In vitro infectivity of the Hepatitis C Virus in the context of humoral immunity and immune escape

Amruta S. Naik

Department of Medicine
National University of Ireland,
University College Cork,
Cork, Ireland.

2017

ucc
Coláiste na hOllscoile Corcaigh, Éire
University College Cork, Ireland

Thesis submitted for the Degree of

Doctor of Philosophy

Supervisors

Dr. Liam J. Fanning (Department of Medicine, UCC),

Dr. Orla Crosbie and Dr. Elizabeth Kenny-Walsh

(Department of Hepatology, Cork University Hospital)

Contents

Acknowledgements

Foremost, I would like to thank my supervisor Dr. Liam J. Fanning for his supervision, motivation and support throughout my PhD. I am also grateful to my co-supervisors Dr. Elizabeth Kenny-Walsh and Dr. Orla Crosbie for their guidance and providing the clinical samples. I must express my very profound gratitude to Molecular Medicine Ireland and University College Cork, Ireland for providing me with the research funding and giving me this opportunity.

I am sincerely thankful to Dr. Arvind H. Patel and Dr. Ania Owsianka for training me in the HCV pseudoparticle assays and for their invaluable thoughts on my research. I am obliged to Dr. Arvind H. Patel for sharing their laboratory reagents with us. I take this opportunity to thank Professor Francois Louis-Cosset for sharing the HCV pseudoparticle generation system with us.

I must mention Kathleen O'Sullivan for her valuable guidance in statistical analysis of my data. I am indebted to Dr. Brendan A. Palmer for his insightful comments and assistance throughout my PhD. I thank Dr. Kevin Hegarty, John Levis, Bernadette Crowley, Jacqueline Kelly, Dr. Owen Cronin, Dr. Gabriella Rizzo, Declan White, all the students and staff for making my stay enjoyable in the Department of Medicine. A special thanks to Rita Lynch for her constant support during my stay in the department.

I need to extend a huge thanks to the 'Suki Calves Group' (Mary Claire O'Regan, Dr. Ciara Harty, Dr. Niamh Denihan, Dr. Charlotte O'Donnell and Dr. Philana Fernandes). I am indebted to Dr. Philana for proof reading my thesis. I am thankful to 'Marathi Mandal Cork' for their constant support during these four years. I must acknowledge my housemates and friends for being there for me.

I could not have done this without my father, late mother and sister. Thank you for being there always. To my cousins, uncles and aunts, thank you for your love and encouragement. To my teachers in India, thank you for motivating me and help me achieve this. I am grateful to each and every individual in my life for helping me accomplish this task.

Declaration

I hereby declare that all work presented in this thesis is original and entirely my own unless otherwise stated. This thesis has not been submitted in whole or in part for a higher degree to this or any other university. Any assistance and contribution by others to this work is acknowledged within the text.

Amruta Naik

Amruta S. Naik, B.Sc. M.Sc.

Statement of Contribution

In this thesis I developed the Total IgG/ VF-Fab: AAV negative viraemic sera challenge protocol. I amplified, cloned, and expressed the full length AAV-E1E2 glycoproteins. I generated infectious HCV pseudoparticles, carried out neutralisation assays and analysed the data. To generate infectious HCV pseudoparticles MLV-Gag-Pol packaging vector, phCMV-ΔC/E1/E2 H77 construct were acquired from Professor Francois Louis-Cosset, INSERM, France by material transfer agreement. MLV-luciferase reporter vector and mouse monoclonal antibodies AP33, ALP98, and luciferase reporter vector were kindly gifted by Dr. Arvind H. Patel, Centre for Virus Research, University of Glasgow, UK. Epitope mapping service was outsourced to Pepscan Presto, Lelystad, Netherlands and further analysis of epitope data was done by me.

Dr. Ania Owsianka (Dr. Arvind H. Patel laboratory, CVR, University of Glasgow, UK) provided training with respect to the HCV pseudoparticle generation. Kian Harty (Bachelor of Science student, UCC), Ciaran J. O'Halloran (Bachelor of Science student, UCC), Nicole Walsh (Research Master student, MVDRL, Department of Medicine, UCC) carried out site directed mutagenesis of cloned E1E2 and contributed in downstream infectious assays. Jessica Neville (Bachelor of Science student, UCC) contributed in GNA ELISA assays of HEK lysates used for generating infectious HCV pseudoparticles.

All other work was performed by me.

This work was funded by Molecular Medicine Ireland, European Regional Development Fund, Department of Enterprise Trade and Innovation and the Higher Education Authority.

List of Publications

This work has been published in the following formats:

Journal Article:

1. **Amruta S. Naik,** Brendan A Palmer, Orla Crosbie, Elizabeth Kenny-Walsh, Liam J. Fanning **Humoral immune system targets clonotypic antibody associated Hepatitis C Virus** (J. Gen Virology, 2016 Nov)

2. **Amruta S. Naik,** Brendan A Palmer, Orla Crosbie, Elizabeth Kenny-Walsh, Liam J. Fanning **A single amino acid change in the hypervariable region 1 of HCV genotype 4a aids humoral immune escape. (**J. Gen Virology, 2016 Jun ;97(6):1345-9)

3. **Amruta S. Naik**, Ania Owsianka, Brendan A. Palmer, Ciaran J. O'halloran**,** Nicole Walsh, Orla Crosbie, Elizabeth Kenny-Walsh, Arvind H. Patel, Liam J. Fanning **Reverse epitope mapping of the E2 glycoprotein in antibody associated Hepatitis C Virus (**
   PLOS ONE-PONE-D-17-02203R1 *In Press*)

Research Presentations:

1. Oral Presentation at **New Horizons in Medical Research** – Dec 2016, Cork, Ireland. E2 glycoprotein epitope mapping in antibody associated hepatitis C virus.

2. Poster presentation at **EASL Special Conference**-"**New perspectives in hepatitis C virus infections – The roadmap for cure**"-September 2016, Paris, France**.** E2 glycoprotein epitope mapping in antibody associated hepatitis C virus.

3. Poster presentation at **15th International Symposium on Viral Hepatitis and Liver Diseases (ISVHLD)**, July 2015, Berlin, Germany**.** Immunoglobulin purified from antibody associated virus from hepatitis C viraemic sera exhibit selective targeting of homologous HCV genotype.

4. Oral Presentation at **New Horizons in Medical Research** – Dec 2015, Cork, Ireland. Mutations of the immunodominant epitopes lead to humoral immune escape of Hepatits C Virus.

5. Oral presentation at **MMI Education & Training Annual Scientific Meeting** - Mar 2015, Dublin, Ireland. Investigation Of antibody associated hepatitis C virus in the quasispecies pool.

List of Abbreviations

3D	Three dimensional
ΔHVR1	HCVpp lacking HVR1
AASLD	American Association for the Study of Liver Disease
AAV	Antibody associated virus
AFV	Antibody free virus
AMP	Ampicillin
APO	Apolipoprotein
BSA	Bovine Serum Albumin
bNAbs	Broadly neutralising antibodies
cDNA	Complementary DNA
CLIPS	Chemically linked peptides on scaffolds
CLDN1	Claudin 1
CTL	Cytotoxic T lymphocytes
DAA	Direct acting antiviral
DMEM	Dulbecco's Modified Eagle Medium
EASL	European Association for the Study of Liver
EBOV	Ebola Virus
EDTA	Ethylenediaminetetraacetic acid
EIA	Enzyme immunoassays
ER	Endoplasmic reticulum
FBS	Foetal Bovine Serum
FcDART	Fc dual-affinity retargeting

GNA	*Galanthus Nivalis* Agglutinin
HAV	Hepatitis A virus
HBV	Hepatitis B virus
HBsAg	Hepatitis B surface antigen
HCV	Hepatitis C virus
HCVpp	HCV pseudoparticle
HCVcc	HCV cell culture derived
HEK	Human embryonic kidney
HIV	Human immunodeficiency virus
HLA	Histocompatibility leukocyte antigen
HRP	Horse radish peroxidase
Huh	Human hepatoma 7
HVR	Hypervariable region
IFN	Interferon
IgVR	Inter-genomic variable region
IPS-1	IFN-β promoter stimulator protein 1
IKK-α	IκB kinase
IL	Interleukin
IRES	Internal ribosome entry site
IRF	IFN regulatory factor
ISG	IFN-stimulated genes
JFH1	Japenese Fulminant Hepatitis 1
κVF-Fab	Kappa virus free Fab

λ-VF-Fab	Lambda virus free Fab
LB	Luria Bertani
LD	Lipid droplet
LDL	Low density lipoprotein
LDLR	Low density lipoprotein receptor
LT	Liver transplant
LVP	Lipoviral particles
MAVS	Mitochiondrial antiviral signalling protein
MAb	Monoclonal antibody
MLV	Murine leukemia virus
NANBH	non A, non B hepatitis.
nAbs	neutralising antibodies
NK	Natural killer cells
Neo	Neomycin phosphotransferase
OASs	2',5'-oligoadenylate synthetases
OCLN	Occludin
ORF	Open reading frame
PAMP	Pathogen associated molecular pattern
PAGE	Polyacrylamide gel electrophoresis
PBS	Phosphate Buffered Saline
PBST	PBS-Tween 20
PCR	Polymerase chain reaction
pDC	Plasmacytoid dendritic cells

PEG-IFN-α	Pegylated IFN-α
PHHs	Primary human hepatocytes
PKR	Protein kinase R
PRR	Pattern recognition receptors
qRT-PCR	quantitative real-time PCR
RAV	Resistance associated variants
RBA	Ribavirin
RdRp	RNA dependent RNA polymerase
REM	Replication enhancing mutations
RLR	Retinoic acid-inducible gene I like receptor
RIBA	Recombinant immunoblot assay
RIG-I	Retinoic acid inducible gene I
RPM	Rotation per minute
RT-PCR	Reverse transcriptase polymerase chain reaction
SCARB1	Scavenger receptor class B member 1
sdHCV	Serum-derived HCV
SDM	Site directed mutagenesis
SDS	Sodium dodecyl sulphate
SIV	Simian immunodeficiency virus
STAT	Signal transducer and activator of transcription
SVR	Sustained virologic response
TGF	Transforming growth factor
TLR	Toll like receptor

TNF	Tumour necrosis factor
TRIF	TIR-domain containing adapter-inducing IFN-β
UTR	Un-translated region
VF-Fab	Virus free Fab
VLDL	Very low density lipoproteins

One letter and three letter amino acid abbreviation

Amino acid	Three letter code	One letter code
alanine	ala	A
arginine	arg	R
asparagine	asn	N
aspartic acid	asp	D
asparagine or aspartic acid	asx	B
cysteine	cys	C
glutamic acid	glu	E
glutamine	gln	Q
glutamine or glutamic acid	glx	Z
glycine	gly	G
histidine	his	H
isoleucine	ile	I
leucine	leu	L
lysine	lys	K
methionine	met	M
phenylalanine	phe	F
proline	pro	P
serine	ser	S
threonine	thr	T
tryptophan	trp	W
tyrosine	tyr	Y
valine	val	V

Abstract

The hepatitis C virus (HCV) is an enveloped RNA virus which circulates in infected individuals as a quasispecies. HCV encodes two highly glycosylated envelope glycoproteins E1E2 which is involved in fusion and entry of the virus into the hepatocytes. E1E2 is hypervariable in nature and is a target of the humoral immune system. The humoral immune system responds to chronic HCV infection by producing neutralising antibodies (nAb) (127). The immune system produces antibodies against susceptible virions which are removed from the heterogeneous virus population leading to the emergence of virions with modulated surface envelope proteins (53, 230). The objective of this *corpus* was to analyse *in vitro* infectivity of the HCV in the context of humoral immunity and humoral immune escape.

In this study, viraemic sera from chronically infected HCV individuals with genotype 1a (n=5), genotype 1b (n=12), genotype 3a (n=3) and genotype 4a (n=6) were segregated into antibody free virus (AFV) and antibody associated virus (AAV) populations. All five (n=5/5) (1a), n=5/12 (1b), n=2/3 (3a) and n=1/6 (4a) showed detectable levels of AAV using a reverse transcriptase PCR (RT-PCR) assay. Total IgG and virus free Fab (VF-Fab) obtained from AAV positive sera were used to challenge AAV negative sera which showed no detectable levels of AAV. Selective targeting of clonotypic HCV variants from the quasispecies pool was documented. Furthermore, HCVpp (n=10) from a clonotypic AAV population were generated. A marked difference in the infectivity of AAV E1E2-HCVpp was observed. 40% of the pseudotyped viral particles were identified as being infectious. Additionally, the neutralisation potential of patient-derived VF-Fab obtained from HCV genotype 1a (n=3), genotype 1b (n=7) and genotype 3a (n=1) was studied using a HCVpp system.

We documented a reduction in the infectivity of HCVpp derived from AAV sequence when challenged with VF-Fab.

Potential linear epitopes within the E1E2 gene junction of AAV sequences (residues 364-430) were mapped. Prospective neutralising epitopes within the HVR1 and an additional epitope which overlapped with a broadly neutralising AP33 epitope were identified (amino acid 412-423 in E2). To assess the possible conformational or discontinuous epitope(s) outside the E1E2 gene junction, amino acid region 384-619 was selected. Five binding motifs were targeted by patient-derived VF-Fab upon peptide mapping, of which two shared the residues with previously reported epitopes within CD81 binding region. One epitope lies within an immunodominant HVR1 and two were novel.

Separately, longitudinal ultra-deep pyrosequencing analysis of HCV genotype 4a over 10 years demonstrated the appearance of antibodies at discrete time points and extinction of the antibody associated lineage (230). Additional analysis of 4a sera extending to 13 years demonstrated the presence of antibodies to a viral variant two years after its first appearance. Subsequently, 27 amino acid HVR1 peptides were used to test humoral immune escape. We defined by differential peptide binding of VF-Fab tha immune escape was due to a single amino acid change in the HVR1.

In summary, we provide direct evidence of natural humoral immune escape by HCV within the HVR1 in a chronically 4a infected patient. We successfully used a reverse epitope mapping strategy to identify epitopes targeted by the host humoral immune system. Additionally, we combined VF-Fabs which have shown binding reactivity to the different epitopes to further reduce HCVpp infectivity. A significant reduction in HCVpp infectivity ($p<0.05$) was observed when challenged with a combination of

inter genotype and subtype VF-Fabs. Our data indicate that combining the antigen specificity of different antibodies may be a useful strategy to reduce the *in vitro* infectivity of the HCV.

Chapter 1

1. Introduction:

1.1 Hepatitis C Virus Classification

In the mid-1970's, patients developed symptoms of hepatitis infection after receiving blood from hepatitis A (HAV) and hepatitis B (HBV) virus negative donors. The causative agent of this hepatitis was serologically unrelated to HAV, HBV or any other previously known hepatotropic viruses like Epstein-Barr virus or human cytomegalovirus. In the late 1980s, Choo *et al*. (1989), first characterised HCV as Non-A-Non-B hepatitis (NANBH) (2). Choo *et al.* prepared cDNA libraries using recombinant DNA technology to identify the causative agent of the NANB hepatitis virus (2). Choo *et al*. (1989) screened ten million clones and identified a positive cDNA clone (clone 5-1-1) along with a larger clone (clone 81) which overlapped clone 5-1-1 (2). The maximum size of the RNA was estimated to be 10,000 nucleotides after the RNA derived from an infected chimpanzee was subjected to gel electrophoresis and hybridised to clone 81. Further analysis revealed that the genome is single stranded with a single positive sense open reading frame. HCV was subsequently classified into the family *Flaviviridae*, genus *Hepacivirus* (3, reviewed in 4).

However, Smith *et al.* (2016) have proposed a new nomenclature system for species belonging to the *Hepacivicrus* based on amino acid p-distances for NS2/ NS3 [protease] and NS5B [RNA-dependent RNA polymerase] proteins (5). Smith *et al.* (2016) propose that HCV being the first Hepacivirus to be discovered and the type species of the genus should be assigned to Hepacivirus C rather than Hepacivirus A (5). Nonetheless, individual viral isolates of Hepacivirus C still referred to as Hepatitis C Virus (5).

1.2 Genome Organisation of HCV

The HCV genome consists of a positive sense RNA molecule with a single opening reading frame (ORF) that encodes a ~3,000 amino acid HCV polyprotein. 5' and 3' non-coding regions flank the ORF. The 5'UTR possesses an internal ribosome entry site (IRES) and is 341 nucleotides long (Fig 1.1). The IRES is involved in cap-independent translation. The 3' UTR of HCV harbours a poorly conserved region of 30-40 nucleotides in length, a poly uridine (poly U) and a unique 98 nucleotide sequence which forms a stem loop structure. This stem loop is important for the initiation of replication and is known as the X tail (6).

The HCV polyprotein can be divided into structural and non-structural proteins. HCV polyprotein is cleaved into 10 mature proteins co and post-transnationally (7). The core, E1 and E2 glycoproteins form the structural components of the HCV polyprotein. NS3-NS5B are required for replication of HCV RNA from the non-structural component of the polyprotein whilst P7 and NS2 are required for assembly of the viral particles (reviewed in 6).

The core protein of HCV is located at the N-terminus of the precursor protein. There are two isoforms of core (P23 and P21) which result from multiple proteolytic cleavage events executed by host signal peptidase(s) (reviewed in 6). P23 is the immature form of core protein which is first cleaved from the 5′ terminal of HCV polyprotein. Mature core-P21 is formed by cleaving the 3′ terminal of P23 between amino acids 174 and 191 (8). The core protein forms multimeric complexes which fold into viral capsid protein composed of a hydrophilic domain and a hydrophobic domain (8, 9). Mature core P21 binds to RNA and co-localises with the endoplasmic reticulum (ER). Core also plays a key role in HCV replication (8, 9).

The envelope glycoproteins, E1 and E2, located downstream of the core protein are involved in the cellular entry of HCV. The glycoproteins are heavily glycosylated and are classified as type I transmembrane proteins with an ectodomain and a transmembrane domain. Detailed role of E1 and E2 in cellular entry and immune escape will be described later (Section 1.6.1).

P7 is a 63 amino acid hydrophobic polypeptide and its N and C – termini are both orientated towards the extracellular domain (10). P7 is classified as a viroporin that forms a cationic channel in the lipid bilayers (10). P7 is shown to be crucial in viral assembly and enveloping of newly synthesised viral particles (11).

Genes encoding for non-structural HCV proteins are located downstream of the structural protein region. The nomenclature for HCV polyproteins is similar to Flavivirus protein nomenclature. However, none of the HCV proteins are homologous to Flavivirus NS1, hence HCV non-structural proteins start with NS2 (12). NS2 is located between P7 and NS3 on the HCV polyprotein. Although the NS2/NS3 precursor is not essential for RNA replication, the protease domain of NS2 is indispensable for virus production. NS2 undergoes autocatalytic *cis* cleavage from its precursor protein (12) to generate the active form. NS2 also interacts with host proteins that belong to the phospholipase family such as phosphatidylserine specific phospholipase A1 which are necessary for virion assembly (13).

NS3 contains an N-terminal serine protease domain and an RNA helicase/NTpase domain within its C-terminal domain (12, 14). NS3 forms a non-covalent complex with NS4A, where NS4A functions as a co-factor for the enzymatic activity of NS3 (15). The protease activity of NS3-4A is responsible for the cleavage events downstream of NS2/NS3. NS3-4A interferes with the host immune response by

inhibiting the activity of proteins essential for antiviral response thereby creating an environment susceptible to persistent viral infection. The helicase domain of NS3 is involved in polyprotein cleavage which is vital for HCV replication (14).

NS4B is located downstream from NS4A, cleaved from the polyprotein by NS3/4A serine protease activity (16). It is thought that NS4B forms oligomers and in this way aids the alteration of ER forming a membranous web (reviewed in 17). NS4B interacts with other non-structural proteins and several host proteins during HCV RNA replication assisting in the development of HCV replication complexes, viral replication and assembly (18, 19).

NS5A is a membrane associated protein with three distinct domains namely D1, D2 and D3 (reviewed in 20). NS5A has two differently phosphorylated isoforms of 56 kDa and 58 kDa (reviewed in 20). NS5A was found to induce accumulation of phosphatidylinositol 4-phosphate in membranous web structures which are associated with HCV RNA replication complexes by interacting with phosphatidylinositol 4-kinase III α (PI4K-IIIα) (reviewed in 21). NS5A was also found to interact with apolipoprotein E (ApoE) during the RNA replication (22). NS5A also interacts with ApoJ, glucose stimulated apolipoprotein and co-localises with HCV core protein on the surface of lipid droplets during the HCV infection confirming its role in viral assembly (23).

NS5B is an RNA dependant RNA polymerase. NS5B is highly conserved amongst the HCV strains and is an important target for antiviral drug development (24). NS5B contains an amino acid motif GDD, which is a distinct characteristic of all the RNA dependant RNA polymerases (25). Crystal structure analysis of NS5B has revealed it to be a tail anchored ‘right hand’ membrane protein with palm, thumb and fingers

subdomains (26). It is the lack of error correcting proof reading activity of NS5B and various selection pressures sculpt the HCV quasispecies (Section 1.6.2)

Figure 1.1: HCV genome organisation, polyprotein processing, and protein topology

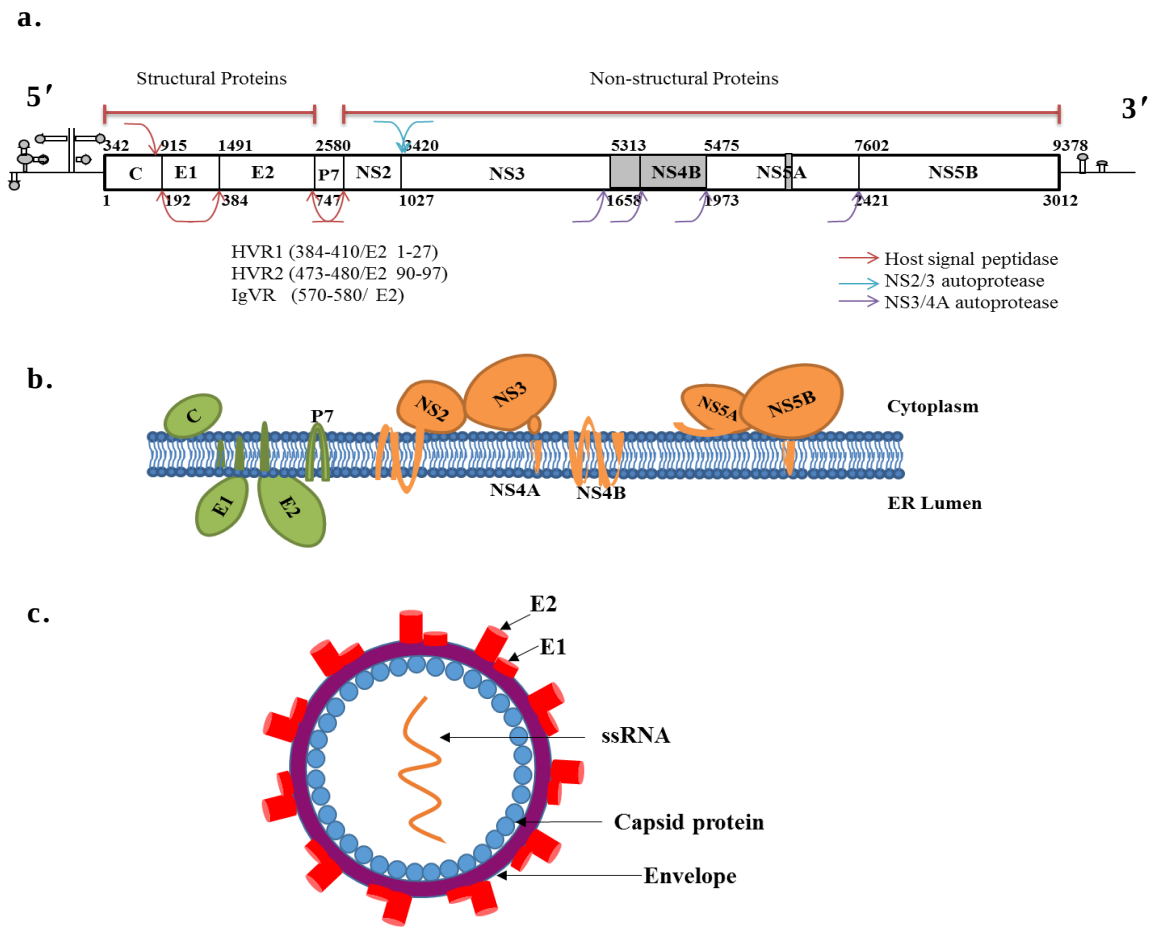

a. Positive sense single stranded HCV RNA flanked by structured 5′ and 3′ UTRs encodes a single open reading frame (ORF) of ~3,000 amino acids. IRES in the 5′ UTR is involved in translation of the ORF, generating a large polyprotein that is organised with structural proteins core (C), two envelope glycoproteins (E1 and E2) in the amino-terminal third of the polyprotein, followed by the NS (NS2, NS3, NS4A/B and NS5A/B) replication proteins. The host and viral proteases cleave the polyprotein co- and posttranslationally to produce the 10 individual HCV proteins. Coloured arrows indicate involvement of host and viral proteases in the proteolytic cleavage **b.** HCV proteins topology relative to the ER membrane. Core (forms a homodimer) and NS5A are anchored to intracellular ER membrane via amphipathic α-helices. NS3 is tethered to membrane through small α-helix and via the cofactor NS4A implanting into the amino-terminal protease domain of NS3. E1E2 forms a heterodimer **c.** three dimensional structure of HCV.

1.2.1 E1E2 envelope glycoproteins

E1E2 is the structural protein which is released by host ER signal peptidase(s). E1 and E2 are type I transmembrane proteins with an amino-terminal ectodomain and carboxy-terminal transmembrane helix (27). E2p7NS2 is produced upon partial cleavage. Later NS2 is cleaved from E2p7NS2 precursor; however, E2p7 is cleaved inefficiently (28). This inefficient cleavage occurs as a result of transmembrane domains of p7 that reduces the productivity of p7/NS2 cleavage (29). This results in the accumulation of E2, E2p7, p7, and NS2 as cleavage products. Additionally, the short distance between the cleavage site of E2/p7 or p7/NS2 and the predicted transmembrane α-helix located downstream of the cleavage sites is thought to further enforce the structural limitations of these cleavage sites (30).

The envelope protein is highly glycosylated and N-linked glycans constitute approximately 50% of the envelope protein ectodomain, with four and 11 potential N-glycosylation sites in E1 and E2 respectively (31, 32). The molecular weights of glycosylated E1 and E2 are approximately 30kDa and 60 kDa respectively (33). The envelope proteins are glycosylated post-translationally by oligosaccharyltransferase (30). Oligosaccharyltransferases add low-branched oligosaccharide chains of nine residues of mannose and three residues of glucose to specific residues. For example, asparagine Asn-X-Ser or Asn-X-Thr sequences are often glycosylated (where X can be any amino acid except for proline) (34, 35). The glycosylation sites on E1E2 are well conserved. The glycosylation of the viral envelope protein is important for the correct folding and assembly of viral particles in the cells. Mutational analysis of envelope protein revealed that glycans E1N1, E2N8, E2N10, and E2N11 are crucial for viral assembly (36). Glycans E2N1, E2N2, E2N4, E2N6, and E2N11 shield neutralisation sensitive epitopes from immunological targeting (36). Additionally,

glycans E2N1, E2N2, E2N4, and E2N6 were shown to have a role in E2 interaction with CD81 (36). The effect of mutations in the glycosylation sites of the envelope protein of HCV 1b and their interaction with the cellular chaperones was studied using insect cell lines (35). It was observed that in insect *Spodoptera frugiperda* cell lines, correctly folded heterodimers of functional E1E2 interact with calnexin whereas misfolded E1E2 dimers interact with calreticulin (35). Mutations at sites N1, N5 in the E1 and N1, N2 or N10 in the E2 lead to misfolding of the E1E2 complex disrupting the conformation of the envelope protein (35). These are the key sites which are involved in stabilisation of the structure, conformation and productive assembly of the viral particles as observed in *Spodoptera frugiperda* cells (35).

After glycosylation, E1E2 either forms a non-covalent functional heterodimer complex by interacting with calnexin or forms non-functional aggregates containing disulphide bridges with the participation of calreticulin. E1 and E2 glycoproteins are major targets of nAb. To date, the structure of E1 (193-383) is not sufficiently characterised. Recently, Falson *et al.* (2015) have shown that E1 protein in HCVcc is trimeric and HCV envelope glycoproteins most probably assemble as stable trimmers of E1E2 heterodimers at the surface of the HCV virion (27). The N-terminal of E1 consists of a highly conserved GXXXG motif a characteristic of transmembrane protein which is involved in intra-membrane protein-protein interactions (27, 37, 38). This GXXXG motif oligomerises to form trimmers via its transmembrane helix-helix association (37, 38). However, it has been observed that E1 is detected as a trimer on HCVcc particles, but identified as a monomer within infected cells, mostly associated with E2 as an E1E2 heterodimer (27, 39). Based on these data Falson *et al*. (2015) suggested that trimerisation of E1 is E2 dependent and is performed by preformed E1E2 during the virion assembly. Falson *et al.* (2015) also proposed that this

trimerisation of E1 could have an important role in the membrane fusion enabling delivery of HCV genome in the infected cells (27).

E2 (384-747) is a well characterised subunit within the E1E2 heterodimer which forms a 334 residue long ectodomain (E2e) and C terminal transmembrane domain (reviewed in 40) (Fig 1.3). The E2 glycoprotein harbours hypervaraible regions (HVR1 384–410; and HVR2, residues 460–485) and an inter-genotypic variable region (IgVR 570-580) (reviewed in 40, Fig 1.3). Structures for some parts of E2c namely HVR1, HVR2 and HVR3 could not be determined due to highly disordered nature and poor diffraction index of these regions (41). Studies using hydrogen deuterium exchange and limited proteolysis have shown that the N terminal regions 384-463 (HVR1 and HVR2) are exposed and flexible (42). The regions within or located near HVRs are assumed to be flexible loops (41).

E2 is mediates viral attachment by interacting with several host proteins that include CD81, scavenger receptor class B type I (SCARB1) and members of the claudin/occludin family (reviewed in 43). Due to the highly glycosylated nature of E2e (11 N-glycosylation and five O-glycosylation sites) with variable degrees of micro-heterogeneity and the difficulty in maintaining the conformation, it has been challenging to determine the complete structure of E2 (32, 40, 42). Circular dichroism and infrared spectroscopy studies have revealed that the E2 comprises of ~35% β-sheets and ~5% α-helices, with a high degree of disorder (40). Recently Kong *et al*. (2013) analysed the crystal structure of engineered E2 core (E2c) spanning from residues 412-645 (Fig 1.3c, H77 isolate, genotype 1a, PDB ID: 4MWF) screening with the bNAb AR3C whereas Khan *et al*. (2014) analysed E2c spanning 456–656 (J6 isolate, genotype 2a, PDB ID: 4NX3) (reviewed in 40). Both the studies found that E2c contains a central Ig-like domain (492-566) formed by four stranded lower, two

stranded upper β-sheets and a C- terminal four stranded β-sheets (32, 42). The Ig domain is surrounded by α-helices (32, 42). Negative staining of cryoelectron microscopic reconstruction of the E2e without TM domain (384-717) with Fab AR3C revealed it to be a compact globular structure (32). The truncated N-terminal region from E2c (384-421), which includes HVR1, likely fits next to the β-sandwich. Another largely truncated region 454-491 which includes HVR2 and the N476 is situated in the opposite face of the β-sandwich (32). The C-terminal stalk region (72 residues) can occupy space behind the back layer and IgVR (32) (Fig 1.2b).

Mutagenesis and electron microscopy analysis of the CD81 binding site in the E2 revealed that E2c contains a conserved N-terminal region (412-423), the frontal layer (424-453) and the CD81 binding loop (519-535) (Fig 1.2b) (32, 44). Law *et al.* (2008) identified three antigenic regions (AR) by using an antibody antigen binding fragment (Fab) in phage-display library of 115 clones which were generated from chronically infected HCV individuals (45). AR1 is proximal and AR2 is distal to the CD81 receptor-binding site whereas AR3 is conserved and overlaps the CD81 receptor-binding site (45). The CD81 binding site is a target of many bNAb. It has three distinct conserved antigenic clusters. The first conserved antigenic region within CD81 binding site (AS412, residues 412-423) is targeted by bNAbs AP33, HCV1, HC33.1 and 3/11 (46-49). The second antigenic cluster (AS434, residues 434-446) consists of α-helix and is targeted by bNAbs HC84-1 and HC84-27 (reviewed in 49, 50). The third conserved antigenic region referred to as AR3 is a discontinuous region that consists of the entire frontal layer (which includes AS434) and the CD81 binding loop. A family of bNAbs AR3A, AR3B, AR3C, and AR3D target AR3 (45, 51, 52). E2 also contains 18 cysteine residues which are conserved across all the genotypes. These cysteine residues are essential in maintaining the correct topology and are involved in

conformational rearrangement upon viral attachment that results in the fusion stage (32, 42).

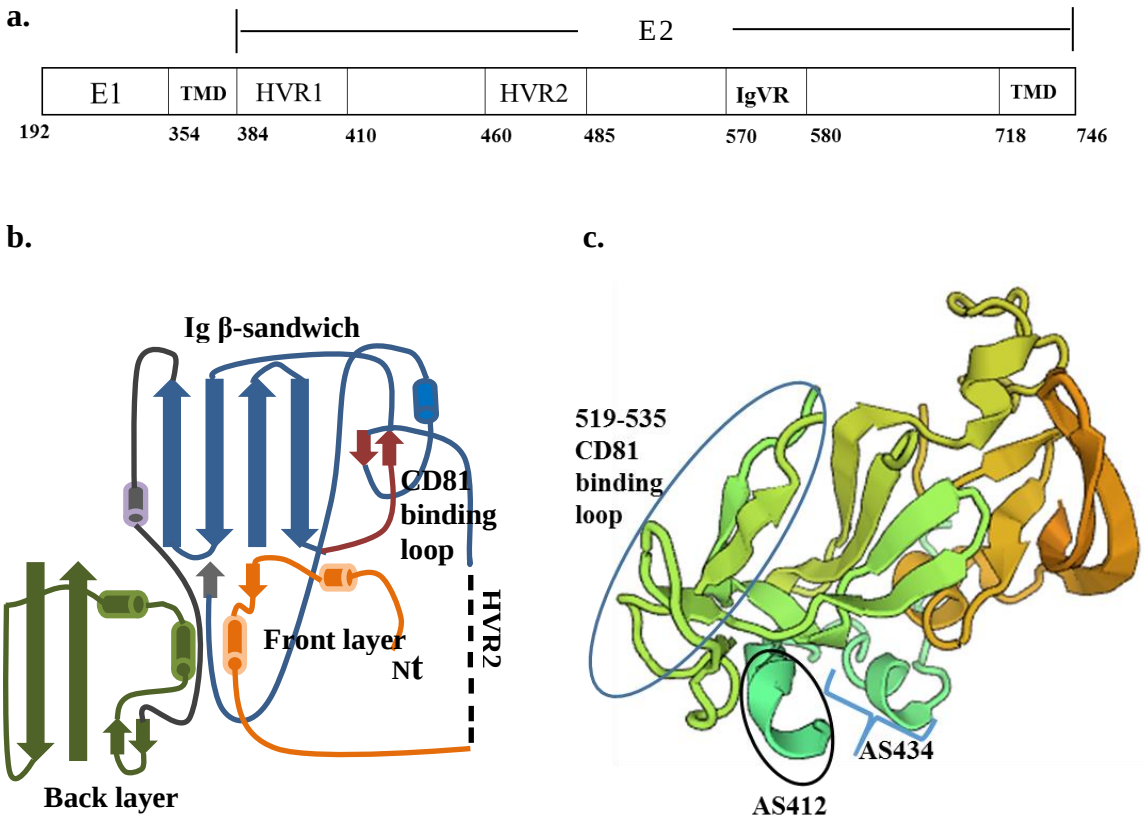

Figure 1.2: Structure of the HCV E1E2 glycoprotein

a. Schematic representation of the E1E2 glycoprotein of the hepatitis C virus showing, transmembrane domains (TMD), hypervariable regions (HVR) and intergenotypic variable region (IgVR) **b.** schematic diagram of E2c (421-645) topology modified from Kong *et al.* (2013) (32). Front layer (orange) is formed by N-terminal region residues 421–453, the Ig β-sandwich (blue) is formed by residues 492-566, the CD81 binding loop is formed by residues 519-535, back layer (green) is formed by residues 597–645. A flexible region HVR2 is denoted by dotted black lines, Nt- N terminus **c.** three dimensional structure of E2c (412-645) modified from Kong *et al.* (2013) using SWISS MODEL showing different antigenic regions (32). AS412, residues 412-423; AS434, residues 434-446 and AR3 includes AS434 and CD81 binding loop (519-535).

1.2.2 Quasispecies and Hypervariable regions

HCV has a high rate of replication with the production of estimated 10^{12}copies/day of virions (53). In an infected individual HCV circulates as a swarm of minor and major phylogenetically closely related diverse variants called as quasispecies (25, 54). RNA dependant RNA polymerase's lack of proof reading activity contributes to the qausipsecies nature of HCV (25). Lack of error correcting activity combined with the high rate of replication results in synonymous and nonsynonymous mutations (55). These mutations undergo either a positive or a negative selection resulting in a dominant variant and other related minor variants. Studies in chimpanzees and infected individuals have shown that cytotoxic T lymphocytes (CTL) drive HCV evolution (reviewed in 56, 57, 58). Erickson *et al.* (2001) studied four chimpanzees, where three animals were chronically infected for five or seven years while one animal was immunised with recombinant HCV glycoprotein before virus challenge (56). Erickson and colleagues observed mutations in multiple epitopes which resulted in impaired class I major histocompatibility complex (MHC) binding and/or CTL recognition (56). Timm and co-workers (2004) studied evolution of immune dominant epitope NS3 in human histocompatibility leukocyte antigen (HLA)-B8 in two acutely infected subjects under PegIFN-RBA treatment in addition to 30 treatment naïve chronically infected individuals (57). They observed mutations within HLA-B8 restricted epitope B8-1395 in subjects with acute HCV infection (57). Chronically infected individuals expressing HLA-B8 allele also showed polymorphism in the epitope B8-1395 (57). Overall, this data supports that amino acid alteration can lead to loss of recognition by CTL giving rise to new escape mutants.

Navas *et al.* (1998) studied the genetic variability in the HVR1 region of HCV obtained from peripheral blood mononuclear cells, liver tissues, and serum samples

from HCV infected patients (59). Phylogenetic analysis of HVR1 sequences demonstrated compartmentalisation of quasipsepcies in PBMC, liver tissues and serum which were obtained at the same time from chronically infected patients (59). Ray *et al.* (2005) studied the genetic variability of HCV obtained from a cohort of women infected with HCV contaminated anti-D immunoglobulin (60). In their research Ray *et al.* (2005) observed the highest rate of nonsynonymous change in the E2 gene with HVR1 being highly divergent, followed by NS2, p7, E1, NS3, and Core (60). These diverse variants have been demonstrated to correlate with the disease outcome in acute HCV infection (55).

Multiple linear epitopes within the 27 amino acid HVR1, in the N terminus of E2 envelope protein, have been identified as the principle target of nAbs (Fig 1.3a) (30, 61-67). It was observed that a more diverse HVR1 population led to the establishment of chronic infection while infection with less diverse HVR1 population was resolved. Research findings by Guan *et al*. (2012) have shown that HVR1 of HCV-H77 has three functional microdomains (68). Residues at positions 14, 15 and 25-27 (397, 398 and 408-410) are dispensable but are important for binding of the HCV envelope protein to the SCARB1 (68). The second microdomain lies between amino acid positions 16-24 (399-407) is a neutralisation epitope, however, not essential for viral entry (68). The third HVR1 microdomain comprised of first 13 amino acids (384-396) can affect HCV infectivity by modulating the binding of the envelope protein to SCARB1, yet not essential for viral entry (68). It has been observed that anti-SCARB1 antibodies do not neutralise HCVpp lacking HVR1 (ΔHVR1) with the same efficiency as that of the wild type HCVpp harbouring HVR1 (69). Moreover, ΔHVR1 particles are less infectious and modulation of SCARB1 resulted into similar outcomes in the infectivity implying HVR1's dependency on the SCARB1 for infectivity (70). Studies

have shown that HVR1 also interacts with low-density lipoprotein receptor (LDLR) (70). It is speculated that interaction of HVR1 with LDLR is mediated by ApoE as anti-ApoE antibodies neutralise wild type HCVpp more efficiently than the ΔHVR1 particles. It was observed that the buoyant density of ΔHVR1 was higher as a result of reduced level of lipid association (70). Recently, Prentoe *et al.* (2015) studied the neutralisation efficacy of IgGs (H06) purified from genotype 1a chronic-phase plasma in animals challenged with a ΔHVR1 clone J6/ JFH (71). They observed complete protection of animals using a heterologous antibody, underlining the important role of HVR1 in shielding the HCV from nAbs *in vivo* (71).

Immunisation of chimpanzees with a peptide corresponding to the HVR1 protected against homologous HCV infection. Antibodies specific for epitopes within HVR1 have been reported to inhibit the binding of E2 glycoprotein to cells and to block HCV infectivity *in vitro* and *in vivo* (72-74). However, the antibody response to the HVR1 region is strain specific and could be non-neutralising too. Mutations within HVR1 are associated with humoral immune escape. On the contrary, HVR2 and IgVR have not been observed to be a target of nAbs (Fig 1.2a) (75). However, Prentoe *et al.* (2015) observed a potential escape mutation, D476G, in the HVR2 in an animal infected with J6 clone harbouring HVR1. The clone with this mutation provided 6.6 fold resistance against H06 IgG as well as 2.0–5.8 fold resistance against MAbs AR3A, AR4A and AR5A (71). Deletion of HVR2 or IgVR affects the E1E2 dimerisation resulting in disrupted folding causing reduced CD81 binding and viral entry in the HCVpp system (reviewed in 76). Deletion of HVR1 and HVR2 resulted in the reduced binding to CD81 by a factor of about half. The available data shows that the variable regions in the E2 glycoprotein affect the binding of nAbs to the CD81 site (reviewed in 77). Alhammad *et al.* (2015) identified two nAbs (MAb33 and MAb36) against epitope

within HVR1. They observed that deletion of IgVR led to reduction in binding of these antibodies to indicating IgVR's involvement in governing conformation and or accessibility to HVR1 (78). However, simultaneous deletion of both IgVR and HVR2 restored the binding partially, suggesting that HVR1, HVR2 and IgVR are linked to the E2 structurally (Figs 1.3a) (78).

1.3 Cellular receptors involved in HCV entry and HCV life cycle

Entry of HCV and its lifecycle in the hepatocytes is shown in Fig 1. 3. HCV entry involves interaction of E1E2 glycoprotein with numerous cellular receptors including the LDLR (79), CD81 (80), SCARB1 (81), mannose binding lectins (82), asialoglycoprotein receptor (83), and glycosaminoglycans (84, reviewed in 85).

It has been demonstrated that low-density lipoprotein receptor (LDLR) and heparin sulphate proteoglycans provide the initial docking for HCV. Experiments using anti-LDLR antibodies and biochemical inhibitors of Low-density lipoprotein (LDL) endocytosis showed inhibition of LDL mediated endocytosis (86). Barth *et al.* (2003) showed that E2 binding was affected by highly sulphated heparan sulphate and heparin, and partial enzymatic degradation of heapran sulphate resulted in the reduction of E2 binding. Thus, the level of sulphation of heparin sulphate influences the binding of E2. As a result of these observations, Barth *et al.* (2003) proposed that E2 interacts with HSPGs which mediate the initial binding of E2 to the target cells and then may be transferred to another receptor for cell entry (84).

After the initial attachment of HCV, the synchronised action of four key receptors facilitates entry of HCV. The receptors are known as SCARB1 (81), tetraspanin CD81 (80) and tight-junction proteins claudin-1 (CLDN1) (87), and occludin (OCLN) (88). Different experimental data suggests that SCARB1 is the first entry factor in the HCV

infection. SCARB1 is a membrane protein with a large extracellular domain that separates the two C-terminal and one N-terminal short internal domains. Scarselli *et al.* (2002) have shown that SCARB1 interacts with HVR1 region in the E2 protein and this interaction is suggested to be important for unmasking the CD81 site (81). SCARB1 binds to lipoproteins and is thought to be engaged in post-attachment productive entry by modifying the lipid composition of the lipoprotein moiety of the virion and exposing the CD81 binding (89).

CD81 is the key receptor involved in HCV attachment and entry. CD81 belongs to the tetraspanin family. CD81 contains two short extracellular loops and two large extracellular loops (80). Many experiments using antiCD81 antibodies in HCVpp and HCVcc system have shown inhibition of infection in primary human hepatocytes or hepatoma cell lines (33, 90-93). Down regulation of CD81 receptor using siRNA in hepatoma cells have been shown to inhibit infectivity of HCVpp and HCVcc (94).

Tight junction protein CLDN1 has been shown to interact with CD81. It is believed that EGFR promotes CD81-CLDN1 complex formation by inducing CD81 diffusion through HRas activation and facilitates CD81-CLDN1 co-internalisation with HCV particles. After interaction with the CD81-CLDN1 complex, the HCV particle also transiently activates the PI3K-AKT pathway in order to facilitate its entry (95). Additionally, one other tight junction protein, OCLN, is also involved as a co-receptor in HCV entry. It has been reported that TNFα, produced by activated macrophages, increases the diffusion coefficient of CD81. In this way, HCV entry is facilitated by relocalising OCLN at the basolateral membrane (96).

HCV particles, associated with CD81 and CLDN1, are then endocytosed by clathrin mediated process (97). Clathrin coated vesicles are delivered to endosomes. Promoted

by interaction with the cell-death-inducing DFFA-like effector b (CIDEB), the acidic pH in endosomes triggers the penetration of the virus by fusing with peptides in the envelope glycoproteins (98). Following the uncoating of the viral particle, positive strand RNA is released into the cytoplasm and host translational machinery is used to directly translate the positive strand RNA. Both viral and host proteases process the HCV polyprotein. The HCV capsid with nascent viral RNA is enveloped in a lipid bilayer harbouring E1E2 glycoprotein buds into ER and is released through host secretory pathways (Fig 1.3).

1.3.1 HCV as lipoviro particle

Thomssen *et al.* in 1992, showed that β-lipoproteins are associated with HCV and hence the HCV particles that circulate in an infected individual vary in their density (99). In 2002, André *et al.* quantified HCV RNA in the low-density fractions of plasma corresponding to the very-low-density lipoprotein (VLDL), intermediate-density lipoprotein, and LDL fractions from treatment naive chronically HCV-infected patients (100). It has been observed that in an infected individual HCV circulates as a 'lipoviral particles' (LVP) which is associated with ApoB, ApoE HCV RNA and the viral core protein (reviewed in 100, 101). Buoyant density of LVPs ranges from <1.03 to ∼1.25 g/ml (reviewed in 101).

It has been proven that for the release of infectious HCV, VLDL assembly is needed. In the first stage microsomal transfer protein creates pre-VLDL species by lipidating ApoB (reviewed in 101). Subsequently pre-VLDLs fuse with triglyceride droplets derived from lipid droplets with the help of ApoE. Nascent HCV particles are released through the VLDL secretory pathway by exocytosis as LVPs. Upon maturation, they are associated with lipoproteins (reviewed in 101).

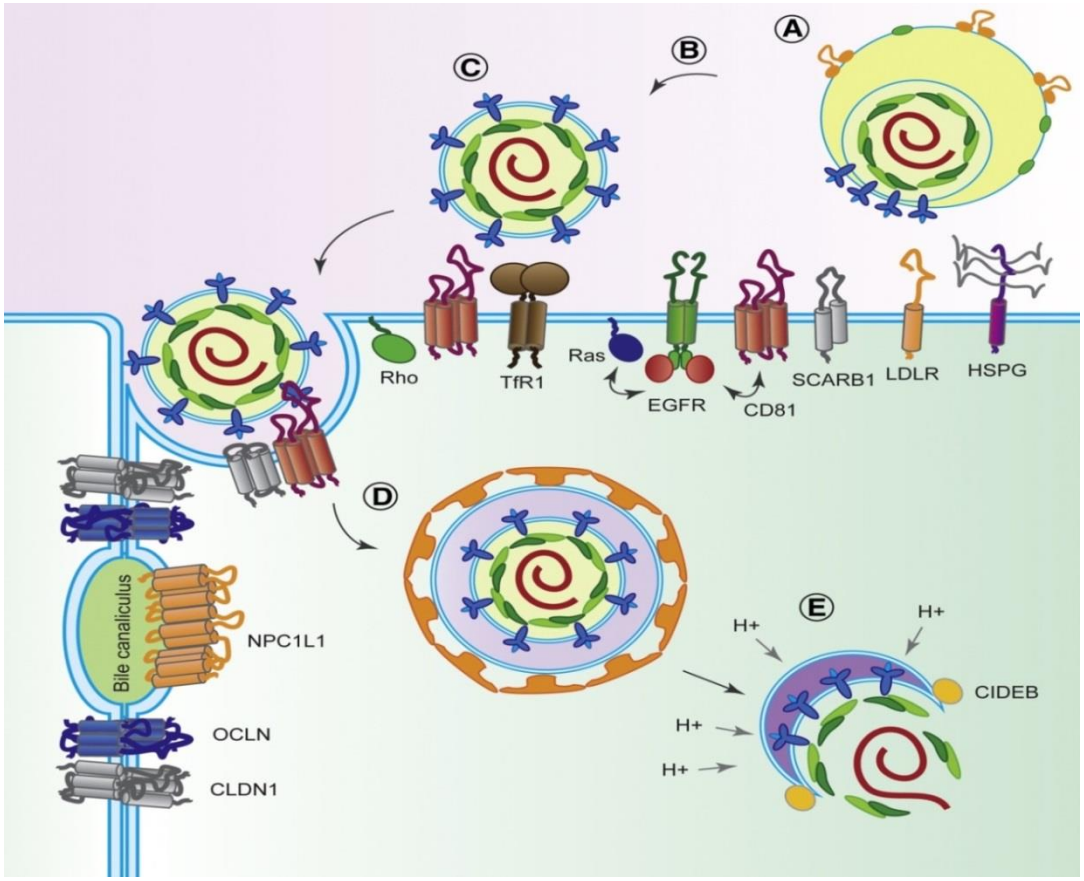

Figure 1.3: Mechanism of HCV Entry

A) HCV circulates as a lipoviral particle. HCV-LPVs first bind to HSPG, LDLR, and SCARB1 B) Binding to SCARB1 induces conformational changes in HCV E2 which facilitates binding of E2 to CD81. C) CD81 binding of HCV results in lateral membrane diffusion of HCV preceded by activation of signalling pathways via EGFR, Ras, and Rho GTPases. CLDN1 and OCLN are engaged in post viral attachment D) Clathrin-mediated endocytosis is initiated by HCV E2-CD81/CLDN1-complex E) The viral envelope and the endosomal membrane undergo fusion in a low-pH environment followed by interaction with cell-death-inducing DFFA-like effector b (CIDEB) (Adopted with permission from (102)).

1.4 Immune response to HCV infection

HCV infection often remains asymptomatic delaying the immune response during acute infection. Neither HCV specific T-cells nor the HCV specific antibodies are observed until 1-2 months of HCV infection. However, HCV RNA can be detected within 1-3 weeks of infection (103-105). A complex interplay between host immune response and viral factors either leads to eradication or establishment of chronic infection.

1.4.1 Innate immune response

The host innate immune system recognises HCV infection via pattern recognition receptors (PRRs). Retinoic acid-inducible gene I (RIG-I)-like receptors (RLRs), the toll-like receptors (TLRs), and the nucleotide oligomerisation domain-like receptors are the three classes of PRRs (106). Double stranded RNA intermediates produced during the replication of HCV serve as a pathogen associated molecular pattern (PAMP) for PRRs. TLRs play a major role in recognising either viral nucleic acid (TLR3, TLR7, TLR9) or viral protein (TLR2 and TLR4) PAMPs. TLR3 recognises ds RNA intermediates. Another PRR, RIG-I binds to the conserved 34 nucleotide poly-uridine core within the poly U/UC region located within the 3'UTR of the virus with 5'ppp motif (107, 108). This leads to a conformational change in RIG-I, followed by ubiquitination by the E3-ubiquitin ligase TRIM2 which in turn recruits mitochondria antiviral signalling protein (MAVS) (109, 110). MAVS then with different signalling partners activates IκB kinase (IKK) and IKK-related kinases (111, 112), TBK1 and IKKε, which phosphorylate the transcription factors IRF3 and IRF7 required for production of IFN-I (IFN-α and IFN-β) and IFN-λ (113). Both IFN-I and IFN-λ induce JAK/STAT pathway resulting in the activation of IFN-stimulated genes (ISGs). RLRs transduce their signals through TIR-domain containing adapter-

inducing IFN-β (TRIF) and IFN-β promoter stimulator protein 1 (IPS-1) resulting in the nuclear translocation of IFN regulatory factor 3 (IRF3), and synthesis of IFN-β respectively (reviewed in 114). IFN-β then binds to the IFN-α/β receptor and activates STAT1 to form homodimers. These homodimers then translocate to gamma (γ) activated sequence elements in ISGs. IFN-β also stimulates uninfected neighbouring hepatocytes to produce ISGs. IFN induced transcriptional upregulation leads to the production of 3-6-base-long, 2'-to-5' linked oligoadenylates (2-5A) from ATP by 2',5'-oligoadenylate synthetases. 2-5A in turn activates latent RNase L enzyme which upon dimerization cleaves single-stranded RNA at UA and UU dinucleotides. RNase L also induces apoptosis of infected cells by degrading cellular mRNAs and rRNAs (reviewed in 115). The ISG 20 kDa protein is also stimulated by IFN which acts as a 3′-5′ exonuclease on ssRNA and supresses viral replication (reviewed in 116). P56 and protein kinase R (PKR) were also identified to inhibit viral and host RNA translation (117).

However, HCV interferes with the IFN response which actually results in the attenuation of its inhibitory effects. The protease activity of NS3/4A protein of HCV cleaves MAVS that leads to dislodging of MAVS from mitochondrial membrane and interferes in the RLR signalling (110, 118). NS3/4A has also been shown to block TLR3 and RIG-I signalling by hydrolysis of TRIF and IPS-1(119). A study on HCV genotype 1b has shown that HCV NS5A inhibited PKR dimerisation and phosphorylation thereby inhibiting its functions (120) . HCV core also interacts with STAT1 and impair IFN-induced STAT1 phosphorylation resulting into inhibition of downstream ISG transcription (121).

Plasmacytoid dendritic cells (pDC) also produce IFN-I in inflamed cells. However, *in vitro* studies have shown that in HCV infection, HCV core and NS3 induce monocytes to produce tumour necrosis factor α (TNF-α) which inhibits IFN-α production resulting into apoptosis of pDCs (122). Nature killer cells (NK) are important effector cells of the innate immune response. NK cells recognise antigen processed by major histocompatibility complexes and produce antiviral cytokines, such as IFN-γ and TNF-α (123). NK cells shape the T cells response directly by secreting cytokines like IFN-γ or by modulating DC. NK cells are capable of killing infected cells thereby increasing the amount of antigen available for cross-presentation to CTLs resulting in an increased $CD8^+$ T cell response (124). Tseng *et al.* (2002) showed that recombinant HCV E2 glycoprotein binds to CD81 on the NK cells and inhibits production of IFN-γ (125). Wang *et al*. (2013) has offered an alternate model suggesting that that HCV may impair the IFN-γ response and proliferation of NK cells by up-regulation of the 'Killer cell lectin-like receptor subfamily G member 1'(126). The NS5A protein of HCV induces the secretion of IL-10 by stimulating monocytes by interacting with TLR-4. IL-10 is an immunosuppressive cytokine that inhibits IL-12, which is an activator of NK cells. IL-10 also induces secretion of transforming growth factor (TGF)-β, thereby down regulating NKG2D on the NK cell surface which results in the functional impairment of NK cells (127).

1.4.2 Adaptive immune response

The adaptive immune response can be divided into the cellular immune response and the humoral immune response. The cellular immune response involves activation of phagocytes, antigen specific CTLs and the release of antiviral cytokines whilst the humoral immune response involves antibody mediated pathogen clearance.

1.4.2.1 Cellular immune response

In HCV infected individuals, up to 40 % people clear the infection spontaneously (reviewed in 128, 129). However, the virus-specific T-cell response determines the course of acute infection. A long-lasting, strong and multi specific CTL response is required for viral clearance (reviewed in 128, 129).

Both $CD4^+$ (T helper cells) and $CD8^+$ T (CTL) cells are produced in response to HCV infection (103, 130). $CD4^+$ T cells play an important role in innate, cellular and antibody mediated immune response. Macrophages and DC secret Interleukin (IL) 12 and IL-18 whereas NK cells produce IFN-γ that promotes growth of $CD8^+$ T cells and $CD4^+$ T helper 1 (Th1) cells (reviewed in 131). DC, macrophages and B cells also produce IL-6. IL-6 production is also stimulated by TNF-α (reviewed in 132). IL-6 then promotes secretion of IL-4, and both IL-6 and IL-4 promote growth and development of $CD4^+$ T helper 2 (Th2) cells (reviewed in 132). Th2 cells mediate B cell activation, antibody production, and the regulation of Th1 responses by secreting IL-4, IL-5, IL-6, IL-10, and IL-13 (reviewed in 133). Antigen presenting cells (DC, macrophages and B cells) capture, process and display the antigen. Endogenous antigens are loaded onto the MHC class I molecule in the ER and are presented to the $CD8^+$ T cells whilst extracellular antigens, internalised by APC are presented to $CD4^+$ T cells by MHC class II molecules (reviewed in 131). $CD4^+$ Th1 cells produce antiviral cytokines IFN-γ, TNF-β and IL-2 (134-136). Sustained $CD4^+$ T cell response is essential in viral clearance in acute HCV infection as they aid with CTL priming, critical in developing a protective response (134, 136). $CD8^+$ T cells are induced at later time points, appearing in the blood after 8-12 weeks of infection (137). Virus-specific $CD8^+$ T-cells are primed by cross presentation of viral antigens from virus-infected dying cells (138). $CD8^+$ T cells kill the target cells and produce non-cytolytic

antivirals cytokines such as IFN-γ which facilitate viral elimination. Studies involving HCV-infected patients and chimpanzees have shown that sustained and multiple epitope specific $CD8^+$ T-cell response leads to spontaneous clearance of acute HCV infection (103, 134, 139, 140).

High level of viral turnover (~10^{12} virions/day) in the absence of proof reading activity by RNA dependant RNA polymerase results into frequent mutations within the viral genome (53). Mutations in the MHC class I restricted T cell epitopes may lead to a delayed T cell response affecting the outcome of cellular response in the infected hepatocytes (141). Escape mutations result in the downregulation of T cell responses and fail to effectively prime new T cells (142). HCV core impairs T cell function by binding to the complement component C1q (gC1qR) which leads to inhibition of Lck/Akt activation, decreased production of IL-12 and T cell function. Mutations in the T cell epitopes cause decrease in the expression of the inhibitory receptor programme death-1 (PD-1) (143, 144). PD-1 expression on CD4+ and CD8+ T cells is upregulated in HCV infection. PD-1 interacts with its ligand programme death ligand-1, PD-L1 (145). There are two subsets of HCV-specific CTL; the PD-1^+/$CD127^-$ subset that do not have expansion ability and are prone to apoptosis and the PD-1^+/$CD127^+$ subset which maintains the proliferation capacity (146). Upon reaching the liver, HCV-specific CTLs acquire a PD-1^{++}/$CD127^-$ phenotype, thus promoting anergy in activated T cells resulting into decreased T-cell proliferation and cytokine release (146). It has been observed that CD4+ regulatory T cells are induced at a high frequency in HCV infection resulting in the increased production of IL-10 and TGF-β which ultimately leads to the suppression of HCV-specific CTL in patients (147). IL10 inhibits T cell activity by aborting T cell function when present during priming (148). IL-10 decreases stimulatory molecule expression on MHC class I and

II antigen presenting cells leading to decreased cytokine production and maturation of T cells (149).

1.4.2.2 Humoral immune response

Both structural and NS viral proteins are targeted by the antibodies in HCV infection. In HCV infection, nAbs and non-neutralising antibodies (non-nAbs) are produced. An antibody or immunoglobulin (Ig) is a "Y" shaped molecule with two identical heavy chains (50kDa) and two identical light chains (25kDa) connected by disulphide bonds. Immunoglobulins are divided into five different classes based on the type of the heavy chain as IgA (α), IgD (δ), IgE (ε), IgG (γ), and IgM (μ) with different effector functions. There are two types of Ig light chains namely kappa (κ) and lambda (λ) (reviewed in 150).. Each Ig molecule has a constant domain (C_L, C_H1, C_H2, C_H3, IgE and IgM have four constant regions per heavy chain) and an amino terminal antigen binding variable domain (V_L, V_H). The variable domain has three hypervariable regions in the complementarity determining regions (reviewed in 150). Antibodies exhibit several antiviral activities *in vivo*,- i) by binding to the envelope protein of virus by blocking the viral attachment to the host cell and interfering with the entry process ii) by Fc-mediated effector system by activating complement fixing pathway iii) this can lead to cell lysis or clearance by antibody-dependent cellular cytotoxicity or complement-dependent cytotoxicity (CDC) (reviewed in 151).

IgM is the first antibody which appears shortly (average 3.7 weeks) after onset of the hepatitis, more specifically to the HCV capsid antigen (152). Anti-HCV IgM antibodies appear in both acute and chronic (71-86%) HCV infection (152-154). Appearance of IgM in chronic infection is an indication of constantly evolving viral antigenic epitopes resulting in secondary IgM response (153). IgGs appear almost

concurrently with IgM in HCV infection (152, 153). Chen *et al.* (1999) have shown that IgG to core protein appear first than to envelope or NS proteins (155). Chen and colleagues (1999) observed that with the exception of core protein, the IgG response to E2, NS3, NS5 and NS4 was restricted to IgG1 isotype and was low in titre (155). This limited class switching could be a result of limited T helper cell function and skewing of T helper cell subsets to HCV antigens. Regardless, absolute presence of anti-HCV antibodies does not differentiate between acute or chronic HCV infection. Cross reactive nAbs are generated against HCV envelope protein E1E2 which is a major target of the anti HCV humoral immune system (73, 156, 157). bNAbs which target conserved regions of the E1E2 glycoprotein have been shown to control HCV infection in cell culture and in animal models of HCV (158-160). E1 has been observed to generate nAb response, but E1 specific antibodies are produced in low titre in infected individuals (161-163). Two nAb epitopes in E1 encompassing residues 192–202 and 264–327 have been documented (164, 165). Recently, Kong *et al.* (2015) have identified a nearly conserved immunogenic epitope within amino acid region 313-328 in the E1 region (166). This region was recognised by sera from 30 of 92 HCV infected patientss and 15 of 41 vaccinee sera (166). The induction of anti E1 specific antibodies against E1E2 heterodimer has been found to be more difficult to stimulate than to E1 alone (167). Besides, all the characterised nAb epitopes are located in the E2 region of envelope glycoprotein (reviewed in 61).

Antibodies specific for epitopes within HVR1 have been reported to inhibit the binding of E2 glycoprotein to cells and to block HCV infectivity *in vitro* and *in vivo* (Fig 1.4) (72-74). However, there is no evidence that antibodies against HVR1 are broadly cross-neutralising and HCV pseudoparticle (HCVpp) and cell culture derived HCV (HCVcc) experiments have shown poor cross-neutralisation potential of isolate

specific nAb response to HVR1 (30, 67, 76) (129, 168, 169). A neutralising epitope directly downstream of HVR1 (residues 412-423) has been observed to induce nAbs (HCV1, AP33). These Abs block the interaction with CD81 via contact with W_{420} residue (170). However, these nAbs lead to emergence of immune escape mutants as a result of immune selection pressure. Furthermore, findings by Tarr *et al.* (2007) suggest that this region is less immunogenic *in vivo* as less than 5% of spontaneous resolvers have been observed to target this region (171). Additionally, two MAbs AR4A and AR5A target the E1E2 glycoprotein complex require correct folding of the envelope protein (51). Their mechanism of neutralisation is currently unknown (51). The CD81 binding loop within E2c has been found to elicit antibody response (32, 42, 47). Several studies have shown that MAbs target amino acid residues 396-424, 436-447 and 523-540 in the E2 glycoprotein (Fig 1.4) (32, 61, 172, 173). Recently, Deng *et al.* (2015) have identified three epitopes in the HCV E2 glycoprotein. The major epitope is located in the neutralisation face within amino acid region 421-453 and other two in amino acid regions 594–618 and 624–653 of E2 (Fig 1.4) (174). Nevertheless, in patients with persistent HCV infection, it is often observed that high titres of nAbs are developed yet fail to clear the infection. One of the reasons behind the failed humoral immune response is strain specificity of nAbs (reviewed in 58, 173).

von Hahn *et al.* (2007) undertook a longitudinal study involving neutralisation of HCVpp generated from prototype strains H and H77 using nAbs obtained from patient H, from 3 weeks to 26 years post HCV infection (1977, 1991, 1992, 1995, and 2002). von Hahn and co-workers (2007) observed that serum samples before seroconversion failed to neutralise HCVpp. Reduced neutralisation efficiency was observed for HCVpp bearing envelope proteins from concurrent and later time point for nAbs collected in 1992, 1995, and 2002 in contrast to their higher neutralisation efficacy for

HCVpp from earlier time points (175). HCVpp clones generated in 2002 were resistant to neutralisation by nAbs collected at all time points. However, nAbs from unrelated patients efficiently neutralised all the HCVpp in the study (175). This data suggested that generated antibodies clear the established viral variants, but fail to neutralise emerging viral quasispecies leading to persistent HCV viraemia (175).

a.

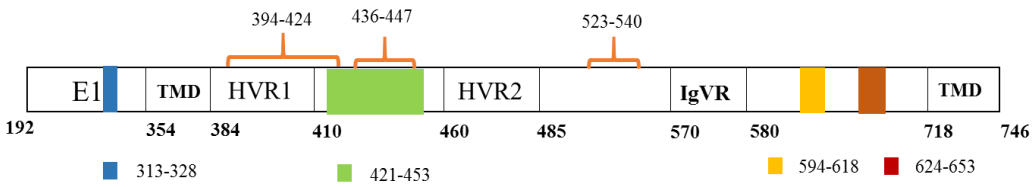

b.

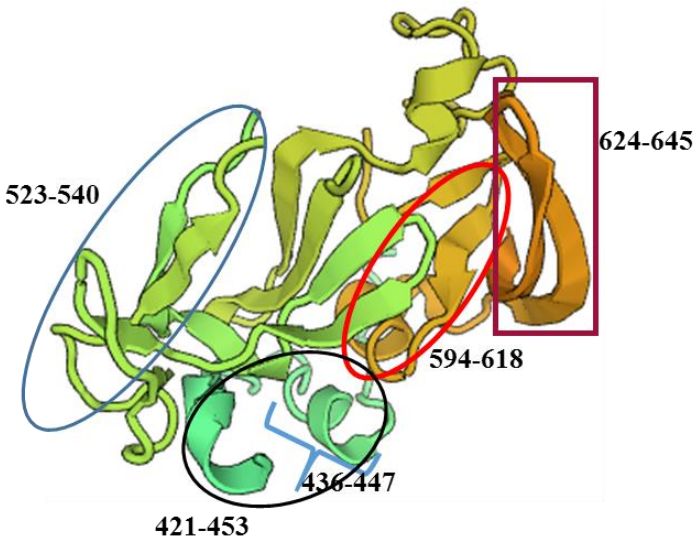

Figure 1.4: Major monoclonal antibody epitopes in the E1E2 glycoprotein

a. Schematic representation of monoclonal neutralising antibody epitopes in the E1E2 glycoprotein of hepatitis C virus **b.** three dimensional structure of E2c (412-645) modified from Kong *et al.* (2013) using SWISS MODEL (32). Different neutralising epitopes targeted by MAbs are highlighted in the 3D structure.

1.5 Epidemiology and geographical distribution

The liver is one of the most transplanted organs. There are a number of reasons for liver transplantation including the damage caused by viral hepatitis (reviewed in 176, 177). HCV is a causative agent of viral hepatitis and approximately 3% of the world's population is chronically infected with HCV (178). Globally, HCV has infected around 150-170 million people with 3-4 million new infections per year (179).

HCV is a blood borne virus, transmitted primarily through contaminated blood and blood products associated with intravenous drug use and sexual contact. Hepatitis C is found worldwide. Egypt (22%), Pakistan (4.8%) and China (3.2%) have the highest prevalence of chronic HCV infection (180). It has been observed that following initial infection, up to 80% people remain asymptomatic both in the acute and early chronic stages (reviewed in 177). Approximately 15-40% of infected individuals resolve the HCV infection and 50-80% people develop chronic hepatitis (reviewed in 176, 177). Persistent HCV infection can lead to inflammation, liver fibrosis, cirrhosis, hepatocellular carcinoma and end stage liver disease (180).

HCV exhibits a high degree of genetic diversity and differs by 30-35% within different genotypes at the nucleotide level (1). Based on the phylogenetic and sequence analyses of HCV genome, it is classified into seven genotypes (1-7) and further categorized into 67 confirmed and 20 provisional subtypes (1, 181, 182). At the nucleotide level each sub genotype differs by 15% (1). HCV genotype 1 is the most prevalent genotype with 83.4 million cases worldwide (46.2%, North America and Western Europe 75.8% and 59.0% respectively), to which East Asia constitutes 1/3 cases in total (1). Genotype 3 is the second most prevalent with 54.3 million cases (30.1%, North America 10.4% and Western Europe 24.8%), followed by genotypes 2 (North America 12.0% and

Western Europe 10.8%), 4 and 6 contributing 22.8% of all the cases while genotype 5 constitutes <1% (1) (Fig 1.1). HCV genotypes 1a, 1b, 2a, and 3a are widely distributed globally. Genotypes 1 and 2 are primarily observed in West Africa, 3 in South Asia, 4 in Central Africa and the Middle East, 5 in Southern Africa, and 6 in South East Asia (1, reviewed in 4) (Fig.1.1). There has been only one genotype 7 infection reported to date, which was isolated from a central African immigrant in Canada (182).

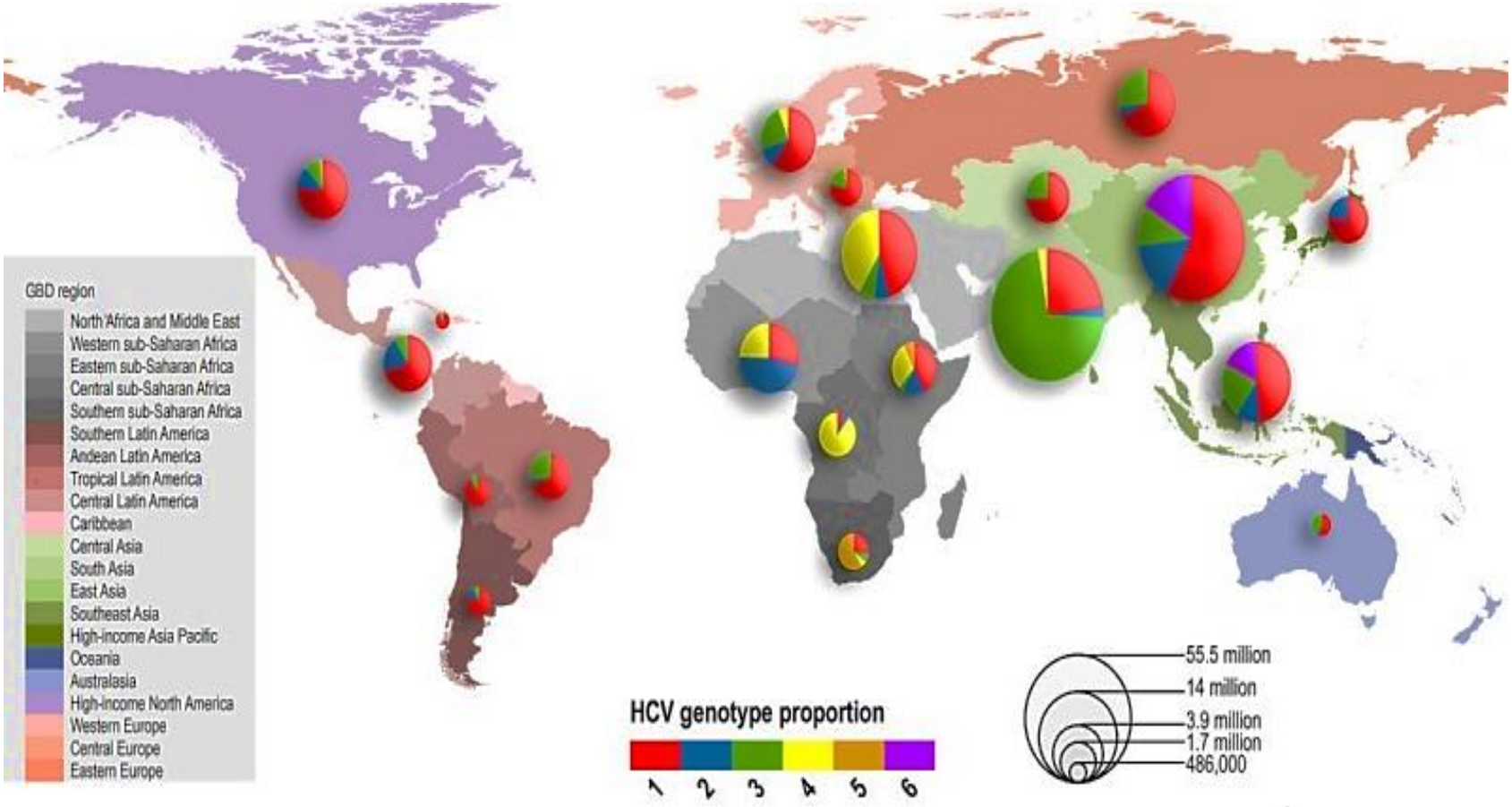

Figure 1.5: Global Prevalence of HCV

Relative distribution of HCV genotypes depending on global burden of disease region (GBD) as described by World Health Organisation. Coloured GBD regions correspond to the countries. Pie chart corresponds to the prevalence of particular genotype in that country. Adopted with

1.6 Diagnosis

HCV infection is determined by detecting the presence of anti-HCV antibodies and HCV RNA. The recombinant immunoblot assay (RIBA) and enzyme immunoassays (EIA) were historically used for the detection of HCV infection (183). Third generation assays which detect a broad spectrum anti-HCV antibodies that target a mixture of HCV epitopes from core, NS3, NS4 and NS5 are now routinely used (184).

Anti-HCV antibody based diagnosis is unreliable, as the seroconversion can occur after a long window period, of up to six months post infection (reviewed in 185). Hence, for early phase pre-window period diagnosis of HCV infection, techniques based on viral RNA detection are essential. Polymerase chain reaction (PCR) based techniques are used for viral RNA detection and Real time PCR offers greater sensitivity relative to standard PCR. Currently, the Real time PCR based automated platforms that are used for HCV diagnosis are sensitive and include a broader range of detection, detecting as low as 10-15 IU/ml (186).

1.7 Signs and Symptoms

Eighty percent of the infected individuals remain asymptomatic in acute HCV infection and are therefore undiagnosed (187). Elevated levels of liver enzymes-alanine aminotransferase and asparagine aminotransferase are the primary signs of acute phase HCV infection (185). Up to 40% of the infected individuals clear the HCV infection spontaneously, the rest develop chronic hepatitis (reviewed in 128, 129).

1.8 HCV treatment

Until 2011, the standard therapy to treat chronic HCV infection was pegylated interferon-α (PEG-IFN-α) and ribavirin (RBA) treatment (188). Success of the treatment is measured as a sustained virological response (SVR). A patient is said to achieve a SVR if they remain aviraemic 24 weeks following antiviral treatment. This method of treatment has worked well for those infected with genotype 2 and 3, 5 and 6 with 78%-82% demonstrating a SVR with an intermediate SVR for genotype 4 (188, 189). However, the SVR for genotype 1 is markedly lower ranging between 42%-46% (188). A genome wide association study of >1600 patients in a clinical treatment trial with Peg-IFN-α RBA identified a single nucleotide polymorphism on chromosome 19q13, rs12979860, which is associated with SVR (190, 191). This SNP is located near the IL28B gene (3 Kb upstream) which encodes type III interferon IFN-λ3. This gene is upregulated during the HCV infection. It was also observed that patients with the C/C genotype attained two fold higher SVR than patients with the C/T and T/T genotypes (192). However, this allele associated SVR is also dependant on the ethnicity of an infected individual (190, 192). Moreover, Peg-IFN-α RBA treatment can be associated with severe health side effects such as neuropsychiatric symptoms, anaemia, alopecia, pruritus, endocrine disorders, angina.

In 2011, telaprevir and boceprevir both targeting the HCV NS3-4A serine protease were approved as the first generation direct-acting antivirals (DAAs) to treat HCV genotype 1 infection. Both were used in combination with PegIFN-RBA. This was termed as a triple therapy regimen which achieved a SVR of 65-75% (193, 194). Nonetheless, these drugs also had serious hematological and gastrointestinal side effects and the costs per SVR in advanced liver disease patients were found to be high (193, 194). The American Association for the Study of Liver Disease (AASLD) and

the European Association for the Study of the Liver (EASL) no longer recommends telaprevir and boceprevir in HCV management (195).

Following recent developments in DAA research, the EU licensed three new antivirals as a part of combination therapies in 2014. These DAAs include i) simeprevir an NS3-4A protease inhibitor which controls the HCV infection by blocking NS3 dependant cleavage of the HCV polyprotein. This can further lead to inhibition of RNA replication by blocking the likely quantity of the NS5B replicase ii) daclatasvir, a pangenotypic NS5A inhibitor which inhibits formation of membranous web and thereby reducing the HCV RNA replicationand iii) sofosbuvir, a pangenotypic nucleotide analogue inhibitor of HCV RNA-dependent RNA polymerase which interferes with the formation of double stranded RNA (195). Each of these DAAs in combination with PegIFN-RBA yielded SVR of 60-100% and are better tolerated than boceprevir or telaprevir alone (196, 197).

The current focus in HCV management is to achieve viral clearance via an IFN-free treatment regimen. An IFN-free combination of sofosbuvir and simeprevir with or without RBA was tested in genotype 1 infected patients (COSMOS study) (195, 198) and 80 - 95% SVR rates were observed (199). Similarly, a combination of sofosbuvir with or without RBA resulted in 81-89% SVR rates for genotype 1 infection (200). Other DAAs have been approved by FDA recently, including the NS3 protease inhibitors Paritaprevir, the NS5A inhibitors Ledipasvir and Omitasvir; and the non-nucleos(t)ide inhibitor, Dasabuvir. DAAs daclatasvir, sofosbuvir, ledipasvir, simeprevir and dasabuvir (used with ombitasvir/paritaprevir/ritonavir) have been added to the WHO Essential Medicines List (WHO/HIV/2016.20).

Although these new DAAs achieve high SVR rates, resistance associated variants (RAVs) are a challenge. Most commonly detected RAVs with respect to the DAA and their class are listed in table 1 (201). The Q80K polymorphism, observed in HCV from 5%-48% of the patients infected with genotype 1, confers resistance to simeprevir reducing SVR to 58% (in combination with PegIFN-RBA) (reviewed in 202). A combination of simeprevir with sofosbuvir improves the performance of DAAs in such patients; however, this treatment regimen is limited to patients without cirrhosis. The S282T mutation is associated with sofosbuvir resistance. Additionally, L159F and V321A mutations are associated with sofosbuvir treatment resistance (reviewed in 202). DAAs have become very important in HCV management; however, it is clear that the occurrence of RAVs and treatment associated variants needs to be carefully monitored. Additionally, prohibitive costs realistically limit DAA access to discrete patient cohorts with cirrhosis and end stage liver disease (203).

A generic drug is a bioequivalent to the branded product with analogous dosage form, safety, strength, route of administration, quality and performance. Although the high costs of DAAs present a financial challenge, results of generic alternatives of these DAAs are promising. Data presented by Freeman *et al.* (2016) at The International Liver Congress™ organised by EASL in Barcelona, Spain, showed high SVR rates after treatment with generic ledipasvir/sofosbuvir (98%), and sofosbuvir/daclatasvir (96%) (204). In case of HCV, 12 week treatment with a branded drug sofosbuvir (Sovaldi©) by Gilead costs $84,000 (USD). This is in comparison to the generic alternative costing less than $1000 (205). An agreement on Trade Related Aspects of Intellectual Property Rights prepared by World Trade Organisation allows lesser developed countries to produce patented medications for their internal use (205). Recently, eleven Indian generic pharmaceutical manufacturers have signed an

agreement with Gilead to develop generic versions of sofosbuvir (Sovaldi©), ledipasvir/sofosbuvir (Harvoni©) and an investigational sofosbuvir/velpatasvir as a single tablet regimen to distribute in 101 developing countries. Bristol-Myers Squibb also has signed a royalty-free voluntary licensing agreement for daclatasvir with the Medicines Patent Pool for selling the drug to 115 low and middle-income countries. An approval from WHO Prequalification Programme or a stringent drug regulatory authority is still essential for the licensees to sell the generic drug.

Table 1.1: Most Frequent resistant associated variants (RAVs) connected with the DAAs

Sr No	Class of DAA	Name of DAA	RAV	Associated (sub)genotype	% occurrence
1	NS3/4A protease inhibitor	Simeprevir	NS3- Q80K	1a	37.6
			NS3-S122T	1b	5.5
2	NS5A inhibitor	Daclatasvir	NS5A-H58P	2a	50.8
			NS5A-Q30K	3a	29.2
		Ledipasvir	NS5A-Q30K	3a	29.2
		Omitasvir	NS5A-Q30R	4,6	55.3%,24.2%
3	NS5B nucleotide inhibitor	Sofosbuvir	NS5A-L31M,P58S, Y39H	1b	3.8-9.7
			NS5B-L159F	1b	3.8-9.7
4	NS5B non-nucleotide inhibitor	Dasabuvir	NS5B-S556G	1b	3.8-9.7

1.8.1 HCV immunoglobulin therapy

Potential HCV vaccine candidates are in clinical development since the discovery of HCV (reviewed in 129). There are two approaches to develop vaccine against HCV, one is prophylactic and the other is therapeutic vaccine for clinical use. The goal for a prophylactic vaccine is to induce nAbs to envelope glycoproteins E1E2 or to induce a broad T-cell response (Table 1.2). Additionally, the non-structural genes of HCV are also targets of therapeutic vaccine (Table 1.2) (206). The goal for a therapeutic vaccine is to strengthen the immune response of an infected individual by passive immunisation. Generation of memory B cells and CD8+ T cells require help from CD4+ cell. In order to develop a successful preventive and/or therapeutic vaccine, following aspects are required to be considered i) a vaccine should be effective against multiple circulating HCV quasispecies ii) should induce a vigorous, sustained, long lived CD4+ and CD8+ T cell response targeting multiple HCV regions. should generate memory CD8+ T cells that can activate effector CD8+ T cells when come in contact with viral peptide(reviewed in 207, 208). There are several challenges in developing vaccine for HCV i) high rate of replication and error prone polymerase ii) highly hypervariable genome and heterogeneity oh HCV iii) overcoming the mechanisms by which HCV evades cellular as well as humoral immune response iv) limited animal models to study the efficacy of HCV vaccine v) designing and execution of efficacy clinical trials as it becomes important to prevent the development of chronic HCV infection. Although DAAs function by ultimately inhibiting the completion of the viral life cycle, however, vaccination is the most effective long-term means of controlling this infectious disease. Currently, there is no prophylactic or therapeutic vaccine available to treat HCV (76).

Table 1.2: Prophylactic and therapeutic HCV vaccine candidates in preparation

Sr. No	Name	Vaccine Type	Vaccine candidate	Stage
1	C**hrion** (Novartis)	Prophylactic	Recombinant E1E2 (MF59C.1)	Phase I
2	Okarios		Adenoviral vector expressing HCV NS3-NS5B	Phase II
3	IC41 (Intercell AG)	Immunetherapeutic	HCV peptide cocktail with polyargenine	Phase II with PEG IFN
4	GI-5005 (Globe Immune)		Core-NS3 protein expressed by yeast cells	Phase II with PEG IFN RBV
5	Civacir© (Biotest)		Pooled polyclonal IgGs	Phase III
6	TG4040 (Transgene)		Modified vaccinia Ankara virus expressing NS3-NS5B HCV proteins	Phase I

Both neutralising and non-neutralising antibodies are produced in response to HCV infection. anti-HCV antibodies that target core, NS3, NS4 and NS5 which are used in serological tests are diagnostic antibodies and are non-neutralising in nature (184). A minority of infected individuals clear HCV infection spontaneously and this requires a rapid, rigorous and multi-specific antiviral response by the host immune system (reviewed in 66, 176, 177). Several experiments using HCV pseudopartcile (HCVpp) and HCV cell culture derived (HCVcc) systems have revealed that point mutations of immune dominant epitopes within viral E2 envelope protein aid humoral immune escape (reviewed in 209). HCVpp and HCVcc are used to measure the neutralisation efficacy of antibodies (reviewed in 209). HVR1 is one target of nAbs (30, 64-67). It has been observed that selection pressure from nAb response shapes the evolution of the viral envelope protein (210-213). Mutations within HVR1 are associated with humoral immune escape (Fig 1.3a). Over time, immune pressure drives replication of HCV variants to escape targeting by nAbs raised against dominant variants, even in

cohorts infected with same inoculum (60, 67). Recent findings by Kong *et al.* (2013) and Khan *et al.* (2014) have shown that the CD81 binding loop located in the E2 core region (residues 519-535, GenBank accession number: AF009606) and residues 421–453 of E2 are ideal candidates for vaccine design (Fig 1.3) (32, 42, 47). Numerous studies have shown that broadly neutralising antibodies (bNAbs) are elicited in the infection process (103, 214, 215). bNAbs are observed only in subset of patients and arise after lengthy period of infection . These bNAbs are effective against multiple strains of HCV while NAbs which are produced in almost all infected individuals are mostly strain specific (reviewed in 216).

As a prophylactic vaccine development strategy, Choo *et al.* (1994) immunised seven chimpanzees with recombinant E1E2 vaccine (derived from HCV 1a). Choo *et al.* (1994) observed development of protective immunity against homologous HCV 1a genotype. Moreover, upon re-immunisation of four chimpanzees followed by subsequent challenge with the heterologous HCV 1a showed that three chimpanzees resolved the infection (217). Meunier *et al.* (2011) used the serum from five of the chimpanzees from the Choo study (n=7) to neutralise HCVpp and HCVcc expressing envelope glycoproteins from genotypes 1-6. A cross neutralisation activity against genotypes 1a, 4a, 5a and 6a, with limited reactivity against 2a and 3a in HCVpp and HCVcc system was observed, showing potential for development of a recombinant vaccine (218). In 2010, Frey *et al.* published findings on immunogenicity and safety of E1E2/MF59C.1 vaccine. A prophylactic vaccine was developed by constitutive expression of recombinant E1E2 derived from HCV genotype 1a in a Chinese hamster ovarian cell line (219). Further Phase I randomized, double-blind, placebo-controlled dose-escalation study involving 60 healthy subjects who received three different doses of HCV E1E2/MF59C.1 vaccine was carried out (219). At the end of the study,

antibody response was confirmed by anti E1E2 ELISA, CD81 blocking and VSV/HCVpp neutralisation experiment. The vaccine successfully induced a strong T helper cell response. However, the neutralising antibody response to VSV/HCVpp was low and insignificant underlining low immunogenicity of the vaccine (219). Law *et al.* (2013) further used the antisera from the phase I clinical trial to assess the cross neutralisation activity in HCVcc expressing E1E2 glycoprotein from HCV genotype 1-7. A cross neutralisation activity in two of the three tested sera against the representative HCV genotypes was observed (220). Wong *et al.* (2014), recently mapped epitopes within E1E2 using antisera from goat and humans immunised with recombinant E1E2 vaccine. Wong and colleagues observed a strong competition between antisera from vaccinated humans (MF59C.1) with five well characterised MAb AP33 (CD81-Mouse MAb $E2_{412-423}$), AR3B (CD81), AR4A, AR5A, and IGH526. AR4 and AR5 require properly folded E1E2 and their binding is obstructed by mutations within 201–206 in E1 and regions 657–659 and 692 in E2 (221). IGH526 targets region 313-327 in E1. These results showed that the anti-HCV vaccine generated broadly cross- neutralising responses by targeting multiple epitopes in the E1E2 glycoprotein and shows promising results for clinical development of recombinant E1E2 HCV vaccine (221). However, studies by Frey *et al.* (2010) and Law *et al.* (2013) identified low titres of cross-neutralising antibody which hinders the vaccine efficacy (219, 220). Further research is warranted to enhance the immunogenicity of the vaccine either by using alum based adjuvants which enhance uptake of antigen by DC or immune potentiator type adjuvants that induce DC to produce cytokines.

New data suggests that MAb and polyclonal antibodies have the ability to provide protection against HCV infection as a mean of passive immunisation (reviewed in 61,

222). bNAbs, which target conserved regions of the E1E2 glycoprotein, have been shown to control HCV infection in cell culture and in animal models of HCV (158-160). Potent bNAbs are widely being considered as a potential therapy to treat viral infections (223-225). Chung and co-workers (2013) developed a fully humanised MAb-HCV1 which targets conserved epitope within 412-423 in the E2. A randomised, double-blind, placebo-controlled study in patients with HCV genotype 1a undergoing liver transplant (LT) was carried out (226). Chung *et al.* (2013) observed control of viraemia for 7-28 days post transplantation. A significant delayed time in viral rebound was observed in individuals treated with MAb-HCV1 was observed (226). Recently, Bukh *et al*. (2015) have demonstrated that polyclonal antibodies purified from chronic HCV patients can suppress the homologous virus in a chimpanzee for 18 weeks (227). Recently, Biotest Pharmaceutical has developed an investigational polyclonal antibody Civacir© to prevent recurrence of the hepatitis C virus after liver transplant surgery (Table 1.2). Recent results from randomized, open-label Phase III trial for Hepatitis C Immune Globulin (HCIG-Civacir©) have shown promising outcomes with liver transplant patients in the US (228). A study by Biotest showed that Civacir© dose-dependently neutralised HCVpp and HCVcc expressing different patient derived E1E2 glycoproteins which also included variants resistant to host antibodies and DAAs.

Similarly, IC-41 peptide based therapeutic vaccine which targets seven HCV T cell epitopes induced IFNγ producing CD4+ and CD8+ cells in healthy and difficult to treat subjects (reviewed in 229). TG4040 also induced T cell based immune response in 153 HCV 1a treatment naïve patients in Phase II study (230). GI-5005 also has been shown to induce antigen specific host CD4+, CD8+ immune response in clinical trial (231) (Table 1.2).

Targeting a single neutralising epitope may not be the ideal approach in HCV infection as sites near the nAb binding site may then mutate resulting in resistance to nAbs (160). Combining antigenic specificities of nAbs presents a new approach to treat viruses with a hypervaraible genome. A new study on H5N1 strain of influenza virus has shown promising use of a bispecific antibody as prophylactic and therapeutic agent (232). This bispecific molecule combines the neutralising capacity and specificities of two different neutralising monoclonal antibodies from human and murine sources. The hemagglutinin (HA) protein of the influenza virus harbours neutralising epitopes. However, the most exposed and accessible epitopes on the globular head of HA protein are highly variable. Zanin *et al.* (2015) have developed a bispecific Fc fusion protein, the Fc dual-affinity retargeting (FcDART) molecule. FcDART targets the conformational epitopes in antigenic sites located on the globular head of HA. FcDART provided 100% protection in mice against A/Vietnam/1203/04 challenge (232). Similarly, a combination of a cocktail of ZMab and MB003 (ZMapp-c13C6, c2G4, and c4G7) has been shown to provide 100% protection in nonhuman primates post 5 days of EBOV infection (225). The MAbs c2G4, and c4G7 bind to the membrane proximal part of the viral glycoprotein thereby neutralising viral infectivity. MAb c13C6 is a non-neutralising antibody, however, it binds to the tip of the glycoprotein and has been suggested to be involved in the complement fixing pathway (225).

Recently, Gautam *et al.* (2016) in their research have shown that a combination of four anti-HIV-1 neutralising monoclonal antibodies (VRC01, VRC01-LS, 3BNC117, and 10-1074) can confer protection in macaques against the repeated administration of a low-dose of clade B simian/human virus $(SIV/HIV)_{AD8}$ (233). Antibodies VRC01

(234)and 3BNC117 (235) target the gp120 CD4bs and antibody 10-1074 (236) is dependent on the presence of HIV-1 gp120 N332 glycan. Overall, the available data suggests that nAbs can be a potential tool of passive immunisation either singly or in combination.

1.9 Laboratory models to study HCV

After the discovery of HCV, various attempts were made to study the infection and replication of HCV in animal and cell culture models. Initially, due to a lack of suitable animal and cell culture models to study HCV, attempts to develop vaccine or the alternative therapies were met with difficulties. However, in recent years several new study models have emerged to study HCV.

1.9.1 In-Vivo models

The chimpanzee (*Pan troglodytes*), being closely genetically related to human and susceptible to HCV infection, has served as the only experimental model to study HCV to date. The chimpanzee model was used for early establishment of characteristics of HCV. Chimpanzees were used to establish HCV infectious clones and to study the immune response to HCV infection which is crucial in vaccine development (237-240). However, chimpanzees are an endangered species, and are costly to maintain. Furthermore being subject of ethical debates, other animals like *Tupaia belanger cinensis* (tree shrews, phylogenetically close to primates, tamarins and marmosets (new world monkeys), transgenic mice, immunodeficient mice or tolerised rats transplanted with human hepatocytes have been used to study HCV infection (241-244). Although xenograft models are the most advantageous of all small animal models, obtaining xenomic chimeras is still expensive and time consuming, limiting their use.

1.9.2 In-vitro models

In recent years different cell culture experimental systems have been established to study HCV. Although most of these models provide a limited outlook on isolated aspects of viral life cycle, replication and pathogenicity, they have been proven to be invaluable source of information.

1.9.2.1 Serum derived HCV

Several attempts were made to culture HCV derived from infected patients however, due to low infectivity and difficulty in detecting RNA replication, they have been unsuccessful. Primary cultured human hepatocytes, B-cell lines and T-cell lines were successfully infected with viraemic serum. However, RNA replication was very low and was only detectable by quantitative real-time polymerase chain reaction (qRT-PCR). Additionally, primary cells from humans or chimpanzees have been used to propagate HCV in cell culture. Iacovacci *et al.* (1993, 1997) infected primary foetal human hepatocytes with viraemic sera (54, 245). They detected a 20-fold increase in HCV positive strand RNA 5 days post infection. Rumin *et al.* (1999) infected primary human hepatocytes for 4 months with HCV and found a gradual increase in the RNA titre from $\sim 10^3$ to $\sim 6 \times 10^4$ genome equivalents per ml (246). However, results obtained from the sera were not reproducible partly because of the presence of HCV specific antibodies in sera and the fact that results were largely donor dependent.

1.9.2.2 HCV Replicon System

Lohmann *et al.* (1999) from Bartenschlager's lab created a sub genomic replicon based on genotype 1b that lacked structural genes (core, E1E2), p7 and NS2 with a selectable marker for neomycin phosphotransferase (neo) under the control of the HCV IRES, followed by a second IRES from encephalomyocarditis virus that controlled

expression of NS3-NS5B (Fig 1.6) (247). Synthetic RNA obtained from this construct in the human hepatoma cell line Huh-7 and G418 selection produced high amounts of self-replicating HCV RNA (1,000–5,000 positive-strand RNA molecules per cell). However, it has been observed that these replicons acquire 'replication enhancing mutations' (REM) in order to replicate more efficiently in transduced Huh7 cell lines. REMs were mainly located in the N-terminus of NS3, at two distinct amino acids in NS4B and in the central domain of NS5A in 1b replicons (248-251). In the case of the genotype 1a replicon, REMs were identified in NS3, NS4B, or NS5A (248, 252-254). These mutations are not observed *in vivo* so it is unclear how they influence viral replication. Genotype 6a and 2a replicons also have been made (249, 255).

1.9.2.3 Retroviral pseudoparticles

Retroviral pseudoparticle system emerged as the most successful experimental model to study the role of HCV glycoproteins in virus entry (Fig 1.6). The pseudotyped viral particles express full length HCV E1E2 glycoprotein. The system involves co-transfection of human embryonic kidney cells (HEK293T) with a packaging vector encoding gag-pol proteins of either murine leukemia virus (MLV) or human immunodeficiency virus (HIV), an expression vector encoding HCV E1E2 and a retroviral genome encoding a reporter gene (green fluorescent protein/luciferase) (33, 256). Upon viral protein translation, retroviral particles encapsidate replication-defective reporter gene sequences which helps in detection of productive infection and are released into the media after acquiring the HCV envelope glycoprotein. HCVpp are then used to study the role of E1E2 glycoprotein in viral entry, various neutralisation assays involving antiE2 specific monoclonal antibodies or infected patient sera (33, 66, 256-258). HCVpp have also been widely used to study entry events and host cell receptors involved in the infection. For example, HCVpp were

used to identify and verify role of CD81, SCARB1, CLDN, OCLN, glycosaminoglycans, LDLR, dendritic cell-specific intercellular adhesion molecule-3-grabbing non-integrin in viral entry (reviewed in 102).

However, generating reliable infectious pseudoparticles from highly divergent populations of HCV is quite challenging (90, 92, 210). Urbanowicz *et al.* (2015) cloned E1E2 glycoproteins from patients at different stages of HCV infection and found 118 out of 493 clones to be infectious, each harbouring an open reading frame for E1E2 (258). Urbanowicz *et al.* (2015) also noticed a marked difference in the infectivity pattern of closely related clones in HCVpp system. Recently, Urbanowicz *et al.* (2016) observed a number of factors to be responsible for the infectivity of HCVpp. These include differences in the amounts of plasmid used, the species of packaging construct utilised (an appropriate retrovirus backbone) and a balance of delivery of plasmids encoding the packaging vector versus those encoding glycoproteins (172). HCVpp are produced in a non-liver cell line where they assemble in post-golgi compartments and/or the plasma membrane like retroviruses and hence do not represent the close association of HCV particles with lipoproteins as observed naturally.

Nonetheless, HCVpp can be produced in large quantities and they provide flexibility in terms of incorporation of marker genes and allow investigation of viral entry independently of replication. HCVpp system has been proved to be indispensable in antibody screening in immunoglobulin based therapy and characterisation of several host factors and fusion mechanism involved in entry.

1.9.2.4 Cell cultured HCV

In 2001, Kato *et al.* constructed a subgenomic replicon from a genotype 2a HCV strain, termed JFH-1, from a patient with fulminant hepatitis (Fig 1.6). The replicon was reported to be highly replicative without acquiring REMs (249, 259) and was hailed a major breakthrough in HCV research. With this replicon, it was possible to study viral entry, replication, genome packaging, virion assembly, maturation and release of viral particles. Viral particles generated using this system closely resemble the HCV viral particles, being 50–65 diameter (nm) (93, 260). Due to the ability of the replicon to interact with lipoproteins, it was now possible to study the role of lipoproteins in the entry of HCV (93, 260, 261). HCVcc-infected chimpanzees develop symptoms similar to those infected with human derived HCV (93, 260, 261).

Similar to the HCVpp, cell culture derived HCV has been used in neutralisation assays. HCVcc is also neutralised by CD81 specific antibodies, confirming the CD81 dependent entry of viral particle. Currently, many chimeric genomes are constructed by combining the JFH1 isolate with heterologous strains of the major HCV genotypes. In these chimeric replicons, core-NS2 regions are derived from another genotype retaining the replicase proteins necessary for generating the membrane-bound replicase complex and nontranslated regions of the JFH1 isolate. An infectious, fully replicating HCVcc system for genotype 1a (H77-S) was developed by Yi *et al.* (2006) which was infectious for chimpanzees. However, H77-S was less infectious in comparison with JFH1 *in vitro* (262).

However, one limitation of the cell-culture derived HCVcc is that the NS5B gene of JFH-1 appears to be a major determinant for efficient RNA replication (263, 264). Furthermore, chimeric JFH1 replicons grow in low titres and are of limited use in drug

discovery. Moreover, HCVcc have a higher density than plasma-derived particles (~1.15 g/ml), and mostly lack ApoB (reviewed in 265). In Huh7 cells, ApoB-containing VLDL precursors do not fuse to ApoE-containing precursors and hence their biochemical characteristics differ from the LPVs isolated from infected individuals (reviewed in 265).

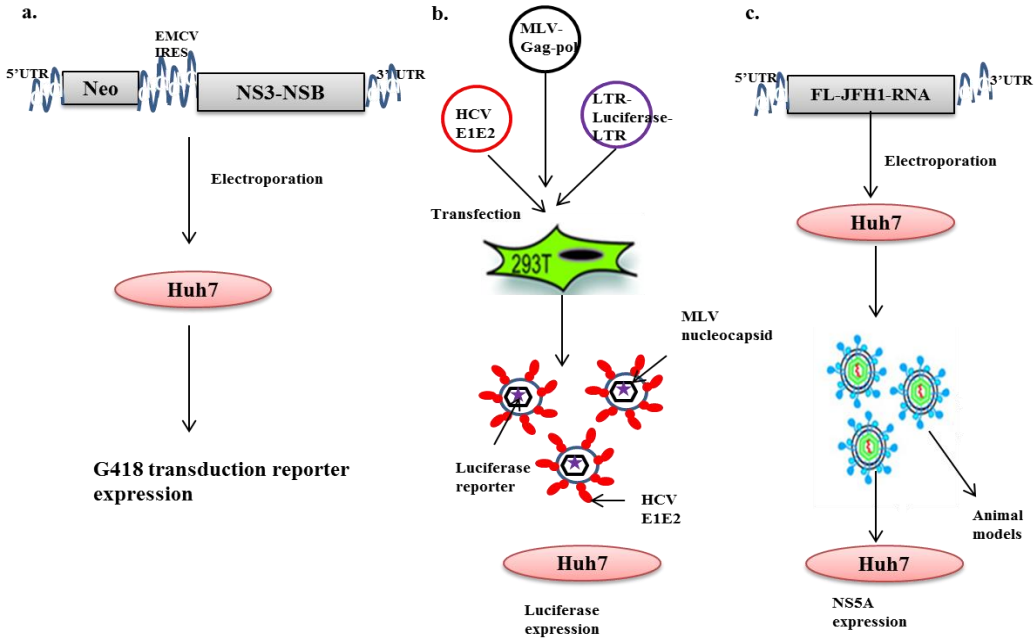

Figure 1.6: Systems for the study of HCV replication, entry, and infectivity

a. Huh7 cells are electrophoresed with bicistronic replicon RNAs, encoding the HCV replicase proteins (NS3-NS5B) under control of a heterologous IRES from EMCV and a selectable marker (Neo^r) under control of the HCV IRES. This system helps to monitor replication events of HCV **b.** HCVpp are produced by co-transfection of HEK-293T cells with gag-pol of either murine leukemia virus (MLV) or human immunodeficiency virus (HIV), an expression vector encoding HCV E1E2 and a retroviral genome encoding a reporter gene (green fluorescent protein/luciferase). HCVpp provides a method to investigate entry events mediated by envelope protein in the HCV life cycle **c.** Human hepatocytes are electrophoresed with either JFH-1 HCV genomic RNA or chimeras of this genome with heterologous sequences to yield HCVcc. The HCVcc can be used to infect naïve cells or animal models. Productive infection is measured either by expression of reporter genes or expression of NS5A, or by direct measure of viral RNA.

1.10 Thesis research outline

HCV establishes a chronic infection and limits the host's capacity to develop protective immunity by evading the adaptive immune system (237). In an infected individual, HCV circulates as a population of closely related, yet heterogeneous, sequences: the quasispecies. The quasispecies nature of HCV allows for immune evasion by mutations in the epitopes which are the targets of nAbs and persistence may therefore require continuous virus sequence change to evade B-cell based immunity (266).

In HCV infected individuals, either HCV will be targeted by antibody assisted immune clearance or it will evade the humoral immune system. Moreau *et al.* (2008) hypothesised that if an infected individual has generated an immune response against HCV, then an immune complex of antibody-virus may circulate in the blood and HCV virions can be separated into IgG depleted and IgG enriched virus subpopulations (Fig 1.7). To test this hypothesis Moreau *et al.* (2008) used Qproteome Albumin/ IgG depletion columns that use immobilised MAb which have high affinity towards human serum albumin and human IgG. A serum sample from treatment naive patient who was infected chronically with HCV genotype 4a was fractionated using Qproteome Albumin/ IgG depletion column (267). Clonal analysis at the HVR1 from IgG enriched fraction showed a homogenous population when compared with the IgG depleted and unfractionated serum (267). Results from Moreau study showed that homogenous sequence isolated from IgG enriched fraction was strongly recognised by humoral immune system. Analysis of both these fractions at the genomic level revealed that the IgG fraction can be diverse, whereas IgG enriched fraction is of limited heterogeneity even clonotypic in nature (212, 267, 268).

Similarly, longitudinal analysis of chronic hepatitis C viral infection has shown that the virus has several adaptive strategies that maintain persistence and infectivity over time. Analysis of the IgG enriched viral population from infected individuals present an opportunity to improve our understanding of humoral immune escape and viral envelope protein evolution.

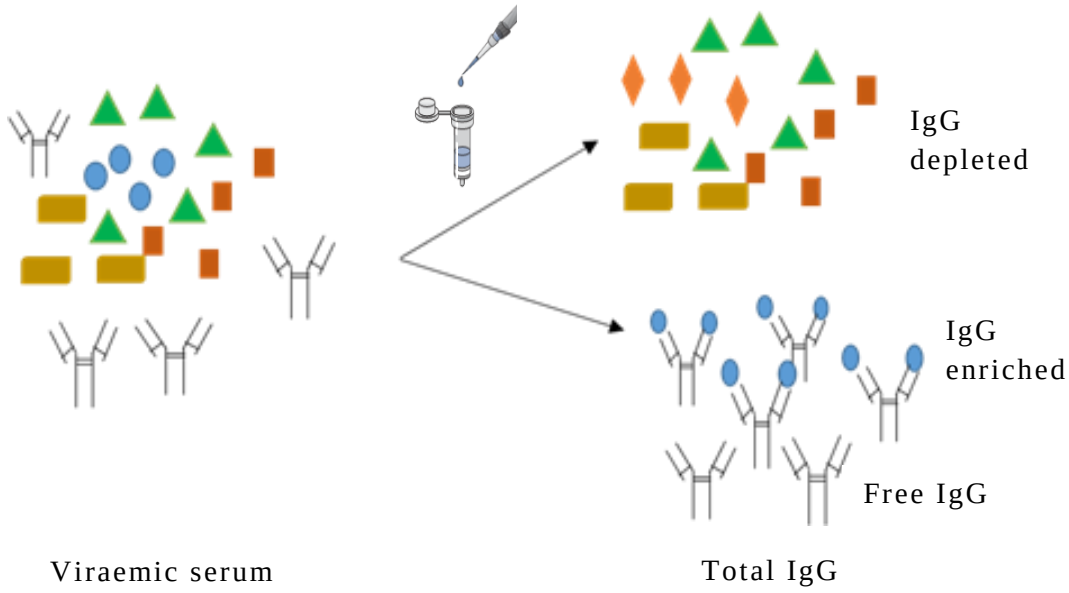

Figure 1.7: Column based pull down of IgG enriched viral population from viraemic serum

schematic representation of column based separation of unbound IgG depleted fraction and IgG enriched fraction using Qproteome Albumin/ IgG depletion columns (267) **.** Different coloured shapes represent quasispecies nature of HCV.

It therefore becomes crucial to study humoral immune escape mechanism of HCV in context with mutating epitopes against which nAbs are produced.

1) Based on previous research in Molecular Virology and Diagnostic Research Lab, Department of Medicine, University College Cork, in this project it was hypothesised that humoral immune system targets homogenous viral population from quasispecies population.In order to prove this hypothesis, we used protein G Ab Spin Trap Column (GE healthcare) to segregate antibody associated virus (AAV) and antibody free virus (AFV) from sera obtained from chronically HCV infected patients. Total IgG and virus free Fab (VF-Fab) were used to challenge the genotype/subtype matched sera where AAV was not detected and/or below the detectable level.

2) E1E2 glycoprotein sequences isolated from clonotypic AAV fractions were hypothesised to be infectious in the HCVpp system. To test this hypothesis, sequences obtained from AAV population were amplified, cloned and expressed in pcDNA3.1 directional cloning vector. Furthermore, pseudoparticles were generated from these E1E2 clones to study their infectivity *in vitro* in Huh7 cells.

3) Based on the available research data, it was hypothesised that E1E2 glycoprotein sequence from AAV fraction harbours neutralising epitopes. This was achieved by conducting linear and conformational epitope mapping analysis using virus free Fab (VF-Fab) fragments obtained from viraemic sera positive for the presence of AAV. In order to demonstrate that VF-Fab from AAV positive sera are neutralising in nature, HCVpp neutralisation assays were carried out.

4) Previous investigation of serum samples from a treatment naïve chronically infected HCV 4a patient over 10 years has shown emergence, dominance and disappearance of distinct lineage in presence of humoral immune response. It was

observed that sequences targeted by humoral immune system had a single amino acid substitution. It was hypothesised that, a single amino acid substitution can lead to immune escape. To prove this, a proof of concept immune escape mutant in HCV 4a genotype was studied by designing peptides comprising amino acid substitution within the HVR1 region

Chapter 2

2.1 Materials

All reagents were stored and prepared according to the manufacturer's guidelines.

2.1.1 Reagents

AB buffer kit -GZ28903059 (GE healthcare)

Ab Spin Trap Column 11703329 (GE healthcare)

Agarose A9414 (Sigma Aldrich)

Anti-Human IgG (H+L), HRP conjugate W4031 (Promega)

Bovine Serum Albumin A9418 (Sigma Aldrich)

BCA Protein Assay Reagents A and B 23223 and 23224 (Thermo Scientific, IL, USA)

Calcium phosphate transfection reagent IK278001 (Invitrogen)

Cell Freezing Media C6164 (Sigma Aldrich)

Clone JET PCR cloning Kit K1231 (Thermo Scientific)

Dulbecco's Modified Eagle Medium D5796 (Sigma Aldrich)

Dulbecco′s Phosphate Buffered Saline (DPBS) D8537 (Sigma Aldrich)

100mM dNTP set 10966-030 (Biosciences)

EcoRI R0101S (New England Bioscences)

Expand High Fidelity PCR system 11732641001 (Roche)

Fetal Bovine Serum (FBS) F9665 (Sigma Aldrich)

GeneJET PCR Purification Kit K0702 (Thermo Scientific)

GloLysis buffer E2661 (Promega)

GloBright E2620 (Promega)

HEPES buffered saline 51558 (Sigma Aldrich)

HindIII R0104S (New England BioLabs)

HisGrab metal chelate plates 15143 (Thermo Scientific)

6x-His Epitope tag antibody (His-H8) MA1-21315 (Thermo Scientific)

HRP labelled mouse anti-Human IgG Fab antibody orb216300 (biorbyt)

Immobilon Western Chemiluminiscent HRP substrate WBLUF0500 (Merck Millipore, MA, USA)

Lectin from *Galanthus nivialis* (Sigma Aldrich)

Luria-Bertani broth L3022 (Sigma Aldrich)

Luria-Bertani Agar(Lennox) L2897 (Sigma Aldrich)

Natural human IgG Fab fragment ab90352 (Abcam)

NcoI R0193S (New England BioLabs)

One Shot Top 10 Chemically Competent E.Coli C404006 (Invitrogen)

One Step RT-PCR- HCV (Primer Design)

pcDNA 3.1 Directional Cloning kit K490001 (Invitrogen)

Pfu DNA Polymerase EP0501 (Thermo Scientific)

Phosphate Buffered Saline D8662 (Sigma Aldrich)

Protease inhibitor cocktail I 539131 (Merck Millipore)

PureYield Plasmid Maxiprep System A2393 (Promega)

QIAamp RNA mini kit 52904 (Qiagen)

Random Hexamer Primers FQ-SO142 (Thermo Scientific)

RNaseOUT™ Recombinant Ribonuclease Inhibitor 10777-019 (Invitrogen)

RNeasy Plus Mini Kit 74134 (Qiagen)

Sigma Stop solution (Sigma Aldrich)

SuperScript® II Reverse Transcriptase 18064022 (Invitrogen)

SURE2 SuperComp Cells 200152 (Agilent Tech)

TMB substrate 34021 (Thermo Scientific)

TransIT-X2 Dynamic Delivery System MIR6003 (Mirus)

Trypsin EDTA (Sigma Aldrich)

Uracil DNA glycosylase M0280S (New England BioLabs)

Xho1 R0146S (New England BioLabs)

2.1.2 Plasmids

MLV-Gag-Pol packaging vector, phCMV-ΔC/E1/E2 H77 constructs were acquired from Dr. Francois Louis-Cosset, INSERM, France through material transfer agreement. . MLV-Luciferase reporter vector was a kind gift from Dr. Arvind Patel, CVR, University of Glasgow, UK.

2.1.3 Antibodies

Mouse monoclonal antibody AP33 and ALP98 were a kind gift from Dr. Arvind H. Patel, CVR, University of Glasgow, UK.

2.1.4 HCV serum samples:

This study was approved by Clinical Research Ethics Committee of the Cork Teaching Hospital and written consent from patients was obtained (by Elizabeth Kenny-Walsh and Orla Crosbie). Initial characterization of patient sera was done using Versant HCV Genotype Assay (LiPA), HCV Amplification 2.0 kit according to the manufacturer's instruction. Serum samples were stored at -80^{o}C at the Molecular Virology Diagnostic & research Laboratory, Cork University Hospital. Details of serum samples used in this study are given in Table 2.1

Table 2.1: Serum samples

Patient Identifier	#Sample Identifier	Date of Collection	Other information
P1a-1	1a-1-1	30/04/2007	
P1a-1	1a-1-2	01/08/2013	N/A
P1a-1	1a-1-3	02/01/2014	
P1a-2	1a-2-1	09/12/2013	N/A
P1a-2	1a-3-1	12/12/2013	N/A
P1b-1	1b-1-1	23/12/2002	
P1b-1	1b-1-2	17/12/2013	anti D
P1b-1	1b-1-3	18/03/2014	
P1b-2	1b-2-1	10/12/2013	anti D

P1b-3	1b-3-1	09/12/2013	Co-HIV
P1b-4	1b-4-1	20/05/2014	anti D
P1b-5	1b-5-1	24/06/2014	BT
P1b-6	1b-6-1	24/06/2014	anti D
P1b-7	1b-7-1	23/09/2014	anti D
P1b-8	1b-8-1	07/10/2014	anti D
P1b-9	1b-9-1	07/10/2014	anti D
P1b-10	1b-10-1	14/10/2014	anti D
P3a-1	3a-1-1	10/12/2013	N/A
P3a-2	3a-2-1	07/05/2014	N/A
P3a-3	3a-3-1	20/03/2014	N/A
P4a-1	4a-1-10-T10	17/11/2011	N/A
P4a-1	4a-1-11-T11	15/11/2012	N/A
P4a-1	4a-1-12- T12	13/06/2013	N/A
P4a-1	4a-1-13 –T13	21/11/2013	N/A
P4a-1	4a-1-14- T14	08/05/2014	N/A
P4a-1	4a-1-15- T15	01/12/2014	N/A

[#] Sample identifier: Genotype/Subtype-patient identifier, N/A: Not applicable

2.2 Methods

2.2.1 Fractionation of viraemic sera

2.2.1.1 Validation of Ab spin trap column

The Ab Spin Trap™ columns were used to separate the samples into (i) antibody associated virus (AAV) and (ii) antibody free virus (AFV) populations following the manufacturer's protocol with a few modifications (GE healthcare Life Sciences). The protein G columns are used to purify Total IgG from serum or plasma. Natural infection with Hepatitis B Virus (HBV) leads to humoral immune response against Hepatitis B surface antigen (HBsAg) which, in most cases, confers protective immunity (269). A positive and negative antibody HBV serum sample was prepared for validation studies and assay performance. HBV serum and anti-HBs (antibodies against Hepatitis B surface antigen) were diluted 1:100. HBV serum was incubated for 2 h at 37^{o}C with proteinase K (5 mg/ml) with end-over-end mixing followed by overnight incubation at room temperature (RT) to digest the antigenic epitopes on HBV (HBV Negative). The volume of serum sample used in the validation experiment was 100 µl. HBV positive and proteinase K treated HBV negative serum samples were mixed with equal amounts of anti-HBs. These samples were incubated for 2 h at 37^{o}C. Patient serum was applied to the column followed by incubation for 15 minutes at RT with end-over-end mixing. The first flow-through (W0) was retained as the AFV fraction. Eight washes (W1-W8) of 300 µl of binding buffer were applied to the column while the last wash (W8) tested by PCR amplicon analysis to confirm the absence of virions (2.2.2.2). The column was then incubated for five minutes with 200 µl of elution buffer with end-over-end mixing. The elute was collected in 30 µl of neutralisation buffer. The elute is now identified as Total IgG. Total IgG contains

AAV (virus targeted by antibodies), along with free antibodies (IgGs) bound by the column.

2.2.1.2 Separation of antibody associated virus (AAV) and antibody free virus (AFV) fractions

Initial characterisation of patient sera was carried out using the Versant HCV Genotype Assay (LiPA), HCV Amplification 2.0 kit according to the manufacturer's instruction. Serum samples were stored at -80^{o}C at the Molecular Virology Diagnostic & Research Laboratory, Department of Medicine, Cork University Hospital, University College Cork. Details of serum samples used in this study are given in Table 2.1. 200 µl of each sample was applied to the Ab Spin trap column™. The separation protocol was followed as described in section 2.1.1

2.2.1. Dissociation of antibody-virion complexes and collection of VF-Fab, λ-VF-Fab and κ-VF-Fab

Proteinase K was used to dissociate the antibodies from antibody-virion complex (AAV). This was achieved by adding 1:1 volume of proteinase K (5 mg/ml) to AAV positive sera. The Ab Spin Trap™ protocol was followed post proteinase K treatment. Virus free status of this proteinase K treated antibody preparation was determined by the absence of an E1E2 specific amplicon (318 base pair) following RT-PCR as described under section 2.2.2. We analysed the functional component in post proteinase K treated samples using HiTrap LambdaFabSelect™ and KappaSelect™ pre-packed columns (GE healthcare Life Sciences). These columns have a ligand which binds to the constant region of lambda or the kappa light chain of human IgG respectively. Briefly, 1 ml of proteinase K treated serum samples were passed through both the columns as per the manufacturer's protocol. Columns were washed to remove

unbound material with 5 volumes of binding buffer (Phosphate Buffered Saline, pH 7.4). Fab fragments were eluted with 0.5 ml of elution buffer (0.1 M glycine buffer, pH 2.5 for KappaSelect™, 0.1 M acetate buffer, pH 3.5 for LambdaFabSelect™). The eluted fractions were concentrated by Amicon Ultra-0.5 centrifugal unit with Ultracel 50 (Millipore). Confirmation of the virus free status of this proteinase K treated preparation was determined by the absence of an E1E2 specific amplification following RT-PCR (section 2.2.2). Furthermore, elutes obtained post proteinase K treatment from Ab Spin Trap™ (VF-Fab), LambdaFabSelect™ (λ-VF-Fab) and KappaSelect™ (κ-VF-Fab) were analysed by western blotting. Elutes, natural human IgG Fab fragment protein (ab90352, Abcam) and control IgG obtained from human plasma CTM (-) C (Roche Molecular systems), were blotted on a nitrocellulose membrane. The samples were then incubated with HRP labelled mouse anti-Human IgG Fab antibody (biorbyt) at 1:10,000 concentration in 0.05% PBST.

2.2.1.4 Antibody- Sera (non-detectable AAV) pull down assay

Total IgG which contains AAV (hereafter referred as 1^{o}AAV) along with free antibodies, VF-Fab, λ-VF-Fab and κ-VF-Fab were used to challenge the AAV negative sera in 1:5 ratios. This mixture was then incubated at 37^{o}C for 2 h. AP33 is a mouse MAb which targets the partially confirmation dependent epitope within amino acid residues 412-423 (a kind gift from Dr. Arvind Patel, University of Glasgow, UK). Simultaneously, we challenged the sera with both intact AP33 and Ab Spin Trap™ eluted post proteinase K treated AP33 (25 µg/ml). The Ab Spin Trap™ protocol was followed (section 2.1.1) and the challenged samples were tested for the presence of a newly formed 2^{o}AAV by PCR (section 2.2, 2.3).

2.2.2 Molecular Techniques

2.2.2.1 Nucleic acid isolation and cDNA synthesis

2.2.2.1a RNA isolation from serum

RNA was isolated from unfractionated serum, AAV and AFV fraction using QIAamp Viral RNA mini kit (Qiagen, Manchester, UK) using a combination of silica membrane and the speed of microspin based purification protocol. The kit uses highly denaturing conditions to inactivate RNases for isolation of intact viral RNA. These conditions are provided by buffer AVL carrier RNA which enhances the binding of viral nucleic acid to the QIAamp Mini membrane and reduces the chance of RNA degradation. 140 µl AAV, AFV and unfractionated serum samples were lysed using 560 µl of AVL containing 5.6 µl of carrier RNA (1 µg/ µl) for 10 minutes at room temperature after vortexing for 15 seconds. The lysed sample was then added with an equal volume (560 µl) of pure ethanol (96-100 %) and mixed by pulse-vortexing for 15 seconds. The solution(s) were immediately processed using QIAamp mini columns according to manufacturer's protocol. The column was centrifuged at 8000 rpm for one minute. The collection tube was discarded and columns were placed in a fresh collection tube. The column was then washed with 500 µl of buffer AW1 at 8000 rpm for 1 minute followed by a wash with buffer AW2 at 14000 rpm for three minutes. QIAamp mini column was placed into a fresh collection tube and was centrifuged at 14000 rpm for one minute to prevent buffer carryover and residual contaminants. The column was then placed into a fresh 1.5ml centrifuge tube and was equilibrated at room temperature with 60 µl of buffer AVE for one minute and RNA was eluted by centrifugation at 8000 rpm for one minute.

2.2.2.1b cDNA synthesis

cDNA synthesis from isolated RNA was carried out using previously optimised RT-PCR protocol (270). Briefly, 11 µl of RNA was mixed with one µl of random hexamer primer (Thermo Scientific) and was incubated at 75^{o}C for 10 minutes. Eight µl of reaction mixture was then added to each sample. Components of the reaction mixture are enlisted in table 2.2. Samples were then incubated in a thermo cycler for 60 minutes at 42^{o}C followed by heat inactivation of reverse transcriptase at 95^{o}C for three minutes.

Table 2.2: Reverse Transcriptase PCR reaction components

Reaction component	**Volume (µl)**
5X First Strand Buffer	4.0
0.1 M DTT	2.0
10mM dNTP	1.0
RNase OUT	0.25
SuperScript II Reverse Transcriptase	0.25
Nuclease free H_2O	Up to 20 µl

2.2.2.2 Amplification of the E1E2 region encompassing HVR1 and full length E1/E2 gene

Primers for PCR (Table 2.3) were designed with the aid of online primer designing tool Integrated DNA Technologies online OligoAnalyzer http://eu.idtdna.com/analyzer/Applications/OligoAnalyzer/. Primers were synthesised by Eurofins Genomics (Ebersberg, Germany). Amplification of the E1E2 region encompassing HVR1 in the E2 glycoprotein of HCV was amplified as previously described (270). All the PCR reactions were carried out using proofreading Pfu DNA

polymerase (2.5 U/µl) (Thermo Scientific) to ensure the accurate amplification of template due to quasispecies nature of HCV. The resulting PCR fragment is of 318 base pairs (bp) in size which corresponds to 1296-1614 of HCV genotype 1a (AF011751) (271). To amplify full length E1E2 glycoprotein, nested PCR approach was used (reaction conditions as outlined in Fig 2.1a). The outer primers are placed in the flanking regions in the HCV core (Core Fwd, upstream nucleotide 280-304) and NS2 (Rev Specific 2, downstream nucleotide 3394-3416) coding sequence. The inner primers are located such that encoded ORF following amplification encompassing amino acids 170-746 (with respect to the polyprotein of strain H77c; GenBank accession number AF011751). The primers artificially introduce a start codon at the 5' end of the proposed signal peptide of E1, and a stop codon following the last amino acid of the mature E2 protein (underlined in Table 2.3, Fig 2.1b-c). This permits expression of the genes in mammalian cell culture, and incorporation of their products into retroviral pseudoparticles. The inner sense primers also include the sequence CACC at the 5' end (in bold Table 2.3) to facilitate directional cloning into the TOPO family of cloning vectors (Invitrogen). We used Expand High Fidelity PCR system for amplification of the full length E1E2. The components of the reaction mixture are outlined in Table 2.4.

Table 2.3: Oligonucleotide Primers

Primer Name	**Tm**	Primer Sequence
Outer forward(I,II)	47.3	5'-ATGGCATGGGATATGAT-3'
Outer reverse(I)	53.7	5'-AAGGCCGTCCTGTTGA-3'
Inner forward (I)	49.9	5'-GCATGGGATATGATGATGAA-3'
Inner reverse (I,II)	52.4	5'-GTCCTGTTGATGTGCCA-3'
Core FWD	60.5	5'-CTTGTGGTACTGCCTGATAGGGTG-3'
REV Spec-2	59	5'- GGTTCTTGTCCCGGCCTGTGAGG -3'
HCV Mod Tarr Fwd	66.7	5'-**CACC**ATGGGTTGCTCYTTYTCTATCTTCC-3'
HCV 1a-pcDNA Rev	63.6	5'-TTAYGCCTCCRCYTGGGATATGAG-3'
HCV 1b-pcDNA Rev	66.3	5'-TTARGCCTCRGYCTGRGCTAYCAR C-3'
HCV 3a-pcDNA Rev	61.4	5'-TTATATCATBAGCATCARCCARARRGC-3'

Table 2.4: Reaction components used in E1E2 amplification

Reaction component	**Volume (µl)**
Expand High Fidelity Buffer (10×) with 15 mM $MgCl_2$	5.0
10 mM dNTP	1.0
10 pm/µl Forward Primer	1.5
10 pm/µl Reverse Primer	1.5
Expand High Fidelity Enzyme mix	0.5
cDNA/ Primary PCR product	5.0
Nuclease free H_2O	Up to 50 µl

5 µl of the first-round product is then used as a template in a second round PCR amplification using the genotype-specific inner sense and antisense primers. Amplification parameters for the 1st and 2nd round of PCR are outlined below (Fig 2.1a-c). Correct PCR amplification results in an amplification product of between 1,734 and 1,752 bp.

Figure 2.1a: Amplification parameters for 1st round of PCR with primers Core Fwd and Reverse Specific 2

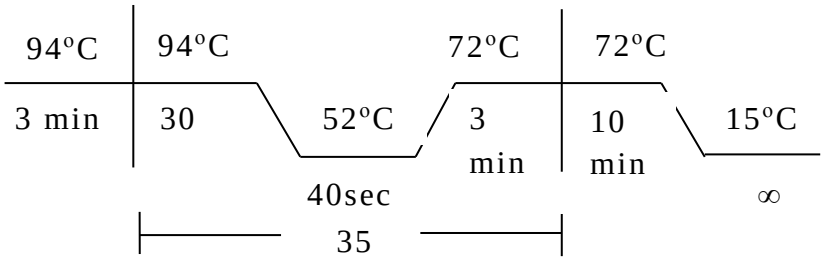

Figure 2.1b: Amplification parameters for 2nd round of PCR for HCV genotype 1a and 1b with primer HCV Mod Tarr Fwd and HCV 1a-pcDNA Rev or HCV 1b-pcDNA Rev

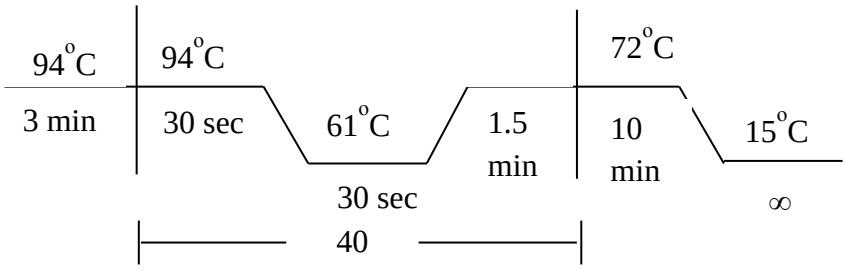

Figure 2.1c: Amplification parameters for 2nd round of PCR for HCV genotype 3a with primer HCV Mod Tarr Fwd and HCV 3a-pcDNA Rev

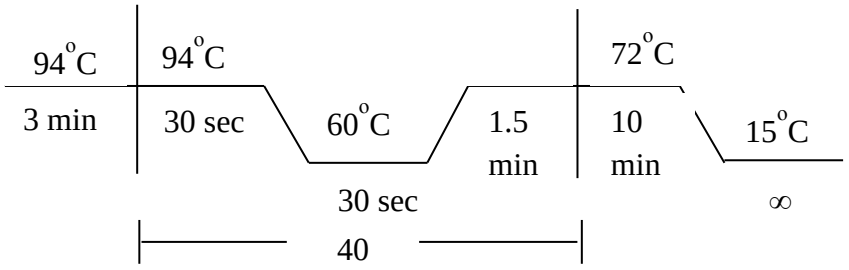

2.2.2.3 Site Directed mutagenesis

QuickChange Lightening Site Directed mutagenesis kit (Agilent Tech) was used to perform site directed mutagenesis (SDM). Primers for SDM were designed using Agilent's web based tool http://www.genomics.agilent.com/primerDesignProgram.jsp?_requestid=707517 . Primers used for SDM are enlisted in the Table 2.5. Reactions were carried out as per the manufacturer's instruction.

Table 2.5: Oligonucleotide Primers for site directed mutagenesis

Primer Name	**Tm**	Primer Sequence
a655g I-V P4 F	74.1	5'-GGAGACCCATACG**G**TAGGGGGGAGCGC-3'
a655g I-V P4 R	74.1	5'-GCGCTCCCCCCTA**C**CGTATGGGTCTCC-3'
t677c V-A P4 F	75	5'-CGCGAGCCGTGC**C**GCCCACCGCG-3'
t677c V-A P4 R	75	5'-CGCGGTGGGC**G**GCACGGCTCGCG -3'
a367g T-A P4 F	67.9	5'-TCTCTCAGCTGTTC**G**CCTTCTCGCCTCGC-3'
a367g T-A P4 R	67.9	5'- GCGAGGCGAGAAGG**C**GAACAGCTGAGAGA-3'

Bold letters indicate nucleotide site for mutation

2.2.2.4 Agarose gel electrophoresis

PCR products were analysed by eletrophoresis alongside either GeneRuler^{TM} 50bp DNA ladder (50-1000 bp) or GeneRuler^{TM} 1kb DNA ladder (250-10,000 bp) (Thermo Scientific) depending upon the expected size of PCR product. 1% agarose gel was prepared by boiling agarose in 1× tris-acetate ethylene diamine tetra acetic acid (TAE) buffer. TAE was prepared with 40mM Trizma base, 20mM glacial acetic acid and 1mM ethylene diamine tetra acetic acid (EDTA). SYBR Safe DNA Gel Stain (Thermo Fisher Scientific) was added prior to casting the gel (5 µl / 100 ml). Ten µl of PCR products were added to 2 µl of 6× loading buffer (Thermo Fisher Scientific). Samples were resolved at 90V for 40-50 minutes. Subsequently DNA was visualised using UV trans-illuminator (UVP). The result of each amplification was then recorded photographically.

2.2.2.5 Purification of PCR products

PCR products of verified size were purified using GeneJET PCR Purification Kit (Thermo Scientific) according to manufacturers' protocol. One volume of the binding buffer, which contains a chaotropic agent that denatures proteins and facilitates binding of DNA to the silica membrane of column, was mixed with one volume of PCR product. In case of the PCR product less than 500 bp, 100 µl of isopropanol was added to 100 µL of product combined with 100 µl of binding buffer. The mixture was then applied to the GeneJET purification column and was then centrifuged for 30 seconds at 10,000 rpm. Flow through was discarded. To remove unincorporated nucleotides, primers, enzyme and salts, 700 µl of wash buffer was applied to the GeneJET purification column and was centrifuged for 30 seconds at 10,000 rpm. To remove all the traces of wash buffer, the column was further spun for one minute at

14,000 rpm. DNA was then eluted with 30 µl of the elution buffer and the quantified by spectrophotometry and stored at -20ºC.

2.2.2.6 Cloning of PCR purified products and transformation

2.2.2.6a Cloning of 318 bp product in Clone JET PCR cloning Kit

We ligated 318 bp PCR purified product generated by using Pfu polymerase in the pJET1.2/blunt cloning vector (Thermo Scientific). The 5' ends of the vector contain phosphoryl groups, therefore, phosphorylation of the PCR primers is not required. This kit makes use of blunt cloning strategy. pJET1.2 harbours a lethal gene which is disrupted by ligation of a DNA insert into the cloning site. This results in the growth of only cells with the recombinant plasmids which eliminates the need for blue/white screening. The optimal insert: vector ratio is 3:1. Vector pJET1.2/blunt is provided at a concentration of 0.05 pmol DNA ends/µl. The optimal amount of the PCR product for ligation (0.15 pmol of DNA ends) was calculated using www.thermoscientific.com/reviewer. The ligation reaction was set on the ice. Reaction components involved in ligation mix are mentioned in table 2.6.

Table 2.6: Regents used for ligation into pJET1.2/blunt vector

Reaction component	**Volume (µl)**
2X Reaction Buffer	10.0
purified PCR product/other blunt-end DNA fragment	0.15 pmol ends
pJET1.2/blunt Cloning Vector (50 ng/µl)	1 (0.05 pmol ends)
T4DNA ligase	1.0
Nuclease free H_2O	Up to 20 µl

Ligation mix was incubated at room temperature (22°C) for five minutes. Ligation mix was then used for transformation.

2.2.2.6b Transformation of pJET1.2 in One Shot Top 10 chemically competent E.Coli

Transformation was performed on 50 µl aliquots of One Shot Top 10 chemically competent *E.Coli* by adding 20 µl of ligation. It was then incubated on the ice for 30 minutes followed by heat shock treatment at 42^{o}C for 30 seconds following brief incubation on the ice. 250 µl of SOC media provided with the kit was added and culture was incubated at 37^{o}C with shaking at 225 rpm for one hour without antibiotics. To select bacteria with the plasmid having 318 bp insert, culture was seeded on Luria-Bertani (LB) Agar (Lennox, Sigma Aldrich) plates with ampicillin (50 µg/ ml). After overnight incubation at 37^{o}C, fifteen colonies from the plate were picked for further screening.

2.2.2.6c Cloning of full length E1E2 glycoprotein into pcDNA3.1D/V5-His-TOPO vector (Invitrogen)

Purified HCV E1E2 product which were amplified using Expand High Fidelity enzyme system and with a directional cloning signal- CACC at the 5' end of forward primer (Mod Tarr Fwd) were ligated into a pcDNA3.1D/V5-His-TOPO vector (Invitrogen). The linearised vector has a single 3' thymidine overhang and is covalently bound to topoisomerase I of *Vaccinia* virus. The TOPO cloning technique eliminates the need for post PCR procedures. The optimal ratio of insert: vector is between 0.5:1–2:1. However, we observed insert: vector ratio varies with the genotype of HCV. Cloning was performed according to the manufacturer's instructions with the modification of half reaction volumes. The reaction components required for the ligation are outlined in table 2.7. After 30 minutes of incubation at room temperature, 6 µl of ligation mix were added to SURE2 SuperComp Cells (Agilent Tech).

Table 2.7: Reagents used for ligation into pcDNA3.1D/V5-His-TOPO vector

Reaction component	**Volume (µl)**
Purified PCR product	0.5-4
Salt Solution	1
TOPO® vector	1
Nuclease free H_2O	Up to 6 µl

2.2.2.6d Transformation of pcDNA3.1D/V5-His-TOPO vector in SURE2 SuperComp cells

Transformation procedure for the SURE 2 Supercompetent cells was followed according to the manufacturer's protocols. Cells were thawed on ice and 100 µl was aliquoted to a pre-chilled 14 ml BD Falcon polypropylene round-bottom tube with 2 µl β-mercaptoethanol. The tubes were incubated on ice for 10 minutes with intermittent swirling. 6 µl of ligation reaction was added to cells and tubes were incubated on ice for 30 minutes. Cells were then heat-pulsed at 42°C in a water bath for 30 seconds followed by incubation on ice for two minutes. 900 µl pre-heated (42°C) NZY+ broth with filter sterilized 1 M $MgCl_2$ and 20% (w/v) glucose (or 10 ml of 2 M glucose) (Lab M, Lancashire, UK) was added and tubes were incubated at 37°C for 1 h with shaking at 225 rpm. Cells were then centrifuged for 30 seconds at 10,000 rpm. The cell pellet was then suspended in 50 µl of NZY+ broth and this transformation mixture was plated on LB Agar plates with ampicillin (50 µg/ ml) and incubated overnight at 37°C.

2.2.2.7 Restriction digestion

Restriction enzymes used in this study were purchased from New England Biolabs (Hertfordshire, UK). Recognition sequences and incubation temperatures of used restriction enzymes are listed in Table 2.8.

Table 2.8: Restriction enzymes
^ denotes point of cleavage

Restriction Enzyme	Target Sequence(5'-3')	Incubation temperature
HindIII	A^AGCTT	37°C
Nco I	C^CATGG	37°C
XhoI	C^TCGAG	37°C

Following restriction enzymes and buffer were used to confirm the ligation of 318 bp product.

Table 2.8.1: Reaction components used in restriction digestion of 318 bp product

Reaction component	Volume (µl)
Cutsmart buffer	2.0
NcoI	0.5
XhoI	0.5
Plasmid DNA	5.0
Nuclease free H_2O	Up to 20

Restriction enzymes used for double digestion of full length E1E2 cloned into pcDNA3.1D/V5-His-TOPO vector are enlisted in table 2.8.2

Table 2.8.2: Reaction components used in restriction digestion of 318 bp product

Reaction component	Volume (µl)
Buffer 2.1	2.0
Hind III	0.5
Xho I	0.5
Plasmid	5.0
Nuclease free H_2O	Up to 20

Digested products were analysed on 1% agarose gel as described in section 2.2.2.4 with appropriate DNA marker.

2.2.2.8 Miniprep

Bacterial colonies from LB agar were inoculated in 5 ml of LB broth with ampicillin (50 µg/ ml). The cultures were grown overnight at 37°C on incubator shaker at 225 rpm. Bacterial cells were harvested by centrifugation at 6000 rpm for 15 minutes at 4ºC. The cell pellet was then suspended in 250 µl of ice cold resuspension solution (containing RNase A) and was transferred to 1.5 ml tube. The bacterial cells were then subjected to SDS/alkaline lysis by adding 250 µl of lysis solution and mixed by inverting for 4-5 times until the solution becomes clear. The mix was then neutralised by adding 350 µl of neutralisation solution and tubes were mixed thoroughly by inverting. Cell debris and chromosomal DNA was pelleted by centrifuging the tubes at 10,000 rpm for five minutes. Supernatant was then applied on to the GeneJET spin column and column was then centrifuged for one minute at 10,000 rpm. Further it was washed with 500 µl of wash solution twice for one minute at 10,000 rpm. An additional one minute spin was given to remove the residual wash solution. Plasmid DNA was eluted in 50 µl of elution buffer after equilibrating at room temperature for

two minutes. Plasmid concentration was determined using spectrophotometer and following formula. Absorbance ratio at 260nm/280nm >1.7 indicated good quality of plasmid. Plasmid DNA was stored at -20^{o}C.

µg/ml= absorbance at 260nm x dilution factor x constant (50)

2.2.2.9 Maxiprep

A single colony was picked from a freshly streaked selective plate and inoculated in a starter culture of 5 ml LB ampicillin (50 µg/ ml) upon confirming the full length E1E2 plasmids by restriction digestion and sequencing. Culture was incubated for 8 h at 37°C with shaking at 225 rpm. This starter culture was used to inoculate 200 ml LB ampicillin (50 µg/ml) in order to obtain sufficient volumes of HCV E1E2 containing plasmids for mammalian cell transfections. High-quality plasmid was isolated using The Pure Yield^{TM} Plasmid Maxiprep System (Promega). The bacterial pellet was resuspended in a 12 ml of cell resuspension solution containing RNaseA and was mixed by pipetting and vortexing. Cells were lysed by addition of 12 ml alkaline lysis cell lysis solution. It was then mixed by inverting gently for 4-5 times followed by incubation at RT for five minutes. Cell debris were precipitated by addition of 12 ml neutralisation solution. Lysate was centrifuged at 6000 rpm for 30 minutes at 4^{o}C to pellet the cell debris. A column stack was assembled by placing a blue PureYield™ Clearing Column on the top of a white PureYield™ Maxi Binding Column. The assembly was placed onto the vacuum manifold. Supernatant obtained after centrifugation was poured in to the clearing column and vacuum was applied. PureYield™ Clearing Column was discarded. 5 ml of Endotoxin Removal Wash was given to the PureYield™ Maxi Binding Column on vacuum manifold. Contaminants were removed by adding 20 ml of column wash solution. The membrane on binding column was allowed to dry. Column was equilibrated with one ml nuclease free water

at room temperature for two minutes. Plasmid DNA was then eluted in a new 50 ml disposable plastic centrifuge tube by centrifuging the binding column in swinging bucket rotor at room temperature, 2,000 × g for two minutes.

2.2.2.10 Sequencing

Purified PCR products and plasmids were sent for sequencing to Eurofins genomics (http://www.eurofinsgenomics.eu/), Germany. 318 bp and full length E1E2 sequences were aligned with reference sequences using BioEdit v5.2. All the trace files were manually validated and curated using the electrophoregram wherever necessary.

2.2.3 HCVpp based work

2.2.3.1 Cell lines

Two different mammalian cell lines were used for the phenotypic analysis of HCV E1E2 glycoprotein: Human Embryonic Kidney (HEK) cells 293T and Human hepatoma (Huh) 7 cells (272). Genomic profile of Huh7 was established by analysing clinically relevant seven human SNPs which were previously published (271). HEK293T cells and Huh7 cells were cultured in DMEM (Sigma) with 10% Foetal Bovine Serum (FBS), 1% of Pen/Strep (10,000 units penicillin and 10 mg streptomycin per ml in 0.9 % NaCl) and 1% of non-essential amino acids (Gibco). Both the cells lines were grown in T-75 ml flasks at 37ºC and 5% CO2. Cells were passaged when they have reached confluency of 80-90%. After washing with the PBS, cells were trypsinised for 5-10 minutes. Trypsin was neutralised by addition of DMEM with FBS and cells were seeded in the fresh media. Cell stocks were stored in 1 ml of cell freezing media (Sigma) in liquid nitrogen. Cell lines were regularly tested for mycoplasma contamination by using PlasmoTest^{TM} Mycoplasma Detection Kit (Invivogen) according to the manufacturer's instruction.

2.2.3.2 Expression of E1E2 glycoprotein in HEK293T cells

HEK293T cells were seeded in 6 well plate at 2.5 $X10^5$ cell density prior transfection. Cells were then transfected with the pcDNA3.1D/V5-His-TOPO vector containing E1E2 sequence at 70% confluency using TransIT-X2^{TM} Dynamic Delivery System (Mirus).TransIT-X2 is a non-liposomal system which comprises a novel class of polymers that helps in efficient nucleic acid complex formation, uptake and endosomal release. The optimal concentration of DNA: TransIT-X2 worked out to be 2 µg of DNA: 6 µl of transfection reagent. Each well was transfected with different pcDNA 3.1 clones in 250 µl serum free DMEM and was incubated at room temperature for 30 minutes. The TransIT-X2 and plasmid DNA complexes were added to each well and were supplemented with 2.5 ml DMEM. Cells were incubated for 48 hours at 37^{o}C in 5% CO2. Cells were then lysed and analysed for expression of E1E2 glycoprotein by western blotting.

2.2.3.3 Analysis of expressed E1E2 glycoproteins

The transfected HEK cells were lysed in 500 µl lysis buffer 2 (LB2; 20 mM Tris-HCl, pH 7.4; 20 mM iodoacetamide; 1mM EDTA; 150mM NaCl; 1% Igepal C630, protease inhibitor was added just before lysis) for 30 minutes on ice. Clarified supernatant was collected by centrifuging the lysate at 13,000 rpm for five minutes (the clarified lysate may be stored at -20^{o}C).

2.2.3.4 Sodium Dodecyl Sulphate-Polyacrylamide gel electrophoresis (SDS-PAGE) and western Blotting

15 µl volume of transfected cell lysates were mixed with 5 µl of 1X Bolt® LDS(Lithium dodecyl sulphate) sample buffer and 5 µl of 1X Bolt ® sample reducing buffer and were denatured at 95^{o}C for five minutes. Denatured lysates were then separated

on a gradient of 4-12% Bis-Tris Plus gel in the mini gel tank system (Thermo Scientific) along with a biotinylated protein molecular weight marker (Sigma). SDS-PAGE was then electrophoresed for 20 minutes at 200V. Resolved proteins were then transferred onto nitrocellulose membrane using iBolt® 2 transfer stacks and iBolt® gel transfer dry electro-blotting system (Thermo Scientific) at 20V for seven minutes. 100 µg of total protein was transferred on the nitrocellulose membrane was visualised by staining with Ponceau. The membrane was destained with 0.05% PBST until the pink stain was removed. The membrane was blocked for 1 h with a 5% milk solution in Phosphate Buffered Saline-0.05% Tween-20 followed 3× washes with 5 ml of PBST. The membrane was then incubated with the mouse monoclonal antibody (MAb) AP33 and ALP98 at a concentration of 1 µg/ml in 5 ml of blocking buffer for 1 h at room temperature followed by 3× washes with 5 ml of PBST. A mixture of primary antibodies was used to enhance the expression signal. Membrane was then incubated with the secondary antibodies, goat anti-mouse IgG, conjugated to horseradish peroxidase and anti-biotin antibody at a dilution of 1:10000 in blocking buffer at room temperature for 1 h. Finally, the membrane was washed 3× 10 minutes with PBST. Proteins were developed by adding the 1ml of Luminata forte western HRP substrate solution for five minutes on the membrane. Images were visualised in LAS-3000 and recorded at 16 bit.

2.2.3.5 Generation of HCV pseudotyped particles

HCV pseudoparicle (HCVpp) is a retrovirus-based system developed by Bartosch *et al.* (2003) (33). It involves co-transfecting HEK293T cells with plasmids expressing the HCV glycoproteins, the murine leukaemia virus (MLV) Gag-Pol, and the MLV transfer vector carrying the green luciferase reporter gene. MLV gag-pol particles encapsidate the replication-defective genome carrying the luciferase sequence and

acquire the HCV glycoprotein-containing envelope before being released into the medium when expressed in HEK293T cells (Fig 2.2).

Day 1

HEK cells were seeded at the 1.5×10^6 cells density in 100cm diameter tissue culture plate in ~15ml DMEM with 10% FBS, 1% Pen-Strep and 1% non-essential amino acids.

Day 2

At 16 h cells should be about 40% confluent. HEK cells were then transfected using calcium phosphate transfection kit (Invitrogen) (do not change the medium before adding precipitate). The reagents required for transfection are enlisted in table 2.9. All the reagents must be kept ice cold. To prepare no envelope control pseudoparticles, pcDNA 3.1 plasmid was replaced with tissue culture grade water.

For one 100cm diameter plate, following components were added in a 1.5 ml tube in the order listed in table 2.9. The components were then mixed by pipetting. 500 µl of 2XHBS was aliquoted into 50 ml tube. The components from 1.5 ml tubes were added dropwise to the tube containing 2XHBS while bubbling it continuously. The mixture in 50 ml tube should turn cloudy. It was then vortexed briefly and allowed to precipitate for 20 minutes at room temperature. This one ml precipitate was then distributed over the HEK culture dish. The contents were mixed gently and incubated overnight at 37ºC in 5% CO2.

Table 2.9: Reagents required for transfection of HEK293T cells

T/C dish:	**100mm**	**60mm**	**35mm**
Area:	48cm^2	21cm^2	8.5cm^2
HEK cells:	1×10^6	4×10^5	2×10^5
p-luciferase	8 µg	3 µg	1.5 µg
pMLV-gag-pol	8 µg	3 µg	1.5 µg
pcDNA3.1-E1E2	3 µg	1.2 µg	0.5 µg
H_2O up to	400 µl	160 µl	80 µl
2 M $CaCl_2$	100 µl	40 µl	20 µl
2X Hepes Buffered Saline(HBS)	500 µl	200 µl	100 µl
Total	1000 µl	400 µl	200 µl

Day 3

Medium from the HEK plate was changed with the 6 ml of fresh medium containing 10mM HEPES buffer and plate was incubated overnight at 37ºC in 5% CO2.

Day 4

Pseudoparticles were harvested 24 h after the media change. Supernatant from the HEK culture dish was passed through 0.45µm filter. The culture dish was again replenished with the fresh 6 ml medium and incubated overnight. The first harvest of HCVpp was stored at 4ºC.

Day 5

The second harvest of pseudoparticles was collected as described on day 4. Both 1st and 2nd harvests were used to infect Huh 7 cells. Remaining HCVpp were stored in aliquots at -70ºC however, this can result in loss in infectivity.

HEK cells which have expressed E1E2 glycoprotein and no envelope glycoproteins were lysed in 5 ml of lysis buffer on ice for 30 minutes. Lysis buffer consists of 40 mM Tris pH 7.5, 1mM EDTA, 150 mM NaCl, 1% Igepal CA-630. These components can be stored at 4^{o}C as 10X stock. 20 mM iodoacetamide (3.7 mg/ml) and protease inhibitor cocktail (PICT, Millipore) must be added to 1x buffer directly before use. Lysate of cells was centrifuged at 5000 rpm for 15 minutes and clear supernatant was stored at -20^{o}C for protein expression analysis.

Figure 2.2: Schematic diagram of HCV pseudoparticle generation

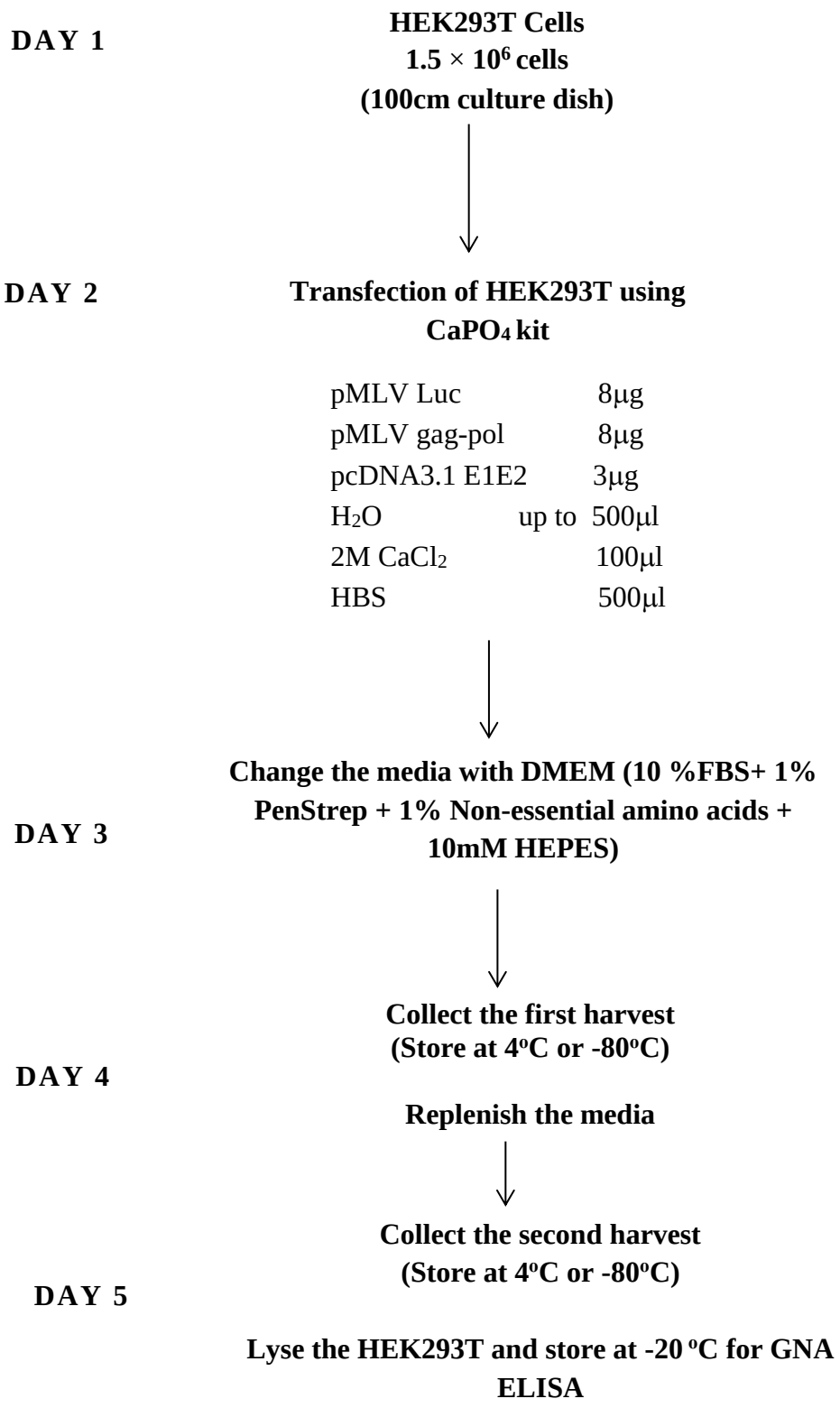

2.2.3.6 Infectivity assay

Huh 7 cells were seeded one day prior to HCVpp infection. Cells were infected with HCVpp inoculum as per table 2.10. The plate was incubated at 37ºC for 3 to 4 h, then the inoculum was removed and cells were re-fed with 150 µl of fresh DMEM. After 72 h of incubation, media was discarded. Cells were lysed in 50 µl lysis buffer at room temperature for 15 minutes. The lysate was then transferred to a white plate and luciferase assay was performed according to manufacturer's protocol using 50 µl firefly luciferase substrate BrightGlo (Promega). Relative light unit emission was read using a luminometer (Promega GloMax system)

Table 2.10: Infection table

Huh7 target cells were seeded one day prior to infection as below:

TC dish:	**6-well**	**12-well**	**24-well**	**48-well**	**96-well**
Area:	$8.5cm^2$	$3.8cm^2$	$2.0cm^2$	$0.8cm^2$	$0.25cm^2$
Huh7 cells:	$1x10^5$	$4.5x10^4$	$2.5x10^4$	$1.0x10^4$	$4.0x10^3$
HCVpp inoculum:	600 µl	300 µl	150 µl	90 µl	50 µl

2.2.3.7 VF-Fab-mediated neutralisation of HCVpp infection

To test the neutralising capability of VF-Fab directed against HCV glycoproteins, HCVpp were pre-incubated with VF-Fabs at 37ºC for 1 h. For unambiguous results, VF-Fabs were serially diluted from the highest concentration of 0.400 mg/ml to 0.05 mg/ml. After 1 h incubation HCVpp-VF-Fab inoculum was added to the Huh7 cells (Section 2.2.3.6).

2.2.3.8 GNA capture ELISA

5 gm of *Galanthus Nivalis* Agglutinin (GNA-Sigma) was dissolved in the 50 ml Phosphate Buffered Saline (PBS). It was then diluted as 1:50 PBS. 96-well high binding, F, ELISA plates (Sarstedt) were coated with 0.25 µg/well GNA in 100 µl PBS. Plates were incubated overnight at 4ºC. Excess GNA was washed from the wells 3 times with 250 µl of PBS-Tween 20 (0.05%) (PBST). The plate was then blocked with 2% skimmed milk powder in PBST, 200 µl/well for 2 h at room temperature. Blocking solution was discarded and traces were removed by washing the plate 3 × with PBST (at this stage the plate can be stored at -20ºC).

Total protein content from the HEK lysates was estimated using the BCA Protein Assay (Thermo -Scientific). 100 µg of the E1E2 expressed HEK lysates were added to plate and were incubated for 2 h at RT (or 4ºC overnight). The plate was washed three times by dipping into 1L beaker of PBST. The test VF-Fabs were added at the concentration of 50 µg in 100 µl of PBST. Mouse monoclonal antibody AP33 was used at the concentration of 1:10,000. Plate was incubated for 1 h at RT followed by washing three times with PBST. 100 µl of 1:10,000 anti-mouse horse radish peroxidase (HRP) conjugate in PBST was added to the well containing AP33. For human VF-Fab, 100 µl of 1:5000 anti-human (H+L) HRP conjugate (Promega) was added. Plate was incubated for 1 h at RT Plate was then washed 6 times with PBST. 100 µl of TMB substrate was added to each well and incubated at RT for 30 minutes. The plate was inspected intermittently to check the development of colour and the reaction was stopped by the addition of 100 µl /well of 0.5 M H_2SO_4. Absorbance was recorded at 450nm and 560nm in GLOMAX®-MULTI, Promega.

2.2.4 Colorimetric ELISA assay

To confirm the escape phenotype hypothesis, three N-terminally 6xHis tagged, 27 amino acid HVR1 peptides were synthesised, i.e

P1: H-HHHHHHETHITGAVASSNAQK**F**TSLFTFGPQQN-OH,

P2: H-HHHHHHETHITGAVASSNAQK**L**TSLFTFGPQQN-OH

P3:H-HHHHHHETHITGAVASS**H**AQK**F**TSLFTFGPQQN-OH

(Pepscan Presto, Netherlands). Peptides were reconstituted in 100% DMSO at a concentration of 1 mg/ml and stored at −20°C. 100 ng/µl of peptide was used in an ELISA based method. These peptides were incubated with VF-Fab at 1:10 dilution for 1 h followed by incubation with anti-human IgG (H&L) HRP conjugate secondary antibody (Promega, W4031) at 1:5000 dilution for 1 h. Plate was incubated for 1 h at RT. Plate was then washed 3X with PBST. 100 µl of TMB substrate was added to each well and incubated at RT for 30 minutes. The plate was inspected intermittently to check the development of colour and the reaction was stopped by the addition of 100 µl/well of 0.5M H_2SO_4. Absorbance was recorded at 450nm and 560nm in GloMax system.

2.2.5 Epitope Mapping

2.2.5.1 Epitope mapping of amino acid region 364-430

Linear peptides were synthesized for 1^{o}AAV and 2^{o}AAV covering amino acid region 364-430 in the E1E2 glycoprotein to study the epitopes targeted by host immune system.

Two sets (hence, set 1 and set 2) of overlapping peptides of 15 amino acid lengths with an overlap of 14 were synthesized for these sequences (Table 2.11). Set 2 comprised linear peptides of 15 amino acid length however, amino acids at position 10 and 11 were replaced by Ala. When a native Ala would occur on either position, it was

replaced by Gly. Control peptides unrelated to our test sequences which are propriety of Pepscan were designed based on epitopes of monoclonal antibodies 57.9 and 3C9 (273). The binding of VF-Fab to peptides was assessed in a Pepscan-based ELISA as described below (Pepscan Presto, Lelystad) (274). Each well in the card contained covalently linked peptides that were incubated overnight at 4^{o}C with VF-Fab between 0.1 to 10% pepscan buffer and preconditioning blocking buffer (SQ) (a mixture of horse serum, Tween 80 and ovalbumin in PBS). After washing, the plates were incubated with goat anti-human HRP conjugate (1:1000, Southern Biotech 2010-05) for 1 h at 25^{o}C. After further washing, peroxidase activity was assessed using substrate (2, 2'-azino-di-3-ethyl-benzthiazolinesulfonate and 20 µl/ml of 3% H_2O_2. The colour development was quantified after 60 minutes using a charge-coupled device camera and an image-processing system.

SET 1

Mimic Type : Linear peptides

Label : LIN

Description : Linear peptides of length 15 derived from the regions 364-430 with the one residue offset.

SET 2

Mimic Type : Linear peptides

Label : LIN.AA

Description: Peptides of set 1, but with residues on positions 10 and 11 replaced by Ala. Native Ala on either position was replaced by Gly. This set contains limited amounts of peptides.

Table 2.11: list peptides used for linear epitope mapping (First 10)

SET 1	SET 2
MVGNWAKVLIVMLLF	MVGNWAKVLAAMLLF
VGNWAKVLIVMLLFA	VGNWAKVLIAALLFA
GNWAKVLIVMLLFAG	GNWAKVLIVAALFAG
NWAKVLIVMLLFAGV	NWAKVLIVMAAFAGV
WAKVLIVMLLFAGVD	WAKVLIVMLAAAGVD
AKVLIVMLLFAGVDG	AKVLIVMLLAGGVDG
KVLIVMLLFAGVDGR	KVLIVMLLFGAVDGR
VLIVMLLFAGVDGRG	VLIVMLLFAAADGRG
LIVMLLFAGVDGRGT	LIVMLLFAGAAGRGT
IVMLLFAGVDGRGTY	IVMLLFAGVAARGTY

Refer to one letter amino acid code

2.2.5.2 Conformational epitope mapping of E2 glycoprotein (residues 384-619)

A library of peptides that covers residues 384-619 in E2 glycoprotein of HCV was synthesised using chemically linked peptides on scaffolds (CLIPS) technology (275) (Pepscan Presto; Lelystad, Netherlands). HCVpp1b-1-3 being highly neutralisation sensitive was chosen as a reference sequence for peptide synthesis. Four different peptide libraries were generated for the peptide microarray at Pepscan Presto, Lelystad as following: (1) Linear peptides of 15 mer were derived from the target sequence with an offset of one residue; (2) Loop mimics of constrained peptides of length 17 were constructed. Positions 2-16 were occupied by 15 mer sequences derived from the target sequence of HCV-E1E2 glycoprotein. To introduce structural constraints Cys were inserted on positions 1 and 17, which then were constrained by mP2 CLIPS; (3) Structured peptides of length 23 derived from the target sequence with an offset of one

residue were synthesised to mimic the helical structure. Cys residues on positions 1 and 5 were joined by mP2 CLIPS; and (4) Structured peptides of length 22 were constructed to mimic β-turn. 20-mer sequences on positions 2-21 were derived from the target sequence of HCV-E1E2 glycoprotein with an offset of one residue. Pro, Gly ("PG") residues supplant the residues present on positions 10 and 11. Cys residues on positions 1 and 22 were joined by mP2 CLIPS. Native Cys were protected by acetamidomethyl in all the libraries (Table 2.12).

The binding of VF-Fab to each of the synthesised peptides was tested in a PEPSCAN-based ELISA (274). The peptide arrays were incubated with VF-Fab (overnight at 4°C). After washing, the peptide arrays were incubated with a 1:1000 dilution of goat anti-human HRP conjugate (Southern Biotech 2010-05) for 1 h at 25°C. After washing, the peroxidase substrate 2,2'-azino-di-3-ethylbenzthiazoline sulfonate and 20 µl/ml of 3% H_2O_2 were added. After 1 h, the colour development was measured. The colour development was quantified with a charge coupled device camera and an image processing system.

SET 3

Mimic Type : linear

Label : LIN

Description: Linear peptides of length 15 derived from the target sequence of HCV-E1E2 glycoprotein with an offset of one residue. Cys are protected by acetamidomethyl (Acm; denoted "2").

SET 4

Mimic Type : Loop, mP2 CLIPS

Label : LOOP

Description: Constrained peptides of length 17. On positions 2 – 16 are 15-mer sequences derived from the target sequence. To introduce structural constraints Cys were inserted on positions 1 and 17, which then were constrained by mP2 CLIPS. Native Cys are protected by Acm (denoted "2").

SET 5

Mimic Type : Helical mimic, mP2 CLIPS

Label : HEL

Description Structured peptides of length 23 derived from the target sequence on page 7 with an offset of one residue. On positions 1 and 5 are Cys residues which are joined by mP2 CLIPS. Native Cys are protected by Acm (denoted "2").

SET 6

Mimic Type : β-turn mimic, mP2 CLIPS

Label : BET

Description: Structured peptides of length 22. On positions 2- 21 are 20-mer sequences derived from the target sequence of HCV-E1E2 glycoprotein with an offset of one residue.

"PG" residues supplant the residues present on positions 10 and 11. On positions 1 and 22 are Cys residues which are joined by mP2 CLIPS. Native Cys are protected by Acm (denoted "2").

Table 2.12: List of peptides used in conformational epitope mapping (first 10)

SET 3	SET 4	SET 5	SET 6
*2GPVY2FTPSPVVVG	CETHTVGGSASRAAHRC	CETHCVGGSASRAAHRVTTFIT	CHRVTTFITRPGSQNIQLINTC
TALN2NDSLNTGFLA	CTHTVGGSASRAAHRVC	CTHTCGGSASRAAHRVTTFITR	CTYTR2GSGPPGTPR2MVHYPC
NRTALN2NDSLNTGF	CHTVGGSASRAAHRVTC	CHTVCGSASRAAHRVTTFITRG	CQNIQLINTNPGWHINRTALNC
SWGENETDVLLLNNT	CTVGGSASRAAHRVTTC	CTVGCSASRAAHRVTTFITRGP	CNDTLT2PTDPGRKHPEATYTC
DTLT2PTD2FRKHPE	CVGGSASRAAHRVTTFC	CVGGCASRAAHRVTTFITRGPS	CNETDVLLLNPGRPPRGNWFGC
STGFTKT2GGPP2NI	CGGSASRAAHRVTTFIC	CGGSCSRAAHRVTTFITRGPSQ	CETDVLLLNNPGPPRGNWFG2C
GVPTYSWGENETDVL	CGSASRAAHRVTTFITC	CGSACRAAHRVTTFITRGPSQN	CP2GIVPAAQPGGPVY2FTPSC
KHPEATYTR2GSGPW	CSASRAAHRVTTFITRC	CSASCAAHRVTTFITRGPSQNI	C2RPIDKFAQPGGPITHTEPPC
KFAQGWGPITHTEPP	CASRAAHRVTTFITRGC	CASRCAHRVTTFITRGPSQNIQ	CDSLNTGFLAPGFYTHRFNASC
WFG2TWMNSTGFTKT	CSRAAHRVTTFITRGPC	CSRACHRVTTFITRGPSQNIQL	CHYAPRP2GIPGAAQV2GPVYC

* Native Cys are protected by Acm are denoted “2”

Chapter 3

3. Humoral immune system targets clonotypic antibody associated Hepatitis C Virus

3.1 Introduction

HCV virions can be segregated into antibody associated and antibody free virus (AFV) subpopulations (267). Analysis of both these fractions at the genomic level has revealed that the AFV fraction can be diverse; whereas the AAV fraction is of limited heterogeneity even clonotypic in nature (212, 268). Longitudinal analysis of HCV genotype 4a over a 10 years has demonstrated the appearance of antibodies at discrete time points and extinction of an antibody associated lineage (212). Short term pyrosequencing analysis of genotype 3a infection has also been used to demonstrate the extinction of discrete viral variants in the presence of AAV(276). The vacant viraemic space is often replaced by previously existing minor variants.

In current study we tested a hypothesis that patient derived IgG target clonotypic viral variants in genotype/subtype matched Hepatitis C sera.

To examine this hypothesis we,

- Segregated viraemic HCV sera into AFV and AAV fraction
- Challenged the AAV negative sera with Total IgG purified from AAV positive sera
- Dissociated the antibody-virus complex in AAV positive sera and used virus free Fab (VF-Fab) to challenge the AAV negative sera

This work has been published in J. Gen Virology, 2016 Nov,-

Amruta S. Naik, Brendan A Palmer, Orla Crosbie, Elizabeth Kenny-Walsh, Liam J. Fanning **Humoral immune system targets clonotypic antibody associated Hepatitis C Virus** – Appendix IV

3.2 Methods

Following methods were used to test the hypothesis. Please refer to the outlined sections for further details,-

3.3 Results

3.3.1 Validation of Ab Spin Trap™ column

Initially we examined whether Ab Spin Trap™ columns, specifically designed for IgG purification, could also purify IgG associated virus. This was validated by mixing anti-HBsAg (antibody against Hepatitis B surface antigen) with proteinase K treated viraemic HBV serum (anti-HBsAg negative) followed by Ab Spin Trap™ protocol. Anti-HBsAg antibodies were obtained from a patient who had cleared HBV infection naturally. HBV amplicon from the Total IgG should only amplify if it has an IgG-virus complex. However, proteinase K treatment of HBV serum should lead to digestion of antigenic epitopes, resulting in no antibody-virus (antiHBsAg-HBV) complex formation. This was confirmed by absence of HBV specific 319 bp amplicon in a PCR amplification reaction. The expected 319 bp fragment was amplified from the untreated mix of HBsAg-HBV serum from the Ab Spin Trap™ elute (Fig 3.1).

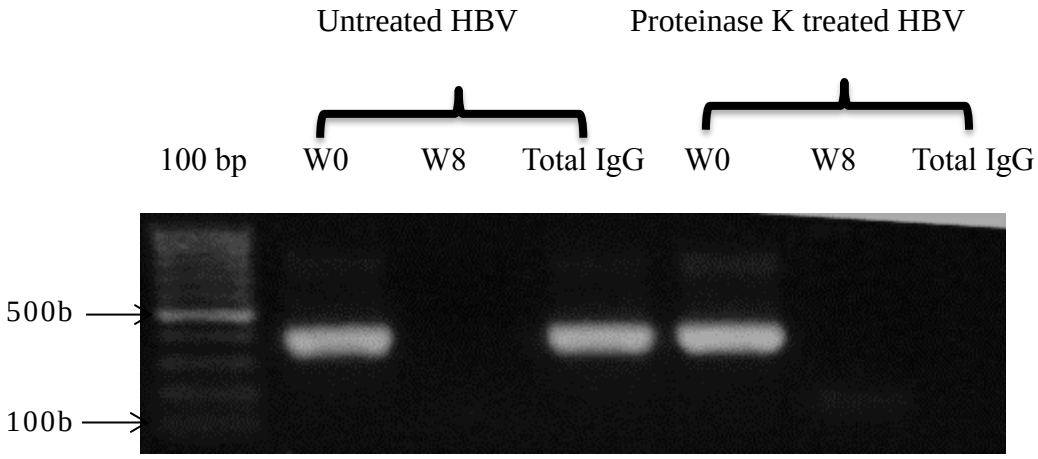

Figure 3.1: Validation of Ab Spin Trap™ protocol

A serum sample positive for hepatitis B virus was treated with proteinase K to digest the antigenic epitopes. Both treated and untreated HBV serum samples were mixed with the anti-HBsAg. Untreated HBV serum sample when mixed with the anti-HBsAg was able to form antibody associated virus (AAV) complex. W0: first flow-through, W8: last wash. DNA isolated from the Total IgG fraction showed presence of 319bp HBV specific amplicon upon PCR amplification. However, DNA isolated from the Total IgG fraction of proteinase K treated HBV sample failed to amplify upon PCR amplification (n=2).

3.3.2 Separation of viraemic sera into antibody associated virus and antibody free virus fraction

Viraemic serum samples were obtained from sixteen unrelated patients (Table 3.1). Out of 18 specimens; n=3/3 (GT 1a), n=5/12 (GT 1b), and n=2/3 (GT 3a) were positive for AAV. Previous research on clonal analysis of antibody based fractionation of viraemic sera has shown that AAV can be of limited heterogeneity with a diverse AFV fraction (212, 267, 268). In the current study, for the initial investigation we analysed both the AAV and AFV fractions by direct amplicon sequencing only. Direct sequencing of the AAV fraction revealed a single, homogeneous nucleotide sequence. Multiple peaks in an electropherogram may indicate heterogeneous sequences within the amplicon sample. For the AFV sequences multiple peaks were observed (A representative electrophoregram shown in Fig 3.2a). Detailed analysis of electropherograms for AAV showed a read of single peaks across the amplicon sequence indicating presence of homogenous sequence (Fig 3.2b). A positive PCR amplification from cDNA obtained from 1:100 diluted 1^{o}AAV also ensured that the results outlined were not subjected to template resampling.

A phylogenetic tree for amino acid sequences was constructed using maximum likelihood estimation method with a bootstrap value of 1000 (MEGA 5.2). Genotype 1a, 1b, 3a and 4a sequences were downloaded from GenBank (amino acid 319-424, from here onwards every nucleotide and amino acid sequence numbering is described against reference sequence AF011751- GT 1a). We acknowledge that only amplicon AFV sequences were used to construct phylogram which do not represent the entire quasispecies profile of the samples. However, the amplicon sequence likely indicates most frequently occurring sequence in the heterogeneous AFV fraction. Based on this, sequences with 100% similarity were clustered together, whereas sequences with

distinct amino acid profile branched out (Fig 3.3a). Further investigation at the HVR1 level revealed that antibody free fractions were distinct in comparison to antibody associated fractions (Fig 3.3b). Mostly changes in the amino acids were restricted to HVR1, however, substitutions at amino acid 322 for sample 1a-1-3; 372 for sample 1a-2-1 and 332, 348, 414 for sample 1a-3-1 were observed. A similar observation was made for genotype 1b. Other than HVR1, sample 1b-1-2 showed changes at amino acid positions 422, 423; 1b-2-1 at 344, 411, 416, 417 and sample 1b-10-1 at 365 and 422 (Fig 3.3b). Conversely, sequences obtained from samples 1b-5-1, 3a-1-1 and 3a-2-1 showed a 100% similarity in both the fractions (Fig 3.3c). In the absence of clonal density data for samples 1b-5-1, 3a-1-1 and 3a-2-1, it is likely that the homogenous sequences for these sera are under purifying selection pressure.

Table 3.1: Sample characteristics used in the current study

Genotype	No. of Samples	1° AAV	Patient Identifier	Sample # Identifier	Accession number AFV¥	Accession Number 1°AAV‡
1a	3	+	P1a-1	1a-1-3	KT873141	KT873142
		+	P1a-2	1a-2-1	KT873143	KT873144
		+	P1a-3	1a-3-1	KT873145	KT873146
1b	12	-	P1b-1	1b-1-1*,†	KT873147-57	-
		+	P1b-1	1b-1-2*,†	KT873158	KT873159
		+	P1b-1	1b-1-3*,†	KT873160	KT873161
		+	P1b-2	1b-2-1*	KT873162	KT873163
		-	P1b-3	1b-3-1	KT873164-71	-
		-	P1b-4	1b-4-1*	KT873173-81	-
		+	P1b-5	1b-5-1	KT873182	KT873183
		-	P1b-6	1b-6-1*	KT873184-94	-
		-	P1b-7	1b-7-1*	KT873195-04	-
		-	P1b-8	1b-8-1*	KT873205-11	-
		-	P1b-9	1b-9-1*	KT873212-17	-
		+	P1b-10	1b-10-1*	KT873218	KT873219
3a	3	+	P3a-1	3a-1-1	KT873220	KT873221
		+	P3a-2	3a-2-1	KT873234	KT873233
		-	P3a-3	3a-3-1	KT873222-32	-

AFV : Antibody free virus

1°AAV: Antibody associated virus

+ : Detectable AAV by RT-PCR

- : No detectable levels of AAV by RT-PCR

Sample identifier: Genotype/Subtype-patient identifier

*Source of infection: contaminated anti-D immunoglobulin (277)

†Obtained from the same patient at three different time points (2002, 2013 and 2014, respectively). Genotype/Subtype-patient identifier- sample number

¥ Samples positive for 1°AAV, both AFV and 1° AAV sequences were analysed by direct sequencing only

‡Samples without accession numbers had no detectable levels of AAV

a.

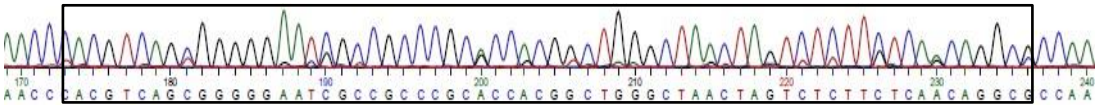

b.

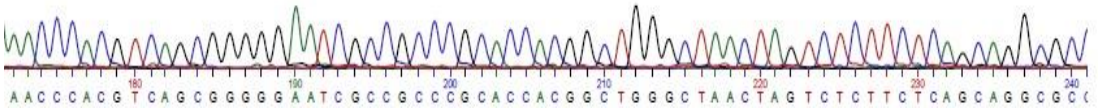

Figure 3.2: AFV fraction shows multiple peaks in the electrophoregram

Multiple peaks in the electrophoregram indicate nucleotide variation at that nucleotide position in the sequence. **a.** Electropherogram segment of HVR1 of AFV fraction of a 1a-2-1. Multiple peaks are shown in the black box **b.** Electropherogram segment of HVR1 of AAV fraction of a 1a-2-1 with clean single peaks indicating homogenous population.

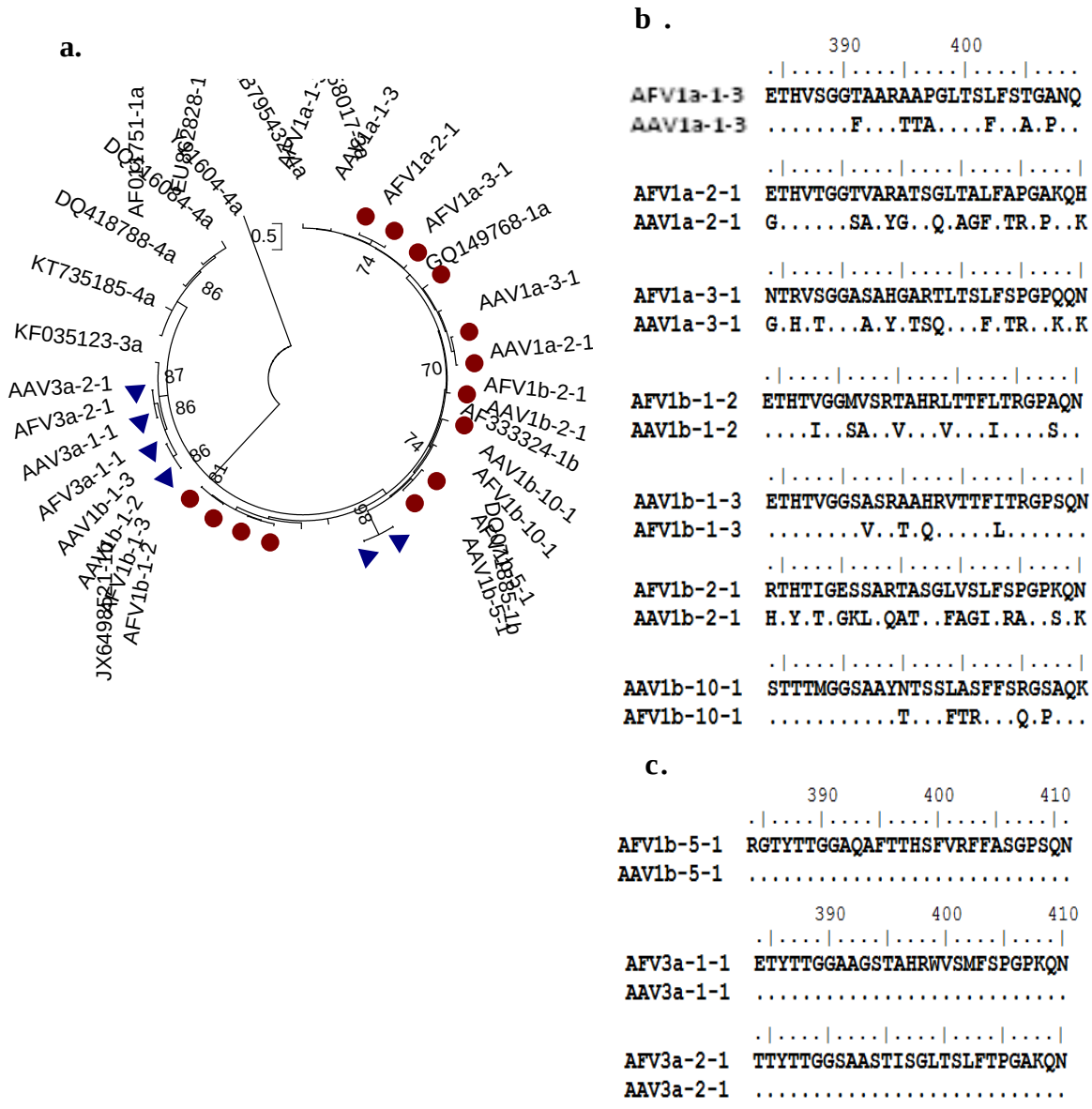

Figure 3.3: Phylogenetic and multiple sequence amino acid analysis for AAV and AFV

a. A phylogenetic tree of AAV and AFV amino acid sequences obtained by direct sequencing (Maximum likelihood, bootstrap-1000, MEGA5.2). Confidence values >70 are shown on the branches. Reference sequences for HCV genotype 1a, 1b, 3a and 4a were downloaded from GenBank. Amino acid sequences with 100% similarity in both AAV and AFV fraction clustered together (blue triangle). Sequences with distinct amino acid profile are shown in brown circle **b.** Direct sequencing amino acid analysis of AFV and AAV for HCV genotype 1 was distinct in the HVR1 (384-410) **c.** Serum samples 1b-5-1, 3a-1-1 and 3a-2-1 showed a 100% similarity in the HVR1 at the amino acid level in both the fractions. 28 amino acid HVR1 domain was observed in AFV and AAV fraction of 1b-5-1. Insertion indicated by a black arrow on the top of the sequence.

3.3.3 Antibodies from AAV positive sera capture viral variants from unrelated patients

It was postulated that antibodies with targeted discrete viral variants in AAV positive sera are isolate specific in the context of a complex mix of variants (212, 268, 276). In order to test this hypothesis, sera identified as negative for detectable AAV were challenged with antibodies purified from sera which were classified as AAV positive (referred as 1^{o}AAV) (Table 3.2, Fig 3.4). Total IgG purified from sera which showed detectable levels of 1^{o}AAV were mixed with the sera which were defined as negative for the presence of detectable AAV. The presence of a newly formed AAV (referred as 2^{o}AAV) in addition to the pre-existing parental DNA sequence in 1^{o}AAV was identified by clonal analysis (schematic representation in Fig 3.4). Total IgG from 1b-5-1 targeted a viral variant from 1b-4-1 and 1b-6-1, total IgG from sample 1b-10-1 captured a variant from sample 1b-7-1 and antibodies from sample 3a-2-1 were bound to a viral variant in 3a-3-1. However, 2^{o}AAV for 1b-8-1 when mixed with the total IgG from 1b-5-1 were not detectable.

The molecular phylogenetic analysis was inferred by using the Maximum Likelihood method for amino acid sequences of 1^{o}AAV and 2^{o}AAV. From the phlyogram it was clear that 2^{o}AAV sequence targeted by the antibody were non-identical with the 1^{o}AAV sequence (Fig 3. 5a). Amino acid sequence for the 2^{o}AAV of 1b-7-1 and 3a-3-1 showed different clade in the phylogenetic analysis. It should be noted that the phylogenetic analysis included 106 amino acids for E1E2 gene junction. BLAST analysis at nucleotide (318 bp) and amino acid (106) level of 1b-7-1 and 3a-3-1 sequences revealed that they belong to genotype 1b and 3a respectively. Additionally, a separate nucleotide BLAST analysis of partial E1 region (nucleotide 1293-1490) and the partial E2 region (nucleotide 1491-1611) in 318 bp E1E2 gene junction of both

1b-7-1 and 3a-3-1 for 2^{o}AAV sequence was performed. Partial E1 and E2 region of 2^{o}AAV 1b-7-1 showed 97% and 88% similarity with genotype 1b sequences JX649813 and AB154190, respectively. Similarly, partial E1 and E2 regions of 2^{o}AAV 3a-3-1 showed 96% and 89% similarity with genotype 3a sequences KC964933 and DQ505847, respectively. Rearrangement of the clusters can be explained as phylogenies based on sequences with little information are susceptible to reordering if the sequences have homoplasy. Due to the high genetic variations in the primer binding sites, attempts to amplify the full length E1E2 glycoprotein for further analysis were not successful.

Similarly, total IgG purified from samples 1b-4-1, 1b-6-1, 1b-7-1, 1b-8-1 and 1b-9-1 which were initially classified as AAV negative were mixed from these experiments in a cross-panel pull down assay (e.g., Total IgG from 1b-4-1 were mixed with serum samples 1b-6-1, 1b-7-1, 1b-8-1 and 1b-9-1). It was observed that total IgG purified from AAV negative sera did not capture any viral variant (Table 3.2).

Separately, amino acid sequence analysis observed that, 1b-5-1 has a 28 amino acid HVR1 domain with an in-frame 3 bp insertion at nucleotides 1492-94 at the 5' end of E2 (Fig 3.5b, Table 3.2). An atypical 30 amino acid HVR1 sequence in both 2^{o}AAV and AFV fractions of serum 1b-4-1 (Fig 3. 5b, Table 3.2), as a result of 9 bp in-frame insertion at 5' end from nucleotide 1492-1500 was identified. Also, as a consequence of an in-frame deletion at the 5' end from nucleotide 1491-93, a 26 amino acid HVR1 profile from specimen 1b-7-1 (Fig 3.5b) was observed. The rest of the targeted 2^{o}AAV sequences harboured a classic 27 amino acid HVR1 (Fig 3.5b).

Table 3.2: Antibody pull down of serum samples without detectable AAV following initial fractionation

AAV negative Sera[#]	1°AAV positive sera	Antibody Pull down[*]						Unique HVR1[‡]	Accession numbers of 2°AAV
		Total IgG	AP33	VF-Fab	λ-VF-Fab	κ-VF-Fab	AP33		
		untreated		proteinase k treated					
1b-1-1[†]	1b-2-1[†]	-	N/D	+	-	N/D	N/D	1	KT873154-57
1b-3-1[†]	1b-2-1[†]	N/D	N/D	+	N/D	N/D	N/D	1	KT873166, 70-71
1b-4-1	1b-5-1	+	-	+	+	-	-	1	KT873176-77,80-81
	1b-10-1	-	-	-	-	-	-	-	-
1b-6-1	1b-5-1	+	-	+	-	-	-	1	KT873186,194
	1b-10-1	-	-	-	-	-	-	-	-
1b-7-1	1b-5-1	-	-	-	-	-	-	-	-
	1b-10-1	+	-	+	+	-	-	1	KT873195, 97-204
1b-8-1	1b-5-1	+	-	+	-	-	-	1	KT873205-11
	1b-10-1	-	-	-	-	-	-	-	-
1b-9-1[†]	1b-2-1[†]	+	+	+	-	N/D	+	1	KT873216-17
3a-3-1	3a-2-1	+	+	+	+	-	+	1	KT873229

[#]Patient sera without detectable AAV following initial fractionation were subsequently challenged with genotype/subgenotype matched 1°AAV positive sera (as per Table 3.1)

[*]Individual antibody preparations originating from 1°AAV positive serum or AP33 are described in Material and Methods section

[†]Insufficient amounts of AAV negative sera and/or 1°AAV positive sera limited the number of possible experimental combinations (N/D-Not Done)

[‡]Cumulative number of unique HVR1 amino acid sequences identified in 2° AAV positive sample

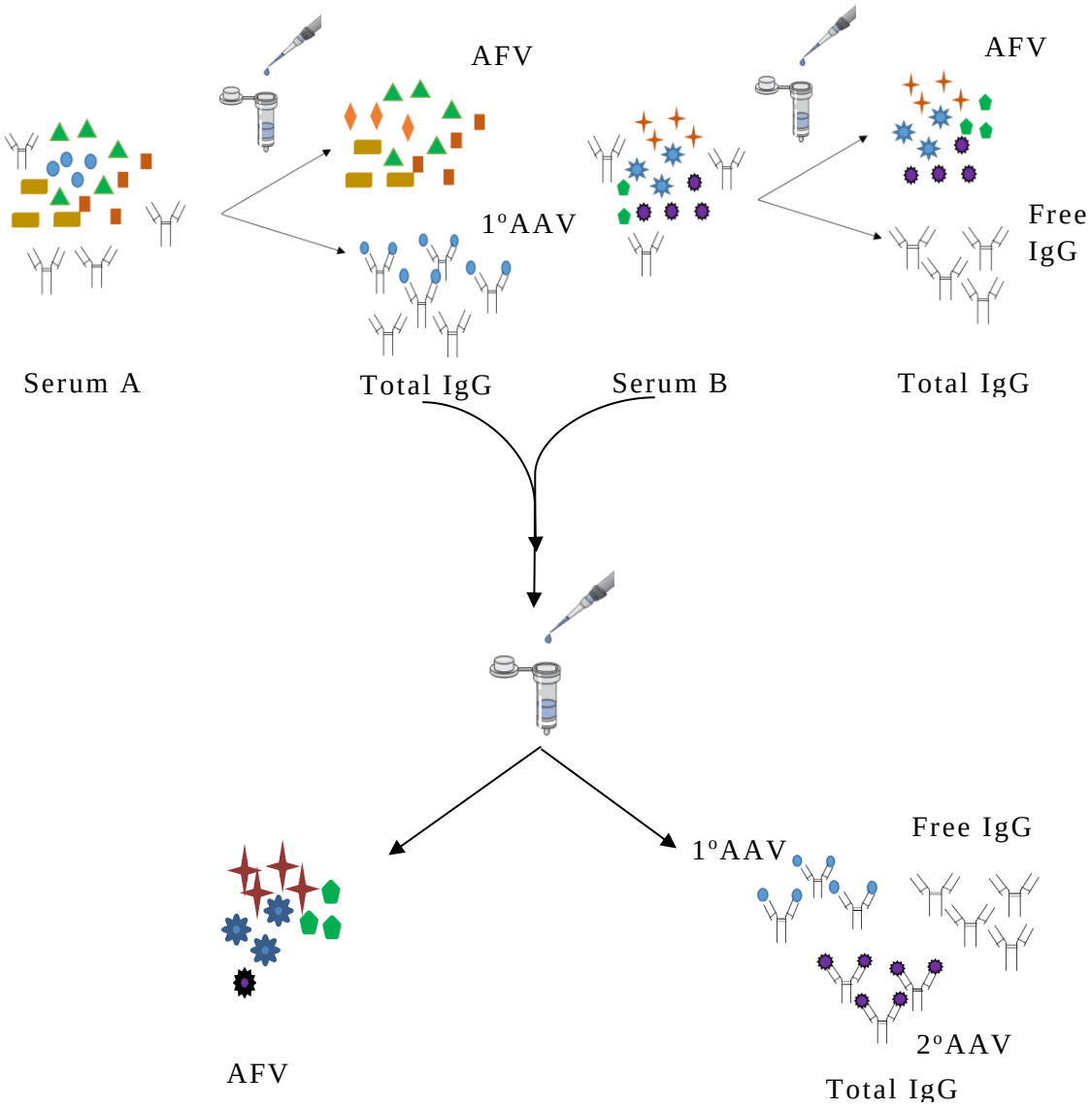

Figure 3.4: Separation of antibody free virus from antibody associated virus from viraemic serum

Schematic diagram of column based separation of unbound antibody free virus (AFV) and 1° antibody associated virus (1°AAV) fraction as described in methods**.** Different coloured shapes represent quasispecies of HCV**.** Total IgG from 1°AAV positive sample (Serum A) were used to pull down viral variants from an unrelated serum sample (Serum B) which had previously been classified as AAV negative. The output of this pull down assay was capture of a newly formed viral variant 2°AAV additional to the pre-existing parental 1°AAV

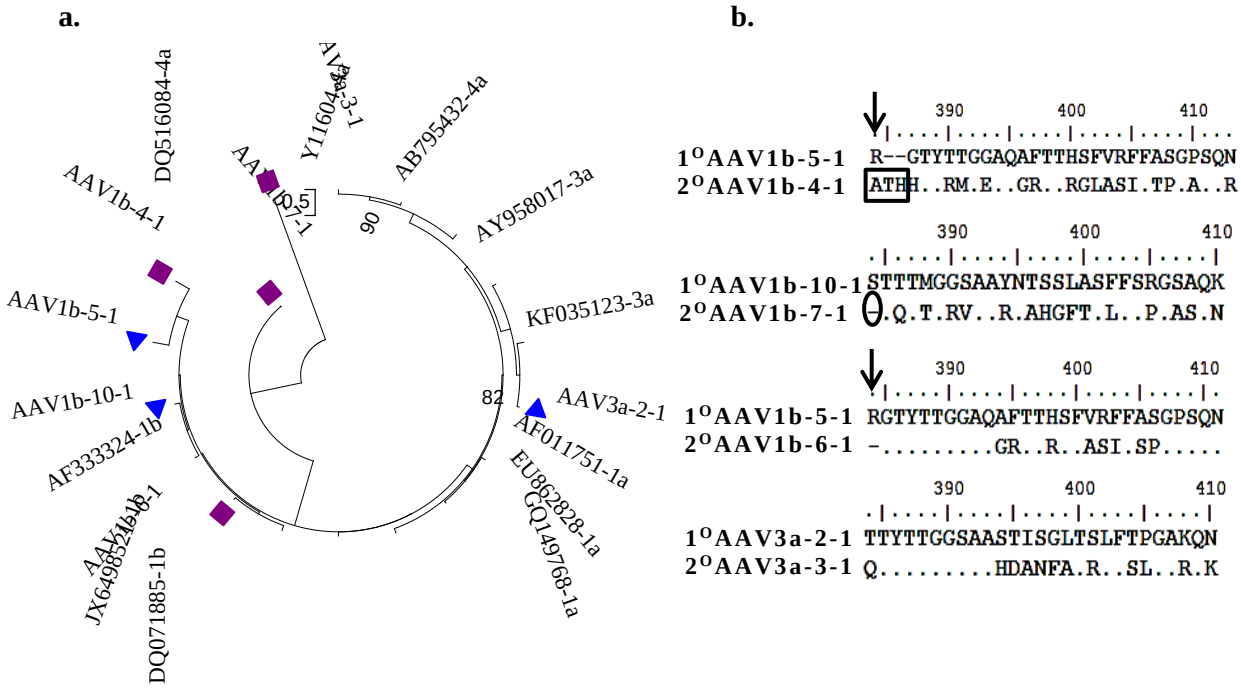

Figure 3.5: 1°AAV (parental) sequence is distinct from 2°AAV sequence (newly formed)

a. A phylogenetic tree of 1°AAV and 2°AAV amino acid sequences (Maximum likelihood, bootstrap-1000, MEGA5.2). Confidence values >70 are shown on the branches. 1°AAV sequences are marked with blue triangle and 2°AAV sequences are marked with purple squares. 2°AAV sequences cluster away from 1°AAV at the different nodes indicating their distinct amino acid profile. Rearrangement of 1b-7-1 and 3a-3-1 amino acid sequence could be due to inclusion of short length of amino acid sequence **b.** 1°AAV sequence from 1b-5-1 has a 28 amino acid HVR1 (Insertion is shown by a black arrow on the top). Total IgG 1b-5-1 captured a 2°AAV [KT873177] from 1b-4-1 which harbours a non-classical 30 amino acid HVR1 (Black box shows insertion). 2°AAV [KT873195] from 1b-7-1 harbours a non-classical 26 amino acid HVR1 that was captured by Total IgG from 1b-10-1 (Black circle shows the deletion). Total IgG from 1b-5-1 captured two more viral variants (2°AAV) from unrelated sera which harboured a classical 27 amino acid HVR1 profile. Similar observations were made for Total IgG from 3a-2-1 which captured a viral variant from serum 3a-3-1 [KT873229]. Sequence analysis of 1°AAV with 2°AAV complex revealed to be non-identical.

3.3.4 Dissociation of antibody-virion complex

Virus free antibody fractions were obtained by treating AAV positive sera with proteinase K. The absence of E1E2 junction specific PCR products confirmed the virus free status of the post proteinase K treated samples (Fig 3.6). Products of proteinase K treated sera eluted from Ab spin trap™, LambdaFabSelect™ and KappaSelect™ were analysed using a 4-12% bis-tris gradient gel. Analysis revealed that in the process of dissociating the antibody-virus complex, the intact antibody was fractionated into several peptides. An intact Fab like fragment was identified at ~50 kDa from all three fractionation procedure (Fig 3.7). The exact cleavage site of the proteinase K on IgG has not been identified in this study. However, the SDS-PAGE, western blot and functional analysis of virus free fragment fraction indicates that this fraction contains Fab like fragment; henceforth this Fab like molecule will be referred to as either "VF-Fab" (Ab spin trap™), "λ-VF-Fab" (LambdaFabSelect™), or "κ-VF-Fab" (KappaSelect™), as appropriate (Fig 3.7).

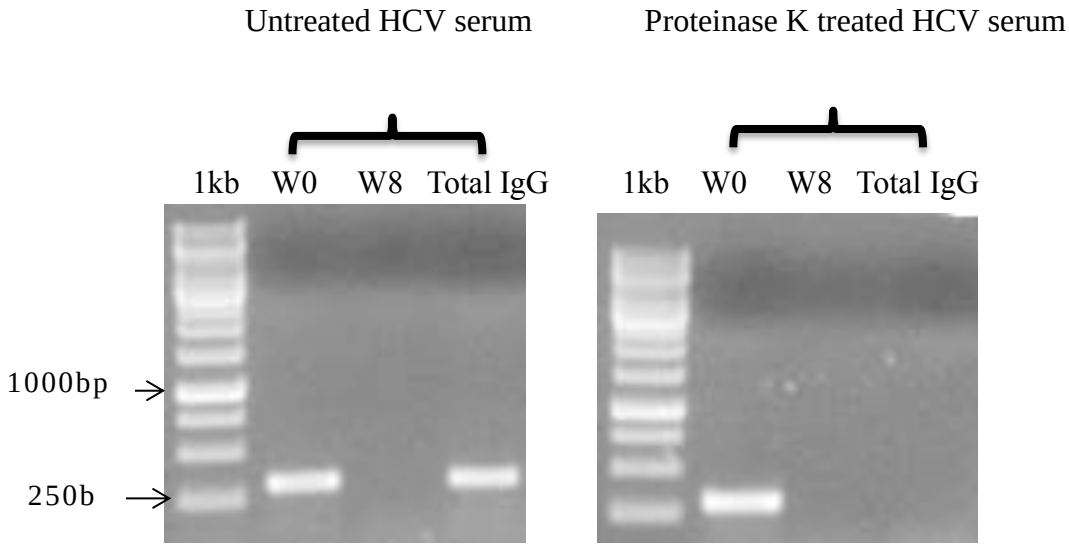

Figure 3.6: Confirmation of of antibody-virion complex dissociation

Serum sample positive for presence of AAV was treated with proteinase K to digest the antigenic epitopes. Both untreated and proteinase K treated HCV serum samples were segregated into AFV (W0) and AAV (Total IgG) complex using Ab spin trap™. W0: first flow-through, W8: last wash. PCR analysis of Total IgG fraction showed presence of 318 bp HCV E1E2 junction specific amplicon. However, Total IgG fraction of proteinase K treated HCV serum failed to amplify the expected 318 bp amplicon indicating virus free status of total IgG fraction.

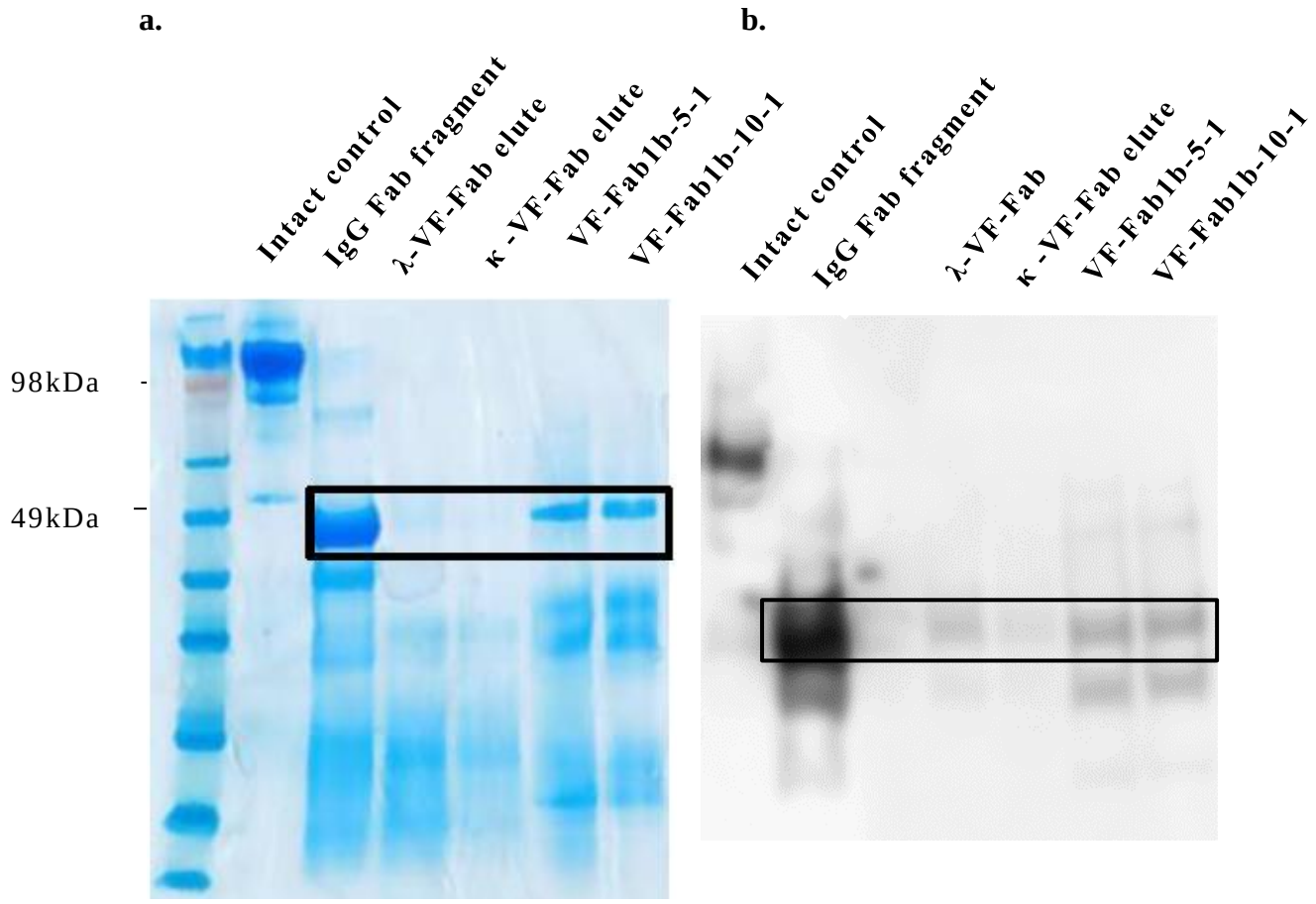

Figure 3.7: Analysis of proteinase K treated serum sample

a. Samples (25 µg) post proteinase K treatment after eluting from three different columns were analysed on 4-12% bis-tris gradient gel in a non-reducing condition. The black box indicates Fab positive control (5 µg) aligning with the test samples. κ-VF-Fab was not detectable in SDS-PAGE. Control IgG was purified from human plasma CTM (-)C, Roche Molecular systems Inc, a commercial natural human IgG Fab fragment was used (ab90352) **b.** Separately, independent preparations of elutes were transferred onto nitrocellulose membrane. The blot was developed using HRP labelled mouse anti-Human IgG Fab antibody (biorbyt). We identified intact Fab fragment post proteinase K treatment.

3.3.5 Patient derived VF-Fab selectively targets homologous genotype

Total IgG, which contains AAV (hereafter referred to as 1°AAV) along with free antibodies, VF-Fab, λ-VF-Fab and κ-VF-Fab was used to pull down the viral variants from the AAV negative sera (Table 3.2, Fig. 3.8). The quantity of HCV specific antibodies in the Total IgG and VF-Fab preparations was not known. The bed volume for Ab Spin Trap™ column is 100 µl and is capable of purifying >1mg of IgG. Considering these factors the ratio of antibodies: AAV negative sera was set to 1:5. This mixture was then incubated at 37°C for 2 h. AP33 is a mouse MAb which targets the partially confirmation dependent epitope within amino acid residues 412-423 (a kind gift from Dr. Arvind Patel, University of Glasgow, UK). Simultaneously, these sera (Table 3.1.3.2) were challenged with both intact AP33 and Ab Spin Trap™ eluted post proteinase K treated AP33 (25 µg/ml) (278). The Ab Spin Trap™ protocol was followed and the challenged samples were tested for the presence of a newly formed 2°AAV by PCR. We observed that VF-Fabs (n=8/12) were able to capture viral variants in all instances in comparison to λ-VF-Fab (n=3/12) and κ-VF-Fab (n=0/12) (Table 3.2). Seven genotype 1b and one genotype 3a serum samples which originally did not show detectable levels of the AAV were successfully retained (on the Ab spin trap™ column) when mixed with the VF-Fabs from a patient infected with the same HCV genotype (Table 3.2). A completely homogenous virus population was recovered from all the newly formed 2°AAV fractions when analysed clonally at the amino acid level (Accession numbers: Table 3.2).

Both intact MAb-AP33 and proteinase K treated AP33 retained identical viral variants from 1b-9-1 and 3a-3-1, only (Table 3.2). The AAV fraction obtained from 1b-9-1 and 3a-3-1 sera yielded a homogenous virus population of [KT873217] and [KT873229], respectively when mixed with AP33. This mirrors the identical viral variants captured

by VF-Fab1b-2-1 and VF-Fab3a-2-1 preparations implying the immunogenicity of the variants. Detailed analysis at the amino acid level demonstrated that serum samples 1b-9-1 and 3a-3-1 harbour epitope $E_{412\text{-}423.}$ MAb AP33 targets epitope $_{412}$QLINTNGSWHIN$_{423}$ ($E2_{412–423}$) (257). The epitope $E2_{412–423}$ is conserved across samples 1b-3-1, 1b-4-1, 1b-6-1, 1b-7-1 and 3a-3-1 (Fig 3.9). In our samples, amino acid isoleucine (I) was replaced with valine (V) at position in 414 in the sequences obtained from 1b-1-1 (40%), 1b-8-1 (100%) and 1b-9-1 (100%). Natural $E2_{412–423}$ variant $_{412}$QL**V**NTNGSWHIN$_{423}$ has been observed in genotype 1a (18.5%), genotype 3a (52%) and genotype 6 (25%) (171).

Both, VF-Fab and λ-VF-Fab derived from respective homologous genotypes captured identical viral variants from 1b-4-1, 1b-7-1 and 3a-3-1 forming a 2^{o}AAV (Table 3.2). κ-VF-Fab did not capture viral variant from any of the AAV negative sera.

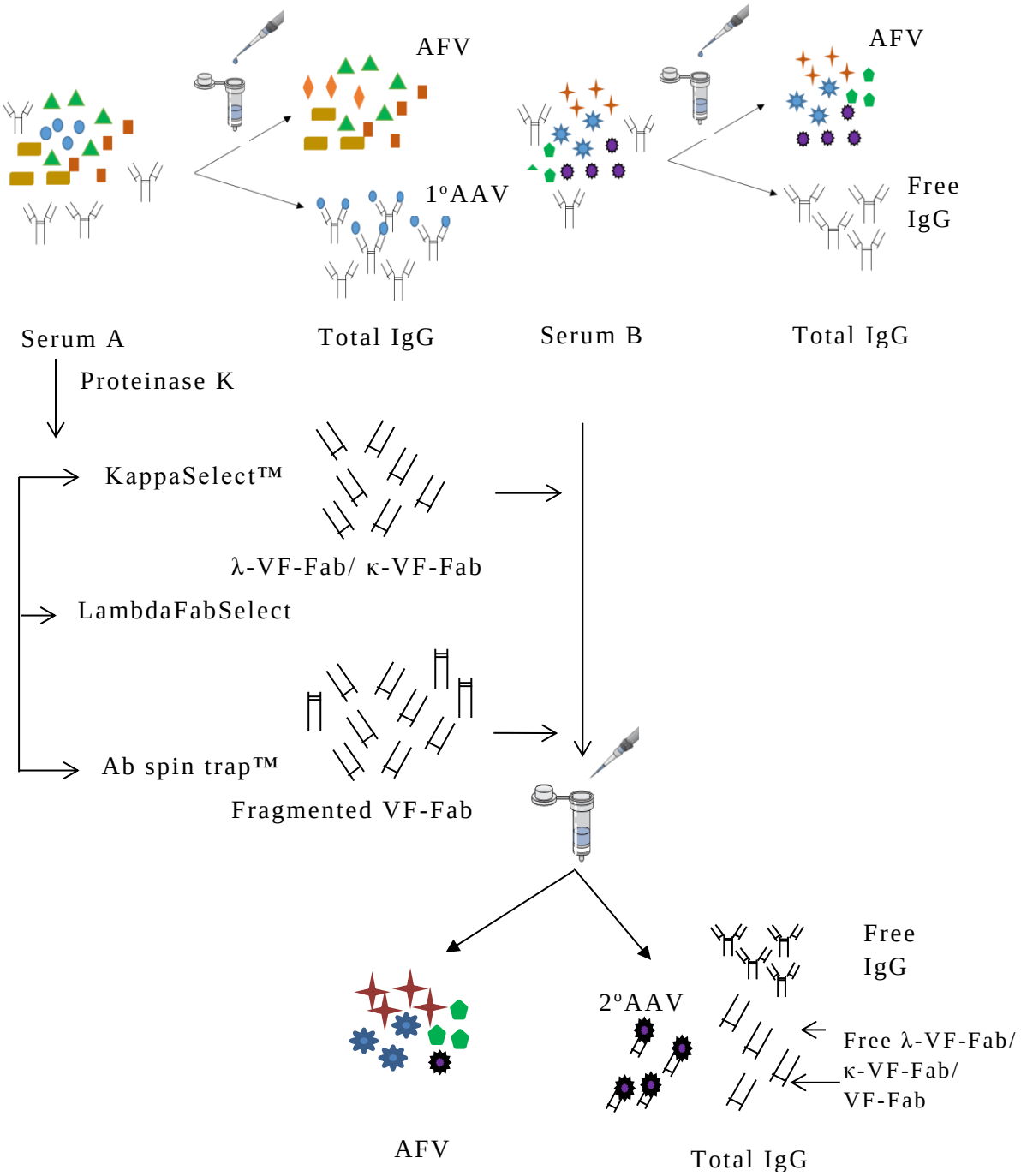

Figure 3.8: Separation of antibody-virion complex

Schematic diagram of separation of antibodies from virion in AAV positive serum sample as described in methods. Different coloured shapes represent quasispecies nature of HCV. λ-VF-Fab, κ-VF-Fab and VF-Fab from 1°AAV positive sample (Serum A) were used to pull down variants from an unrelated (obtained from a different patient) serum sample of same genotype/subtype (Serum B) which had previously been classified as AAV negative. The output of this pull down assay was capture of a newly formed 2°AAV.

Figure 3.9: Weblogo of epitope $E_{412\text{-}423}$ targeted by MAb AP33 observed in sera with no detectable antibody associated virus (Table 3.2)

Amino acid Weblogo of epitope $_{412}$QLINTNGSWHIN$_{423}$ targeted by MAb AP33. Amino acids are grouped and colour coded as Black: non polar, Green: polar, Red: acidic, Blue: basic and Purple: neutral. The x-axis depicts the amino acid position and the height of the individual letter reflects relative frequency of each amino acid at that position. Sequences obtained from AAV negative sera 1b-1-1, 1b-8-1 and 1b-9-1 showed I414V mutation.

3.3.6 Source of VF-Fab does not affect the selective binding to viral variants

VF-Fab1b-2-1 was obtained from a serum which belongs to the anti-D cohort (277). Patients in the anti-D cohort were iatrogenically infected with the same source of HCV genotype 1b (277). Three of four HCV 1b sera which were mixed with VF-Fab1b-2-1 were from the anti-D cohort (1b-1-1, 1b-8-1, and 1b-9-1) (Table 3.2). However, viral variants from only two of viraemic sera (1b-1-1, 1b-9-1) were captured by the VF-Fab1b-2-1. Interestingly, serum sample from which VF-Fab1b-5-1 was obtained does not belong to the anti-D cohort yet successfully retained virus from the anti-D serum 1b-4-1, 1b-6-1 and 1b-8-1. On the other hand, 1b-7-1 was targeted by VF-Fab1b-10-1, obtained from another anti-D serum. Of note, no shared reactivity with respect to capture viral variants (2^{o}AAV) for VF-Fab1b-5-1 or VF-Fab1b-10-1 was observed.

Moreover, similar to the previous observation, amino acid substitutions were restricted to HVR1 in 1b-3-1, 1b-9-1, 1b-4-1, 1b-8-1 and 1b-7-1. The relative percentages of 2^{o}AAV clonal population (amino acid at the HVR1 level) identified in AFV ranges from 10-100% (Fig 3.10). Supplementary clonal analysis of unfractionated sample 3a-3-1 showed presence of 2^{o}AAV in the unfractionated sample indicating this variant was a minor variant of the quasispecies pool. It is likely that VF-Fab3a-2-1 has targeted all the available 2^{o}AAV 3a-3-1 variants in serum (Fig 3.10). However, in some of the viral samples changes in the amino acid profile were also observed outside the HVR1 (Fig 3.11). For genotype 1a, 1b-1-1 showed changes at the amino acid positions 344, 347, 355, 373 and 414. In case of genotype 1b, the amino acid positions 319, 345, 347, 373 and 379 showed variation in 1b-6-1 and positions, 339 and 346 in 1b-8-1. In 3a-2-1, variations in the amino acid profile were observed at positions 337, 345, 383 and 415.

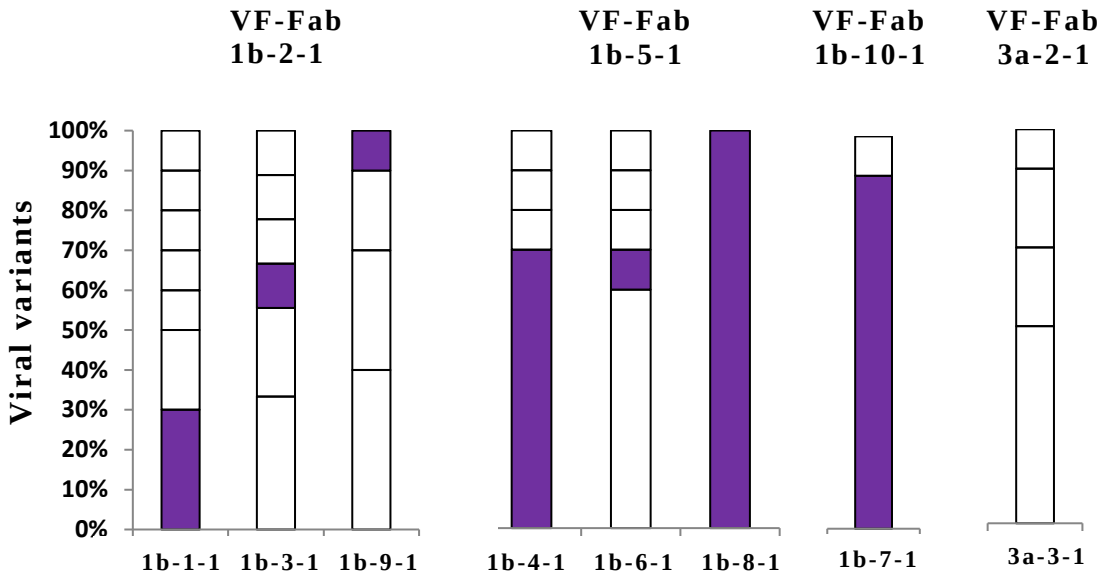

Figure 3.10: Clonal density per sample in AFV fraction

The histogram represents the clonal density of 2ºAAV (when mixed with VF-Fabs) identified in antibody free fraction of parental sample at the amino acid level in HVR1 domain. Ten clones per serum sample were analysed. The X axis depicts homologous genotypes mixed with patient derived VF-Fab (Table 3.2). The vertical bars represent the percentage of unique variants within each specimen. The purple boxes indicate proportion of 2ºAAV detected in AFV fraction after challenging the viraemic sera with VF-Fab from homologous genotype. A single viral variant in 1b-1-1, 1b-3-1 and 1b-9-1 was targeted by VF-Fab1b-2-1. A unique viral variant in 1b-4-1, 1b-6-1 and 1b-8-1 was successfully retained by VF-Fab1b-5-1. A unique viral variant from 1b-7-1 was targeted by VF-Fab1b-10-1. A unique variant from 3a-3-1 was retained by VF-Fab3a-2-1 was identified in unfractionated serum sample 3a-3-1. Accession numbers for 2ºAAV are enlisted in Table 3.2.

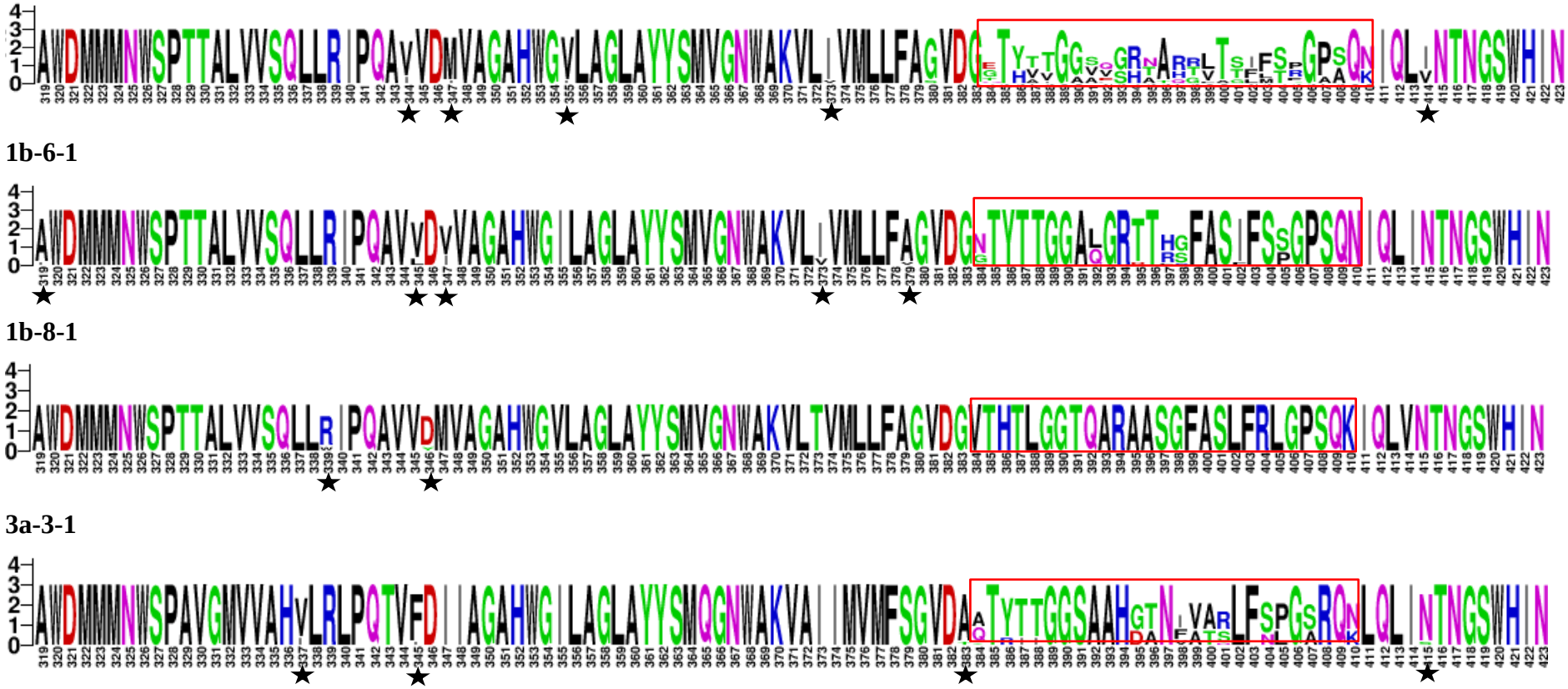

1b-6-1

1b-8-1

3a-3-1

Figure 3.11: Quasispecies heterogeneity in the partial E1E2 glycoprotein of AFV population in HCV at the amino acid level

1b-1-1

Amino acid Weblogo of partial E1E2 glycoprotein sequence (residues 319-424, ref: AF011751). Amino acids are grouped and colour coded as Black: non polar, Green: polar, Red: acidic, Blue: basic and Purple: neutral. The x-axis depicts the amino acid position and the height of the individual letter reflects relative frequency of each amino acid at that position. Red boxes show heterogeneity at the HVR1 level. Stars below the x- axis depict changes in the amino acid composition outside HVR1.

3.4 Discussion

Both the proof-reading activity of HCV RNA polymerase and the high mutation rate of HCV contribute to the rapid evolution in HCV (279). The phenotypes of virus population can change in short periods of time. The biological impact of this variability includes the appearance of escape mutants, alterations in cell tropism and changes in virulence and host range giving rise to fitter virus populations. HCV genome is heterogeneous except for the conserved 5' UTR, with higher diversity in the envelope genes (280). The HVR1 undergoes significant genomic variation (279). It has been observed that selection pressure from nAb responses shape the evolution of viral envelope protein (210-213). Previous research has shown that HCV virions can be segregated into AAV and AFV subpopulations (267). Analysis of both these fractions at the genomic level has revealed that the AFV can be diverse, whereas AAV can be of limited heterogeneity, even clonotypic in nature (268). Investigation of the AAV from immunologically active individuals provide an opportunity to advance our understanding of immune escape mutants and viral envelope protein evolution.

In the current study, viraemic HCV sera were fractionated into AAV and AFV subpopulations to investigate the viral variants targeted by host humoral immune system (Fig 3.2). Furthermore, virus free Fab (VF-Fab) were obtained from the AAV complexes and used to mix homologous genotype/subtype matched sera where AAV was not detected previously (Fig 3.4). This study assessed the ability of Total IgG and VF-Fab to target viral variants from unrelated patients in serum derived HCV system. To our knowledge, this is the first successful attempt where Total IgG and VF-Fab preparations purified from AAV positive sera captured viral variant from viraemic HCV sera classified as AAV negative (Figs 3.4, 3.8). Findings from this study demonstrated that inter-patient viral variants can be targeted by using antibodies from

homologous AAV positive sera (Figs 3.3, 3.5). It has been shown in HCVpp and HCVcc *in vitro* infection systems that antibodies obtained from patient sera are broadly reactive (reviewed in 61). In this instance, however, in the complex serum environment, antibodies targeted unique viral variants from the quasispecies pool from unrelated patient sera which were previously not encountered by the patient B cells (Table 3.2, Figs 3.3, 3.5).

Patient derived anti-HCV VF-Fab fragments either crude (Ab Spin Trap™) or purified λ-VF-Fab (HiTrap LambdaFabSelect™) have the same targeting potential (against defined E2 epitopes) as that of the intact Total IgG (Fig 3.8, Table 3.2). This indicated that antigen binding site was intact post proteinase K treatment. Lack of κ-VF-Fab to capture any viral variant can be explained by its very low concentration, as observed in western blot analysis (Fig 3.7b). Protein G, a surface protein purified from Streptococci group C or G has been shown to bind to the broader range of IgG subclasses. Protein G binds to the interface between C_H2 and C_H3 region of Fc portion in IgG (281). Antibodies purified from proteinase K treated serum samples resulted in fragmentation (Fig 3.7a). SDS-PAGE analysis of fragments obtained from Ab Spin Trap™ showed Fab like fragment along with other fragments (Fig 3.7). It has been previously shown that C_H1 domain of the Fab arm has a binding site for streptococcal protein G (282). This is a likely explanation to how we obtained functional VF-Fab from proteinase K treated AAV positive serum samples (Fig. 3.7).

It is of note that, although six samples were from the Irish anti-D cohort (277), VF-Fab showed a selective targeting of viral variant in homologous subtyped matched HCV 1b sera, irrespective of the common source of HCV infection (Fig 3.5b). Analysis of relative distribution of 2°AAV at the HVR1 level suggests that the viral

variant targeted by VF-Fab need not dominate the heterogeneous virus population (Fig 3.9). Multiple sequence and phylogenetic analysis indicated amino acid diversity of distinct 2^{o}AAV targeted by VF-Fab (Fig 3.5). This data suggests that the variants targeted by VF-Fab must share a common epitope. In an infected individual HCV is associated with ApoB, ApoE and circulates as a lipoviral particle (reviewed in 100, 101). This limits the accessibility to the immunogenic epitope. Furthermore, the immunogenicity and antibody-epitope binding kinetics play a crucial role in selecting the clonotypic population out of the diverse mixture of variants in patient sera. Competition between the antibodies produced against different viral variants is another potential reason for the clonotypic selection of the virion. Additional unknown factors in the serum could also contribute to the selective targeting of viral variant(s).

The HVR1 in the E2 undergoes significant genomic variation (279). A recent study by Palmer *et al.* (2015) involved ultra-deep pyrosequencing analysis of HVR1 phenotypes isolated from 23 treatment naïve chronically infected patients where samples were collected for 16 weeks biweekly (276). Based on the HVR1 variation, quasispecies were distinguished as stationary viromes (purifying immune pressure) phenotype and antigenic drift (positive selection pressure) phenotype (276). Several studies have documented the existence of neutralisation epitopes within HVR1 (30, 61-67), hence making it vulnerable to antibody mediated immune selection pressure. Positive selection pressure results in immune evasion of variants from antibody responses and HCV successfully establishes persistent infection in the face of continual production of neutralising antibodies (nAb) (268, 283, 284). In the present work, we observed that variations in the amino acid profile were largely concentrated within HVR1, which supports the already published data that HVR1 is constantly under immune selection pressure (Fig 3.3b-c and 3.5b) (266, 268, 283, 284). A

dominant homogenous HVR1 population with no variations in the amino acid profile outside HVR1 was observed for samples 1b-4-1 (70%), 1b-8-1 (100%) and 1b-7-1 (90%), implying the variants are under purifying selection pressure (Fig 3.10). The partial E1 sequence (319-383) showed very few amino acid substitutions (Fig 3.11). E1 is a transmembrane protein, which limits its exposure to the antibodies (27, 37, 38). This may be explained partially as E1 being a poor immunogenic region and hence subject to less immune pressure (161-163, 167).

Insertion-deletion events in HVR1 are a feature of HCV biology (212, 267, 285). This study reports the capture of a non-classic 30 amino acid HVR1 (from sample 1b-4-1, Fig 3.5b) using VF-Fab1b-5-1 from an unrelated sample. The variant in AAV positive 1b-5-1 harboured a non-classical 28 amino acid HVR1 (sample 1b-5-1, Fig 3.5b). These data indicate that the three amino acid insertion at the N-terminus of HVR1 did not interfere with the binding capacity of aforementioned VF-Fabs from sample 1b-5-1. Guan *et al*. (2012) in their experiments have shown that first 13 amino acids do not affect the infectivity in HCVpp system. This is likely because nAbs target C terminus of HVR1 and hence deletion or insertion at the N terminus doesn't affect this phenomenon (129).

Epitope $_{412}$QLINTNGSWHIN$_{423}$ targeted by MAb AP33 is a highly conserved epitope downstream from the HVR1 is broadly neutralising and conserved across different genotypes (53.4%) (171, 257). Importantly, MAb AP33 (either intact or proteinase K treated) was able to retain epitope positive viral variant(s) from only 1b-9-1 and 3a-3-1 (Table 3.2, Fig 3.9). In our study, sequences obtained from samples 1b-1-1 (40%), 1b-8-1 (100%) and 1b-9-1 (100%) harboured I414V mutation in the E2$_{412–423}$ epitope (Fig 3.9). Tarr *et al.* (2006) observed that alanine replacement at positions L413, N415,

G418 and W420 resulted in a reduction in binding (>75%) (286). In another study in 2007 they observed that alanine substitution at I414 and T416 resulted into 60% reduction in binding (171, 286). However, AP33 showed >100% reactivity to I414V natural variant in genotype 1a, 3a and 6 (171). Tarr *et al.* (2007) also noted that antibodies obtained from less than 2.5% acute and chronically infected individuals were reactive to $E2_{412–423}$ epitope (genotype 1- 4%, genotype 2- 1% and genotype 3- 1%) (171). These findings suggested that $E2_{412–423}$ presentation is genotype specific (171). This explains despite of the I414V mutation how AP33 targeted viral variant in sample 1b-9-1.

Dreux *et al.* (2006) have shown that high density lipoproteins in serum can shield the CD81 binding site making it unavailable for binding of MAbs like AP33 (287). Recently, Deng *et al.* (2015) have found no detectable antibody response to a peptide (PUHI 19) harbouring $E2_{412–423}$ epitope (409-423) suggesting weak immunogenicity of the epitope (174). Another study by Li *et al.* (2015) shows that $E1_{412\text{-}423}$ assumes different conformations leading to decreased immunogenicity in the infected individuals (288). Li *et al.* (2015) showed that epitope $E2_{412–423}$ in complex with antibody HC33.1 (Human MAb to $E2_{412–423}$) assumed a conformation intermediate to a β-hairpin and coil (288) in contrast to its β-hairpin structure in complex with AP33 and other two MAbs HCV1 and Hu5B3.v3 (48). These findings suggest that $E2_{412–423}$ is a flexible region. This is due to the fact that the epitope structure depends on the polypeptide sequence up and/or downstream of the antigenic site. $E2_{412–423}$ is preceded by a highly disordered and variable region which is assumed to form a flexible loop like structure (41) implying that strain or isolate specific amino acid variation may modulate the epitope presentation thereby altering the neutralisation efficiency. Overall, the available data suggest that structural flexibility of $E2_{412–423}$ renders it less

immunogenic depending upon the individual quasispecies heterogeneity, partly explaining as to why AP33 failed to target some of the viral variant(s) in our serum-AP33 pull down experiments.

From our results it was not possible to determine whether, i) the antibodies which targeted 1°AAV are the same antibodies that targeted 2°AAV, and/or ii) the antibodies were not saturated by 1°AAV. Moreover, Total IgG purified from AAV negative sera were not capable of capturing viral variants from other AAV negative sera. In this context, absence of AAV might represent a period when antibody sensitive viral variants were removed (from a quasispecies pool) or below the detection level leaving behind the humoral immune escape mutants. Nonetheless, we acknowledge that these AAV negative sera might have nAbs against previously culled viral variants from the quasispecies pool (Section 5.3.2).

In summary, we segregated the chronically infected viraemic sera from HCV infected patients into a diverse population of AFV and a clonotypic AAV fraction. Our study highlights that mutations in the HVR1 of AAV provide an insight into the dynamics of viral evolution. Presence of AAV signifies an active host immune response in the context of a complex serum based environment. We show differential binding of patient derived anti-HCV antibodies, VF-Fab and murine MAb AP33 in unrelated viraemic sera (Table 3.2). The data presented here shows that selective binding is independent of the source of infection and/or mutations within the HVR1. Thus our data strengthen the hypothesis that antibodies derived from HCV infected patients target viral variant(s) from homologues genotype/subtype matched sera.

Chapter 4

4. Amplification, cloning and expression of full length E1E2 glycoprotein from antibody associated HCV

4.1 Introduction

HCV pseudoparticle system has been proven to be an efficient *in vitro* system to study the role of E1E2 glycoprotein in HCV life cycle (33, 51, 165, 256). Recently, Urbanowicz *et al*. (2015) assessed the infectivity of a diverse panel of patient derived HCV envelope glycoproteins and their neutralisation using monoclonal antibodies (MAb) (258). Urbanowicz *et al*. (2015) observed variance in the infectivity and neutralisation sensitivity of these patient derived HCV glycoproteins. In the previous chapter we have shown that the humoral immune system targets clonotypic viral variants from the quasispecies population. In this chapter, we tested the hypothesis that the E1E2 sequences generated from the antibody associated virus fraction are infectious in the HCV pseudoparticle (HCVpp) system.

To examine this hypothesis we,

- Amplified, cloned and expressed the full length AAV- E1E2 glycoprotein
- Generated HCV pseudoparticles using MLV based packaging vector in the HEK293T cells
- Carried out infectivity assay in the Huh7 cells

Part of this work has been published in J. Gen Virology, 2016 Nov,-

Amruta S. Naik, Brendan A Palmer, Orla Crosbie, Elizabeth Kenny-Walsh, Liam J. Fanning **Humoral immune system targets clonotypic antibody associated Hepatitis C Virus** – Appendix IV

4.2 Methods

Following methods were used to test the hypothesis,

4.3 Results:

4.3.1 Cloning and expression of E1E2 glycoprotein sequence derived from AAV

A panel of viraemic sera positive for HCV genotype 1a (n=3), 1b (n=7), 3a (n=1) were selected from eight chronically infected patients at different time points (Table 3.2.3.1). Six out of seven 1b serum samples were acquired from a cohort of Irish women infected with HCV genotype 1b via contaminated anti-D immunoglobulin (277). cDNA sequences encoding full-length E1E2 were amplified from RNA extracted from Total IgG fraction using Expand High Fidelity PCR system (Roche) (Table 4.1, Fig 4.1a). Ten out of eleven samples successfully amplified expected ~1.7 kb E1E2 sequences. Several attempts to amplify E1E2 from 1b-6-1 were unsuccessful. Heterogeneity in the region of interest, from the signal peptide of E1 to the cytoplasmic domain of E2 presents a significant challenge in successful recovery of the PCR product. The resulting ten E1E2 sequences were cloned into the pcDNA3.1 V5his D-TOPO expression vector (Life Technologies) (Section 2.2.2.6c). The E1E2 proteins expressed in transfected HEK 293T cells were assessed by western blot (Section 2.2.3.4) (Fig 4.1b). E1E2 sequence from 1a-1-2 was not expressed whereas 1b-8-1 showed very low level of expression (Fig 4.1b).

Table 4.1: Sample characteristics used in the current study.

Genotype	No. of samples	AAV positive samples	Patient Identifier	Sample [#] identifier	Date of collection	Accession Number AAV	[$]VF-Fab
1a	3	+	P1a-1	1a-1-1	04/2007	KY031948	1a-1-1
		+	P1a-1	1a-1-2	08/2013	KY031950	1a-1-2
		+	P1a-1	1a-1-3	01/2014	KY031949	1a-1-3
1b	7	+	P1b-1	1b-1-2*	12/2013	KY031951	1b-1-2
		+	P1b-1	1b-1-3*	03/2014	KY031952	1b-1-3
		-	P1b-4	1b-4-1*	05/2014	KU888835[¥]	1b-4-1
		+	P1b-5	1b-5-1	04/2015	KU888834	1b-5-1
		-	P1b-6	1b-6-1*	06/2014	N/A	1b-6-1
		-	P1b-8	1b-8-1*	10/2014	KU888836[¥]	1b-8-1
		+	P1b-10	1b-10-1*	04/2015	KU888837	1b-10-1
3a	1	+	P3a-1	3a-1-1	12/2013	KY031953	3a-1-1

[#] Sample identifier: Genotype/Subtype-patient identifier- sample number

*Source of infection: contaminated anti-D immunoglobulin (277)

[¥] KU888835 and KU888836 targeted by VF-Fab1b-5-1 and VF-Fab1b-10-1 forming 2[o]AAV

[$] VF-Fab - Virus free Fab obtained from sera positive for AAV complex

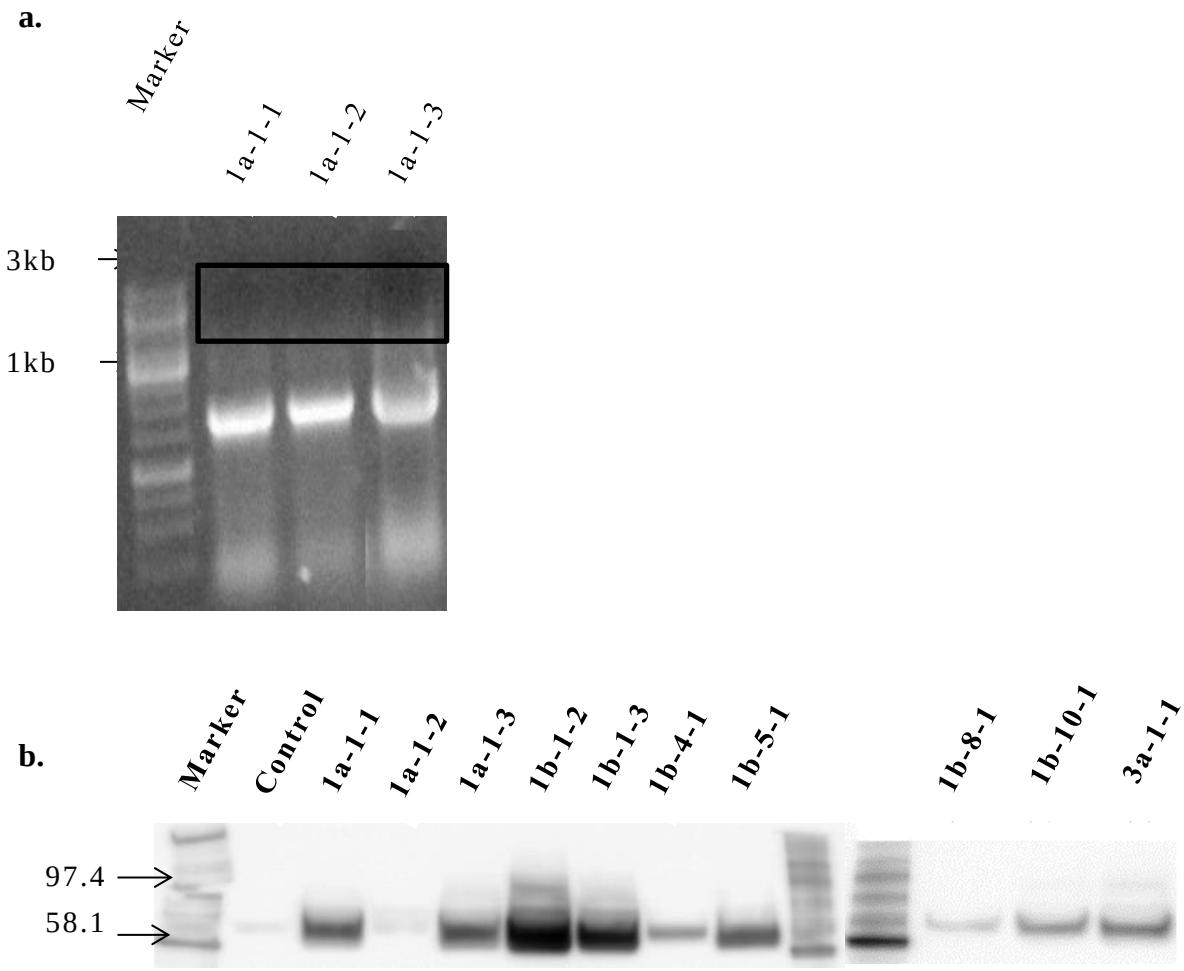

Figure 4.1 Cloning and Expression of E1E2 glycoprotein

a. PCR amplification of ten selected E1E2 sequences associated with AAV. RNA was extracted from patient sera and cDNA generated using specific primers (Section 2.3, Table 2.3). ~1.7kb PCR product was visualised on 1% agarose gel (shown in a black box). M: GeneRuler™ 1 kb DNA ladder (250-10,000 base pair). Only representative samples are shown in this figure **b.** Western blot of E2 glycoprotein (50 μg/well) detected with a mixture of anti-E2 MAbs AP33 (amino acid residues 412-423) and ALP98 (amino acid residues 644-651). M: Biotinylated molecular weight marker (6,500-180,000 Da).

4.3.2 Difference in the infectivity of HCVpp

Ten pseudotyped HCV particles were generated in this study according to the Bartosch *et al*. (2003) protocol (Section 2.2.3.5) (33). The pseudoparticles were screened for their infectivity, as previously described (Section 2.2.3.6) (258). No envelope control was used as a baseline to determine the infectivity of the pseudoparticles. Out of ten pseudotyped viruses, four were identified as being infectious in our entry assay (Fig 4.2). H77 pseudoparticles were included as a reference standard in each experiment (Fig 4.2). HCVpp1b-4-1 yielded a 10 fold greater relative luminescence value (RLU) than no envelope control in 48 well plate only (Section 2.2.3.6) (Fig. 4.2). HCVpp1b-1-2 were highly infectious yielding 657 times greater RLU followed by HCVpp1b-1-3 with 440 times greater RLU than no envelope control. Even though these pseudoparticles express E1E2 derived from patient P1b-1 at different time points, the difference in their infectivity was consistent from batch-to-batch. HCVpp1a-1-3 showed 61 fold higher RLU than the no envelope control (Fig 4.2). HCVpp1a-1-1, HCVpp1a-1-2, HCVpp1b-5-1, HCVpp1b-8-1, HCVpp1b-10-1 and HCVpp3a-1-1 were non-infectious as they did not pass the threshold set for infectivity (10 times higher than the no envelope control) (258). Lack of infectivity could be due to individual mutations in the E1E2 gene or the ratios of plasmids used in transfection and/or Murine Leukaemia virus reporter system (172).

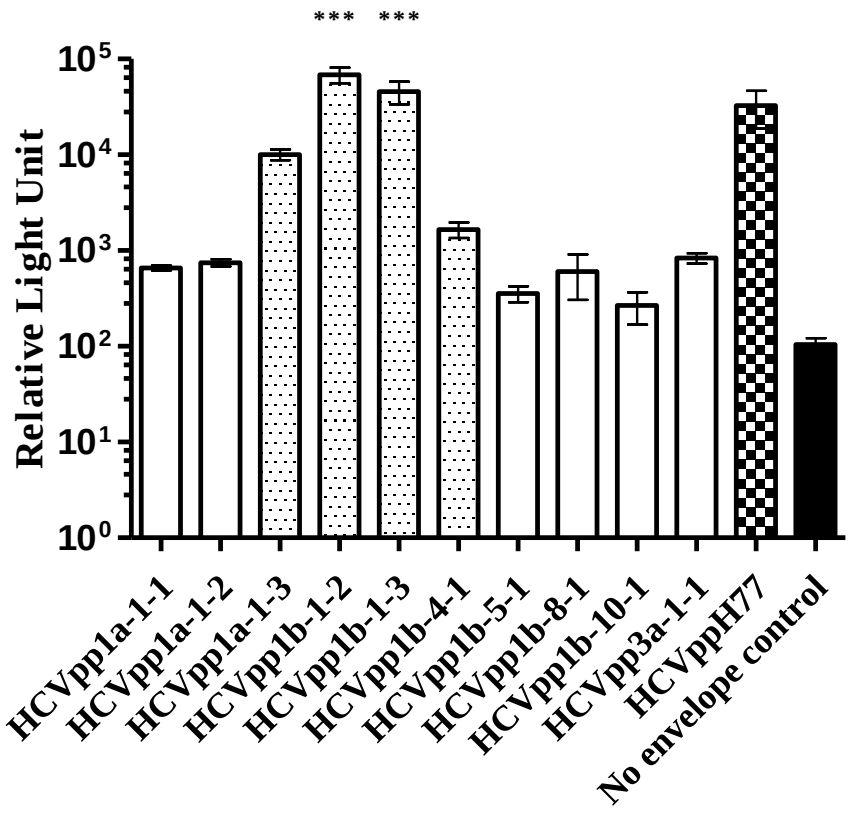

Figure 4.2: Varying degree of infectivity of E1E2 glycoproteins derived from AAV HCVpp

HCVpp generated from E1E2 associated with AAV showed varying degree of infectivity. HCVpp generated from phCMV-ΔC/E1/E2 H77 were used as reference HCVpp. No envelope control reproducibly gave RLU values less than 100, therefore a cut-off of 1000 RLU was used to determine the infectivity of a clone (*$p<0.0001$, one way ANOVA, Dunnett's posthoc test). phCMV-ΔC/E1/E2 H77 was used as a reference clone. From a panel of 1°AAV and 2°AAV E1E2, four pseudoparticles were found to be infectious (dotted boxes). The X axis depicts HCVpp clones in this study. Y axis infectivity in RLU (Log10). Black box represents no envelop control Error bars indicate standard deviation. All the experiments were repeated four times with three technical replicates each. The RLUs were normalised with the values from no envelop control.

4.3.3 Analysis of E1E2 glycoprotein from the cell extracts

100 µg of HEK cell extracts of all ten E1E2 clones were used to further characterise the reactivity of MAb AP33, MRCT10 (HCV envelope glycoprotein E2 fragment 412-423 with humanised and affinity-matured antibody, 4HS6-PDB) and VF-Fab in GNA (*Galanthus nivalis)* capture ELISA (Section 2.2.3.8). The absorbance range for GLOMAX®-MULTI has a photometric measuring range of 0-4 with the OD accuracy of <2% at OD 4. AP33 is mouse MAb which targets an epitope within amino acid region 412-423 in the E2 glycoprotein (257). Equivalent binding efficiency in ELISA was observed when probing GNA captured E2 with AP33 and its humanised version MRCT10 to all the glycoproteins (Fig 4.3a). Cell extracts from HCVpp1a-1-2, HCVpp1b-4-1 and HCVpp1b-8-1 showed a low binding signal (O.D. 0.033-0.073) for AP33 which mirrors the western blot results for these E1E2 glycoproteins (Figs 4.1b, 4.3a). Moreover, all the VF-Fab were able to bind to the glycoproteins in the HEK cell lysate (Fig 4.3b-d). HCVpp1a-1-2 showed a low signal for VF-Fab from genotype 1a (O.D. 0.14-0.40) (Figs 4.3a and 4.3b). VF-Fab derived from genotype 1a showed higher affinity towards cell extracts from HCVpp1a-1-1, HCVpp1a-1-3, HCVpp1b-1-2, HCVpp1b-1-3 and HCVppH77 (O.D. 0.55-1.96) (Fig 4.3b). Whereas VF-Fab derived from genotype 1b showed more affinity (O.D. 0.79-2.00) towards cell extract from HCVpp1b-1-2 and 1b-1-3 which were extracted from cells infected with HCVpp from genotype 1b (Fig 4.3c). VF-Fab1b-5-1 appeared to be highly efficient (O.D. 0.02-2.09) in binding to all the E1E2 extracts in this study (Fig 4.3c). Similarly, VF-Fab derived from 3a-1-1 showed highest binding signal (O.D. 0.88) to HEK extract from HCVpp3a-1-1 (Fig 4.3d). Equal amounts of HEK cell extracts were used to analyse the expression of the E1E2 glycoproteinp (172). , this cannot be directly correlated to the infectivity of the HCVp – you need to develop this a little more or else leave out

Figure 4.3

a.

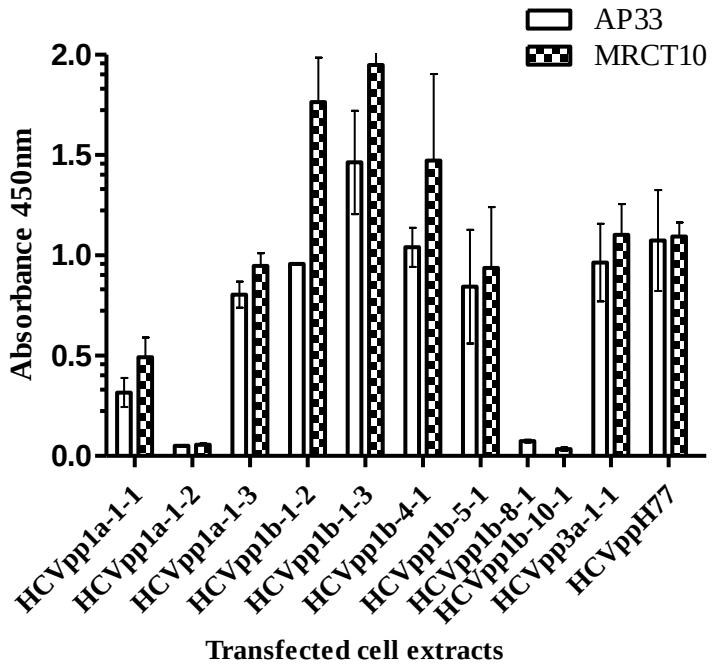
AP33
MRCT10
Absorbance 450nm
2.0
1.5
1.0
0.5
0.0
HCVpp1a-1-1
HCVpp1a-1-2
HCVpp1a-1-3
HCVpp1b-1-2
HCVpp1b-1-3
HCVpp1b-4-1
HCVpp1b-5-1
HCVpp1b-8-1
HCVpp1b-10-1
HCVpp3a-1-1
HCVppH77
Transfected cell extracts

b.

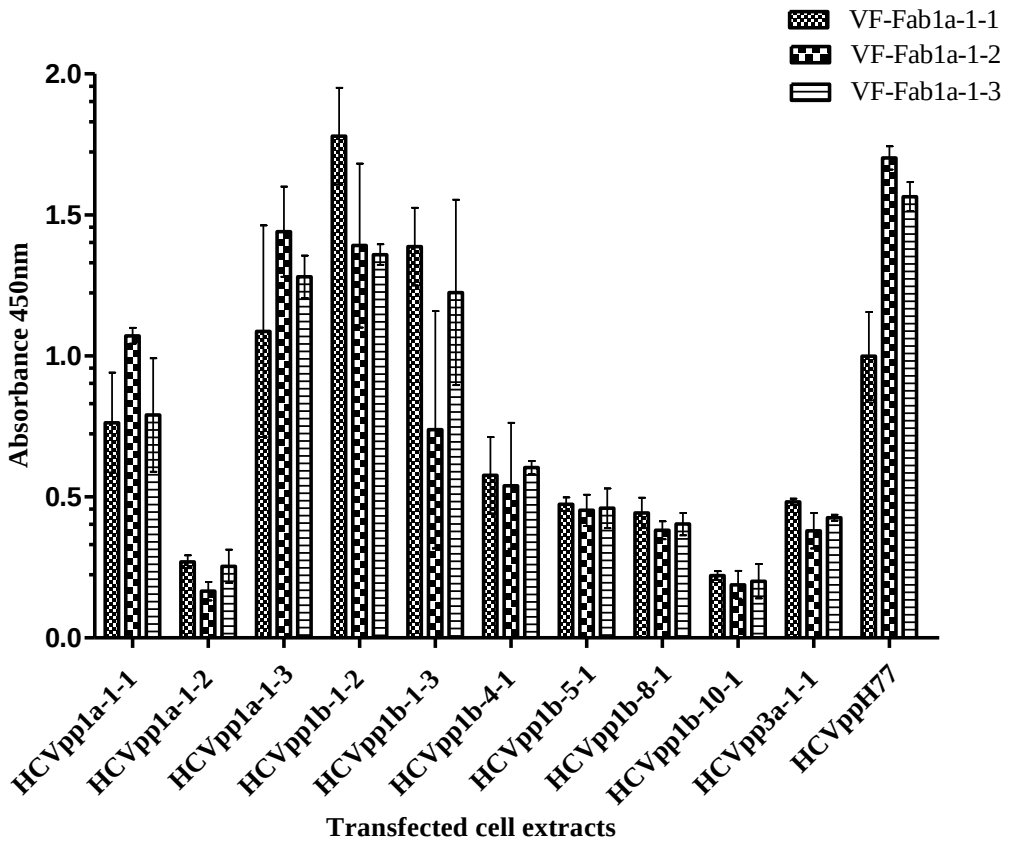
VF-Fab1a-1-1
VF-Fab1a-1-2
VF-Fab1a-1-3
Absorbance 450nm
2.0
1.5
1.0
0.5
0.0
HCVpp1a-1-1
HCVpp1a-1-2
HCVpp1a-1-3
HCVpp1b-1-2
HCVpp1b-1-3
HCVpp1b-4-1
HCVpp1b-5-1
HCVpp1b-8-1
HCVpp1b-10-1
HCVpp3a-1-1
HCVppH77
Transfected cell extracts

c.

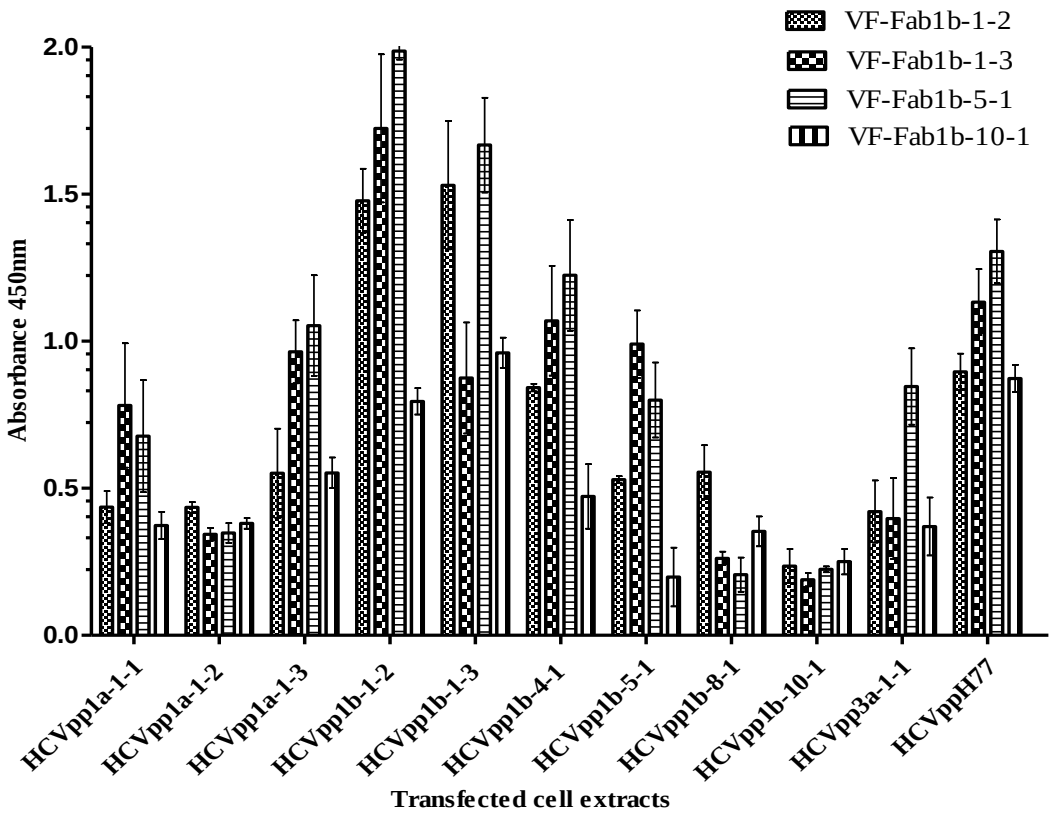
VF-Fab1b-1-2
VF-Fab1b-1-3
VF-Fab1b-5-1
VF-Fab1b-10-1
Absorbance 450nm
2.0
1.5
1.0
0.5
0.0
HCVpp1a-1-1
HCVpp1a-1-2
HCVpp1a-1-3
HCVpp1b-1-2
HCVpp1b-1-3
HCVpp1b-4-1
HCVpp1b-5-1
HCVpp1b-8-1
HCVpp1b-10-1
HCVpp3a-1-1
HCVppH77
Transfected cell extracts

d.

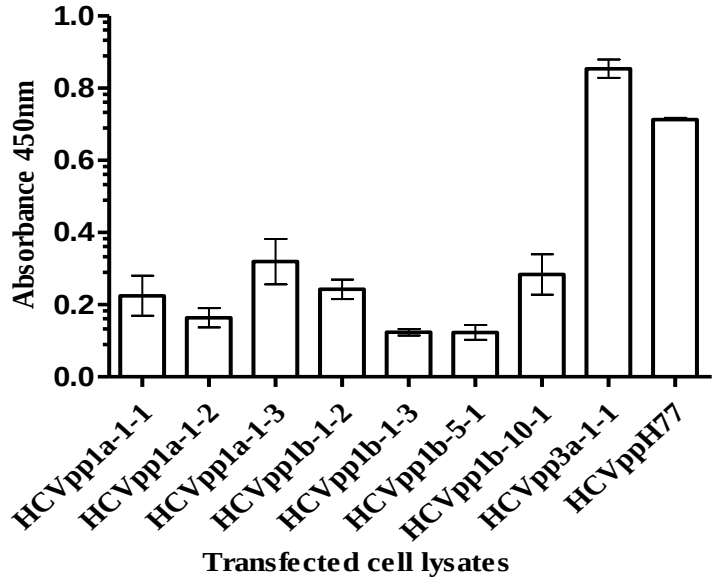
Absorbance 450nm
1.0
0.8
0.6
0.4
0.2
0.0
HCVpp1a-1-1
HCVpp1a-1-2
HCVpp1a-1-3
HCVpp1b-1-2
HCVpp1b-1-3
HCVpp1b-5-1
HCVpp1b-10-1
HCVpp3a-1-1
HCVppH77
Transfected cell lysates

Figure 4.3: GNA capture ELISA of transfected HEK cell extracts

a. Cell extracts of HEK (100 µg) 293T co-transfected with MLV packaging vector, pcDNA3.1 expressing E1E2 (different genotypes, Table 4.1) were analysed for the presence of E2 by GNA capture ELISA using MAb AP33 (at 1µg/ml, 1:10,000) and humanised version of AP33, MRCT10 (1:10,000) **b.** VF-Fab obtained from genotype 1a **c.** VF-Fab genotype 1b (50µg/ml) **d.** VF-Fab genotype 3a. Error bars represent standard deviation. *MRCT10 experiments were done at CVR, University of Glasgow, UK. MRCT10 was not available for HCVpp1b-8-1 and HCVpp1b-10-1.

4.3.4 Mutations at 292 in the E1 and 388 in the HVR1 of glycoprotein modify infectivity of HCVpp1b-1-3

It was observed that HCVpp1b-1-2 was 1.5 times more infectious than HCVpp1b-1-3. It is interesting to note that these 1b HCVpp expressing E1E2 glycoproteins were obtained from P1b-1 at two different time points (Table 4.1). However, HCVpp1b-1-2 differed from HCVpp1b-1-3 by only three amino acids at positions 292 (C-terminal of E1), 388 and 395 (HVR1 of the N-terminal of E2) in the E1E2 glycoprotein sequence and yet showed differences in the infectivity (Fig. 4.4a). It was hypothesised that these three amino acid correlates were responsible for the difference in their infectivity. As a reference range, infectivity of HCVpp1b-1-2 was set to 1. Individual mutants, 1b-1-2$_{\mathbf{I388V}}$ and 1b-1-2$_{\mathbf{V395A}}$, generated 1.34 and 2.12 fold greater levels of infectious particles compared to that of HCVpp1b-1-2 respectively (Fig 4.4b). These results indicated that alanine substitution at position 395 plays a more significant role in enhancing HCVpp infectivity *in vitro* than wild type valine. A mutation in the E1 at T292A dramatically decreased the HCVpp infectivity by 0.74 fold for $_{\mathbf{T292A}}$HCVpp1b-1-2$_{\mathbf{I388V}}$ and 1.04 fold $_{\mathbf{T292A}}$HCVpp1b-1-2$_{\mathbf{V395A}}$ in comparison to the individual mutant clones HCVpp1b-1-2$_{\mathbf{I388V}}$ and HCVpp1b-1-2$_{\mathbf{V395A}}$ (Fig 4.4b). Importantly, the $_{\mathbf{T292A}}$HCVpp1b-1-2$_{\mathbf{DM}}$ clone (0.76 fold) closely replicates the infectivity of the HCVpp1b-1-3 (0.83 fold) wild type (Fig 4.4b). These results indicate a potential role for the amino acid at position 292 (within E1) in governing the degree of infectivity *in vitro* (Fig 4.4a). Simultaneously 162 GenBank sequences for genotype 1a, 1b, 3, 4, 5 and 6 (GT 1a=44, GT 1b= 21, GT 2=19, GT 3=21, GT4=20, GT 5=17 and GT 6=20) were compared to E1$_{265\text{-}296}$ sequence from HCVpp1b-1-3. Out of 159 sequences, GenBank sequences of 78 clones used by Urbanowicz and colleagues for neutralisation assay were included in the analysis (GenBank accession numbers in

appendix 1) (258). At position $E1_{292}$ amino acid T was replaced by I (5.06%), V (1.89%) in genotype 2 and with S (11.3%) in genotype 4 (Fig 4.4a). Only our clone HCVpp1b-1-3 harboured T292A substitution. This bioinformatics analysis revealed that T292 is a nearly conserved amino acid in rest of the genotypes. Subsequent western blotting analysis of HEK extracts of the mutated isolates revealed decreased expression of E2 glycoprotein for clones HCVpp $^{\mathbf{T292A}}$1b-1-2$^{\mathbf{I388V}}$, HCVpp $^{\mathbf{T292A}}$1b-1-2$^{\mathbf{V395A}}$, HCVpp 1b-1-2$^{\mathbf{DM}}$ and HCVpp $^{\mathbf{T292A}}$1b-1-2$^{\mathbf{DM}}$ as compared to the wild type HCVpp1b-1-2 and HCVpp1b-1-3 (Fig 4.5).

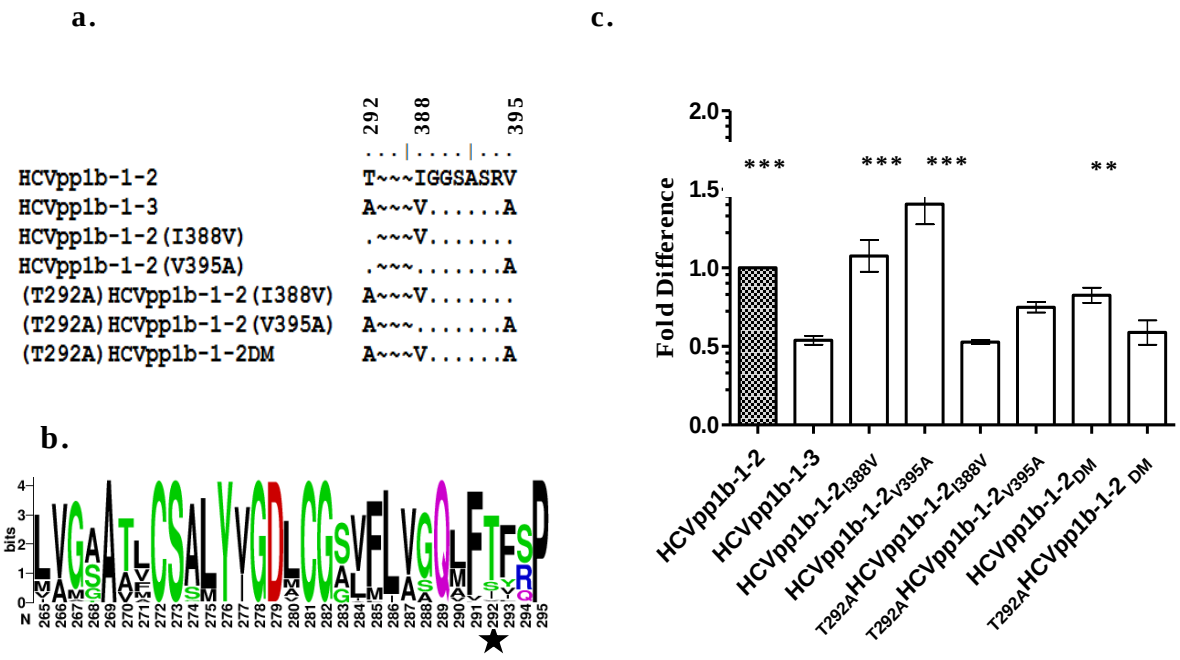

Figure 4.4: Site directed mutagenesis of HCVpp1b-1-2

a. Amino acid sequence alignment of wild type HCV1b-1-2, HCVpp1b-1-3 and sequential site directed mutagenesis at positions 292 in the E1, 388 and 395 in the HVR1 of E2 glycoprotein **b.** Amino acid Weblogo of partial E1 glycoprotein sequence (residues 265-296, ref: AF011751). Black: non polar, Green: polar, Red: acidic, Blue: basic and Purple: neutral. The x-axis depicts the amino acid position and the height of the individual letter reflects relative frequency of each amino acid at that position. Star below the x-axis denotes a conserved amino acid threonine (T) at position 292 in E1 **c.** Six mutant clones were generated for highly infectious HCVpp1b-1-2 as follows, 1b-1-2$_{I388V}$, 1b-1-2$_{V395A}$, $_{T292A}$1b-1-2$_{I388V}$, $_{T292A}$1b-1-2$_{V395A}$, 1b-1-2$_{DM}$ and $_{T292A}$1b-1-2$_{DM}$ (DM corresponds to double mutant $I_{388}V$ and $V_{395}A$). Wild type clones HCVpp1b-1-2 and HCVpp1b-1-3 were used as controls. Mutation in the E1 glycoprotein reduces the infectivity of HCVpp1b-1-2. Pairwise mutation at position 292 and 388 ($_{T292A}$1b-1-2$_{I388V}$) and $_{T292A}$1b-1-2$_{DM}$ corresponds to wild type HCVpp1b-1-3 which was less infectious in comparison to HCVpp1b-1-2. Pairwise mutation at position 292 and 388 ($_{T292A}$1b-1-2$_{I388V}$) and $_{T292A}$1b-1-2$_{DM}$ corresponds to wild type HCVpp1b-1-3 (*p<0.0001, one way ANOVA, Dunnett's posthoc test). All the experiments were repeated four times with three technical replicates each. The X axis depicts infectious mutant HCVpp clones in this study. Y axis denotes infectivity in fold difference. ~~~ denotes the break in the amino acid sequence for the presentation purpose. Error bars indicated standard deviation.

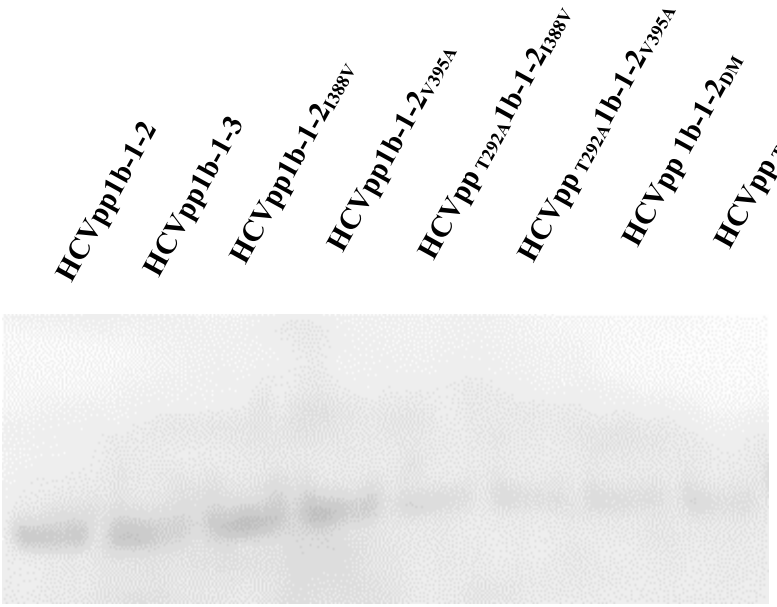

Figure 4.5: Western blot analysis of HEK extracts expressing wild type and mutated E1E2 glycoproteins.

HEK extracts (50µg/well) were analysed on 4-12% bis-tris gradient gel in reducing condition followed by transferring onto a Nitrocellulose membrane. DM corresponds to double mutant $I_{388}V$ and $V_{395}A$. The blot was developed using a primary mouse MAb AP33 and ALP98 (a kind gift from Dr. Arvind Patel, University of Glasgow, Scotland) and secondary HRP labelled goat anti-mouse antibody. It was observed that proteins with E1 mutation showed low level of expression as compared to individual mutants. Wild type HCVpp1b-1-3 harbouring all three mutations showed high level of protein expression than $_{T292A}$1b-1-2$_{DM.}$ Error bars represent standard deviation.

4.3.5 HCVpp entry is CD81 dependent

It has been shown that CD81 receptors play a key role in the entry of HCV 5µl (289). AntiCD81 antibody (BD, Pharmingen, JS-81) can block the entry of viral particles. In this study, antiCD81 antibody was used to test the role of CD81 in infectivity of HCVpp in three different treatment groups (5µg/ml**)** (289).

1. HCVpp – HuH7 cells were infected with different HCVpp without antiCD81 antibody

2. HCVpp+antiCD81 - antiCD81 antibody was added 1 h post HCVpp inoculation

3. AntiCD81+HCVpp - antiCD81 antibody was added 1 h prior to HCVpp inoculation

Addition of antiCD81 antibodies prior to HCVpp inoculation rendered greater reduction the infectivity as compared to the group where antibodies were added 1 h post inoculation (Fig 4.6). This data implies that antiCD81 blocks the CD81 receptors on the Huh7 cells affecting the cellular entry of HCVpp.

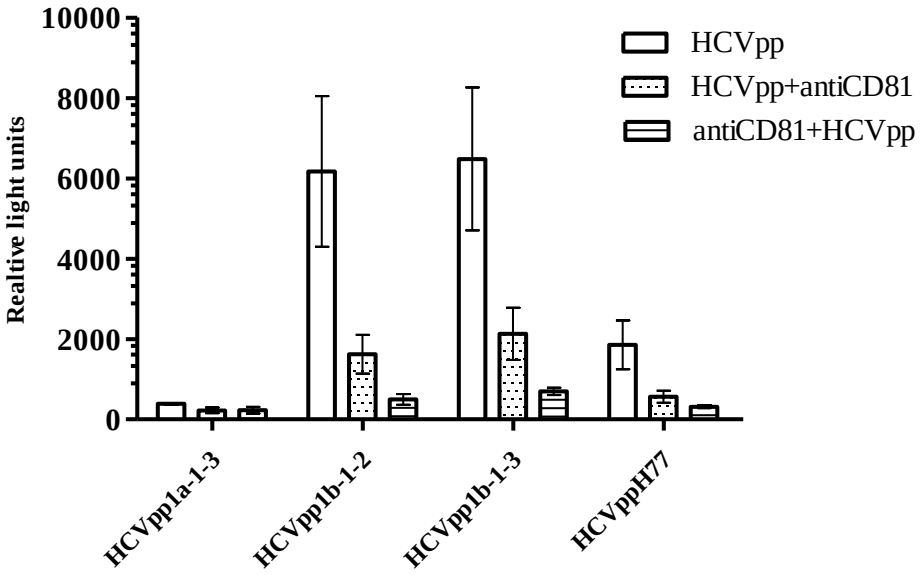

Figure 4.6: antiCD81 antibody (5µg/ml) reduces HCVpp infection dependent

HCVpp1a-1-3, HCVpp1b-1-2, HCVpp 1b-1-3 and HCVppH77 were used to infect Huh7 cells. Huh7 cells were treated in three different treatment groups. **a**. HCVpp – Huh7 cells were infected with different HCVpp without antiCD81 antibody **b.** HCVpp+antiCD81 – antiCD81 antibody was added 1 h post HCVpp inoculation **c.** antiCD81+HCVpp – antiCD81 antibody was added 1 h prior to HCVpp inoculation. In treatment groups' **b** and **c** HCVpp infectivity was reduced as a result of CD81 receptor blocking. Error bars represent standard deviation.

4.4 Discussion

Surface glycoprotein E1E2 play a key role in the HCV cell entry and are the major targets of neutralising antibodies (nAbs) (63). Hepatitis C virus pseudoparticle system (HCVpp) is robustly used to study the neutralisation epitopes and conserved host cellular receptors involved in entry (256). To date nAb response is measured in cell culture using HCVpp and HCVcc bearing glycoproteins of prototype strains and which does not reflect the diversity of the virus population targeted by the host immune system (33, 51, 165, 256). Generation of HCVpp involves co-transfection of HEK293T cells with a retroviral vector harbouring Gag-Pol gene, vector carrying a reporter gene and a vector that encodes E1E2 glycoproteins of HCV (33, 256).

In this study HCVpp were generated using sequence information from the clonotypic antibody bound virus population (Table 4.1). We were able to amplify, clone and express ten full length E1E2 which were targeted by host antibodies however, not all were infectious in the HCVpp system. Only 40% of glycoprotein clones yielded infectious HCVpp (Fig 4.2). Generation of infectious psuedoparticles from a diverse HCV population presents some challenges. It has been previously reported that for glycoproteins isolated from chronic and acute infections, only 24-27% yielded infectious clones (258). Recently, Urbanowicz *et al.* (2015) screened 883 E1E2 clones from 3909 patients. Of these clones, they identified 493 clones with E1E2 ORF; however, only 118 clones (24%) were infectious in the infectivity assay (258). Further investigation into determinants of HCVpp infectivity lead to the following outcomes, i) different ratios of packaging vectors and glycoprotein expression constructs largely influences infectivity which could be due to the difference in the incorporation of glycoproteins into pseudoparticles ii) species of retroviral packaging.

vector used (172). Increasing the concentration of glycoprotein expression vector beyond threshold, however, lead to reduced infectivity as a result of likely increase in the autophagy of expressed proteins becoming toxic to the producer cells or reduction in expression of capsid protein causing decrease in the budding of retrovirus (172). Additionally, when the species of packaging vector was changed, some HCVpp which were infectious in MLV-based HCVpp system turned out to be non-infectious in HIV-1 based packaging construct while some were equally infectious in both the packaging vectors (172). In MLV-based vector, HCV E1E2 glycoproteins are likely to be incorporated in an intracellular compartment. E1E2 polymorphism could influence their cellular localisation resulting into difference in the incorporation into particles (172). In case of HIV-1 as a packaging vector, the E1E2 expression construct can alter the site of Gag/glycoprotein co-localisation (290), resulting in decreased levels of intracellular envelope (291). Nevertheless, role of genetic variations of the E1E2 glycoprotein in localisation of envelope protein with Gag needs to be studied in more detail. Factors such as concentration and species of the packaging vector used to express the E1E2 sequence and polymorphism of the glycoprotein may influence the difference in the infectivity of the HCVpp observed in our experiments. The technical difficulties in generating infectious HCVpp can be overcome by implementing aforementioned methods by Urbanowicz *et al.* (2016). However, no significant difference was observed in the neutralisation curves for HCVpp generated with altered plasmid ratios (172).

HCVpp1b-1-2 and HCVpp1b-1-3 were closely related but differed in their infectivity (Fig 4.4b). Urbanowicz *et al.* (2016) have shown that difference in the infectivity of closely related E1E2 clones is due to isolate specific mutations in these genes (172). Site directed mutagenesis in current study showed that mutations in the HVR1 of E2

maintained the physicochemical properties by replacing hydrophobic amino acid ($V_{395}A$ and $I_{388}V$) and thereby infectivity of HCVpp (Fig 4.4). Pe´rez-Berna *et al.* (2006) showed that residues 265-296 in the E1 glycoprotein are hydrophobic and have membranotropic characteristics making them a candidate for membrane fusion (292). Weblogo of residues from 265-296 (150 GenBank sequences) revealed that position T_{292} was conserved (Fig 4.4a). In the E1 glycoprotein of HCVpp1b-1-3, a polar amino acid (T) was replaced by a hydrophobic (A) amino acid at position 292 which might have affected the membrane fusion ability of E1. It was also observed that pairwise mutation at position 292 and 388 lead to decrease in the HCVpp infectivity similar to the clone harbouring all three mutations (HCVpp1b-1-3). Western blot analysis of HEK extracts (from which HCVpp were generated) showed decreased expression of HCVpp1b1-1-2 mutants harbouring T292A substitution (Fig 4.5). However, it has been shown that expression of glycoprotein cannot be directly correlated with their infectivity (172). In the absence of well-defined structure for E1 and the hypervaraible region in the E2, this data provides an insight into probable engagement of $E1_{292}$ and $E2_{388}$ in the infectivity of viral particle (Fig 4.4b). The observed substitutions outside HVR1 may have an impact on the variant's fitness at the entry level. In this instance, our data supports the hypothesis that these amino acid coordinates play an important role in the infectivity of HCVpp1b-1-3 specifically. This result also highlights the sensitivity of HCVpp system to the small but relevant genetic change in the E1E2 glycoprotein influences infectivity of pseudoparticles (44, 172).

E1E2 glycoproteins from the clarified lysates of transfected HEK293T cells were captured onto GNA lectin (Sigma Aldrich) coated microtiter plates and then detected with the anti-E2 mouse MAb AP33, MRCT10 and a panel of VF-Fab (Fig 4.3). The GNA capture enzyme immunoassay, validated that all the clones were expression

competent (Fig 4.3). Isolates HCVpp1a-1-2, HCVpp1b-8-1 and HCVpp-1b-10-1 a low absorbance signal for AP33, MRCT10 and VF-Fab likely because of no detectable or low levels of E2 resulting into non-infectious HCVpp (Fig 4.1b). The highest reactivity was observed between VF-Fab obtained from the homologous genotype, possibly due to genotype-restricted targeting of the epitopes (Fig 4.3). VF-Fab1a-1-3, VF-Fab1b-1-2, VF-Fab1b-1-3 were able to recognise all the E1E2 lysates, this cross-reactivity likely resulted from targeting the conserved epitopes in the glycoprotein (Fig 4.3). Epitope mapping study might help in knowing the conserved epitopes targeted by these VF-Fab preparations. However, why some of the HCVpp expressing E1E2 glycoproteins were non-functional in entry assay is not clear (Figs 4.1, 4.3).

Many studies have shown involvement of CD81 receptor in the HCV entry. In the liver CD81 is expressed on hepatocytes and sinusoidal endothelium. It has been shown that antibodies against large extracellular loop of CD81 inhibit the entry of HCVpp, HCVcc and serum-derived HCV (32, 42, 44, 69, 293). It has been shown that CD81 binding region of the E2 glycoprotein encompasses discontinues epitopes and requires correctly folded E2 for the interaction to occur (294). Recent crystal structure by Kong *et al.* (2013) has established that several amino acid residues (427–430 and 442–444) in the frontal layer of E2 and residues 523, 526-531, 535, 538, 540 and 550 in CD81 binding loop are involved in CD81 interaction (32). Hence, antibodies blocking CD81 interaction have garnered much attention in the Hepatitis C research. Ectopic expression of CD81 receptor on the non-permissive cell lines like HepG2, HH29 cells and also some sub-clones of Huh-7 cells enables entry of HCVpp and HCVcc, underlining involvement of CD81 receptor in HCV cell entry (43, 91, 295, 296). Numerous studies involving bNAbs have shown that HCVpp, HCVcc are neutralised by blocking the CD81 interaction with the E2 glycoprotein (32, 42, 44, 69, 293).

Similarly, in this study antiCD81 antibodies were used to block the entry of HCVpp in Huh7 cells. Our data showed that even though anti-CD81 antibodies were added 1 h post HCVpp inoculation, they still reduced the infectivity by interfering with the CD81 dependent entry (Fig 4.6) (43, 93, 295, 297, 298). It will be interesting to study the involvement of patient derived antibodies in targeting of CD81 epitopes in the clonotypic antibody associated HCVpp (Section 5.3.4, 5.4).

In summary, here we have shown that not all the E1E2 sequences which were targeted by humoral immune system were infectious in the HCVpp system. Nonetheless, the E2 glycoprotein was expressed in both infectious and non-infectious HCVpp. Small but relevant genetic variation in the E1E2 glycoprotein can modify the infectivity of the closely related sequences underscoring the potential role of $E1_{292}$ and $E2_{388}$ in the HCVpp infectivity.

Chapter 5

5. Neutralisation and epitope mapping using patient derived VF-Fab

5.1 Introduction

E1E2 glycoproteins are major target of nAbs. Various research studies have shown that MAbs target amino acid residues 396-424, 412-424, 436-447 and 523-540 in the E2 glycoprotein (32, 61, 172, 173). Furthermore, Wong *et al.* (2014) observed a multi-epitope specific antibody response in the sera analysed from individuals vaccinated with recombinant E1E2 glycoprotein (221). In the previous chapter we showed that not all the E1E2 glycoproteins isolated from antibody associated virus are infectious in a pseudoparticle system. Generating reliably infectious HCVpp is very challenging (172, 258). However, the HCVpp system is a robust i*n vtiro* model to study the neutralisation potential of patient derived and monoclonal antibodies. In this chapter we tested the hypothesis that VF-Fab obtained from AAV positive sera are neutralising in nature and target different epitopes in the E1E2 glycoprotein. Based on the available anti-HCV monoclonal nAb mapping information we selected amino acid region 384-619 for conformational epitope mapping**.**

To examine this hypothesis we,

- Carried out neutralisation assay with VF-Fab obtained from AAV positive sera
- Carried out neutralisation assay with post proteinase K treated Total IgG obtained from AAV negative sera
- Mapped epitopes in the amino acid region 364-430 in AAV using patient derived VF-Fab
- Based on the available anti-HCV monoclonal nAb mapping information mapped amino acid region 384-619 for conformational epitope mapping using patient derived VF-Fab.

- Combined the antigenic specificity of different VF-Fabs to achieve a greater neutralisation range in HCVpp expressing AAV associated E1E2 glycoproteins.

Amruta S. Naik, Ania Owsianka, Brendan A. Palmer, Ciaran J. O'Halloran**,** Nicole Walsh, Orla Crosbie, Elizabeth Kenny-Walsh, Arvind H. Patel, Liam J. Fanning **Reverse epitope mapping of the E2 glycoprotein in antibody associated Hepatitis C Virus,** PLOS ONE-PONE-D-17-02203R1 *In Press*

5.2 Methods

Following methods were used to test the hypothesis,

5.3 Results

5.3.1 Neutralisation of antibody associated E1E2 HCVpp

In this chapter, in order to determine the neutralisation potency of patient derived virus free Fabs (VF-Fab), the source sera were treated with proteinase K (Section 2.2.3.7). The sera were obtained from the same patients who were positive for presence of AAV (Table 5.1). Neutralisation assays were carried out to assess whether patient derived VF-Fabs block the virus attachment and entry of HCVpp into Huh7 cells. HCVpp generated from phCMV-ΔC/E1/E2 H77 were used as reference. Initially, a neutralisation assay for HCVppH77 was carried out using defined concentrations of VF-Fab ranging from 0.006-0.400 mg/ml of VF-Fab1b-5-1 and VF-Fab1b-10-1 (Fig 5.1). Percentage infectivity is expressed as the average of three independent experiments. VF-Fab1b-5-1 at the concentration of 0.167 mg/ml was highly neutralising, reducing the HCVppH77 infection by 85% (Fig 5.1). VF-Fab1b-10-1 reduced HCVppH77 infection by 75% at 0.400 mg/ml (Fig 5.1). HCVpp1b-4-1 showed 10 fold greater relative light values (RLU) than the no envelope control. VF-Fab1b-5-1 reduced HCVpp1b-4-1 infection by 88% at 0.167 mg/ml (Fig 5.2). VF-Fab1b-10-1 showed 72% of inhibition of infection for HCVpp1b-4-1 at 0.400 mg/ml (Fig 5.2).

Similarly, eight VF-Fabs (0.006-0.400 mg/ml), from genotype 1a (n=3), genotype 1b (n=4) and genotype 3a (n=1) were each tested for neutralisation of HCVppH77, HCVpp1a-1-3, HCVpp1b-1-2, HCVpp1b-1-3. The IC_{50} are presented in Table 5.2 and the corresponding neutralisation curves are presented in Fig 5.2. The panel of patient derived VF-Fab cross-neutralised genotype 1 HCVpp efficiently. VF-Fab1a-1-2, VF-Fab1b-1-2, VF-Fab1b-1-3, VF-Fab1b-5-1 and VF-Fab1b-10-1 showed greatest neutralisation breadth, reducing the infection, by at least 50% for all the HCVpp clones

(Fig 5.2). The neutralisation sensitivity to each VF-Fabs varied across the HCVpp panel, with HCVpp1b-1-3 being highly neutralisation sensitive (relative infection range 2-32%), HCVpp1a-1-3, HCVpp1b-1-2 being moderately neutralisation resistant (relative infection range 10-65%) to each of the tested VF-Fabs. HCVpp generated from phCMV-ΔC/E1/E2 H77 were resistant to the VF-Fab1a-1-1 and VF-Fab3a-1-1 neutralisation and showed varying degree of sensitivity to the VF-Fab1a-1-2 (81%), VF-Fab1a-1-3 (66%), VF-Fab1b-1-2 (62%), VF-Fab1b-1-3 (66%) and VF-Fab1b-10-1 (73%) (Fig 5.2). VF-Fab1b-5-1 at the concentration of 0.200 mg/ml and VF-Fab1b-10-1 at 0.400 mg/ml were highly neutralising inhibiting the infectivity of all the HCVpp clones by average 75-96% (Fig 5.2). Despite showing highest neutralisation potential, unique fit for VF-Fb1b-5-1 was not identified. This can be corrected by including either higher concentration of VF-Fab or constraining the values for the top and/or bottom parameters (GraphPad Prism guidelines). However, at 200 μg/ml concentration VF-Fab1b-5-1 reduced the infectivity by average 80-98% in HCVpp. In this situation using concentration higher than 200 μg/ml was not ideal. Hence, values for the bottom parameter for VF-Fab1b-5-1 were constrained to zero.

Table 5.1: Sample characteristics used in the current study

Genotype	No. of samples	AAV positive samples	Patient Identifier	Sample [#] identifier	Date of collection	Accession Number AAV	[$]VF-Fab
1a	3	+	P1a-1	1a-1-1	04/2007	KY031948	1a-1-1
		+	P1a-1	1a-1-2	08/2013	KY031950	1a-1-2
		+	P1a-1	1a-1-3	01/2014	KY031949	1a-1-3
1b	7	+	P1b-1	1b-1-2*	12/2013	KY031951	1b-1-2
		+	P1b-1	1b-1-3*	03/2014	KY031952	1b-1-3
		-	P1b-4	1b-4-1*	05/2014	KU888835[¥]	1b-4-1
		+	P1b-5	1b-5-1	04/2015	KU888834	1b-5-1
		-	P1b-6	1b-6-1*	06/2014	N/A	1b-6-1
		-	P1b-8	1b-8-1*	10/2014	KU888836[¥]	1b-8-1
		+	P1b-10	1b-10-1*	04/2015	KU888837	1b-10-1
3a	1	+	P3a-1	3a-1-1	12/2013	KY031953	3a-1

AAV: Antibody associated virus

[#] Sample identifier: Genotype/Subtype-patient identifier- sample number

*Source of infection: contaminated anti-D immunoglobulin (277)

[¥]E1E2 sequences were obtained from 2[o]AAV (Table 3.2)

[$] VF-Fab - Virus free Fab obtained from sera positive for AAV complex

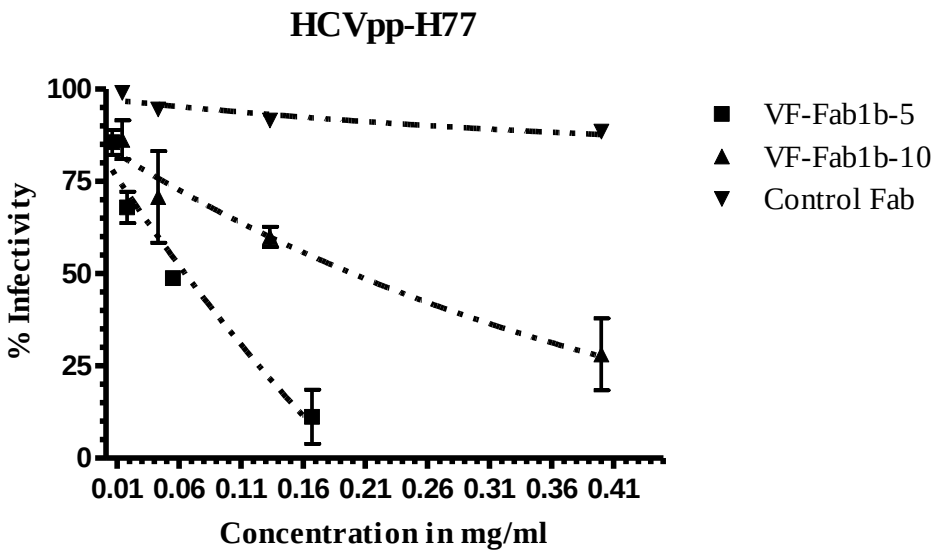

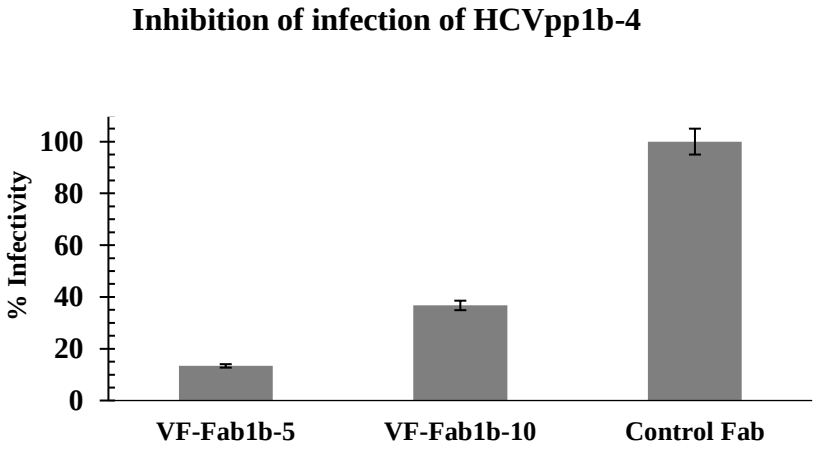

Figure 5.1: Neutralisation of E1E2- HCVpp isolated from antibody associated virus

Neutralisation curve for HCVpp-H77 shows 0.167 mg/ml and 0.400 mg/ml as the most effective concentration to inhibit the HCVpp infection for VF-Fab1b-5-1 and VF-Fab1b-10 by 85% and 75% respectively **b.** VF-Fab1b-5 at 0.167 mg/ml inhibits 88% of HCVpp1b-4 infection whereas VF-Fab1b-10 at 0.400 mg/ml inhibits only 72% of infection. Each experiment was repeated three times with two technical replicates. Error bars indicate standard deviation.

Figure 5.2

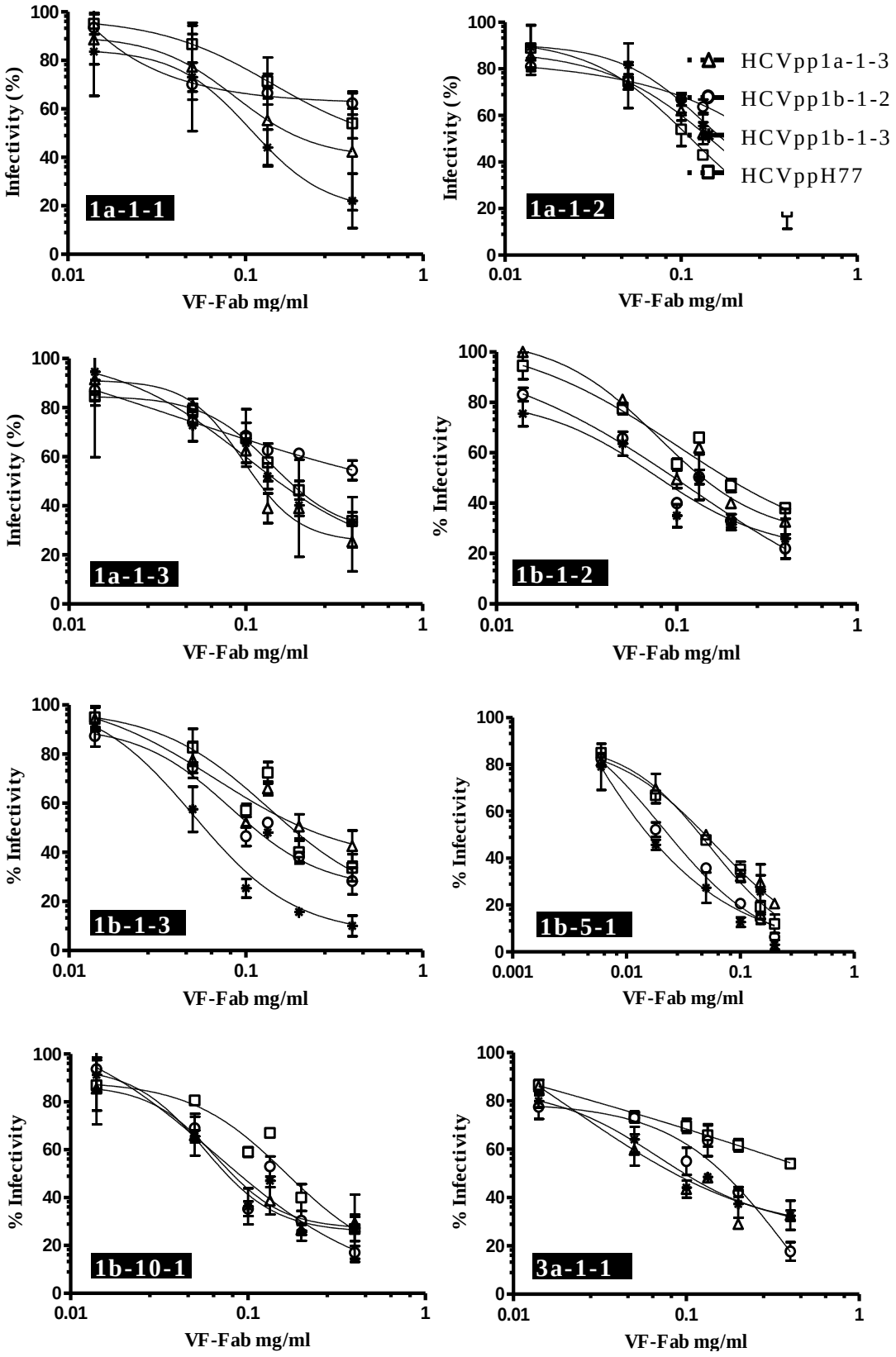
HCVpp1a-1-3
HCVpp1b-1-2
HCVpp1b-1-3
HCVppH77
1a-1-1
1a-1-2
1a-1-3
1b-1-2
1b-1-3
1b-5-1
1b-10-1
3a-1-1
Infectivity (%)
% Infectivity
VF-Fab mg/ml

Figure 5.2: Patient derived VF-Fab display varying degree of neutralising ability to different E1E2 HCV pseudoparticles

VF-Fab were obtained from antibody-virus complex. VF-Fab1a-1-1, VF-Fab1a-1-2, VF-Fab1a-1-3 were purified from a patient infected with HCV genotype 1a. VF-Fab1b-1-2, VF-Fab1b-1-3 and VF-Fab1b-10-1 were purified from a patients infected with genotype 1b whose common source of infection was HCV infected anti D immunoglobulin (30). VF-Fab1b-5-1 were purified from a blood transfusion patient infected with genotype 1b. VF-Fab3a-1-1 was purified from a patient infected with HCV genotype 3a (Table 5.1). HCVpp incorporating E1E2 derived from genotype 1a (HCVpp1a-1-3, HCVppH77), 1b (HCVpp1b-1-2 and HCVpp1b-1-3) were pre-incubated with different concentrations (0.006 to 0.4 mg/ml) of purified VF-Fabs prior to infection of Huh7 cells. No envelope control was used to normalise the data. The neutralising activity of the VF-Fab is expressed as percentage of inhibition of the infectious titres. Prism was unable to find unique fit for VF-Fb1b-5-1, hence, as per prism guidelines, bottom values were constraint to zero for that data set only. Each experiment was repeated three times with two technical replicates. IC_{50} for each VF-Fab is detailed in Table 5.2. Error bars indicate standard deviation. * Limited quantity of VF-Fab1a-1-1 restricted the number of concentration points used for neutralisation assay.

5.3.2 Total IgG derived from sera without detectable AAV shows neutralisation activity

In the previous chapter, we have shown that Total IgG purified from sera classified as AAV negative do not demonstrate viral variant targeting activity in the viraemic HCV sera (Chapter 3, Section 3.3.3) (299). In the current work, the ability of Total IgG from AAV negative sera to neutralise HCVpp was tested. The AAV negative sera were treated with proteinase K (Section 2.2.1.3). HCVpp1b-1-3 and HCVppH77 were highly neutralisation sensitive to VF-Fab1b-4-1 and VF-Fab1b-8-1, reducing the infectivity by 75% and 85% respectively (Fig 5.3). However, HCVpp1a-1-3 and HCVpp1b-1-2 were resistant to neutralisation by VF-Fab1b-4-1, VF-Fab1b-6-1 and VF-Fab1b-8-1 (Fig 5.3). Although the VF-Fabs were derived from sera from an anti-D cohort, a varying degree of neutralisation breadth was observed in HCVpp1b-1-2 and HCVpp1b-1-3, which were also derived from an anti-D patient serum P1b-1.

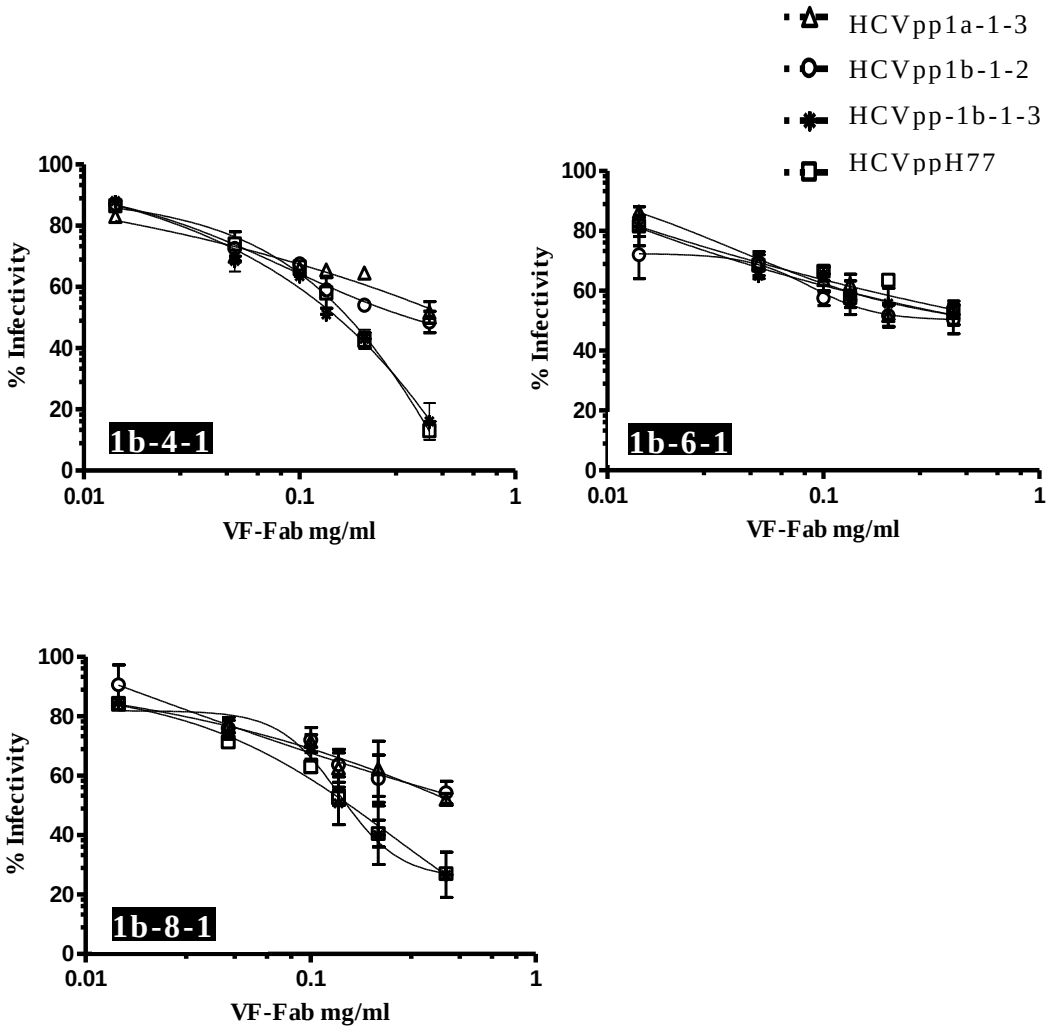

Figure 5.3: VF-Fab from sera without detectable AAV shows neutralisation activity

VF-Fab1b-4-1, VF-Fab1b-6-1, VF-Fab1b-8-1 were purified from three unrelated patients infected with HCV genotype 1b that were negative for presence of AAV. HCVpp incorporating E1E2 derived from genotype 1a (HCVpp1b-1-3, HCVppH77) and 1b (HCVpp1b-1-2, HCVpp1b-1-3) were pre-incubated with different concentrations (0.006 to 0.4 mg/ml) of purified VF-Fabs prior to infection of Huh7 cells. A no envelope control was used to normalise the data. The neutralising activity of the VF-Fabs is expressed as percentage of inhibition of the infectious titres. Each experiment was repeated three times with two technical replicates. IC_{50} for each VF-Fabs is detailed in Table 5.2.

Table 5.2: IC_{50} values (mg/ml) of neutralisation curves in Figure 5.1 and Figure 5.2 for each VF-Fabs.

GT 1a

HCVpp	VF-Fab 1a-1-1	VF-Fab 1a-1-2	VF-Fab 1a-1-3	VF-Fab 3a-1-1
1a-1-3	0.088	0.161	0.097	0.023
1b-1-2	-	-	0.041	0.399
1b-1-3	0.108	0.133	0.100	0.069
H77	0.142	0.111	0.140	-

GT 1b

HCVpp	VF-Fab 1b-1-2	VF-Fab 1b-1-3	VF-Fab 1b-4-1	VF-Fab 1b-5-1*	VF-Fab 1b-6-1	VF-Fab 1b-8-1	VF-Fab 1b-10-1
1a-1-3	0.080	0.067	-	0.061	0.038	-	0.066
1b-1-2	0.117	0.081	0.087	0.021	0.087	-	0.066
1b-1-3	0.075	0.036	-	0.015	-	0.132	0.057
H77	0.100	0.134	-	0.054	-	0.235	0.165

* Prism was unable to find unique fit for VF-Fb1b-5-1, hence, as per prism guidelines, bottom values were constraint to zero for that data set only.

5.3.3 Potential epitopes targeted by VF-Fab1b-1 and VF-Fab1b-10-1

Based on the previous research by Guan *et al.* (2012), initially the partial E1E2 region which covers both the HVR1 and AP33 epitope was explored for potential binding motifs targeted by the humoral immune system (68). Linear peptides were synthesised for 1^{o}AAV 1b-5-1 [KU888834], 1b-10-1 [KT873219] and 2^{o}AAV 1b-4-1 [KU888835], 1b-7-1 [KT873204], 1b-8-1 [KU888836] covering amino acid region 364-430 in the E1E2 glycoprotein to study the epitopes targeted by host immune system. Full length sequences for 1b-7-1 [KT873204] and 1b-10-1 [KT873219] were not available so peptides were designed for region 364-423.

Five different potential binding motifs were observed for 1b-4-1, 1b-5-1 and 1b-8-1 sequences (Table 5.3, Appendix II). All the peptides in this study were designed as 15 mers with overlapping 14 mer peptides. Outliers representing best fitting epitope candidates were evaluated based on raw ELISA intensity profiles with subtracted background values. Background was calculated as a mean value of ELISA signals corresponding to the interaction between test samples and unrelated control peptides designed from epitopes of monoclonal antibodies 57.9 and 3C9 (273). VF-Fab1b-5-1 targeted a motif which shares amino acid residues 412, 413, 415-423 with epitope $E2_{412\text{-}423}$ (QLINTNGSWHIN) targeted by MAb AP33 in 1^{o}AAV fraction of 1b-5-1 and 2^{o}AAV fraction of 1b-8-1 (Table 5.3) (257). VF-Fab1b-10-1 targeted motif 396-407 within the HVR1 domain of 2^{o}AAV fraction of 1b-4-1 [KU888835] and 1b-8-1 [KU888836] and 1^{o}AAV fraction of 1b-5-1 [KU888834], it is the same antigenic domain targeted by MAb 3C7 and 9/27 (Table 5.3) (reviewed in 300).

A heatmap representation of scaled and centred data for each VF-Fabs is shown in Fig 5.4. Heat maps give a visual overview of complex data sets in matrices. In this data set, column represents VF-Fabs and each row represents ELISA score obtained from

a peptide for the VF-Fabs under analysis (Table 5.3). Rows were arranged sequentially with respect to the target sequence. Colour key shows the colour-coded Z-score distribution of the displayed dataset. Scaling and centering was performed for each sample individually meaning that ELISA signal of each peptide was compared with ELISA signals obtained with all other peptides for a sample (Raw data appendix II).

Here, the Z-score is the result of scaling and centering applied to data from a VF -Fab and was calculated by subtracting the mean of the column from every value and then dividing the resulting values by the standard deviation of the column. In this case, magnitude of the magenta colour indicates 'Z' score (Fig 5.4). In our data set the Z-scores range from ± 4 standard deviation which defines the magnitude of magenta. This is a visual representation of the binding affinity of the VF-Fabs to that particular peptide (Fig. 5.4).

Table 5.3: Binding Motifs targeted by VF-Fabs

VF-Fabs	Target Sequence	Accession numbers	Putative Epitope
VF-Fab1b-5-1	1b-5-1	KU888834	$_{410}$NIQLVNTNGSWHINR$_{424}$
	1b-8-1	KU888836	$_{410}$KIQLVNTNGSWHINR$_{424}$
VF-Fab1b-10-1	1b-4-1	KU888835	$_{388}$MGEAQGRTTRGLA$_{400}$
	1b-5-1	KU888834	$_{398}$GFASLFRLGPSQ$_{409}$
	1b-8-1	KU888836	$_{397}$HSFVRFFASGPSQ$_{410}$

Figure 5.4:

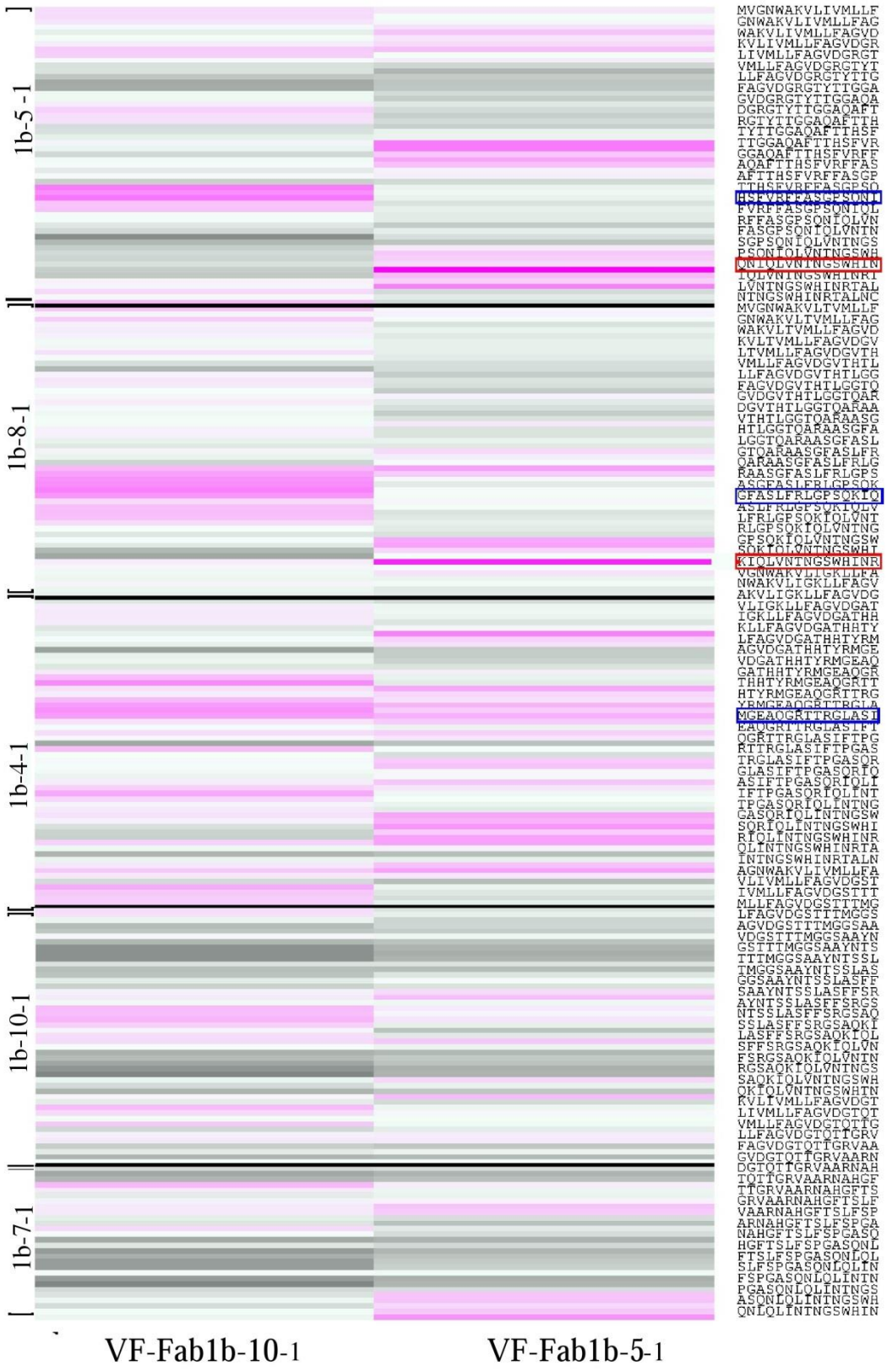

Figure 5.4: Heatmap overview of peptides targeted by VF-Fabs

1°AAV fractions of 1b-5-1, 1b-10-1 and 2°AAV fractions of 1b-4-1, 1b-7-1, 1b-8-1 were assessed for epitope mapping with VF-Fab1b-5-1 and VF-Fab1b-10-1 from amino acid 364-430 including the HVR1 in E2. Individual peptides are listed on the right-hand side and VF-Fabs is indicated at the base of the heatmap. Black horizontal lines show start position of a new target sequence in that particular set of peptides. Target sequences are flanked by black brackets on the left. The magnitude of colour (dark magenta) with higher Z score represents the binding affinity of Fab to the peptide. Sequence in a red box (in right) represents motif targeted by VF-Fab1b-5-1. Sequence in a blue box (in right) represents motif targeted by VF-Fab1b-10-1. In order to make Heatmap legible, only every second peptide in the study has been included in the figure.

5.3.4 Conformational epitope mapping of E2

The linear peptide mapping suggested that there might be additional conformational epitopes in the E2 region (32, 42, 76, 78, 170, 173). Based on the available anti-HCV monoclonal nAb mapping information and E2 structure, selected amino acid residues that cover HVR1 (384-410), HVR2 (460-482), E2 β-sandwich (492–566) and IgVR (572-588) spanning up to amino acid 619 were selected for conformational epitope mapping (32, 42, 76, 78, 170, 173). Five different binding motifs were targeted by VF-Fab1a-1-3, VF-Fab1b-1-3, VF-Fab1b-5-1 and VF-Fab3a-1-1 in HCVpp1b-1-3 sequence upon peptide mapping (Table 5.4, Fig 5.5, Appendix III). Amino acid variation in the epitopes targeted by patient derived VF-Fabs in infectious HCVpps from this study are shown in Fig 5.5a. The 3D model of sequence mapped for potential epitopes (HCVpp1b-1-3) is shown in Fig 5.5b.

The epitope mapping data showed that all the VF-Fabs targeted an immunodominant epitope within region 393-405, henceforth, AN1 within HVR1 (Table 5.4). The regions within or located near HVRs are assumed to be flexible loops (VR1, VR2 and IgVR) (41). Of note, VF-Fab1b-5-1, VF-Fab3a-1-1 showed a higher binding affinity towards the β-turn mimics of $AN1_{393-405}$ as compared to the linear mimics by VF-Fab1a-1-3 and VF-Fab1b-1-3 (Fig 5.5). The second motif in the region 433-445. AN2, overlaps with amino acid residues 428-447 (AN3) and is part of discontinuous B cell epitope targeted by MAb AR3C (428-433, 436, 438, 439, 441-443, 446) (32, 42, 301). The $AN4_{539-551}$ epitope is reported for the first time. Residues 549 (CBH7), 540 (AR3A, AR3C) and 550 (H48) are part of conformational epitopes for broadly neutralising anti HCV MAbs (reviewed in 300). Notably, epitope $AN5_{599-608}$ which lies beside $IgVR_{572-588}$ (78) has not been reported previously. In case of conformational epitope mapping high sequence variability of test peptides and signal redundancy

provided by the presence of various epitope mimics corresponding to the same region of the target sequence replaced the need for control peptides. Analysis of 162 GenBank sequences (GT 1a=44, GT 1b= 21, GT 2=19, GT 3=21, GT4= 20 GT 5=17 and GT 6=20, Appendix I) revealed that residues 540, 544, 545, 548, 550 and 551 in AN4 and residues 600, 601, 602, 604, 605 and 607 in AN5 are highly conserved across all the genotypes (Fig 5.5c).

Table 5.4: Putative Epitopes targeted by VF-Fabs

VF-Fabs	Motif	Epitope Name
1a-1-3,1b-1-3,1b-5-1*, 3a-1-1*	$_{393}$SRAAHRVTTFITR*$_{405}$	AN1#
1a-1-3	$_{433}$LNTGFLAALFYTH$_{445}$	AN2
1b-5-1*, 3a-1-1*	$_{428}$NCNDSLNTGFLAALFYTHRF*$_{447}$	AN3
1b-1-3, 1b-5-1*, 3a-1-1*	$_{539}$LLNNTRPPRGNWF$_{551}$	AN4
3a-1-1	$_{599}$SGPWLTPRCM$_{608}$	AN5

*****VF-Fabs binding to β-turn mimics was higher when compared with that of linear mimics [Ref AF011751] (Pepscan Presto; Lelystad, Netherlands)

Figure 5.5

a.

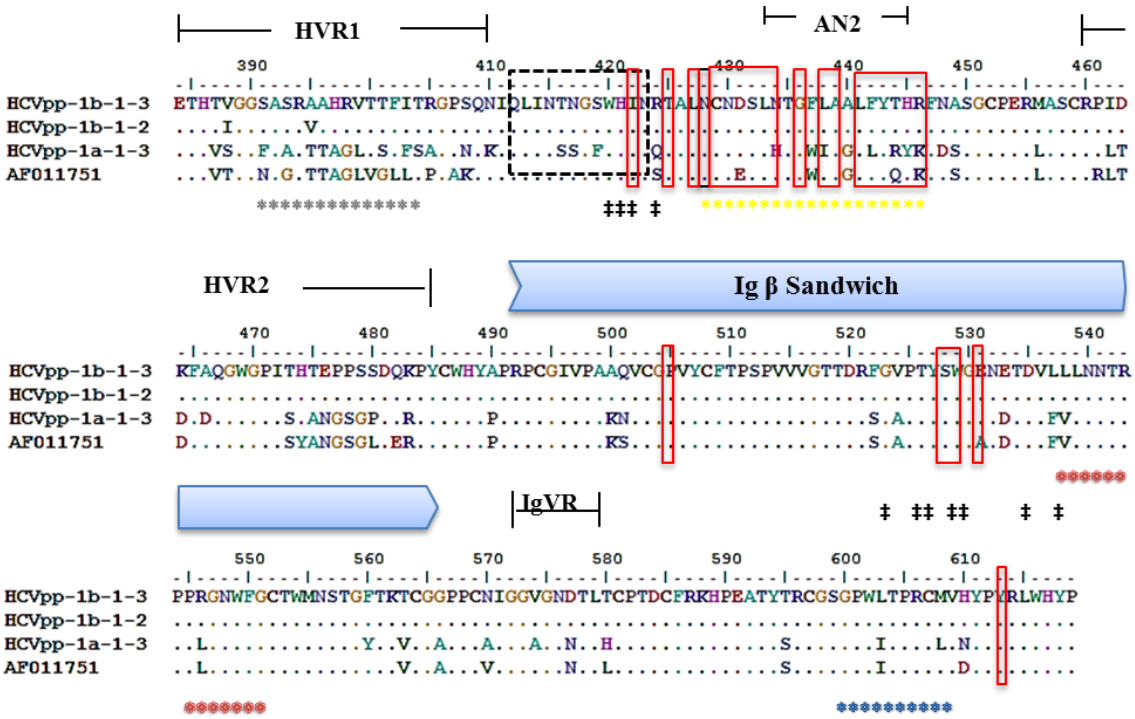

b.

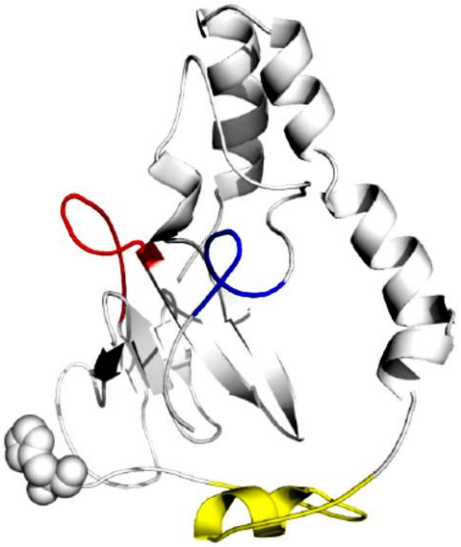

c.

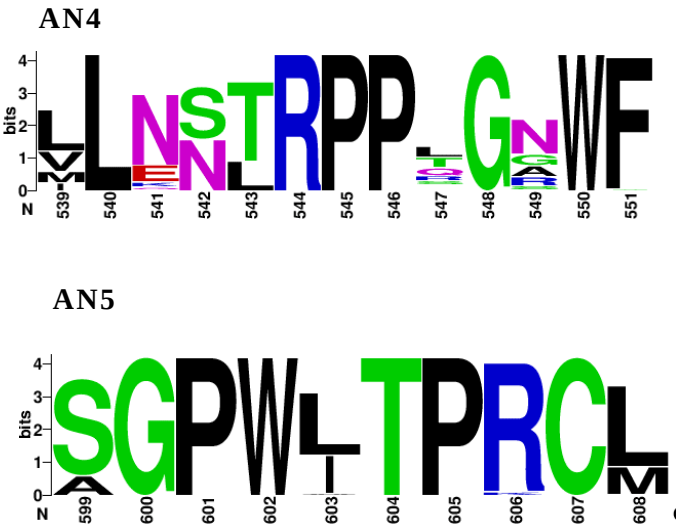

Figure 5.5: Conformational epitope mapping of E2 glycoprotein region starting from amino acid 384-619

a. The multiple sequence alignment (MSA) of the E2 glycoprotein. HCVpp1b-1-3 is a reference sequence; HCVpp1b-1-1, HCVpp1a-1-3 and HCVppH77 were the infectious pseudoparticles. AF011751 is an H77 strain. aa marked with *: targeted by patient derived VF-Fabs. The colour code of the epitopes represent the position of the epitope in 3D structure of E2 glycoprotein (Table 5.5); gray stars: AN1, yellow stars: AN3, red stars: AN4, blue stars: AN5 aa in dashed box: linear epitope targeted by AP33 mouse MAb (257); aa in red box: residues on E2 interact with AR3C HuMAb (32); aa marked with ‡: residues important for CD81 binding (32) **b.** The 3D model of HCV-E1E2 glycoprotein shown in white cartoon with flexible non-modelled E2 N-termini (384-412) labelled with spheres. Sequence $_{428}$NCNDSLNTGFLAALFYTHRF$_{447}$ is highlighted in yellow, $_{539}$LLNNTRPPRGNWF$_{550}$ in red and $_{599}$SGPWLTPRCM$_{608}$ in blue (Pepscan Presto; Lelystad, Netherlands) **c.** Amino acid Weblogo of epitope AN4$_{539\text{-}551}$ and AN5$_{599\text{-}608}$ showing conserved residues. Black: non polar, Green: polar, Red: acidic, Blue: basic and Purple: neutral. The x-axis depicts the amino acid position and the height of the individual letter reflects relative frequency of each amino acid at that position.

5.3.5 Combination of VF-Fabs significantly reduces HCVpp infection

Based on the date of collection of sera, IC_{50}, and epitope mapping data (Tables 5.1, 5.2), VF-Fab1a-1-3, VF-Fab1b-1-3, VF-Fab1b-5-1 and VF-Fab3a-1-1 were selected for mixed VF-Fabs pull down assay. The ratio of the combined VF-Fabs was set by choosing the average $LogIC_{50}$ for each of the selected VF-Fabs (Prism 5 guide lines). Averages of % infectivity for all the HCVpp treated with a particular VF-Fabs combination were chosen for statistical analysis. A significant reduction in HCVpp infectivity with VF-Fab1a-1-3 and VF-Fab1b-1-3, VF-Fab1a-1-3 and VF-Fab1b-5-1, VF-Fab1b-1-3 and VF-Fb1b-5-1 and VF-Fab1b-5-1 and VF-Fab3a-1-1 combinations when compared to the individual VF-Fabs concentration was observed (Dunnett t test, $p<0.05$-0.001) (Table 5.6, Fig 5.6). However, VF-Fab1a-1-3 & VF-Fab3a-1-1 in combination did not show any substantial reduction (in infectivity) compared to individual VF-Fabs concentration (Table 5.5, Fig 5.6).

Table 5.5: Summary of statistical significance of average IC_{50} (mg/ml) of VF-Fab in combination in comparison with the individual VF-Fab

Concentration of individual VF-Fab →	VF-Fab1a-1-3	VF-Fab1b-1-3	VF-Fab1b-5-1	VF-Fab3a-1-1
	0.078	0.078	0.02	0.108
Combination of VF-Fabs ↓				
1a-1-3 & 1b-1-3	**	***	**	***
1a-1-3 & 1b-5-1	**	**	*	**
1a-1-3 & 3a-1-1	ns	ns	ns	ns
1b-1-3 & 1b-5-1	***	***	***	***
1b-1-3 & 3a-1-1	**	***	**	***
1b-5-1 & 3a-1-1	***	***	***	***
1a-1-3	n/a	ns	ns	ns
1b-1-3	ns	n/a	ns	ns
1b-5-1	ns	ns	n/a	ns
3a-1-1	ns	ns	ns	n/a

*p<0.05, **p<0.001, ***p<0.0001, ns = not significant, n/a = not applicable

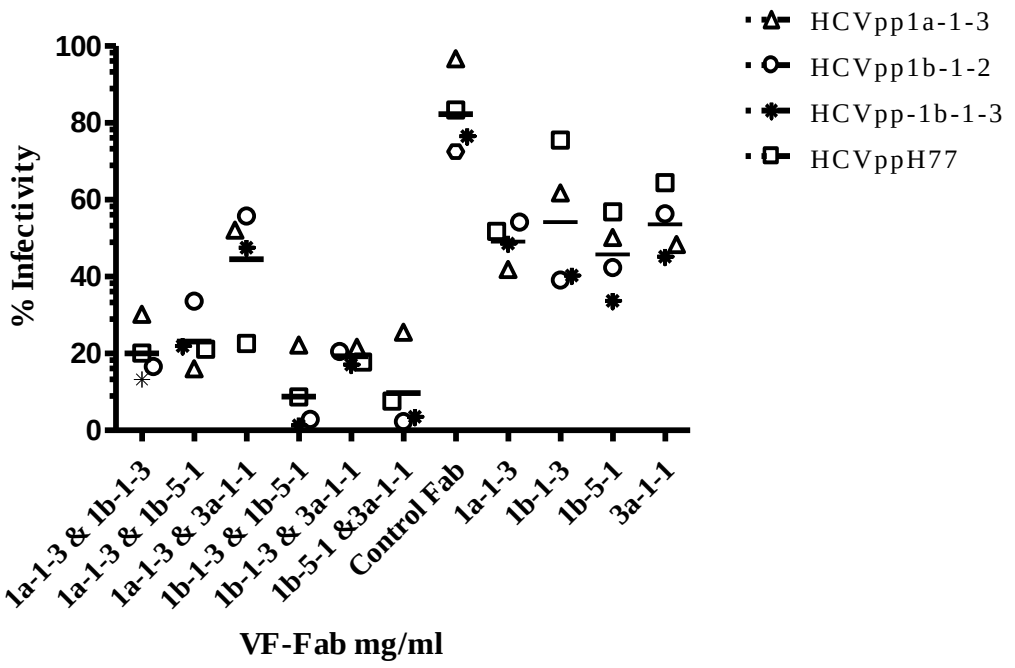

Figure 5.6: Neutralisation of pseudotyped virus with combination of VF-Fabs

HCVpp1a-1-3, HCVpp1b-1-2, HCVpp1b-1-3 and control HCVppH77 were tested for neutralisation using the average Log IC_{50} (mg/ml) for the VF-Fabs in combinations (Table 5). Control Fab were obtained by treating commercially available male AB plasma with proteinase K (SLBK465 V, Sigma). The data was obtained from three independent experiments. Data for all the HCVpp were grouped together for statistical analysis. Averages of % infectivity for all the HCVpp treated with a particular VF-Fabs combination were chosen for statistical analysis Significance was tested using one-way ANOVA with Dunnett t test ($p<0.05$-0.001, Table 5.5). Each VF-Fabs combination was compared against individual VF-Fabs at the concentration used in combination experiments.

5.3.6 Analysis of tolerated amino acid substitution in predicted motifs

Using an *in silico* Sorting Intolerant From Tolerant (SIFT) amino acid analysis, we discovered that epitopes AN2-AN5 were not affected by the (observed) variation at the different positions in the epitopes (Table 5.6). Amino acid residues in the binding motifs of AN2-AN5 were broadly conserved. It is likely that amino acid variations in the aforementioned epitopes of HCVpp sequences were functionally tolerable and hence, were recognised by the VF-Fabs in this study (deleterious variations <0.05, Table 5.6). However, in case of AN1, a single amino acid substitution at position 395 was predicted as tolerable with respect to the VF-Fabs binding (Table 5.6). AN1 lies in the HVR1, an immunodominant region which generates a strain specific immune response.

Based upon the number of sequences submitted to the programme, SIFT presumes that a particular amino acid is well-conserved in the query sequence. The programme then calculates the probability of amino acid based on the most frequent amino acid appearing at each position in the alignment and their physicochemical properties (302). If the position in an alignment contains a hydrophobic amino acid, then residues other than hydrophobic characteristics are predicted to be deleterious for protein function (302). The programme uses a default cut off value of 0.05 for functional intolerance to evaluate the amino acid substitution (302).

Table 5.6: Tolerance to the amino acid substitution in the epitopes targeted by VF-Fab1a-1-3, VF-Fab1b-1-3, VF-Fab1b-5-1 and VF-Fab3a-1-1.

a. AN1

$_{393}$S	R	A	A	H	R	V	T	T	F	I	T	$_{405}$R
A		T	T	A	G	L	V	G	L	F	S	A
G		V						S		L		P
		1	-	-	-	-	-	-	-	-	-	-
1		0.34	1	1	1	1	0	1	1	1	1	1
0		1	0	0	0	0	0	0	0	0	0	0

b. AN3

$_{428}$N	C	N	D	S	L	N	T	G	F	L	A	A	L	F	Y	T	H	R	$_{447}$F
-	-	-	E	-	-	H	-	-	W	I	-	G	-	L	-	Q	Y	K	-
-	-	-		-	-		-	-	-	-	-		-		-	R	-		-
-	-	-	1	-	-	1	-	-	1	1	-	1	-	1	-	1	1	1	-
-	-	-	0.73	-	-	0.46	-	-	0.94	0.61	-	1	-	1	-	0.65	0.68	1	-
-	-	-	-	-	-	-	-	-	-	-	-	-	-	-	-	0.8	-	-	-

c. AN4

$_{539}$L	L	N	N	T	R	P	P	R	G	N	W	$_{551}$F
V								L				
1	-	-	-	-	-	-	-	1	-	-	-	-
1	-	-	-	-	-	-	-	1	-	-	-	-

d. AN5

$_{599}$S	G	P	W	L	T	P	R	C	$_{608}$M
				I					L
-	-	-	-	1	-	-	-	-	1
-	-	-	-	1	-	-	-	-	1

Data presented is analysed and predicted using programme SIFT (http://sift.jcvi.org/www/SIFT_aligned_seqs_submit.html). Row corresponds to a position in the reference epitope. Column corresponds to amino acid variation (observed in our data set) at that position in different HCVpp (Fig 5.5a). Score at a particular position for an amino acid substitution is mentioned below the amino acid variant. The default threshold for functional intolerance used was 0.05 for amino acid substitution.

5.4 Discussion:

The HCVpp system is widely used to study the neutralisation sensitivity to serum-derived antibodies and MAbs (256). In the last chapter, we have shown that not all the E1E2 clones isolated from AAV were infectious in the HCVpp system. This chapter analyses the neutralisation potential of the VF-Fabs in HCVpp generated from AAV-E1E2 clones. Initially, a neutralisation assay was performed using VF-Fab1b-5-1, VF-Fab1b-10-1 on HCVpp-H77 and HCVpp1b-4-1. Both VF-Fab1b-5-1 and VF-Fab1b-10-1 neutralised HCVpp with different efficiencies, VF-Fab1b-5-1 being highly neutralising (Figs 5.1 and 5.2). Subsequently, VF-Fabs obtained from patients P1a-1 and P1b-1 at different time points were tested for their neutralisation efficacy against the HCVpp expressing patient derived glycoprotein (Fig 5.2). In the case of genotype 1a, VF-Fab1a-1-1, VF-Fab1a-1-2 and VF-Fab1a-1-3 were able to neutralise HCVpp1a-1-3, all were acquired from the same patient at different time points (Table 5.1, Fig 5.2). Similar observations were made for VF-Fab1b-1-2 and VF-Fab1b-1-3, which had the ability to neutralise HCVpp1b-1-2 and HCVpp1b-1-3 (Table 5.1, Fig 5.2). The neutralisation of HCVpp by the VF-Fabs derived from antibodies present in the earlier serum samples (Table 5.1) suggests that the viral escape from the humoral immune response continues even after years of chronic infection. Most significantly, we also detected that VF-Fabs from unrelated patient sera 1b-5-1, 1b-10-1 and 3a-1-1 were efficient in reducing the HCVpp infectivity in all cases, suggesting that these VF-Fabs must target common neutralising epitope(s). Proteinase K treated Total IgG purified from AAV negative sera were also used to neutralise the HCVpp in this study (Fig 5.3). In chapter 3 it was shown that proteinase K treated Total IgG from the AAV negative sera were not able to capture any viral variant(s) from a complex serum environment (Section 3.3.3). However, in the HCVpp system VF-Fab1b-4-1 and VF-

Fab1b-8-1 neutralised HCVpp1b-1-3 and HCVppH77. These latter sera likely have nAbs against now extinct viral variants, which, targeted conserved epitopes present in the homogenous HCVpp system of HCVpp1b-1-3 and HCVppH77 (Fig 5.3). Our data supports that viral variants successfully evade the humoral immunity as nAb response elicited in patient lags behind the rapidly evolving glycoprotein sequences present within the quaispecies population *in vitro* (215) (Section 3.4). Our observation emphasises that the epitope evolution is a result of strong immune selection pressure. Our data supports further how the immune response fails to resolve the HCV infection even after nAb response by host.

Several methods can be used for epitope mapping. X-ray crystallography of antigen-antibody complex and multidimensional nuclear magnetic resonance (NMR) are the gold standards for epitope characterisation (303, 304). The biggest advantage of X-ray crystallography is that it provides atomic resolution of residues involved in interaction between both epitope and complementarity-determining regions in the antibody paratope (303, reviewed in 305). X-ray crystallography requires purification of both antigen and antibody followed by crystallisation of the complex. This method of epitope mapping faces complications such as high expertise, difficulties in obtaining diffraction quality crystals and the capital cost (reviewed in 305). Similarly, NMR requires predetermined structure of the free antigen (reviewed in 305). Another approach to determine the presence of epitope(s) is by analysing the binding of antibodies by mutating antigenic determinants (306). Alanine scanning mutagenesis is widely used to screen as many as hundreds to thousands of the proteins for epitope-paratope interaction (306). However, mutation within the epitope does not differentiate to whether the loss in antibody binding is a result of alteration in the protein folding or is genuinely a key interacting residue. Regardless, mutagenesis

along with the crystallography technique has been used to study the contribution of individual residue in the antigen-antibody interaction (307, 308).

Peptide based method is another epitope mapping strategy. In order to study the epitopes targeted by the VF-Fabs in 1°AAV and 2°AAV fractions, the peptide based epitope mapping service was outsourced to Pepscan Presto, Lelystad, Netherlands. Here, microarrays of overlapping peptides that covers sequence of interest are prepared and the binding affinity of antibodies is tested in ELISA format (reviewed in 305, 309). This approach is more suited for linear epitope mapping, yet, discontinuous or constrained peptides can be synthesised using Pepscan's CLIPS technology (Section 2.2.5.2) (275). Peptide based epitope mapping does not necessarily require purified antigen or antibody. The peptide arrays can be used multiple times for screening of antibodies. This method is ideal for linear, discontinues and relatively conformational antigens. Pepscan uses peptide based ELISA format for both linear and constrained epitope mapping (Section 2.2.5).

Primarily, the linear epitope mapping service from Pepscan was used to identify epitopes in the E1E2 gene junction covering the HVR1 and $E2_{412\text{-}423}$ epitopes. To our knowledge, this is the first time a sequence which was targeted by host humoral immune system (AAV) has been used for epitope mapping using patient derived VF-Fabs. Linear epitope mapping analysis revealed that VF-Fab1b-5-1 targeted motifs in 1°AAV fraction of 1b-5-1[KU888834] and 2°AAV fraction of 1b-8-1 [KU888836] that overlap with the well characterised AP33 epitope $E2_{412\text{-}423}$ (Fig. 5.4, Appendix 2). It has been shown that broadly neutralising $E2_{412\text{-}423}$ epitope is conserved across different HCV genotypes (53.4%) (257). Antibodies against $E2_{412\text{-}423}$ epitope inhibit HCV entry by blocking CD81 interaction (257). Our data and others have already

established that HCVpp entry is CD81 dependent (Section 4.3.5) (32, 42, 44, 69, 293). This is a likely explanation why VF-Fab1b-5-1 is highly neutralising. AP33 is a partially conformational dependent epitope and its immunogenicity varies among the infected patients (Section 3.3.5, Fig. 3.9) (171, 310). VF-Fab1b-10-1 targeted epitope within the HVR1 (Table 5.3). Neutralising antibodies against HVR1 are strain specific and of limited cross-reactivity, hence, VF-Fab1b-10-1 is the least neutralising in HCVpp1b-4-1 and HCVppH77 neutralisation assay (reviewed in 61, 300). It should be noted that both VF-Fab1b-5-1 and VF-Fab1b-10-1 did not recognise any epitope in 2^{o}AAV fraction of 1b-7-1 and 1^{o}AAV of 1b-10-1. This data infers a possible conformational or discontinuous epitope(s) outside the HVR1, which was not included in linear epitope mapping analysis.

To further expand the epitope knowledge base, E2 sequence (residues 384-619) from a highly neutralisation sensitive HCVpp1b-1-3 was used to construct conformational peptides (Fig 5.5, Appendix III). The conformational epitope mapping predicted five putative epitopes AN1-AN5 (Table 5.4). $AN1_{393\text{-}405}$ lies in the domain targeted by MAbs 3C7 and 9/27 (Fig. 5.5) (reviewed in 300). Cerino *et al.* (2001) immunised mice with mimitopes (surrogate peptides) of HVR1 obtained from chronically infected patient and obtained a panel of MAbs (311). From the panel of MAbs, 3C7-C3 recognised HVR1 chimeras/linear peptide pairs (truncated E2 protein from H77). 3C7-C3 was also efficient in capturing bona-fide (infected with genotype 2c) and recombinant viral particle (HCV-LP 1a, H77) (311). Hsu *et al.* (2003) showed that mAb 9/27 recognised 396-407 residues in the C terminal of HVR1 and neutralised HIV-H77 E1E2 pseudoparticles. Our study and others have demonstrated that nAbs target epitopes on the C terminus of HVR1 and hence role of HVR1 in neutralisation

is apparent (65, reviewed in 129). However, as of writing, there is no evidence that antibodies against HVR1 are broadly cross-neutralising.

VF-Fab1a-1-3 recognised a second linear epitope $AN2_{433-445}$ which overlaps with epitope AN3 (Fig 5.5). A study by Deng *et al*. (2015) has shown that a major epitope lies on the neutralisation face of E2 glycoprotein, between amino acid 421-543 (174). VF-Fab1b-5-1 and VF-Fab3a-1-1 showed a higher affinity towards the β-turn mimics of epitope $AN3_{428-447.}$ AN3 is a part of the neutralisation face of E2 and intersects with the CBH-2 epitope as well (293). AN3 also shares residues with HuMAb AR3C (Fig 5.5a, red solid boxes) (32). Kong *et al.* (2013) have shown that N-terminal region residues 421 to 453 form a front layer, a part of CD81 binding loop. The crystal structure of this epitope has shown that it is targeted by bNAbs (32). This provides a probable explanation to why VF-Fab1b-5-1 and VF-Fab3a-1-1 showed high affinity towards the β-turn mimics of epitope AN3 (32).

VF-Fab1b-1-3, VF-Fab1b-5-1 and VF-Fab3a-1-1 have targeted a new epitope AN4 (residues 539-551). VF-Fab3a-1-1 also showed binding affinity towards epitope $AN5_{599-608}$. Three CD81 binding regions on E2 glycoprotein have been proposed which includes residues 474-492, 522-551 and 612-619 (reviewed in 41). However, the Kong-E2c structure do not contain region 474-492, but it still binds to CD81 receptor and 612-619 are on different face from the CD81 binding domain (reviewed in 41). This data indicates that contact point between E2c and CD81 likely lies within region 522-551 (reviewed in 41). AN4 amino acid residues 540 and 550 are involved in CD81 binding (32) however; AN4 and AN5's role in HCV infection needs to be further characterised (Fig 5.5c).

A recent study on H5N1 strain of influenza virus has shown promising use of neutralising antibodies as prophylactic and therapeutic agents (312). A cocktail of ZMab and MB003 (ZMapp - c13C6, c2G4, and c4G7) has been shown to provide 100% protection in nonhuman primates post 5 days of EBOV infection (225). Bukh *et al.* (2015) have shown that polyclonal antibodies purified from chronic HCV patient can suppress the homologous virus in the chimpanzee for 18 weeks (227). However, it failed to provide protection against the heterologous strains. Wong *et al.* (2014) documented targeting of multiple epitopes within E1E2 glycoprotein by antisera collected from five human volunteers who were immunised with recombinant E1E2 glycoprotein from genotype 1a. Wong *et al.* (2014) observed antibodies from vaccinee sera competed against well characterised MAb AP33 ($E_{412-423}$), AR3B, AR4A, AR5A and IGH526. AP33 targets epitope $E2_{412-423}$ (221). AR3B targets a discontinuous conformation dependent epitope within amino acid region 396–424, 436–447, and 523–540 in the E2 glycoprotein (313). Both AP33 and AR3B neutralise the HCVpp and HCVcc infection by blocking CD81 interaction (51, 257). AR4A and AR5A require correctly folded E1E2 glycoprotein for the interaction to occur (51). E1 region 201–206 and the E2 regions 657–659 and 692 are critical for binding of both AR4A and AR5A (51). However, their target in the E1E2 glycoprotein and mechanism of action for neutralisation is unknown (51). IGH526 targets residues 313-328 in the E1 region which is nearly conserved and is recognised by 30 of 92 HCV patient sera and 15 of 41 vaccinee sera (166). These studies collectively show the value of using an antibody adjunct to achieve control of viraemia. In our study, we observed that VF-Fabs when used in a combination had an enhanced effect in reduction of the HCVpp infection (Fig 5.6). We posited the following question, is this greater decline in the infectivity of HCVpp due to the targeting of multiple E2 epitopes? The epitope

mapping analysis clearly showed that all the VF-Fabs used in the combination experiment recognised multiple epitopes hence suggesting that these patient derived VF-Fabs do indeed target multiple epitopes in HCVpp (Table 5.4, Fig 5.5). Our data demontrate that a HCV infected individual elicits nAb response to multiple cross-neutralising epitopes. However, the immune response lags behind the continuously evolving viral envelope protein (175).

The observed binding behaviour of these VF-Fabs suggest two possibilities a) VF-Fabs are of polyclonal nature, and/or b) they recognise discontinuous epitopes. The binding capacity of the VF-Fabs pool represented here is inter-genotype and inter-subtype. Immunovirology and bioinformatics analysis of amino acid variation of the putative epitopes predicted that the observed natural changes do not affect the functionality of the targets (Fig 5.7, Table 5.7). SIFT calculates the probabilities for all the possible substitutions at each position and constructs a position-specific matrix considering the physiochemical properties of the amino acids. Positions with normalised probabilities <0.05 are predicted to be deleterious to the VF-Fabs binding (314-316). One drawback of the programme is that it calculates the probability of an amino acid at a given position depending upon the number of sequences submitted. Regardless, SIFT is a valuable tool for primary analysis of variance observed in the protein of interest. In this study, only four sequences which yielded infectious HCVpp were used for SIFT analysis. The observed variation in amino acid residues in the epitopes indicates that there must be preservation of the physicochemical properties and perhaps structural conformation to enable the VF-Fabs to target the previously "unseen" epitopes (probabilities range between 0.34-1.00). Specifically, this may explain (in part) why VF-Fabs, which were never exposed to the unrelated E1E2 glycoprotein, were still able to neutralise the HCVpp in our experiments (Fig 5.1, Fig

5.2). Amino acid substitution analysis hints towards the strain specificity of VF-Fabs in case of AN1 epitope. Campo *et al.* (2012), used a set of 261 HVR1 peptides for enzyme based Immunoassay (317). Of these sequences, 103 synthetic HVR1 peptides from different genotypes were used to immunise mice (317). Campo and colleagues observed 16.2%-20.6% cross immune reactivity between inter- and intra-genotypic pairs, respectively (317). They also identified that capacity of antibody (raised against one viral variant) to recognise variant peptide(s) was inversely proportional to genetic distance between viral variants (317). It should be acknowledged that cross immune reactivity is important but it always doesn't result in cross neutralisation. This possibly explains why all four VF-Fabs were able to recognise the AN1 epitope (Table 5.4, Fig. 5.5).

A well-known caveat that needs to be appreciated when using MAb and serum antibody screening for neutralisation potential in HCVpp system is that the pseudoparticle system provides a homogenous population of E1E2 glycoprotein, as compared to the complex heterogeneity and density of native glycoprotein in HCV virions. A limitation of this study is that this phenomenon was only explored with eleven patient derived VF-Fabs in genotype 1 in an HCVpp system. However, other studies and recent work by Wasilewski *et al.* (2016) collectively have shown that both HCVcc and HCVpp are equivalent with respect to the neutralisation phenotypes (160, 258, 318). Nevertheless, our immunovirological data lays a strong foundation for the investigation of humoral immune targeting of conserved HCV epitopes in antibody associated HCV and adds novel information to the *in vivo* humoral immune response to chronic HCV infection.

We present original and noteworthy findings in terms of the targeting of multiple epitopes, using unrelated patient derived VF-Fabs. The epitope mapping data showed potential antigenic determinants, which are subjected to humoral immune attack *in vivo*. Importantly, two new epitopes have been identified using VF-Fabs obtained from immunologically active patients.

Chapter 6

6. A single amino acid change in the hypervariable region 1 of HCV genotype 4a aids humoral immune escape

6.1 Introduction:

Longitudinal analysis of chronic hepatitis C viral infection has shown that the virus has several adaptive strategies that maintain persistence and infectivity over time. Longitudinal analysis of HCV genotype 4a, over a near 10 year period by Palmer *et al.* (2012) has shown the emergence, dominance and disappearance of distinct but related lineages (L1 and L2) in a treatment naïve patient chronically infected with HCV genotype 4a (268). The vacant viraemic space was replaced by previously existing minor variants (212, 268). Preliminary investigation of sample set T1-T9, by clonal analysis led to the observation of two distinguishable lineages L1 and L2 based on the presence of typical and atypical HVR1 (212). Additional exploration of the same sample set T1-T10 with ultra-deep pyrosequencing revealed the dominance of three sub-lineages (L1a, L1b and L1c) at different time points until T7 (268). L1 dominated the virome for the first eight years of the sampling period prior to population collapse and this led to the concomitant rise to prominence of L2. During this period of dominance, IgG-targeting of the L1 was detected in five of the first seven samples, which in part contributed directly to the humoral immune mediated removal of this group of variants (212, 268). Despite the near total dominance of the L2 sequences in latter samples (96.9% and 99.9% at T9 and T10, respectively), no IgG-targeting of the L2 virions was detected in the study (268). Furthermore, the HVR1 of the L2 variants remained predominantly under purifying selection across the 10 year period with a single principle HVR1 amino acid variant persisting during this time. Follow up clonal analysis indicated that a HVR1 variant with a single point mutation had superseded the principle variant, yet the L2-IgG remained undetectable (268).

In current follow up study we tested a hypothesis that the HVR1 variants which were not targeted by host immune system to be potential humoral immune escape mutants.

To examine this hypothesis we,

- Designed 6x His-tag peptides harbouring three different HVR1 variants.
- Performed a colorimetric ELISA

This work has been published in J. Gen Virology, 2016 Jun ;97(6):1345-9),- there appears to be a change in the font

Amruta S. Naik, Brendan A Palmer, Orla Crosbie, Elizabeth Kenny-Walsh, Liam J. Fanning **A single amino acid change in the hypervariable region 1 of HCV genotype 4a aids humoral immune escape**- Appendix IV

6.2 Methods

Following methods were used to test the hypothesis,

6.3 Results

6.3.1. T13 yields a clonotypic population in AAV fraction (2.3.1-2.3.4, 2.3-2.8)

Upon initial fractionation of HCV 4a serum samples, we observed only one sample (n=4) was positive for detectable levels of AAV (Table 6.1). In their previous research work, *Palmer et al.* (2012) observed that T11 had three different HVR1 amino acid variants, namely; H_{395}-X-X-X-F_{399}, N_{395}-X-X-X-F_{399} and N_{395}-X-X-X-L_{399} (Fig. 6.1a) (subscript numbering identifies specific amino acid positions within the 27 amino acid HVR1 with reference to NC_004102). The presence of HVR1 variant H_{395}-X-X-X-F_{399} in AFV fraction of T12 was confirmed by amplicon sequencing only. The subsequent AFV fraction of T13 also had H_{395}-X-X-X-F_{399} (frequency=0.40) amino acid profile. However, N_{395}-X-X-X-L_{399} variant was now dominant in T13 (frequency=0.60) (Fig. 6.1b). Interestingly, the predicted HVR1 sequence from AAV RNA detected at T13 indicated N_{395}-X-X-X-L_{399} motif targeting. This Leu containing motif was isolated in the succeeding samples, T14 and T15 in AFV fraction. However, AAV was not detected in samples T11, T12, T14 and T15.

Table 6.1 Samples used in this study

Time Point	Date of Collection	Unique HVR1 variants	Accession Number	
			AFV	AAV
T10*	17/11/2011	2	JQ743313-17	-
T11*	15/11/2012	3	KC689336–41	-
T12	13/06/2013	1	KT595215	-
T13	21/11/2013	2	KT595216–21	KT595222-23
T14	08/05/2014	2	KT595225	-
T15	01/12/2014	2	KT595225	-

Figure 6.1: Temporal mapping of quasispecies dominance at different time points

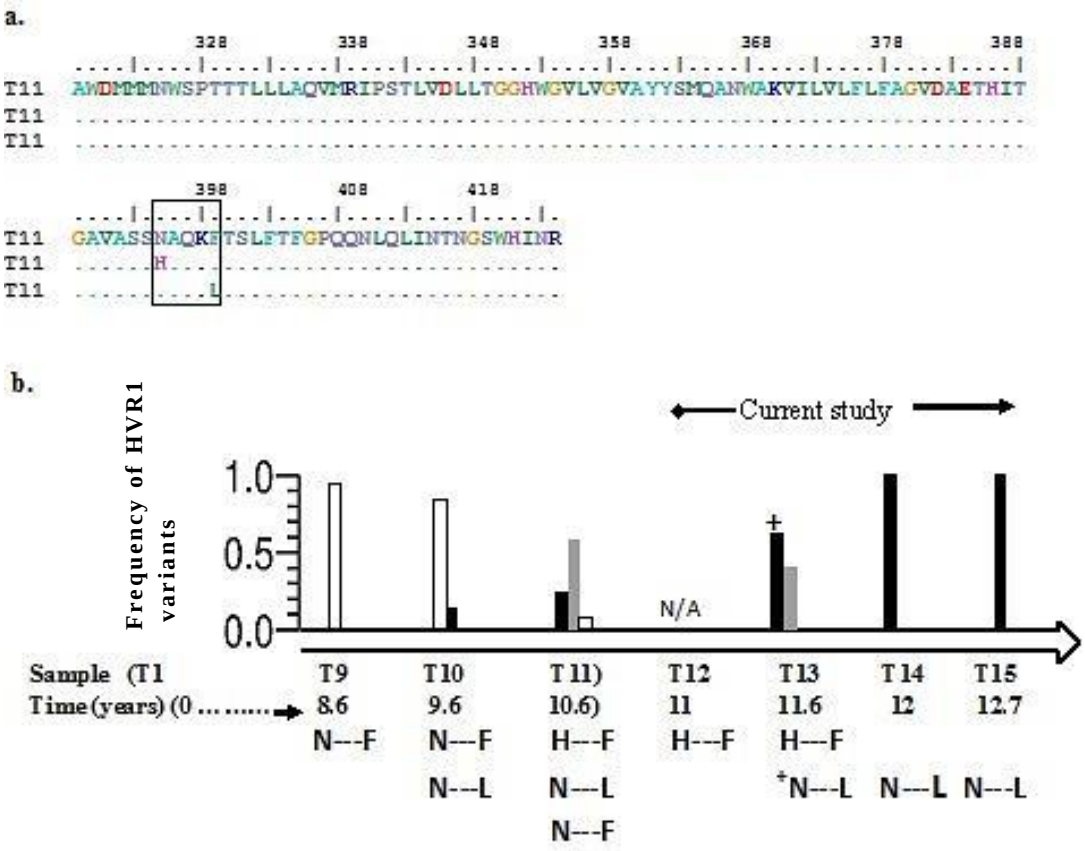

Multiple sequence alignment of T11 AFV fraction at amino acid level using BioEdit v 5.2. T11 had three different clones H_{395}-X-X-X-F_{399}, N_{395}-X-X-X-F_{399} and N_{395}-X-X-X-L_{399} in the HVR1 (black box) **b.** Clonal DNA sequence analysis of the antibody-free fraction of T11 (268), T13–T15 yielded the following predicted amino acid variants: (i) three unique AFV HVR1 variants for T11 (GenBank accession numbers KC689336–KC689341), (ii) two unique AFV HVR1 variants for T13 (GenBank accession numbers KT595216–KT595221), (iii) a clonotype amino acid quasispecies from the AAV in T13 (GenBank accession numbers KT595222 and KT595223), and (iv) an identical amino acid clonotype profile to T13 AAV in T14 (GenBank accession number KT595224) and T15 (GenBank accession numbers KT595225 and KT595226). T12 (GenBank accession number KT595215) was analysed by amplicon sequencing only. Columns are representative of the relative abundance of that sequence at that time point: black, N_{395}-X-X-X-L_{399} (N- - -L); grey, H_{395}-X-X-X-F_{399} (H- - -F); white, N_{395}-X-X-X-F_{399} (N- - -F). In this study the antibody response was detected at T13. The detectable antibody response identified at T13 and the variant associated with it is denoted by a plus sign. NA, Data not available.

6.3.2 Peptide P2 shows high affinity towards VF- T13 Fab (2.18)

Despite of several attempts full length E1E2 amplification of T13-AAV sequence was unsuccessful. The reason behind this is because of likely variable region(s) within the primer binding sites (Section 4.3.1). In this case, to study the immune escape mutant a colorimetric peptide based ELISA approach was taken. To confirm the escape phenotype hypothesis, three N-terminally 6xHis tagged, 27 amino acid HVR1 peptides were synthesised, i.e.

P1: H-HHHHHHETHITGAVASSNAQK**F**TSLFTFGPQQN-OH,

P2:H-HHHHHHETHITGAVASSNAQK**L**TSLFTFGPQQN-OH and

P3:H-HHHHHHETHITGAVASS**H**AQK**F**TSLFTFGPQQN-OH (Pepscan Presto, Lelysted, Netherlands). The HVR1 sequence of P1 and P3 corresponds to the dominant L2 HVR1 variant for the initial 10 years of *in vivo* infection for which no AAV was detected (268). The P2 sequence corresponds to the predicted HVR1 of AAV RNA isolated at T13. The ELISA results confirmed that the peptide containing the N_{395}-X-X-X-L_{399} mutation was recognized by the VF-T13Fab. In order to exclude the possibility that the P2 variant motif containing N_{395}-X-X-X-L_{399} was not accessible to antibodies, we similarly tested VF-T11Fab, VF-T12Fab and VF-T15Fab for binding affinity to the HVR1 peptide variants. The binding phenotype of VF-T13Fab had the strongest affinity towards P2 (P2>>P1>>P3) with Leu at position 399 compared, to the predicted escape variant Phe (P=0.06, Kruskal-Wallis test, GraphPad Prism 4) (Fig 6.2) in-vitro. However, VF-T11Fab, VF-T12Fab and VF-T15Fab did not show any biding affinity towards any of the peptides in this study.

Figure 6.2: Recognition of antigenic epitope within HVR1 by VF-Fab

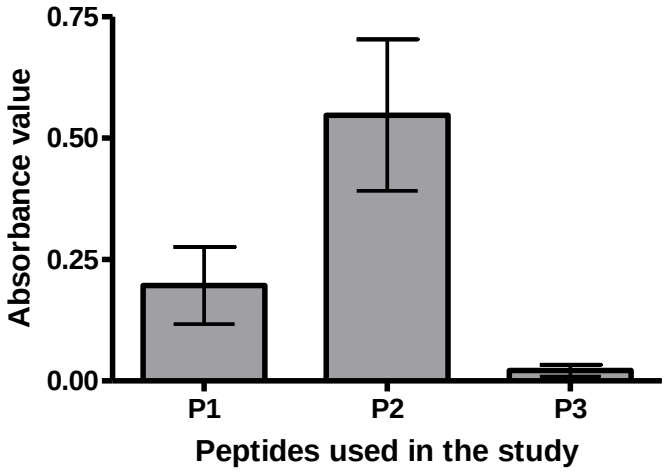

ELISA-based detection of the binding of the VF-T13Fab to the predicted HVR1 derived His $_{6}$-tag peptide epitopes (P1–P3, see text). The P1 and P3 variants were observed in the AFV fraction of T11, and the P2 variant was observed in the AAV fraction of T13. The control reference points included only peptides, peptides with only primary antibodies and peptides with only secondary antibodies. VF-T13Fab showed the strongest affinity towards P2 and baseline activity towards P3. The data were obtained from three independent experiments. The ***x***-axis indicates the peptide used in the ELISA, i.e. P1, P2 and P3. The ***y***-axis indicates the absorbance obtained by subtracting the $\boldsymbol{A}_{450}$ reading from the $\boldsymbol{A}_{560}$. *$\boldsymbol{P}$ = 0.06.

6.4 Discussion:

Longitudinal ultra-deep pyrosequencing analysis of HCV genotype 4a over 10 years has demonstrated the appearance of antibodies at discrete time points and extinction of the antibody associated lineage (268). Short term pyrosequencing analysis of genotype 3a has also been used to demonstrate the extinction of viral variants targeted by the humoral immune system (276). It has been observed that selection pressure from nAb responses shape the evolution of viral envelope protein (210-213). A study by Guan *et al*. (2012) has shown that neutralisation epitopes lies within amino acid positions 16-24 (i.e.399-407) in HVR1 (68). It is interesting to note that in our study, amino acid variation was observed only at amino acid positions 395 and 399 within the entire HVR1. Based on the Guan *et al.* (2012). data, we hypothesised that the HVR1 variants with N_{395}-X-X-X-F_{399} (T11-AFV) and H_{395}-X-X-X-F_{399} (T13-AFV) motif are potential humoral immune escape mutants which have Phe at position 399. Our ELISA results prove that, in this case, a naturally occurring single amino acid change to Phe in the HVR1 alone at position 399 can drive humoral immune escape after more than 10 years of immune silence. Our results demonstrated that none of the VF-T11Fab, VF-T12Fab and VF-T15Fab were bound to the HVR1 peptide variants P1-P3.

In our current study, analysis of serum samples over a 13 year period showed two distinct periods when AAV were present. A window period of five years existed between the two points during which AAV were detectable. The antibody specificity of the latter time point, T13, targeted a different HVR1 lineage from that found previously (212, 268). The HVR1 variant captured by the T13Ab was first observed in pyrosequencing data at T10 (1.1 %) (268). A further two year period elapsed before T13Ab to this latter variant was detected (Fig. 6.1b)

Interestingly, the HVR1 genomic sequence associated with virus captured by T13Ab was found to be present in the subsequent samples, i.e., T14 and T15. Analysis of samples T14 and T15 revealed that the T13Ab response was not sustained to detectable levels. The loss of nAb is a recognised feature of the natural history of HCV infection (319). Additionally, it is also recognised that a sustained antibody response is likely a prerequisite for complete removal of viral variant(s). The short life span of the antibody response could be because of lack of establishment of memory B cells (175). The notable absence of a sustained and neutralising antibody response (in T14 and T15) and likely fitness superiority explains why the motif (N_{395}-X-X-X-L_{399}) persisted in subsequent samples.

In conclusion, our proof of concept study has confirmed that antibodies were naturally generated against a discrete viral variant (Fig 6.2). We have additionally confirmed that naturally occurring amino acid variations in this epitope represent one mechanism by which HCV escapes humoral immunity.

Conclusion

Conclusion

In May 2016, during the World Health Assembly, the World Health Organisation (WHO) put forward a global strategy which aims to eliminate viral hepatitis as a public threat by 2030 (320, 321). In support of the WHO's Global Strategy for Viral Hepatitis, 36 countries had developed national plans to eradicate HCV. Ireland is one of the member states to adopt this strategy. The Health Service Executive (HSE) in Ireland established a National Hepatitis C Treatment Programme in 2016, outlining a strategic programme direction for 2016-2026 leading to the potential elimination of HCV in Ireland by 2026 **(**http://www.hse.ie/eng/about/Who/primarycare/hepcprogramme%20.html**).**

WHO plans to achieve eradication of viral hepatitis as a major public health burden by using a combination of available treatments and aims to achieve 80% reduction in new cases of HCV infection (321). Direct acting antivirals (DAAs) have emerged as an effective HCV treatment and are promising in the effective management of HCV.

Although the available DAAs provide a successful outcome in HCV management, there still exists a need to explore the immunoglobulin based therapy. In this thesis, we investigated E1E2 glycoprotein associated with AAV and the target epitopes in the antibody associated clonotypic virus population. Primarily, we segregated viraemic sera into AAV and AFV. AAV was observed to be homogenous in nature implying immunogenicity of the sequence in quasespecies pool targeted by the host humoral immune system. Although sequences obtained from AAV negative sera were positive for $E2_{412\text{-}423}$ epitope, only two samples showed reactivity to MAb AP33. This indicates genotype/subtype/patient specific epitope presentation of the epitope. We provide significant data that Total IgG or VF-Fab target viral variant in homologous genotype/subtype matched sera irrespective of source of the antibody. The targeted

viral variant need not be a dominant within the heterogeneous quasispecies. We analysed the E1E2 glycoprotein sequences associated with the AAV complex. AAV-associated E1E2 sequences obtained from patients at different time points provided us with an insight into the diversity of the envelop protein targeted by humoral immune system. Furthermore, variance in the infectivity of HCVpp was observed. This variability relates to the individual polymorphism of the envelope glycoprotein targeted by host humoral immune system at that point. SDM analysis also showed that small genetically related changes govern the infectivity of HCVpp. Our data also showed that AAV negative sera carried nAbs against viral variants which were removed from the population. This data strengthened the findings that the *in vivo* nAb response to HCV infection lags behind the constantly evolving HCV and aids in immune escape.

Lastly, we successfully identified epitopes targeted by patient derived VF-Fabs in the antibody associated HCV using a reverse epitope mapping approach. Our data shows that VF-Fab are broadly reactive against viral variants which were previously not encountered by the immune system. Primary investigation of E1E2 gene junction revealed that HVR1 and $E2_{412\text{-}423}$ epitope (AP33) are targeted by a panel of unrelated VF-Fab derived from different patients. This implied immunogenicity of the epitope varies amongst the infected individuals. Conformational epitope mapping analysis showed five binding motifs. Similarly, in this analysis, VF-Fab recognised HVR1 epitope (AN1) further strengthening the role of HVR1 in HCV biology. Two epitopes AN2 and AN3 overlap with the discontinuous epitope targeted by a broadly neutralising antibody AR3C which blocks the CD81 interaction with E2 glycoprotein. This data indicates some infected individuals generate antibodies to block the CD81 interaction. However, the lack of sustained, multi specific, vigorous antibody response

results in failure to clear the virus. We identified two new epitopes, AN4 and AN5, whose role in HCV infection needs to be established. Moreover, when we combined the antigenic specificities of VF-Fab in the neutralisation experiments we observed significant greater reduction ($p<0.05$-0.0001) in the infectivity of HCVpp. Together our neutralisation assay and epitope mapping data signifies that combining broadly nAbs which target different epitopes could enhance the neutralisation efficacy.

We provide unique evidence that natural humoral immune escape of HCV (4a genotype) can occur within the HVR1.

In summary, the data presented here provides new information on humoral immune targeting of viral variants in qausispecies pool and the potential epitopes in the envelope protein involved in this interaction.

Future Directions

Future Directions

Identifying a conserved epitope(s) across all the HCV genotypes is a very big challenge in HCV vaccine development. Broadly neutralising MAbs have been identified to target a discontinuous CD81 epitope in the E2, yet have only been tested in HCVpp and HCVcc. *In vivo,* quasispecies are much more complex than these HCV models. This thesis presents opportunities for further research into immunovirology of HCV infection.

In this thesis, we observed that MAb AP33 was able to capture viral variant in only two out of eight $E2_{412\text{-}423}$ epitope positive samples. Importantly, the targeted variant was found to be clonotypic in nature. This implied that immunogenicity of the epitope is genotype specific and varies with the individual. Additional research using a panel of polyclonal antibodies (from patients who have resolved HCV infection) and MAbs to challenge the HCV sera is warranted. Furthermore, a larger panel of HCVpp and corresponding HCVcc needs to be explored following the antibody-HCV sera pull down experiments. These investigations have the potential to aid in the identification of viral variant(s) targeted by antibodies which will enhance our understanding of immunogenicity of the sequences targeted from a heterogeneous virus population.

From our neutralisation assays, we observed that VF-Fab from 1b-5-1 was most neutralising. Peripheral blood mononuclear cells from patient 1b-5 can be obtained and B cells from that patient can be immortalised. Another approach to obtain B cells is isolating them from tonsils of patient 1b-5. The cells can be then screened for the secretion of antibodies. These antibodies then can be used in the neutralisation assays. Furthermore, combinatorial antibody libraries can be prepared. Four types of antibody libraries can be built. i) Immune libraries: here information from V gene of VF-Fab1b-5-1 can be used to target E2 glycoprotein ii) Semi-synthetic libraries: here unarranged

V genes from pre-B cells from patient 1b-5-1 can be used or complementary determining region (CDR) H3 from VF-Fab1b-5-1 can be randomised iii) Synthetic libraries: can be constructed by randomising the CDR cassettes where V, D and J gene segments are assembled in vitro iv) Naïve libraries: V gene segment from unimmunised or healthy individuals can be rearranged or synthetic V gene segment can be constructed. Our epitope mapping data presents opportunities for translational research. Methods to identify roles of the two new epitopes AN4 and AN5 have been discussed in Chapter 5. Similarly, the information on AN4 and AN5 epitope can be further used to develop monoclonal antibodies against these epitopes. Our bioinformatics analysis has shown that AN4 and AN5 epitopes are conserved across the genotypes. Moreover, AN4 epitope is located within the Ig like domain of the E2 glycoprotein which is conformationally flexible. Proteins with Ig like domain have conserved sequence patterns and been shown to be involved in the protein-protein or protein-ligand interactions. Peptides corresponding to AN4 and AN5 epitopes can be designed and used to immunise the animals to produce MAbs. A step by step site directed mutagenesis of epitope followed by HCVpp neutralisation assay can be used to study whether the MAbs against AN4 and AN5 are neutralising or non-neutralising. Similarly, this approach can be used to identify role of AN4 epitope in governing the conformation of the E2 glycoprotein.

Furthermore, using information from already well characterised MAbs, antigenic targeting potential of these MAbs can be combined which will provide us further insight in the prospective use of a combination of antibodies to control HCV infection, as a possible adjunct therapy.

References

1. **Messina JP, Humphreys I, Flaxman A, Brown A, Cooke GS, Pybus OG, Barnes E.** 2015. Global distribution and prevalence of hepatitis C virus genotypes. Hepatology **61:**77-87.
2. **Choo QL, Kuo G, Weiner AJ, Overby LR, Bradley DW, Houghton M.** 1989. Isolation of a cDNA clone derived from a blood-borne non-A, non-B viral hepatitis genome. Science **244:**359-362.
3. **Lauer GM, Walker BD.** 2001. Hepatitis C virus infection. N Engl J Med **345:**41-52.
4. **Simmonds P.** 2013. The origin of hepatitis C virus. Curr Top Microbiol Immunol **369:**1-15.
5. **Smith DB, Becher P, Bukh J, Gould EA, Meyers G, Monath T, Muerhoff AS, Pletnev A, Rico-Hesse R, Stapleton JT, Simmonds P.** 2016. Proposed update to the taxonomy of the genera Hepacivirus and Pegivirus within the Flaviviridae family. J Gen Virol **97:**2894-2907.
6. **Tan SL.** 2006. *In* Tan SL (ed), Hepatitis C Viruses: Genomes and Molecular Biology, Norfolk (UK).
7. **Penin F, Dubuisson J, Rey FA, Moradpour D, Pawlotsky JM.** 2004. Structural biology of hepatitis C virus. Hepatology **39:**5-19.
8. **Santolini E, Migliaccio G, La Monica N.** 1994. Biosynthesis and biochemical properties of the hepatitis C virus core protein. J Virol **68:**3631-3641.
9. **Miyanari Y, Atsuzawa K, Usuda N, Watashi K, Hishiki T, Zayas M, Bartenschlager R, Wakita T, Hijikata M, Shimotohno K.** 2007. The lipid droplet is an important organelle for hepatitis C virus production. Nat Cell Biol **9:**1089-1097.
10. **Pavlovic D, Neville DC, Argaud O, Blumberg B, Dwek RA, Fischer WB, Zitzmann N.** 2003. The hepatitis C virus p7 protein forms an ion channel that is inhibited by long-alkyl-chain iminosugar derivatives. Proc Natl Acad Sci U S A **100:**6104-6108.
11. **Sakai A, Claire MS, Faulk K, Govindarajan S, Emerson SU, Purcell RH, Bukh J.** 2003. The p7 polypeptide of hepatitis C virus is critical for infectivity and contains functionally important genotype-specific sequences. Proc Natl Acad Sci U S A **100:**11646-11651.
12. **Bartenschlager R, Ahlborn-Laake L, Mous J, Jacobsen H.** 1993. Nonstructural protein 3 of the hepatitis C virus encodes a serine-type proteinase required for cleavage at the NS3/4 and NS4/5 junctions. J Virol **67:**3835-3844.
13. **Guo M, Pei R, Yang Q, Cao H, Wang Y, Wu C, Chen J, Zhou Y, Hu X, Lu M, Chen X.** 2015. Phosphatidylserine-specific phospholipase A1 involved in hepatitis C virus assembly through NS2 complex formation. J Virol **89:**2367-2377.

14. **Gwack Y, Kim DW, Han JH, Choe J.** 1996. Characterization of RNA binding activity and RNA helicase activity of the hepatitis C virus NS3 protein. Biochem Biophys Res Commun **225:**654-659.
15. **Morikawa K, Lange CM, Gouttenoire J, Meylan E, Brass V, Penin F, Moradpour D.** 2011. Nonstructural protein 3-4A: the Swiss army knife of hepatitis C virus. J Viral Hepat **18:**305-315.
16. **Pietschmann T, Lohmann V, Rutter G, Kurpanek K, Bartenschlager R.** 2001. Characterization of cell lines carrying self-replicating hepatitis C virus RNAs. J Virol **75:**1252-1264.
17. **Gouttenoire J, Penin F, Moradpour D.** 2010. Hepatitis C virus nonstructural protein 4B: a journey into unexplored territory. Rev Med Virol **20:**117-129.
18. **Dimitrova M, Imbert I, Kieny MP, Schuster C.** 2003. Protein-protein interactions between hepatitis C virus nonstructural proteins. J Virol **77:**5401-5414.
19. **Jones DM, Patel AH, Targett-Adams P, McLauchlan J.** 2009. The hepatitis C virus NS4B protein can trans-complement viral RNA replication and modulates production of infectious virus. J Virol **83:**2163-2177.
20. **Dubuisson J.** 2007. Hepatitis C virus proteins. World J Gastroenterol **13:**2406-2415.
21. **Ploen D, Hildt E.** 2015. Hepatitis C virus comes for dinner: How the hepatitis C virus interferes with autophagy. World J Gastroenterol **21:**8492-8507.
22. **Scull MA, Ploss A.** 2012. Exiting from uncharted territory: hepatitis C virus assembles in mouse cell lines. Hepatology **55:**645-648.
23. **Lin CC, Tsai P, Sun HY, Hsu MC, Lee JC, Wu IC, Tsao CW, Chang TT, Young KC.** 2014. Apolipoprotein J, a glucose-upregulated molecular chaperone, stabilizes core and NS5A to promote infectious hepatitis C virus virion production. J Hepatol **61:**984-993.
24. **Bartenschlager R, Lohmann V.** 2000. Replication of the hepatitis C virus. Baillieres Best Pract Res Clin Gastroenterol **14:**241-254.
25. **Clarke B.** 1997. Molecular virology of hepatitis C virus. J Gen Virol **78 (Pt 10):**2397-2410.
26. **Bressanelli S, Tomei L, Roussel A, Incitti I, Vitale RL, Mathieu M, De Francesco R, Rey FA.** 1999. Crystal structure of the RNA-dependent RNA polymerase of hepatitis C virus. Proc Natl Acad Sci U S A **96:**13034-13039.
27. **Falson P, Bartosch B, Alsaleh K, Tews BA, Loquet A, Ciczora Y, Riva L, Montigny C, Montpellier C, Duverlie G, Pecheur EI, le Maire M, Cosset FL, Dubuisson J, Penin F.** 2015. Hepatitis C Virus Envelope Glycoprotein E1 Forms Trimers at the Surface of the Virion. J Virol **89:**10333-10346.

28. **Carrere-Kremer S, Montpellier C, Lorenzo L, Brulin B, Cocquerel L, Belouzard S, Penin F, Dubuisson J.** 2004. Regulation of hepatitis C virus polyprotein processing by signal peptidase involves structural determinants at the p7 sequence junctions. J Biol Chem **279:**41384-41392.
29. **Carrere-Kremer S, Montpellier-Pala C, Cocquerel L, Wychowski C, Penin F, Dubuisson J.** 2002. Subcellular localization and topology of the p7 polypeptide of hepatitis C virus. J Virol **76:**3720-3730.
30. **Lavie M, Goffard A, Dubuisson J.** 2006. HCV Glycoproteins: Assembly of a Functional E1-E2 Heterodimer. *In* Tan SL (ed), Hepatitis C Viruses: Genomes and Molecular Biology, Norfolk (UK).
31. **Whidby J, Mateu G, Scarborough H, Demeler B, Grakoui A, Marcotrigiano J.** 2009. Blocking hepatitis C virus infection with recombinant form of envelope protein 2 ectodomain. J Virol **83:**11078-11089.
32. **Kong L, Giang E, Nieusma T, Kadam RU, Cogburn KE, Hua Y, Dai X, Stanfield RL, Burton DR, Ward AB, Wilson IA, Law M.** 2013. Hepatitis C virus E2 envelope glycoprotein core structure. Science **342:**1090-1094.
33. **Bartosch B, Dubuisson J, Cosset FL.** 2003. Infectious hepatitis C virus pseudo-particles containing functional E1-E2 envelope protein complexes. J Exp Med **197:**633-642.
34. **Burda P, Aebi M.** 1999. The dolichol pathway of N-linked glycosylation. Biochim Biophys Acta **1426:**239-257.
35. **Orlova OV, Drutsa VL, Spirin PV, Prasolov VS, Rubtsov PM, Kochetkov SN, Beljelarskaya SN.** 2015. The role of HCV e2 protein glycosylation in functioning of virus envelope proteins in insect and Mammalian cells. Acta Naturae **7:**87-97.
36. **Helle F, Vieyres G, Elkrief L, Popescu CI, Wychowski C, Descamps V, Castelain S, Roingeard P, Duverlie G, Dubuisson J.** 2010. Role of N-linked glycans in the functions of hepatitis C virus envelope proteins incorporated into infectious virions. J Virol **84:**11905-11915.
37. **Russ WP, Engelman DM.** 2000. The GxxxG motif: a framework for transmembrane helix-helix association. J Mol Biol **296:**911-919.
38. **Senes A, Gerstein M, Engelman DM.** 2000. Statistical analysis of amino acid patterns in transmembrane helices: the GxxxG motif occurs frequently and in association with beta-branched residues at neighboring positions. J Mol Biol **296:**921-936.
39. **Op De Beeck A, Montserret R, Duvet S, Cocquerel L, Cacan R, Barberot B, Le Maire M, Penin F, Dubuisson J.** 2000. The transmembrane domains of hepatitis C virus envelope glycoproteins E1 and E2 play a major role in heterodimerization. J Biol Chem **275:**31428-31437.
40. **Castelli M, Clementi N, Sautto GA, Pfaff J, Kahle KM, Barnes T, Doranz BJ, Dal Peraro M, Clementi M, Burioni R, Mancini**

N. 2014. HCV E2 core structures and mAbs: something is still missing. Drug Discov Today **19:**1964-1970.

41. **Sabahi A, Uprichard SL, Wimley WC, Dash S, Garry RF.** 2014. Unexpected structural features of the hepatitis C virus envelope protein 2 ectodomain. J Virol **88:**10280-10288.
42. **Khan AG, Whidby J, Miller MT, Scarborough H, Zatorski AV, Cygan A, Price AA, Yost SA, Bohannon CD, Jacob J, Grakoui A, Marcotrigiano J.** 2014. Structure of the core ectodomain of the hepatitis C virus envelope glycoprotein 2. Nature **509:**381-384.
43. **Dubuisson J, Helle F, Cocquerel L.** 2008. Early steps of the hepatitis C virus life cycle. Cell Microbiol **10:**821-827.
44. **Owsianka AM, Timms JM, Tarr AW, Brown RJ, Hickling TP, Szwejk A, Bienkowska-Szewczyk K, Thomson BJ, Patel AH, Ball JK.** 2006. Identification of conserved residues in the E2 envelope glycoprotein of the hepatitis C virus that are critical for CD81 binding. J Virol **80:**8695-8704.
45. **Law M, Maruyama T, Lewis J, Giang E, Tarr AW, Stamataki Z, Gastaminza P, Chisari FV, Jones IM, Fox RI, Ball JK, McKeating JA, Kneteman NM, Burton DR.** 2008. Broadly neutralizing antibodies protect against hepatitis C virus quasispecies challenge. Nat Med **14:**25-27.
46. **Kong L, Giang E, Nieusma T, Robbins JB, Deller MC, Stanfield RL, Wilson IA, Law M.** 2012. Structure of hepatitis C virus envelope glycoprotein E2 antigenic site 412 to 423 in complex with antibody AP33. J Virol **86:**13085-13088.
47. **Kong L, Giang E, Robbins JB, Stanfield RL, Burton DR, Wilson IA, Law M.** 2012. Structural basis of hepatitis C virus neutralization by broadly neutralizing antibody HCV1. Proc Natl Acad Sci U S A **109:**9499-9504.
48. **Meola A, Tarr AW, England P, Meredith LW, McClure CP, Foung SK, McKeating JA, Ball JK, Rey FA, Krey T.** 2015. Structural flexibility of a conserved antigenic region in hepatitis C virus glycoprotein E2 recognized by broadly neutralizing antibodies. J Virol **89:**2170-2181.
49. **Zhang P, Wu CG, Mihalik K, Virata-Theimer ML, Yu MY, Alter HJ, Feinstone SM.** 2007. Hepatitis C virus epitope-specific neutralizing antibodies in Igs prepared from human plasma. Proc Natl Acad Sci U S A **104:**8449-8454.
50. **Kong L, Jackson KN, Wilson IA, Law M.** 2015. Capitalizing on knowledge of hepatitis C virus neutralizing epitopes for rational vaccine design. Curr Opin Virol **11:**148-157.
51. **Giang E, Dorner M, Prentoe JC, Dreux M, Evans MJ, Bukh J, Rice CM, Ploss A, Burton DR, Law M.** 2012. Human broadly neutralizing antibodies to the envelope glycoprotein complex of hepatitis C virus. Proc Natl Acad Sci U S A **109:**6205-6210.
52. **Kong L, Lee DE, Kadam RU, Liu T, Giang E, Nieusma T, Garces F, Tzarum N, Woods VL, Jr., Ward AB, Li S, Wilson IA, Law M.** 2016. Structural flexibility at a major conserved

antibody target on hepatitis C virus E2 antigen. Proc Natl Acad Sci U S A doi:10.1073/pnas.1609780113.

53. **Neumann AU, Lam NP, Dahari H, Gretch DR, Wiley TE, Layden TJ, Perelson AS.** 1998. Hepatitis C viral dynamics in vivo and the antiviral efficacy of interferon-alpha therapy. Science **282:**103-107.
54. **Iacovacci S, Manzin A, Barca S, Sargiacomo M, Serafino A, Valli MB, Macioce G, Hassan HJ, Ponzetto A, Clementi M, Peschle C, Carloni G.** 1997. Molecular characterization and dynamics of hepatitis C virus replication in human fetal hepatocytes infected in vitro. Hepatology **26:**1328-1337.
55. **McAllister J, Casino C, Davidson F, Power J, Lawlor E, Yap PL, Simmonds P, Smith DB.** 1998. Long-term evolution of the hypervariable region of hepatitis C virus in a common-source-infected cohort. J Virol **72:**4893-4905.
56. **Erickson AL, Kimura Y, Igarashi S, Eichelberger J, Houghton M, Sidney J, McKinney D, Sette A, Hughes AL, Walker CM.** 2001. The Outcome of Hepatitis C Virus Infection Is Predicted by Escape Mutations in Epitopes Targeted by Cytotoxic T Lymphocytes. Immunity **15:**883-895.
57. **Timm J, Lauer GM, Kavanagh DG, Sheridan I, Kim AY, Lucas M, Pillay T, Ouchi K, Reyor LL, Schulze zur Wiesch J, Gandhi RT, Chung RT, Bhardwaj N, Klenerman P, Walker BD, Allen TM.** 2004. CD8 epitope escape and reversion in acute HCV infection. J Exp Med **200:**1593-1604.
58. **Bowen DG, Walker CM.** 2005. Adaptive immune responses in acute and chronic hepatitis C virus infection. Nature **436:**946-952.
59. **Navas S, Martin J, Quiroga JA, Castillo I, Carreno V.** 1998. Genetic diversity and tissue compartmentalization of the hepatitis C virus genome in blood mononuclear cells, liver, and serum from chronic hepatitis C patients. J Virol **72:**1640-1646.
60. **Ray SC, Fanning L, Wang XH, Netski DM, Kenny-Walsh E, Thomas DL.** 2005. Divergent and convergent evolution after a common-source outbreak of hepatitis C virus. J Exp Med **201:**1753-1759.
61. **Ball JK, Tarr AW, McKeating JA.** 2014. The past, present and future of neutralizing antibodies for hepatitis C virus. Antiviral Res **105:**100-111.
62. **Fafi-Kremer S, Fauvelle C, Felmlee DJ, Zeisel MB, Lepiller Q, Fofana I, Heydmann L, Stoll-Keller F, Baumert TF.** 2012. Neutralizing antibodies and pathogenesis of hepatitis C virus infection. Viruses **4:**2016-2030.
63. **Tarr AW, Khera T, Hueging K, Sheldon J, Steinmann E, Pietschmann T, Brown RJ.** 2015. Genetic Diversity Underlying the Envelope Glycoproteins of Hepatitis C Virus: Structural and Functional Consequences and the Implications for Vaccine Design. Viruses **7:**3995-4046.

64. **Allain JP, Dong Y, Vandamme AM, Moulton V, Salemi M.** 2000. Evolutionary rate and genetic drift of hepatitis C virus are not correlated with the host immune response: studies of infected donor-recipient clusters. J Virol **74:**2541-2549.
65. **Vieyres G, Dubuisson J, Patel AH.** 2011. Characterization of antibody-mediated neutralization directed against the hypervariable region 1 of hepatitis C virus E2 glycoprotein. J Gen Virol **92:**494-506.
66. **Zeisel MB, Baumert TF.** 2009. HCV entry and neutralizing antibodies: lessons from viral variants. Future Microbiol **4:**511-517.
67. **Ray R, Meyer K, Banerjee A, Basu A, Coates S, Abrignani S, Houghton M, Frey SE, Belshe RB.** 2010. Characterization of antibodies induced by vaccination with hepatitis C virus envelope glycoproteins. J Infect Dis **202:**862-866.
68. **Guan M, Wang W, Liu X, Tong Y, Liu Y, Ren H, Zhu S, Dubuisson J, Baumert TF, Zhu Y, Peng H, Aurelian L, Zhao P, Qi Z.** 2012. Three different functional microdomains in the hepatitis C virus hypervariable region 1 (HVR1) mediate entry and immune evasion. J Biol Chem **287:**35631-35645.
69. **Bankwitz D, Steinmann E, Bitzegeio J, Ciesek S, Friesland M, Herrmann E, Zeisel MB, Baumert TF, Keck ZY, Foung SK, Pecheur EI, Pietschmann T.** 2010. Hepatitis C virus hypervariable region 1 modulates receptor interactions, conceals the CD81 binding site, and protects conserved neutralizing epitopes. J Virol **84:**5751-5763.
70. **Bankwitz D, Vieyres G, Hueging K, Bitzegeio J, Doepke M, Chhatwal P, Haid S, Catanese MT, Zeisel MB, Nicosia A, Baumert TF, Kaderali L, Pietschmann T.** 2014. Role of hypervariable region 1 for the interplay of hepatitis C virus with entry factors and lipoproteins. J Virol **88:**12644-12655.
71. **Prentoe J, Verhoye L, Velazquez Moctezuma R, Buysschaert C, Farhoudi A, Wang R, Alter H, Meuleman P, Bukh J.** 2015. HVR1-mediated antibody evasion of highly infectious in vivo adapted HCV in humanised mice. Gut doi:10.1136/gutjnl-2015-310300.
72. **Habersetzer F, Fournillier A, Dubuisson J, Rosa D, Abrignani S, Wychowski C, Nakano I, Trepo C, Desgranges C, Inchauspe G.** 1998. Characterization of human monoclonal antibodies specific to the hepatitis C virus glycoprotein E2 with in vitro binding neutralization properties. Virology **249:**32-41.
73. **Farci P, Shimoda A, Wong D, Cabezon T, De Gioannis D, Strazzera A, Shimizu Y, Shapiro M, Alter HJ, Purcell RH.** 1996. Prevention of hepatitis C virus infection in chimpanzees by hyperimmune serum against the hypervariable region 1 of the envelope 2 protein. Proc Natl Acad Sci U S A **93:**15394-15399.

74. **Owsianka A, Clayton RF, Loomis-Price LD, McKeating JA, Patel AH.** 2001. Functional analysis of hepatitis C virus E2 glycoproteins and virus-like particles reveals structural dissimilarities between different forms of E2. J Gen Virol **82:**1877-1883.
75. **Moradpour D, Penin F.** 2013. Hepatitis C virus proteins: from structure to function. Curr Top Microbiol Immunol **369:**113-142.
76. **Drummer HE.** 2014. Challenges to the development of vaccines to hepatitis C virus that elicit neutralizing antibodies. Front Microbiol **5:**329.
77. **Freedman H, Logan MR, Law JL, Houghton M.** 2016. Structure and Function of the Hepatitis C Virus Envelope Glycoproteins E1 and E2: Antiviral and Vaccine Targets. ACS Infect Dis **2:**749-762.
78. **Alhammad Y, Gu J, Boo I, Harrison D, McCaffrey K, Vietheer PT, Edwards S, Quinn C, Coulibaly F, Poumbourios P, Drummer HE.** 2015. Monoclonal Antibodies Directed toward the Hepatitis C Virus Glycoprotein E2 Detect Antigenic Differences Modulated by the N-Terminal Hypervariable Region 1 (HVR1), HVR2, and Intergenotypic Variable Region. J Virol **89:**12245-12261.
79. **Monazahian M, Böhme I, Bonk S, Koch A, Scholz C, Grethe S, Thomssen R.** 1999. Low density lipoprotein receptor as a candidate receptor for hepatitis C virus. Journal of Medical Virology **57:**223-229.
80. **Pileri P, Uematsu Y, Campagnoli S, Galli G, Falugi F, Petracca R, Weiner AJ, Houghton M, Rosa D, Grandi G, Abrignani S.** 1998. Binding of hepatitis C virus to CD81. Science **282:**938-941.
81. **Scarselli E, Ansuini H, Cerino R, Roccasecca RM, Acali S, Filocamo G, Traboni C, Nicosia A, Cortese R, Vitelli A.** 2002. The human scavenger receptor class B type I is a novel candidate receptor for the hepatitis C virus. EMBO J **21:**5017-5025.
82. **Lozach PY, Amara A, Bartosch B, Virelizier JL, Arenzana-Seisdedos F, Cosset FL, Altmeyer R.** 2004. C-type lectins L-SIGN and DC-SIGN capture and transmit infectious hepatitis C virus pseudotype particles. J Biol Chem **279:**32035-32045.
83. **Saunier B, Triyatni M, Ulianich L, Maruvada P, Yen P, Kohn LD.** 2003. Role of the asialoglycoprotein receptor in binding and entry of hepatitis C virus structural proteins in cultured human hepatocytes. J Virol **77:**546-559.
84. **Barth H, Schafer C, Adah MI, Zhang F, Linhardt RJ, Toyoda H, Kinoshita-Toyoda A, Toida T, Van Kuppevelt TH, Depla E, Von Weizsacker F, Blum HE, Baumert TF.** 2003. Cellular binding of hepatitis C virus envelope glycoprotein E2 requires cell surface heparan sulfate. J Biol Chem **278:**41003-41012.

85. **Bartosch B, Cosset FL.** 2006. Cell entry of hepatitis C virus. Virology **348:**1-12.
86. **Agnello V, Abel G, Elfahal M, Knight GB, Zhang QX.** 1999. Hepatitis C virus and other flaviviridae viruses enter cells via low density lipoprotein receptor. Proc Natl Acad Sci U S A **96:**12766-12771.
87. **Evans MJ, von Hahn T, Tscherne DM, Syder AJ, Panis M, Wolk B, Hatziioannou T, McKeating JA, Bieniasz PD, Rice CM.** 2007. Claudin-1 is a hepatitis C virus co-receptor required for a late step in entry. Nature **446:**801-805.
88. **Ploss A, Evans MJ, Gaysinskaya VA, Panis M, You H, de Jong YP, Rice CM.** 2009. Human occludin is a hepatitis C virus entry factor required for infection of mouse cells. Nature **457:**882-886.
89. **Zahid MN, Turek M, Xiao F, Thi VL, Guerin M, Fofana I, Bachellier P, Thompson J, Delang L, Neyts J, Bankwitz D, Pietschmann T, Dreux M, Cosset FL, Grunert F, Baumert TF, Zeisel MB.** 2013. The postbinding activity of scavenger receptor class B type I mediates initiation of hepatitis C virus infection and viral dissemination. Hepatology **57:**492-504.
90. **Lavillette D, Tarr AW, Voisset C, Donot P, Bartosch B, Bain C, Patel AH, Dubuisson J, Ball JK, Cosset FL.** 2005. Characterization of host-range and cell entry properties of the major genotypes and subtypes of hepatitis C virus. Hepatology **41:**265-274.
91. **Cormier EG, Tsamis F, Kajumo F, Durso RJ, Gardner JP, Dragic T.** 2004. CD81 is an entry coreceptor for hepatitis C virus. Proc Natl Acad Sci U S A **101:**7270-7274.
92. **McKeating JA, Zhang LQ, Logvinoff C, Flint M, Zhang J, Yu J, Butera D, Ho DD, Dustin LB, Rice CM, Balfe P.** 2004. Diverse hepatitis C virus glycoproteins mediate viral infection in a CD81-dependent manner. J Virol **78:**8496-8505.
93. **Wakita T, Pietschmann T, Kato T, Date T, Miyamoto M, Zhao Z, Murthy K, Habermann A, Krausslich HG, Mizokami M, Bartenschlager R, Liang TJ.** 2005. Production of infectious hepatitis C virus in tissue culture from a cloned viral genome. Nat Med **11:**791-796.
94. **Zhang J, Randall G, Higginbottom A, Monk P, Rice CM, McKeating JA.** 2004. CD81 is required for hepatitis C virus glycoprotein-mediated viral infection. J Virol **78:**1448-1455.
95. **Liu Z, Tian Y, Machida K, Lai MM, Luo G, Foung SK, Ou JH.** 2012. Transient activation of the PI3K-AKT pathway by hepatitis C virus to enhance viral entry. J Biol Chem **287:**41922-41930.
96. **Fletcher NF, Sutaria R, Jo J, Barnes A, Blahova M, Meredith LW, Cosset FL, Curbishley SM, Adams DH, Bertoletti A, McKeating JA.** 2014. Activated macrophages promote hepatitis C virus entry in a tumor necrosis factor-dependent manner. Hepatology **59:**1320-1330.

97. **Blanchard E, Belouzard S, Goueslain L, Wakita T, Dubuisson J, Wychowski C, Rouille Y.** 2006. Hepatitis C virus entry depends on clathrin-mediated endocytosis. J Virol **80:**6964-6972.
98. **Tscherne DM, Jones CT, Evans MJ, Lindenbach BD, McKeating JA, Rice CM.** 2006. Time- and temperature-dependent activation of hepatitis C virus for low-pH-triggered entry. J Virol **80:**1734-1741.
99. **Thomssen R, Bonk S, Propfe C, Heermann KH, Kochel HG, Uy A.** 1992. Association of hepatitis C virus in human sera with beta-lipoprotein. Med Microbiol Immunol **181:**293-300.
100. **Andre P, Komurian-Pradel F, Deforges S, Perret M, Berland JL, Sodoyer M, Pol S, Brechot C, Paranhos-Baccala G, Lotteau V.** 2002. Characterization of low- and very-low-density hepatitis C virus RNA-containing particles. J Virol **76:**6919-6928.
101. **Jones DM, McLauchlan J.** 2010. Hepatitis C virus: assembly and release of virus particles. J Biol Chem **285:**22733-22739.
102. **Ding Q, von Schaewen M, Ploss A.** 2014. The impact of hepatitis C virus entry on viral tropism. Cell Host Microbe **16:**562-568.
103. **Thimme R, Oldach D, Chang KM, Steiger C, Ray SC, Chisari FV.** 2001. Determinants of viral clearance and persistence during acute hepatitis C virus infection. J Exp Med **194:**1395-1406.
104. **Netski DM, Mosbruger T, Depla E, Maertens G, Ray SC, Hamilton RG, Roundtree S, Thomas DL, McKeating J, Cox A.** 2005. Humoral immune response in acute hepatitis C virus infection. Clin Infect Dis **41:**667-675.
105. **Sagnelli E, Coppola N, Marrocco C, Coviello G, Battaglia M, Messina V, Rossi G, Sagnelli C, Scolastico C, Filippini P.** 2005. Diagnosis of hepatitis C virus related acute hepatitis by serial determination of IgM anti-HCV titres. J Hepatol **42:**646-651.
106. **Wilkins C, Gale M, Jr.** 2010. Recognition of viruses by cytoplasmic sensors. Curr Opin Immunol **22:**41-47.
107. **Saito T, Owen DM, Jiang F, Marcotrigiano J, Gale M, Jr.** 2008. Innate immunity induced by composition-dependent RIG-I recognition of hepatitis C virus RNA. Nature **454:**523-527.
108. **Schnell G, Loo YM, Marcotrigiano J, Gale M, Jr.** 2012. Uridine composition of the poly-U/UC tract of HCV RNA defines non-self recognition by RIG-I. PLoS Pathog **8:**e1002839.
109. **Liu HM, Loo YM, Horner SM, Zornetzer GA, Katze MG, Gale M, Jr.** 2012. The mitochondrial targeting chaperone 14-3-3epsilon regulates a RIG-I translocon that mediates membrane association and innate antiviral immunity. Cell Host Microbe **11:**528-537.
110. **Horner SM, Gale M, Jr.** 2013. Regulation of hepatic innate immunity by hepatitis C virus. Nat Med **19:**879-888.

111. **Yamamoto M, Sato S, Hemmi H, Hoshino K, Kaisho T, Sanjo H, Takeuchi O, Sugiyama M, Okabe M, Takeda K, Akira S.** 2003. Role of adaptor TRIF in the MyD88-independent toll-like receptor signaling pathway. Science **301:**640-643.
112. **Kawai T, Takahashi K, Sato S, Coban C, Kumar H, Kato H, Ishii KJ, Takeuchi O, Akira S.** 2005. IPS-1, an adaptor triggering RIG-I- and Mda5-mediated type I interferon induction. Nat Immunol **6:**981-988.
113. **Sharma S, tenOever BR, Grandvaux N, Zhou GP, Lin R, Hiscott J.** 2003. Triggering the interferon antiviral response through an IKK-related pathway. Science **300:**1148-1151.
114. **Kawai T, Akira S.** 2008. Toll-like receptor and RIG-I-like receptor signaling. Ann N Y Acad Sci **1143:**1-20.
115. **Silverman RH.** 2007. Viral encounters with 2',5'-oligoadenylate synthetase and RNase L during the interferon antiviral response. J Virol **81:**12720-12729.
116. **Degols G, Eldin P, Mechti N.** 2007. ISG20, an actor of the innate immune response. Biochimie **89:**831-835.
117. **Wang C, Pflugheber J, Sumpter R, Jr., Sodora DL, Hui D, Sen GC, Gale M, Jr.** 2003. Alpha interferon induces distinct translational control programs to suppress hepatitis C virus RNA replication. J Virol **77:**3898-3912.
118. **Li XD, Sun L, Seth RB, Pineda G, Chen ZJ.** 2005. Hepatitis C virus protease NS3/4A cleaves mitochondrial antiviral signaling protein off the mitochondria to evade innate immunity. Proc Natl Acad Sci U S A **102:**17717-17722.
119. **Li K, Foy E, Ferreon JC, Nakamura M, Ferreon AC, Ikeda M, Ray SC, Gale M, Jr., Lemon SM.** 2005. Immune evasion by hepatitis C virus NS3/4A protease-mediated cleavage of the Toll-like receptor 3 adaptor protein TRIF. Proc Natl Acad Sci U S A **102:**2992-2997.
120. **Gale M, Jr., Blakely CM, Kwieciszewski B, Tan SL, Dossett M, Tang NM, Korth MJ, Polyak SJ, Gretch DR, Katze MG.** 1998. Control of PKR protein kinase by hepatitis C virus nonstructural 5A protein: molecular mechanisms of kinase regulation. Mol Cell Biol **18:**5208-5218.
121. **Bode JG, Ludwig S, Ehrhardt C, Albrecht U, Erhardt A, Schaper F, Heinrich PC, Haussinger D.** 2003. IFN-alpha antagonistic activity of HCV core protein involves induction of suppressor of cytokine signaling-3. FASEB J **17:**488-490.
122. **Dolganiuc A, Chang S, Kodys K, Mandrekar P, Bakis G, Cormier M, Szabo G.** 2006. Hepatitis C virus (HCV) core protein-induced, monocyte-mediated mechanisms of reduced IFN-alpha and plasmacytoid dendritic cell loss in chronic HCV infection. J Immunol **177:**6758-6768.
123. **Lee SH, Miyagi T, Biron CA.** 2007. Keeping NK cells in highly regulated antiviral warfare. Trends Immunol **28:**252-259.
124. **Pallmer K, Oxenius A.** 2016. Recognition and Regulation of T Cells by NK Cells. Front Immunol **7:**251.

125. **Tseng CT, Klimpel GR.** 2002. Binding of the hepatitis C virus envelope protein E2 to CD81 inhibits natural killer cell functions. J Exp Med **195:**43-49.
126. **Wang JM, Cheng YQ, Shi L, Ying RS, Wu XY, Li GY, Moorman JP, Yao ZQ.** 2013. KLRG1 negatively regulates natural killer cell functions through the Akt pathway in individuals with chronic hepatitis C virus infection. J Virol **87:**11626-11636.
127. **Yoon JC, Yang CM, Song Y, Lee JM.** 2016. Natural killer cells in hepatitis C: Current progress. World J Gastroenterol **22:**1449-1460.
128. **Dustin LB, Rice CM.** 2007. Flying under the radar: the immunobiology of hepatitis C. Annu Rev Immunol **25:**71-99.
129. **Cashman SB, Marsden BD, Dustin LB.** 2014. The Humoral Immune Response to HCV: Understanding is Key to Vaccine Development. Front Immunol **5:**550.
130. **Chang KM, Thimme R, Melpolder JJ, Oldach D, Pemberton J, Moorhead-Loudis J, McHutchison JG, Alter HJ, Chisari FV.** 2001. Differential CD4(+) and CD8(+) T-cell responsiveness in hepatitis C virus infection. Hepatology **33:**267-276.
131. **O'Farrelly C, Doherty DG.** 2007. A Short Primer on Fundamental Immunology, p 15-24. *In* Gershwin ME, Vierling JM, Manns MP (ed), Liver Immunology: Principles and Practice doi:10.1007/978-1-59745-518-3_2. Humana Press, Totowa, NJ.
132. **Dienz O, Rincon M.** 2009. The effects of IL-6 on CD4 T cell responses. Clin Immunol **130:**27-33.
133. **Paul WE, Seder RA.** 1994. Lymphocyte responses and cytokines. Cell **76:**241-251.
134. **Diepolder HM, Zachoval R, Hoffmann RM, Wierenga EA, Santantonio T, Jung MC, Eichenlaub D, Pape GR.** 1995. Possible mechanism involving T-lymphocyte response to non-structural protein 3 in viral clearance in acute hepatitis C virus infection. Lancet **346:**1006-1007.
135. **Missale G, Bertoni R, Lamonaca V, Valli A, Massari M, Mori C, Rumi MG, Houghton M, Fiaccadori F, Ferrari C.** 1996. Different clinical behaviors of acute hepatitis C virus infection are associated with different vigor of the anti-viral cell-mediated immune response. J Clin Invest **98:**706-714.
136. **Urbani S, Amadei B, Fisicaro P, Tola D, Orlandini A, Sacchelli L, Mori C, Missale G, Ferrari C.** 2006. Outcome of acute hepatitis C is related to virus-specific CD4 function and maturation of antiviral memory CD8 responses. Hepatology **44:**126-139.
137. **Shin EC, Park SH, Demino M, Nascimbeni M, Mihalik K, Major M, Veerapu NS, Heller T, Feinstone SM, Rice CM, Rehermann B.** 2011. Delayed induction, not impaired recruitment, of specific CD8(+) T cells causes the late onset of acute hepatitis C. Gastroenterology **141:**686-695, 695 e681.

138. **Racanelli V, Behrens SE, Aliberti J, Rehermann B.** 2004. Dendritic cells transfected with cytopathic self-replicating RNA induce crosspriming of CD8+ T cells and antiviral immunity. Immunity **20:**47-58.
139. **Cooper S, Erickson AL, Adams EJ, Kansopon J, Weiner AJ, Chien DY, Houghton M, Parham P, Walker CM.** 1999. Analysis of a successful immune response against hepatitis C virus. Immunity **10:**439-449.
140. **Thimme R, Bukh J, Spangenberg HC, Wieland S, Pemberton J, Steiger C, Govindarajan S, Purcell RH, Chisari FV.** 2002. Viral and immunological determinants of hepatitis C virus clearance, persistence, and disease. Proc Natl Acad Sci U S A **99:**15661-15668.
141. **Eckels DD, Wang H, Bian TH, Tabatabai N, Gill JC.** 2000. Immunobiology of hepatitis C virus (HCV) infection: the role of CD4 T cells in HCV infection. Immunol Rev **174:**90-97.
142. **Wolfl M, Rutebemberwa A, Mosbruger T, Mao Q, Li HM, Netski D, Ray SC, Pardoll D, Sidney J, Sette A, Allen T, Kuntzen T, Kavanagh DG, Kuball J, Greenberg PD, Cox AL.** 2008. Hepatitis C virus immune escape via exploitation of a hole in the T cell repertoire. J Immunol **181:**6435-6446.
143. **Golden-Mason L, Palmer B, Klarquist J, Mengshol JA, Castelblanco N, Rosen HR.** 2007. Upregulation of PD-1 expression on circulating and intrahepatic hepatitis C virus-specific CD8+ T cells associated with reversible immune dysfunction. J Virol **81:**9249-9258.
144. **Radziewicz H, Ibegbu CC, Fernandez ML, Workowski KA, Obideen K, Wehbi M, Hanson HL, Steinberg JP, Masopust D, Wherry EJ, Altman JD, Rouse BT, Freeman GJ, Ahmed R, Grakoui A.** 2007. Liver-infiltrating lymphocytes in chronic human hepatitis C virus infection display an exhausted phenotype with high levels of PD-1 and low levels of CD127 expression. J Virol **81:**2545-2553.
145. **Radziewicz H, Ibegbu CC, Hon H, Osborn MK, Obideen K, Wehbi M, Freeman GJ, Lennox JL, Workowski KA, Hanson HL, Grakoui A.** 2008. Impaired hepatitis C virus (HCV)-specific effector CD8+ T cells undergo massive apoptosis in the peripheral blood during acute HCV infection and in the liver during the chronic phase of infection. J Virol **82:**9808-9822.
146. **Larrubia JR, Benito-Martinez S, Miquel J, Calvino M, Sanz-de-Villalobos E, Gonzalez-Praetorius A, Albertos S, Garcia-Garzon S, Lokhande M, Parra-Cid T.** 2011. Bim-mediated apoptosis and PD-1/PD-L1 pathway impair reactivity of PD1(+)/CD127(-) HCV-specific CD8(+) cells targeting the virus in chronic hepatitis C virus infection. Cell Immunol **269:**104-114.
147. **Manigold T, Shin EC, Mizukoshi E, Mihalik K, Murthy KK, Rice CM, Piccirillo CA, Rehermann B.** 2006.

Foxp3+CD4+CD25+ T cells control virus-specific memory T cells in chimpanzees that recovered from hepatitis C. Blood **107:**4424-4432.

148. **Ejrnaes M, Filippi CM, Martinic MM, Ling EM, Togher LM, Crotty S, von Herrath MG.** 2006. Resolution of a chronic viral infection after interleukin-10 receptor blockade. J Exp Med **203:**2461-2472.
149. **Carbonneil C, Donkova-Petrini V, Aouba A, Weiss L.** 2004. Defective dendritic cell function in HIV-infected patients receiving effective highly active antiretroviral therapy: neutralization of IL-10 production and depletion of CD4+CD25+ T cells restore high levels of HIV-specific CD4+ T cell responses induced by dendritic cells generated in the presence of IFN-alpha. J Immunol **172:**7832-7840.
150. **Schroeder HW, Jr., Cavacini L.** 2010. Structure and function of immunoglobulins. J Allergy Clin Immunol **125:**S41-52.
151. **Burton DR.** 2002. Antibodies, viruses and vaccines. Nat Rev Immunol **2:**706-713.
152. **Chen PJ, Wang JT, Hwang LH, Yang YH, Hsieh CL, Kao JH, Sheu JC, Lai MY, Wang TH, Chen DS.** 1992. Transient immunoglobulin M antibody response to hepatitis C virus capsid antigen in posttransfusion hepatitis C: putative serological marker for acute viral infection. Proc Natl Acad Sci U S A **89:**5971-5975.
153. **Nikolaeva LI, Blokhina NP, Tsurikova NN, Voronkova NV, Miminoshvili MI, Braginsky DM, Yastrebova ON, Booynitskaya OB, Isaeva OV, Michailov MI, Archakov AI.** 2002. Virus-specific antibody titres in different phases of hepatitis C virus infection. J Viral Hepat **9:**429-437.
154. **Quiroga JA, Campillo ML, Catillo I, Bartolome J, Porres JC, Carreno V.** 1991. IgM antibody to hepatitis C virus in acute and chronic hepatitis C. Hepatology **14:**38-43.
155. **Chen M, Sallberg M, Sonnerborg A, Weiland O, Mattsson L, Jin L, Birkett A, Peterson D, Milich DR.** 1999. Limited humoral immunity in hepatitis C virus infection. Gastroenterology **116:**135-143.
156. **Logvinoff C, Major ME, Oldach D, Heyward S, Talal A, Balfe P, Feinstone SM, Alter H, Rice CM, McKeating JA.** 2004. Neutralizing antibody response during acute and chronic hepatitis C virus infection. Proc Natl Acad Sci U S A **101:**10149-10154.
157. **Yu MY, Bartosch B, Zhang P, Guo ZP, Renzi PM, Shen LM, Granier C, Feinstone SM, Cosset FL, Purcell RH.** 2004. Neutralizing antibodies to hepatitis C virus (HCV) in immune globulins derived from anti-HCV-positive plasma. Proc Natl Acad Sci U S A **101:**7705-7710.
158. **Keck ZY, Li SH, Xia J, von Hahn T, Balfe P, McKeating JA, Witteveldt J, Patel AH, Alter H, Rice CM, Foung SK.** 2009. Mutations in hepatitis C virus E2 located outside the CD81

binding sites lead to escape from broadly neutralizing antibodies but compromise virus infectivity. J Virol **83:**6149-6160.

159. **Keck ZY, Xia J, Wang Y, Wang W, Krey T, Prentoe J, Carlsen T, Li AY, Patel AH, Lemon SM, Bukh J, Rey FA, Foung SK.** 2012. Human monoclonal antibodies to a novel cluster of conformational epitopes on HCV E2 with resistance to neutralization escape in a genotype 2a isolate. PLoS Pathog **8:**e1002653.
160. **Wasilewski L, Ray S, Bailey JR.** 2016. Hepatitis C virus resistance to broadly neutralizing antibodies measured using replication competent virus and pseudoparticles. J Gen Virol doi:10.1099/jgv.0.000608.
161. **Leroux-Roels G, Esquivel CA, DeLeys R, Stuyver L, Elewaut A, Philippe J, Desombere I, Paradijs J, Maertens G.** 1996. Lymphoproliferative responses to hepatitis C virus core, E1, E2, and NS3 in patients with chronic hepatitis C infection treated with interferon alfa. Hepatology **23:**8-16.
162. **Kachko A, Kochneva G, Sivolobova G, Grazhdantseva A, Lupan T, Zubkova I, Wells F, Merchlinsky M, Williams O, Watanabe H, Ivanova A, Shvalov A, Loktev V, Netesov S, Major ME.** 2011. New neutralizing antibody epitopes in hepatitis C virus envelope glycoproteins are revealed by dissecting peptide recognition profiles. Vaccine **30:**69-77.
163. **Wahid A, Dubuisson J.** 2013. Virus-neutralizing antibodies to hepatitis C virus. J Viral Hepat **20:**369-376.
164. **Keck ZY, Sung VM, Perkins S, Rowe J, Paul S, Liang TJ, Lai MM, Foung SK.** 2004. Human monoclonal antibody to hepatitis C virus E1 glycoprotein that blocks virus attachment and viral infectivity. J Virol **78:**7257-7263.
165. **Meunier JC, Russell RS, Goossens V, Priem S, Walter H, Depla E, Union A, Faulk KN, Bukh J, Emerson SU, Purcell RH.** 2008. Isolation and characterization of broadly neutralizing human monoclonal antibodies to the e1 glycoprotein of hepatitis C virus. J Virol **82:**966-973.
166. **Kong L, Kadam RU, Giang E, Ruwona TB, Nieusma T, Culhane JC, Stanfield RL, Dawson PE, Wilson IA, Law M.** 2015. Structure of Hepatitis C Virus Envelope Glycoprotein E1 Antigenic Site 314-324 in Complex with Antibody IGH526. J Mol Biol **427:**2617-2628.
167. **Garrone P, Fluckiger AC, Mangeot PE, Gauthier E, Dupeyrot-Lacas P, Mancip J, Cangialosi A, Du Chene I, LeGrand R, Mangeot I, Lavillette D, Bellier B, Cosset FL, Tangy F, Klatzmann D, Dalba C.** 2011. A prime-boost strategy using virus-like particles pseudotyped for HCV proteins triggers broadly neutralizing antibodies in macaques. Sci Transl Med **3:**94ra71.
168. **Hu YW, Rocheleau L, Larke B, Chui L, Lee B, Ma M, Liu S, Omlin T, Pelchat M, Brown EG.** 2005. Immunoglobulin

mimicry by Hepatitis C Virus envelope protein E2. Virology **332:**538-549.

169. **Larrubia JR, Moreno-Cubero E, Lokhande MU, Garcia-Garzon S, Lazaro A, Miquel J, Perna C, Sanz-de-Villalobos E.** 2014. Adaptive immune response during hepatitis C virus infection. World J Gastroenterol **20:**3418-3430.
170. **Sautto G, Tarr AW, Mancini N, Clementi M.** 2013. Structural and antigenic definition of hepatitis C virus E2 glycoprotein epitopes targeted by monoclonal antibodies. Clin Dev Immunol **2013:**450963.
171. **Tarr AW, Owsianka AM, Jayaraj D, Brown RJ, Hickling TP, Irving WL, Patel AH, Ball JK.** 2007. Determination of the human antibody response to the epitope defined by the hepatitis C virus-neutralizing monoclonal antibody AP33. J Gen Virol **88:**2991-3001.
172. **Urbanowicz RA, McClure CP, King B, Mason CP, Ball JK, Tarr AW.** 2016. Novel functional hepatitis C virus glycoprotein isolates identified using an optimised viral pseudotype entry assay. J Gen Virol doi:10.1099/jgv.0.000537.
173. **Sabo MC, Luca VC, Prentoe J, Hopcraft SE, Blight KJ, Yi M, Lemon SM, Ball JK, Bukh J, Evans MJ, Fremont DH, Diamond MS.** 2011. Neutralizing monoclonal antibodies against hepatitis C virus E2 protein bind discontinuous epitopes and inhibit infection at a postattachment step. J Virol **85:**7005-7019.
174. **Deng K, Liu R, Rao H, Jiang D, Wang J, Xie X, Wei L.** 2015. Antibodies Targeting Novel Neutralizing Epitopes of Hepatitis C Virus Glycoprotein Preclude Genotype 2 Virus Infection. PLoS One **10:**e0138756.
175. **von Hahn T, Yoon JC, Alter H, Rice CM, Rehermann B, Balfe P, McKeating JA.** 2007. Hepatitis C virus continuously escapes from neutralizing antibody and T-cell responses during chronic infection in vivo. Gastroenterology **132:**667-678.
176. **Chen SL, Morgan TR.** 2006. The natural history of hepatitis C virus (HCV) infection. Int J Med Sci **3:**47-52.
177. **Westbrook RH, Dusheiko G.** 2014. Natural history of hepatitis C. J Hepatol **61:**S58-68.
178. **Hope VD, Eramova I, Capurro D, Donoghoe MC.** 2014. Prevalence and estimation of hepatitis B and C infections in the WHO European Region: a review of data focusing on the countries outside the European Union and the European Free Trade Association. Epidemiol Infect **142:**270-286.
179. **Cloherty G, Talal A, Coller K, Steinhart C, Hackett J, Jr., Dawson G, Rockstroh J, Feld J.** 2016. Role of Serologic and Molecular Diagnostic Assays in Identification and Management of Hepatitis C Virus Infection. J Clin Microbiol **54:**265-273.
180. **Ford N, Kirby C, Singh K, Mills EJ, Cooke G, Kamarulzaman A, duCros P.** 2012. Chronic hepatitis C treatment outcomes in

low- and middle-income countries: a systematic review and meta-analysis. Bull World Health Organ **90:**540-550.

181. **Simmonds P, Alberti A, Alter HJ, Bonino F, Bradley DW, Brechot C, Brouwer JT, Chan SW, Chayama K, Chen DS, et al.** 1994. A proposed system for the nomenclature of hepatitis C viral genotypes. Hepatology **19:**1321-1324.
182. **Murphy DG, Willems B, Deschenes M, Hilzenrat N, Mousseau R, Sabbah S.** 2007. Use of sequence analysis of the NS5B region for routine genotyping of hepatitis C virus with reference to C/E1 and 5' untranslated region sequences. J Clin Microbiol **45:**1102-1112.
183. **Alter MJ, Kuhnert WL, Finelli L, Centers for Disease C, Prevention.** 2003. Guidelines for laboratory testing and result reporting of antibody to hepatitis C virus. Centers for Disease Control and Prevention. MMWR Recomm Rep **52:**1-13, 15; quiz CE11-14.
184. **Pawlotsky JM.** 2002. Use and interpretation of virological tests for hepatitis C. Hepatology **36:**S65-73.
185. **Kamal SM.** 2008. Acute hepatitis C: a systematic review. Am J Gastroenterol **103:**1283-1297; quiz 1298.
186. **Chevaliez S.** 2011. Virological tools to diagnose and monitor hepatitis C virus infection. Clin Microbiol Infect **17:**116-121.
187. **Orland JR, Wright TL, Cooper S.** 2001. Acute hepatitis C. Hepatology **33:**321-327.
188. **European Association for the Study of the L.** 2011. EASL Clinical Practice Guidelines: management of hepatitis C virus infection. J Hepatol **55:**245-264.
189. **Antaki N, Craxi A, Kamal S, Moucari R, Van der Merwe S, Haffar S, Gadano A, Zein N, Lai CL, Pawlotsky JM, Heathcote EJ, Dusheiko G, Marcellin P.** 2010. The neglected hepatitis C virus genotypes 4, 5 and 6: an international consensus report. Liver Int **30:**342-355.
190. **Ge D, Fellay J, Thompson AJ, Simon JS, Shianna KV, Urban TJ, Heinzen EL, Qiu P, Bertelsen AH, Muir AJ, Sulkowski M, McHutchison JG, Goldstein DB.** 2009. Genetic variation in IL28B predicts hepatitis C treatment-induced viral clearance. Nature **461:**399-401.
191. **McHutchison JG, Lawitz EJ, Shiffman ML, Muir AJ, Galler GW, McCone J, Nyberg LM, Lee WM, Ghalib RH, Schiff ER, Galati JS, Bacon BR, Davis MN, Mukhopadhyay P, Koury K, Noviello S, Pedicone LD, Brass CA, Albrecht JK, Sulkowski MS, Team IS.** 2009. Peginterferon alfa-2b or alfa-2a with ribavirin for treatment of hepatitis C infection. N Engl J Med **361:**580-593.
192. **Thomas DL, Thio CL, Martin MP, Qi Y, Ge D, O'Huigin C, Kidd J, Kidd K, Khakoo SI, Alexander G, Goedert JJ, Kirk GD, Donfield SM, Rosen HR, Tobler LH, Busch MP, McHutchison JG, Goldstein DB, Carrington M.** 2009. Genetic variation in

IL28B and spontaneous clearance of hepatitis C virus. Nature **461:**798-801.

193. **Bacon BR, Gordon SC, Lawitz E, Marcellin P, Vierling JM, Zeuzem S, Poordad F, Goodman ZD, Sings HL, Boparai N, Burroughs M, Brass CA, Albrecht JK, Esteban R, Investigators HR-.** 2011. Boceprevir for previously treated chronic HCV genotype 1 infection. N Engl J Med **364:**1207-1217.
194. **Jacobson IM, McHutchison JG, Dusheiko G, Di Bisceglie AM, Reddy KR, Bzowej NH, Marcellin P, Muir AJ, Ferenci P, Flisiak R, George J, Rizzetto M, Shouval D, Sola R, Terg RA, Yoshida EM, Adda N, Bengtsson L, Sankoh AJ, Kieffer TL, George S, Kauffman RS, Zeuzem S, Team AS.** 2011. Telaprevir for previously untreated chronic hepatitis C virus infection. N Engl J Med **364:**2405-2416.
195. **European Association for Study of L.** 2015. EASL Recommendations on Treatment of Hepatitis C 2015. J Hepatol **63:**199-236.
196. **Sanford M.** 2015. Simeprevir: a review of its use in patients with chronic hepatitis C virus infection. Drugs **75:**183-196.
197. **Leroy V, Angus P, Bronowicki JP, Dore GJ, Hezode C, Pianko S, Pol S, Stuart K, Tse E, McPhee F, Bhore R, Jimenez-Exposito MJ, Thompson AJ.** 2016. Daclatasvir, sofosbuvir, and ribavirin for hepatitis C virus genotype 3 and advanced liver disease: A randomized phase III study (ALLY-3+). Hepatology **63:**1430-1441.
198. **Panel AIHG.** 2015. Hepatitis C guidance: AASLD-IDSA recommendations for testing, managing, and treating adults infected with hepatitis C virus. Hepatology **62:**932-954.
199. **Lawitz E, Sulkowski MS, Ghalib R, Rodriguez-Torres M, Younossi ZM, Corregidor A, DeJesus E, Pearlman B, Rabinovitz M, Gitlin N, Lim JK, Pockros PJ, Scott JD, Fevery B, Lambrecht T, Ouwerkerk-Mahadevan S, Callewaert K, Symonds WT, Picchio G, Lindsay KL, Beumont M, Jacobson IM.** 2014. Simeprevir plus sofosbuvir, with or without ribavirin, to treat chronic infection with hepatitis C virus genotype 1 in non-responders to pegylated interferon and ribavirin and treatment-naive patients: the COSMOS randomised study. Lancet **384:**1756-1765.
200. **Seifert LL, Perumpail RB, Ahmed A.** 2015. Update on hepatitis C: Direct-acting antivirals. World J Hepatol **7:**2829-2833.
201. **Chen ZW, Li H, Ren H, Hu P.** 2016. Global prevalence of pre-existing HCV variants resistant to direct-acting antiviral agents (DAAs): mining the GenBank HCV genome data. Sci Rep **6:**20310.
202. **Horner SM, Naggie S.** 2015. Successes and Challenges on the Road to Cure Hepatitis C. PLoS Pathog **11:**e1004854.

203. **Chhatwal J, Kanwal F, Roberts MS, Dunn MA.** 2015. Cost-effectiveness and budget impact of hepatitis C virus treatment with sofosbuvir and ledipasvir in the United States. Ann Intern Med **162:**397-406.
204. **Freeman J, Sallie R, Kennedy A, Hieu PTN, Freeman J, Jeffreys G, Hill AM.** High Sustained Virological Response Rates Using Generic Direct Acting Antiviral Treatment for Hepatitis C, Imported into Australia. Journal of Hepatology **64:**S209.
205. **Freeman JA, Hill A.** 2016. The use of generic medications for hepatitis C. Liver Int **36:**929-932.
206. **Man John Law L, Landi A, Magee WC, Lorne Tyrrell D, Houghton M.** 2013. Progress towards a hepatitis C virus vaccine. Emerg Microbes Infect **2:**e79.
207. **Stoll-Keller F, Barth H, Fafi-Kremer S, Zeisel MB, Baumert TF.** 2009. Development of hepatitis C virus vaccines: challenges and progress. Expert Rev Vaccines **8:**333-345.
208. **Halliday J, Klenerman P, Barnes E.** 2011. Vaccination for hepatitis C virus: closing in on an evasive target. Expert Rev Vaccines **10:**659-672.
209. **Thimme R, Lohmann V, Weber F.** 2006. A target on the move: innate and adaptive immune escape strategies of hepatitis C virus. Antiviral Res **69:**129-141.
210. **Dowd KA, Netski DM, Wang XH, Cox AL, Ray SC.** 2009. Selection pressure from neutralizing antibodies drives sequence evolution during acute infection with hepatitis C virus. Gastroenterology **136:**2377-2386.
211. **Basavapathruni A, Yeh WW, Coffey RT, Whitney JB, Hraber PT, Giri A, Korber BT, Rao SS, Nabel GJ, Mascola JR, Seaman MS, Letvin NL.** 2010. Envelope vaccination shapes viral envelope evolution following simian immunodeficiency virus infection in rhesus monkeys. J Virol **84:**953-963.
212. **Palmer BA, Moreau I, Levis J, Harty C, Crosbie O, Kenny-Walsh E, Fanning LJ.** 2012. Insertion and recombination events at hypervariable region 1 over 9.6 years of hepatitis C virus chronic infection. J Gen Virol **93:**2614-2624.
213. **Palmer BA, Schmidt-Martin D, Dimitrova Z, Skums P, Crosbie O, Kenny-Walsh E, Fanning LJ.** 2015. Network analysis of the chronic Hepatitis C virome defines HVR1 evolutionary phenotypes in the context of humoral immune responses. J Virol doi:10.1128/JVI.02995-15.
214. **Bailey JR, Wasilewski LN, Snider AE, El-Diwany R, Osburn WO, Keck Z, Foung SK, Ray SC.** 2015. Naturally selected hepatitis C virus polymorphisms confer broad neutralizing antibody resistance. J Clin Invest **125:**437-447.
215. **Pestka JM, Zeisel MB, Blaser E, Schurmann P, Bartosch B, Cosset FL, Patel AH, Meisel H, Baumert J, Viazov S, Rispeter K, Blum HE, Roggendorf M, Baumert TF.** 2007. Rapid induction of virus-neutralizing antibodies and viral clearance

in a single-source outbreak of hepatitis C. Proc Natl Acad Sci U S A **104:**6025-6030.

216. **Edwards VC, Tarr AW, Urbanowicz RA, Ball JK.** 2012. The role of neutralizing antibodies in hepatitis C virus infection. J Gen Virol **93:**1-19.
217. **Choo QL, Kuo G, Ralston R, Weiner A, Chien D, Van Nest G, Han J, Berger K, Thudium K, Kuo C, et al.** 1994. Vaccination of chimpanzees against infection by the hepatitis C virus. Proc Natl Acad Sci U S A **91:**1294-1298.
218. **Meunier JC, Gottwein JM, Houghton M, Russell RS, Emerson SU, Bukh J, Purcell RH.** 2011. Vaccine-induced cross-genotype reactive neutralizing antibodies against hepatitis C virus. J Infect Dis **204:**1186-1190.
219. **Frey SE, Houghton M, Coates S, Abrignani S, Chien D, Rosa D, Pileri P, Ray R, Di Bisceglie AM, Rinella P, Hill H, Wolff MC, Schultze V, Han JH, Scharschmidt B, Belshe RB.** 2010. Safety and immunogenicity of HCV E1E2 vaccine adjuvanted with MF59 administered to healthy adults. Vaccine **28:**6367-6373.
220. **Law JL, Chen C, Wong J, Hockman D, Santer DM, Frey SE, Belshe RB, Wakita T, Bukh J, Jones CT, Rice CM, Abrignani S, Tyrrell DL, Houghton M.** 2013. A hepatitis C virus (HCV) vaccine comprising envelope glycoproteins gpE1/gpE2 derived from a single isolate elicits broad cross-genotype neutralizing antibodies in humans. PLoS One **8:**e59776.
221. **Wong JA, Bhat R, Hockman D, Logan M, Chen C, Levin A, Frey SE, Belshe RB, Tyrrell DL, Law JL, Houghton M.** 2014. Recombinant hepatitis C virus envelope glycoprotein vaccine elicits antibodies targeting multiple epitopes on the envelope glycoproteins associated with broad cross-neutralization. J Virol **88:**14278-14288.
222. **Flego M, Ascione A, Cianfriglia M, Vella S.** 2013. Clinical development of monoclonal antibody-based drugs in HIV and HCV diseases. BMC Med **11:**4.
223. **Stiegler G, Katinger H.** 2003. Therapeutic potential of neutralizing antibodies in the treatment of HIV-1 infection. J Antimicrob Chemother **51:**757-759.
224. **Doria-Rose NA, Schramm CA, Gorman J, Moore PL, Bhiman JN, DeKosky BJ, Ernandes MJ, Georgiev IS, Kim HJ, Pancera M, Staupe RP, Altae-Tran HR, Bailer RT, Crooks ET, Cupo A, Druz A, Garrett NJ, Hoi KH, Kong R, Louder MK, Longo NS, McKee K, Nonyane M, O'Dell S, Roark RS, Rudicell RS, Schmidt SD, Sheward DJ, Soto C, Wibmer CK, Yang Y, Zhang Z, Program NCS, Mullikin JC, Binley JM, Sanders RW, Wilson IA, Moore JP, Ward AB, Georgiou G, Williamson C, Abdool Karim SS, Morris L, Kwong PD, Shapiro L, Mascola JR.** 2014. Developmental pathway for potent V1V2-directed HIV-neutralizing antibodies. Nature **509:**55-62.

225. **Qiu X, Wong G, Audet J, Bello A, Fernando L, Alimonti JB, Fausther-Bovendo H, Wei H, Aviles J, Hiatt E, Johnson A, Morton J, Swope K, Bohorov O, Bohorova N, Goodman C, Kim D, Pauly MH, Velasco J, Pettitt J, Olinger GG, Whaley K, Xu B, Strong JE, Zeitlin L, Kobinger GP.** 2014. Reversion of advanced Ebola virus disease in nonhuman primates with ZMapp. Nature **514:**47-53.
226. **Chung RT, Gordon FD, Curry MP, Schiano TD, Emre S, Corey K, Markmann JF, Hertl M, Pomposelli JJ, Pomfret EA, Florman S, Schilsky M, Broering TJ, Finberg RW, Szabo G, Zamore PD, Khettry U, Babcock GJ, Ambrosino DM, Leav B, Leney M, Smith HL, Molrine DC.** 2013. Human monoclonal antibody MBL-HCV1 delays HCV viral rebound following liver transplantation: a randomized controlled study. Am J Transplant **13:**1047-1054.
227. **Bukh J, Engle RE, Faulk K, Wang RY, Farci P, Alter HJ, Purcell RH.** 2015. Immunoglobulin with High-Titer In Vitro Cross-Neutralizing Hepatitis C Virus Antibodies Passively Protects Chimpanzees from Homologous, but Not Heterologous, Challenge. J Virol **89:**9128-9132.
228. **Tawar RG, Heydmann L, Bach C, Schuttrumpf J, Chavan S, King BJ, McClure CP, Ball JK, Pessaux P, Habersetzer F, Bartenschlager R, Zeisel MB, Baumert TF.** 2016. Broad neutralization of hepatitis C virus-resistant variants by Civacir hepatitis C immunoglobulin. Hepatology **64:**1495-1506.
229. **Abdelwahab KS, Ahmed Said ZN.** 2016. Status of hepatitis C virus vaccination: Recent update. World J Gastroenterol **22:**862-873.
230. **Di Bisceglie AM, Janczweska-Kazek E, Habersetzer F, Mazur W, Stanciu C, Carreno V, Tanasescu C, Flisiak R, Romero-Gomez M, Fich A, Bataille V, Toh ML, Hennequi M, Zerr P, Honnet G, Inchauspe G, Agathon D, Limacher JM, Wedemeyer H.** 2014. Efficacy of immunotherapy with TG4040, peg-interferon, and ribavirin in a Phase 2 study of patients with chronic HCV infection. Gastroenterology **147:**119-131 e113.
231. **Habersetzer F, Baumert TF, Stoll-Keller F.** 2009. GI-5005, a yeast vector vaccine expressing an NS3-core fusion protein for chronic HCV infection. Curr Opin Mol Ther **11:**456-462.
232. **Zanin M, Keck ZY, Rainey GJ, Lam CY, Boon AC, Rubrum A, Darnell D, Wong SS, Griffin Y, Xia J, Webster RG, Webby R, Johnson S, Foung S.** 2015. An anti-H5N1 influenza virus FcDART antibody is a highly efficacious therapeutic agent and prophylactic against H5N1 influenza virus infection. J Virol **89:**4549-4561.
233. **Gautam R, Nishimura Y, Pegu A, Nason MC, Klein F, Gazumyan A, Golijanin J, Buckler-White A, Sadjadpour R, Wang K, Mankoff Z, Schmidt SD, Lifson JD, Mascola JR,**

Nussenzweig MC, Martin MA. 2016. A single injection of anti-HIV-1 antibodies protects against repeated SHIV challenges. Nature **533:**105-109.

234. **Zhou T, Georgiev I, Wu X, Yang ZY, Dai K, Finzi A, Kwon YD, Scheid JF, Shi W, Xu L, Yang Y, Zhu J, Nussenzweig MC, Sodroski J, Shapiro L, Nabel GJ, Mascola JR, Kwong PD.** 2010. Structural basis for broad and potent neutralization of HIV-1 by antibody VRC01. Science **329:**811-817.
235. **Scheid JF, Mouquet H, Ueberheide B, Diskin R, Klein F, Oliveira TY, Pietzsch J, Fenyo D, Abadir A, Velinzon K, Hurley A, Myung S, Boulad F, Poignard P, Burton DR, Pereyra F, Ho DD, Walker BD, Seaman MS, Bjorkman PJ, Chait BT, Nussenzweig MC.** 2011. Sequence and structural convergence of broad and potent HIV antibodies that mimic CD4 binding. Science **333:**1633-1637.
236. **Mouquet H, Scharf L, Euler Z, Liu Y, Eden C, Scheid JF, Halper-Stromberg A, Gnanapragasam PN, Spencer DI, Seaman MS, Schuitemaker H, Feizi T, Nussenzweig MC, Bjorkman PJ.** 2012. Complex-type N-glycan recognition by potent broadly neutralizing HIV antibodies. Proc Natl Acad Sci U S A **109:**E3268-3277.
237. **Farci P, Alter HJ, Govindarajan S, Wong DC, Engle R, Lesniewski RR, Mushahwar IK, Desai SM, Miller RH, Ogata N, et al.** 1992. Lack of protective immunity against reinfection with hepatitis C virus. Science **258:**135-140.
238. **Prince AM, Brotman B, Huima T, Pascual D, Jaffery M, Inchauspe G.** 1992. Immunity in hepatitis C infection. J Infect Dis **165:**438-443.
239. **Kolykhalov AA, Agapov EV, Blight KJ, Mihalik K, Feinstone SM, Rice CM.** 1997. Transmission of hepatitis C by intrahepatic inoculation with transcribed RNA. Science **277:**570-574.
240. **Forns X, Payette PJ, Ma X, Satterfield W, Eder G, Mushahwar IK, Govindarajan S, Davis HL, Emerson SU, Purcell RH, Bukh J.** 2000. Vaccination of chimpanzees with plasmid DNA encoding the hepatitis C virus (HCV) envelope E2 protein modified the infection after challenge with homologous monoclonal HCV. Hepatology **32:**618-625.
241. **Feinstone SM, Alter HJ, Dienes HP, Shimizu Y, Popper H, Blackmore D, Sly D, London WT, Purcell RH.** 1981. Non-A, non-B hepatitis in chimpanzees and marmosets. J Infect Dis **144:**588-598.
242. **Karayiannis P, Scheuer PJ, Bamber M, Cohn D, Hurn BA, Thomas HC.** 1983. Experimental infection of Tamarins with human non-A, non-B hepatitis virus. J Med Virol **11:**251-256.
243. **Xie ZC, Riezu-Boj JI, Lasarte JJ, Guillen J, Su JH, Civeira MP, Prieto J.** 1998. Transmission of hepatitis C virus infection to tree shrews. Virology **244:**513-520.

244. **Couto LB, Kolykhalov AA.** 2006. Animal Models for HCV Study. *In* Tan SL (ed), Hepatitis C Viruses: Genomes and Molecular Biology, Norfolk (UK).
245. **Iacovacci S, Sargiacomo M, Parolini I, Ponzetto A, Peschle C, Carloni G.** 1993. Replication and multiplication of hepatitis C virus genome in human foetal liver cells. Res Virol **144:**275-279.
246. **Rumin S, Berthillon P, Tanaka E, Kiyosawa K, Trabaud MA, Bizollon T, Gouillat C, Gripon P, Guguen-Guillouzo C, Inchauspe G, Trepo C.** 1999. Dynamic analysis of hepatitis C virus replication and quasispecies selection in long-term cultures of adult human hepatocytes infected in vitro. J Gen Virol **80 (Pt 11):**3007-3018.
247. **Lohmann V, Korner F, Koch J, Herian U, Theilmann L, Bartenschlager R.** 1999. Replication of subgenomic hepatitis C virus RNAs in a hepatoma cell line. Science **285:**110-113.
248. **Grobler JA, Markel EJ, Fay JF, Graham DJ, Simcoe AL, Ludmerer SW, Murray EM, Migliaccio G, Flores OA.** 2003. Identification of a key determinant of hepatitis C virus cell culture adaptation in domain II of NS3 helicase. J Biol Chem **278:**16741-16746.
249. **Kato T, Date T, Miyamoto M, Furusaka A, Tokushige K, Mizokami M, Wakita T.** 2003. Efficient replication of the genotype 2a hepatitis C virus subgenomic replicon. Gastroenterology **125:**1808-1817.
250. **Maekawa S, Enomoto N, Sakamoto N, Kurosaki M, Ueda E, Kohashi T, Watanabe H, Chen CH, Yamashiro T, Tanabe Y, Kanazawa N, Nakagawa M, Sato C, Watanabe M.** 2004. Introduction of NS5A mutations enables subgenomic HCV replicon derived from chimpanzee-infectious HC-J4 isolate to replicate efficiently in Huh-7 cells. J Viral Hepat **11:**394-403.
251. **Ikeda M, Abe K, Dansako H, Nakamura T, Naka K, Kato N.** 2005. Efficient replication of a full-length hepatitis C virus genome, strain O, in cell culture, and development of a luciferase reporter system. Biochem Biophys Res Commun **329:**1350-1359.
252. **Blight KJ, McKeating JA, Marcotrigiano J, Rice CM.** 2003. Efficient replication of hepatitis C virus genotype 1a RNAs in cell culture. J Virol **77:**3181-3190.
253. **Yi M, Lemon SM.** 2004. Adaptive mutations producing efficient replication of genotype 1a hepatitis C virus RNA in normal Huh7 cells. J Virol **78:**7904-7915.
254. **Lanford RE, Guerra B, Lee H.** 2006. Hepatitis C virus genotype 1b chimeric replicon containing genotype 3 NS5A domain. Virology **355:**192-202.
255. **Yu M, Peng B, Chan K, Gong R, Yang H, Delaney Wt, Cheng G.** 2014. Robust and persistent replication of the genotype 6a hepatitis C virus replicon in cell culture. Antimicrob Agents Chemother **58:**2638-2646.

256. **Tarr AW, Owsianka AM, Szwejk A, Ball JK, Patel AH.** 2007. Cloning, expression, and functional analysis of patient-derived hepatitis C virus glycoproteins. Methods Mol Biol **379:**177-197.
257. **Owsianka A, Tarr AW, Juttla VS, Lavillette D, Bartosch B, Cosset FL, Ball JK, Patel AH.** 2005. Monoclonal antibody AP33 defines a broadly neutralizing epitope on the hepatitis C virus E2 envelope glycoprotein. J Virol **79:**11095-11104.
258. **Urbanowicz RA, McClure CP, Brown RJ, Tsoleridis T, Persson MA, Krey T, Irving WL, Ball JK, Tarr AW.** 2015. A diverse panel of Hepatitis C Virus glycoproteins for use in vaccine research reveals extremes of monoclonal antibody neutralization resistance. J Virol doi:10.1128/JVI.02700-15.
259. **Kato T, Furusaka A, Miyamoto M, Date T, Yasui K, Hiramoto J, Nagayama K, Tanaka T, Wakita T.** 2001. Sequence analysis of hepatitis C virus isolated from a fulminant hepatitis patient. J Med Virol **64:**334-339.
260. **Lindenbach BD, Evans MJ, Syder AJ, Wolk B, Tellinghuisen TL, Liu CC, Maruyama T, Hynes RO, Burton DR, McKeating JA, Rice CM.** 2005. Complete replication of hepatitis C virus in cell culture. Science **309:**623-626.
261. **Zhong J, Gastaminza P, Cheng G, Kapadia S, Kato T, Burton DR, Wieland SF, Uprichard SL, Wakita T, Chisari FV.** 2005. Robust hepatitis C virus infection in vitro. Proc Natl Acad Sci U S A **102:**9294-9299.
262. **Yi M, Villanueva RA, Thomas DL, Wakita T, Lemon SM.** 2006. Production of infectious genotype 1a hepatitis C virus (Hutchinson strain) in cultured human hepatoma cells. Proc Natl Acad Sci U S A **103:**2310-2315.
263. **Binder M, Quinkert D, Bochkarova O, Klein R, Kezmic N, Bartenschlager R, Lohmann V.** 2007. Identification of determinants involved in initiation of hepatitis C virus RNA synthesis by using intergenotypic replicase chimeras. J Virol **81:**5270-5283.
264. **Shavinskaya A, Boulant S, Penin F, McLauchlan J, Bartenschlager R.** 2007. The lipid droplet binding domain of hepatitis C virus core protein is a major determinant for efficient virus assembly. J Biol Chem **282:**37158-37169.
265. **Herker E, Ott M.** 2011. Unique ties between hepatitis C virus replication and intracellular lipids. Trends Endocrinol Metab **22:**241-248.
266. **Farci P, Shimoda A, Coiana A, Diaz G, Peddis G, Melpolder JC, Strazzera A, Chien DY, Munoz SJ, Balestrieri A, Purcell RH, Alter HJ.** 2000. The outcome of acute hepatitis C predicted by the evolution of the viral quasispecies. Science **288:**339-344.
267. **Moreau I, O'Sullivan H, Murray C, Levis J, Crosbie O, Kenny-Walsh E, Fanning LJ.** 2008. Separation of Hepatitis C

genotype 4a into IgG-depleted and IgG-enriched fractions reveals a unique quasispecies profile. Virol J **5:**103.

268. **Palmer BA, Dimitrova Z, Skums P, Crosbie O, Kenny-Walsh E, Fanning LJ.** 2014. Analysis of the evolution and structure of a complex intrahost viral population in chronic hepatitis C virus mapped by ultradeep pyrosequencing. J Virol **88:**13709-13721.
269. **Waters J, Pignatelli M, Galpin S, Ishihara K, Thomas HC.** 1986. Virus-neutralizing antibodies to hepatitis B virus: the nature of an immunogenic epitope on the S gene peptide. J Gen Virol **67 (Pt 11):**2467-2473.
270. **Moreau I, Levis J, Crosbie O, Kenny-Walsh E, Fanning LJ.** 2008. Correlation between pre-treatment quasispecies complexity and treatment outcome in chronic HCV genotype 3a. Virol J **5:**78.
271. **Palmer BA, Menton J, Levis J, Kenny-Walsh E, Crosbie O, Fanning LJ.** 2012. The pan-genotype specificity of the hepatitis C virus anti-core monoclonal antibody C7-50 is contingent on the quasispecies profile of a population. Arch Virol **157:**2235-2239.
272. **Nakabayashi H, Taketa K, Miyano K, Yamane T, Sato J.** 1982. Growth of human hepatoma cells lines with differentiated functions in chemically defined medium. Cancer Res **42:**3858-3863.
273. **Posthumus WPA, Lenstra JA, Vannieuwstadt AP, Schaaper WMM, Vanderzeijst BAM, Meloen RH.** 1991. IMMUNOGENICITY OF PEPTIDES SIMULATING A NEUTRALIZATION EPITOPE OF TRANSMISSIBLE GASTROENTERITIS VIRUS. Virology **182:**371-375.
274. **Langedijk JP, Brandenburg AH, Middel WG, Osterhaus A, Meloen RH, van Oirschot JT.** 1997. A subtype-specific peptide-based enzyme immunoassay for detection of antibodies to the G protein of human respiratory syncytial virus is more sensitive than routine serological tests. J Clin Microbiol **35:**1656-1660.
275. **Timmerman P, Puijk WC, Meloen RH.** 2007. Functional reconstruction and synthetic mimicry of a conformational epitope using CLIPS technology. J Mol Recognit **20:**283-299.
276. **Palmer BA, Schmidt-Martin D, Dimitrova Z, Skums P, Crosbie O, Kenny-Walsh E, Fanning LJ.** 2015. Network Analysis of the Chronic Hepatitis C Virome Defines Hypervariable Region 1 Evolutionary Phenotypes in the Context of Humoral Immune Responses. J Virol **90:**3318-3329.
277. **Kenny-Walsh E.** 1999. Clinical outcomes after hepatitis C infection from contaminated anti-D immune globulin. Irish Hepatology Research Group. N Engl J Med **340:**1228-1233.
278. **Fofana I, Xiao F, Thumann C, Turek M, Zona L, Tawar RG, Grunert F, Thompson J, Zeisel MB, Baumert TF.** 2013. A novel monoclonal anti-CD81 antibody produced by genetic

immunization efficiently inhibits Hepatitis C virus cell-cell transmission. PLoS One **8:**e64221.

279. **Timm J, Roggendorf M.** 2007. Sequence diversity of hepatitis C virus: implications for immune control and therapy. World J Gastroenterol **13:**4808-4817.
280. **Tanaka T, Kato N, Nakagawa M, Ootsuyama Y, Cho MJ, Nakazawa T, Hijikata M, Ishimura Y, Shimotohno K.** 1992. Molecular cloning of hepatitis C virus genome from a single Japanese carrier: sequence variation within the same individual and among infected individuals. Virus Res **23:**39-53.
281. **Kato K, Lian L-Y, Barsukov IL, Derrick JP, Kim H, Tanaka R, Yoshino A, Shiraishi M, Shimada I, Arata Y, Roberts GCK.** 1995. Model for the complex between protein G and an antibody Fc fragment in solution. Structure **3:**79-85.
282. **Derrick JP, Wigley DB.** 1994. The third IgG-binding domain from streptococcal protein G. An analysis by X-ray crystallography of the structure alone and in a complex with Fab. J Mol Biol **243:**906-918.
283. **Lu L, Tatsunori N, Li C, Waheed S, Gao F, Robertson BH.** 2008. HCV selection and HVR1 evolution in a chimpanzee chronically infected with HCV-1 over 12 years. Hepatol Res **38:**704-716.
284. **Ramachandran S, Campo DS, Dimitrova ZE, Xia GL, Purdy MA, Khudyakov YE.** 2011. Temporal variations in the hepatitis C virus intrahost population during chronic infection. J Virol **85:**6369-6380.
285. **Gerotto M, Dal Pero F, Loffreda S, Bianchi FB, Alberti A, Lenzi M.** 2001. A 385 insertion in the hypervariable region 1 of hepatitis C virus E2 envelope protein is found in some patients with mixed cryoglobulinemia type 2. Blood **98:**2657-2663.
286. **Tarr AW, Owsianka AM, Timms JM, McClure CP, Brown RJ, Hickling TP, Pietschmann T, Bartenschlager R, Patel AH, Ball JK.** 2006. Characterization of the hepatitis C virus E2 epitope defined by the broadly neutralizing monoclonal antibody AP33. Hepatology **43:**592-601.
287. **Dreux M, Pietschmann T, Granier C, Voisset C, Ricard-Blum S, Mangeot PE, Keck Z, Foung S, Vu-Dac N, Dubuisson J, Bartenschlager R, Lavillette D, Cosset FL.** 2006. High density lipoprotein inhibits hepatitis C virus-neutralizing antibodies by stimulating cell entry via activation of the scavenger receptor BI. J Biol Chem **281:**18285-18295.
288. **Li Y, Pierce BG, Wang Q, Keck ZY, Fuerst TR, Foung SK, Mariuzza RA.** 2015. Structural basis for penetration of the glycan shield of hepatitis C virus E2 glycoprotein by a broadly neutralizing human antibody. J Biol Chem **290:**10117-10125.
289. **Petracca R, Falugi F, Galli G, Norais N, Rosa D, Campagnoli S, Burgio V, Di Stasio E, Giardina B, Houghton M, Abrignani**

S, Grandi G. 2000. Structure-function analysis of hepatitis C virus envelope-CD81 binding. J Virol **74:**4824-4830.

290. **Bouard D, Sandrin V, Boson B, Negre D, Thomas G, Granier C, Cosset FL.** 2007. An acidic cluster of the cytoplasmic tail of the RD114 virus glycoprotein controls assembly of retroviral envelopes. Traffic **8:**835-847.
291. **Christodoulopoulos I, Droniou-Bonzom ME, Oldenburg JE, Cannon PM.** 2010. Vpu-dependent block to incorporation of GaLV Env into lentiviral vectors. Retrovirology **7:**4.
292. **Perez-Berna AJ, Moreno MR, Guillen J, Bernabeu A, Villalain J.** 2006. The membrane-active regions of the hepatitis C virus E1 and E2 envelope glycoproteins. Biochemistry **45:**3755-3768.
293. **Keck ZY, Saha A, Xia J, Wang Y, Lau P, Krey T, Rey FA, Foung SK.** 2011. Mapping a region of hepatitis C virus E2 that is responsible for escape from neutralizing antibodies and a core CD81-binding region that does not tolerate neutralization escape mutations. J Virol **85:**10451-10463.
294. **Flint M, Dubuisson J, Maidens C, Harrop R, Guile GR, Borrow P, McKeating JA.** 2000. Functional characterization of intracellular and secreted forms of a truncated hepatitis C virus E2 glycoprotein. J Virol **74:**702-709.
295. **Bartosch B, Vitelli A, Granier C, Goujon C, Dubuisson J, Pascale S, Scarselli E, Cortese R, Nicosia A, Cosset FL.** 2003. Cell entry of hepatitis C virus requires a set of co-receptors that include the CD81 tetraspanin and the SR-B1 scavenger receptor. J Biol Chem **278:**41624-41630.
296. **Akazawa D, Date T, Morikawa K, Murayama A, Miyamoto M, Kaga M, Barth H, Baumert TF, Dubuisson J, Wakita T.** 2007. CD81 expression is important for the permissiveness of Huh7 cell clones for heterogeneous hepatitis C virus infection. J Virol **81:**5036-5045.
297. **Molina S, Castet V, Pichard-Garcia L, Wychowski C, Meurs E, Pascussi JM, Sureau C, Fabre JM, Sacunha A, Larrey D, Dubuisson J, Coste J, McKeating J, Maurel P, Fournier-Wirth C.** 2008. Serum-derived hepatitis C virus infection of primary human hepatocytes is tetraspanin CD81 dependent. J Virol **82:**569-574.
298. **Brazzoli M, Bianchi A, Filippini S, Weiner A, Zhu Q, Pizza M, Crotta S.** 2008. CD81 is a central regulator of cellular events required for hepatitis C virus infection of human hepatocytes. J Virol **82:**8316-8329.
299. **Naik AS, Palmer BA, Crossbie O, Kenny-Walsh E, Fanning LJ.** 2016. Humoral immune system targets clonotypic antibody associated Hepatitis C Virus. J Gen Virol doi:10.1099/jgv.0.000659.
300. **Helle F, Duverlie G, Dubuisson J.** 2011. The hepatitis C virus glycan shield and evasion of the humoral immune response. Viruses **3:**1909-1932.

301. **Sun J, Brusic V.** 2015. A systematic analysis of a broadly neutralizing antibody AR3C epitopes on Hepatitis C virus E2 envelope glycoprotein and their cross-reactivity. BMC Med Genomics **8 Suppl 4:**S6.
302. **Ng PC, Henikoff S.** 2003. SIFT: Predicting amino acid changes that affect protein function. Nucleic Acids Res **31:**3812-3814.
303. **Saul FA, Alzari PM.** 1996. Crystallographic studies of antigen-antibody interactions. Methods Mol Biol **66:**11-23.
304. **Liu HL, Hsu JP.** 2005. Recent developments in structural proteomics for protein structure determination. Proteomics **5:**2056-2068.
305. **Abbott WM, Damschroder MM, Lowe DC.** 2014. Current approaches to fine mapping of antigen-antibody interactions. Immunology **142:**526-535.
306. **Benjamin DC, Perdue SS.** 1996. Site-Directed Mutagenesis in Epitope Mapping. Methods **9:**508-515.
307. **Lu J, Witcher DR, White MA, Wang X, Huang L, Rathnachalam R, Beals JM, Kuhstoss S.** 2005. IL-1beta epitope mapping using site-directed mutagenesis and hydrogen-deuterium exchange mass spectrometry analysis. Biochemistry **44:**11106-11114.
308. **Peng L, Oganesyan V, Damschroder MM, Wu H, Dall'Acqua WF.** 2011. Structural and functional characterization of an agonistic anti-human EphA2 monoclonal antibody. J Mol Biol **413:**390-405.
309. **Reineke U.** 2009. Antibody epitope mapping using de novo generated synthetic peptide libraries. Methods Mol Biol **524:**203-211.
310. **Tarr AW, Urbanowicz RA, Jayaraj D, Brown RJ, McKeating JA, Irving WL, Ball JK.** 2012. Naturally occurring antibodies that recognize linear epitopes in the amino terminus of the hepatitis C virus E2 protein confer noninterfering, additive neutralization. J Virol **86:**2739-2749.
311. **Cerino A, Meola A, Segagni L, Furione M, Marciano S, Triyatni M, Liang TJ, Nicosia A, Mondelli MU.** 2001. Monoclonal antibodies with broad specificity for hepatitis C virus hypervariable region 1 variants can recognize viral particles. J Immunol **167:**3878-3886.
312. **Caskey M, Klein F, Lorenzi JC, Seaman MS, West AP, Jr., Buckley N, Kremer G, Nogueira L, Braunschweig M, Scheid JF, Horwitz JA, Shimeliovich I, Ben-Avraham S, Witmer-Pack M, Platten M, Lehmann C, Burke LA, Hawthorne T, Gorelick RJ, Walker BD, Keler T, Gulick RM, Fatkenheuer G, Schlesinger SJ, Nussenzweig MC.** 2015. Viraemia suppressed in HIV-1-infected humans by broadly neutralizing antibody 3BNC117. Nature doi:10.1038/nature14411.
313. **Lapierre P, Troesch M, Alvarez F, Soudeyns H.** 2011. Structural basis for broad neutralization of hepatitis C virus quasispecies. PLoS One **6:**e26981.

314. **Ritchie GR, Flicek P.** 2014. Computational approaches to interpreting genomic sequence variation. Genome Med **6:**87.
315. **Ng PC, Henikoff S.** 2006. Predicting the effects of amino acid substitutions on protein function. Annu Rev Genomics Hum Genet **7:**61-80.
316. **O'Hara M, Rixon FJ, Stow ND, Murray J, Murphy M, Preston VG.** 2010. Mutational analysis of the herpes simplex virus type 1 UL25 DNA packaging protein reveals regions that are important after the viral DNA has been packaged. J Virol **84:**4252-4263.
317. **Campo DS, Dimitrova Z, Yokosawa J, Hoang D, Perez NO, Ramachandran S, Khudyakov Y.** 2012. Hepatitis C virus antigenic convergence. Sci Rep **2:**267.
318. **Swann RE, Cowton VM, Robinson MW, Cole SJ, Barclay ST, Mills PR, Thomson EC, McLauchlan J, Patel AH.** 2016. Broad Anti-Hepatitis C Virus (HCV) Antibody Responses Are Associated with Improved Clinical Disease Parameters in Chronic HCV Infection. J Virol **90:**4530-4543.
319. **Shimizu YK, Hijikata M, Iwamoto A, Alter HJ, Purcell RH, Yoshikura H.** 1994. Neutralizing antibodies against hepatitis C virus and the emergence of neutralization escape mutant viruses. J Virol **68:**1494-1500.
320. **WHO.** 2016. Towards elimination of viral hepatitis by 2030. Lancet **388:**308.
321. **Hellard M, Sacks-Davis R, Doyle J.** 2016. Hepatitis C elimination by 2030 through treatment and prevention: think global, act in local networks. J Epidemiol Community Health doi:10.1136/jech-2015-205454.

Appendices

Appendix I

List of Genebank sequence

Genotype 1a	***Genotype 1a***	***Genotype 1b***	***Genotype 2***
AF011751	KU285170*	AF333324	AB047639
EU862828	KU285171*	DQ071885	AB690461
GQ149768	KU285172*	JX649852	AF169004
KU285151*	KU285178*	KU285191*	AF169005
KU285152*	KU285173*	KU285192*	DQ155560
KU285153*	KU285174*	KU285193*	DQ155561
KU285154*	KU285175*	KU285194*	HQ639939
KU285155*	KU285176*	KU285195*	JF735112
KU285156*	KU285177*	KU285196*	JX227967
KU285158*	KU285179*	KU285197*	KC967476
KU285157*	KU285180*	KU285198*	KF676351
KU285161*	KU285182*	KU285199*	KF700370
KU285162*	KU285181*	KU285200*	KM102770
KU285159*	KU285185*	KU285201*	KU285209*
KU285160*	KU285183*	KU285202*	KU285210*
KU285163*	KU285184*	KU285203*	KU285211*
KU285164*	KU285187*	KU285204*	KU285212*
KU285165*	KU285186*	KU285205*	KU285213*
KU285166*	KU285190*	KU285206*	KU285214*
KU285167*	KU285188*	KU285207*	
KU285168*	KU285189*	KU285208*	
KU285169*	NC_004102		

Accession number of genotypes used in this study (GenBank)

Continued…

Genotype 3	***Genotype 4***	***Genotype 5***	***Genotype 6***
AF046866	AB795432	AF064490	AY545978
AY734985	AY734987	EF043104	DQ480512
AY958020	DQ418784	EF427672	DQ480513
AY958007	DQ418787	KC767829	DQ480514
AY958017	DQ516084	KC767832	DQ480520
AY958012	DQ988073	KC767835	KJ678747
AY957990	DQ988078	KC767838	KJ678754
AY957993	DQ418783	KC767839	KJ678755
AY957997	GU814265	KC767842	KJ678761
DQ437509	GU814266	KC767843	KJ678764
JQ285741	KT735185	KC767844	KJ678765
JQ285790	KU285220*	KC767845	KJ678766
KJ470613	KU285221*	KJ925148	KJ678781
KJ470614	KU285222*	KU285225*	KJ678784
KU285215*	KU285223*	KU285226*	KJ678785
KU285216*	KU285224*	KU871279	KJ678782
KU285217*	KU871289	KU871280	KJ678814
KU285218*	KU871290		KJ678815
KU285219*	KU871291		KU285227*
KX621501	Y11604		KU285228*
KX621530			

* GenBank sequences for HCVpp from Urbanowicz *et al.*(2015)(258)

Appendix II

PEPSCAN

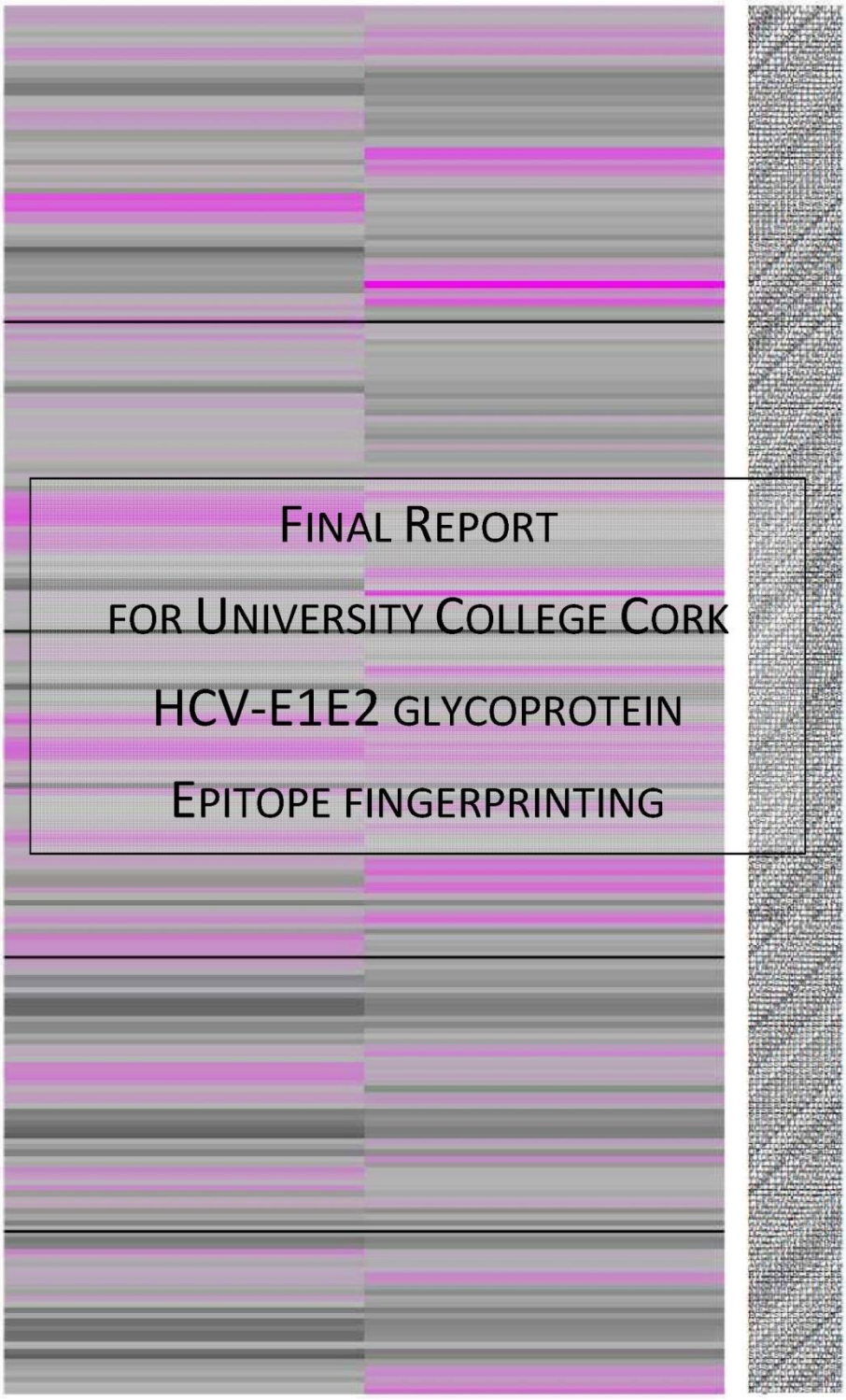
FINAL REPORT
FOR UNIVERSITY COLLEGE CORK
HCV-E1E2 GLYCOPROTEIN
EPITOPE FINGERPRINTING

STUDY REPORT

STUDY NUMBER ES20150924130E+F

TABLE OF CONTENTS

EXECUTIVE SUMMARY

GOAL

To fingerprint the epitopes of two polyclonal antibodies, which recognize HCV-E1E2 glycoprotein.

RESULTS

Pepscan analysis established tentative peptide binding footprints for both antibodies provided for the study. Both antibodies bound linear peptides under reduced stringency conditions.

REFERENCES

The study was conducted at Pepscan Presto BV, (Zuidersluisweg 2, 8243RC Lelystad, The Netherlands). All Pepscan data is stored in the software package Peplab™, a proprietary database application developed in-house and built on a PostgreSQL storage back-end. The database has daily off-site back-ups on a private secure server. The screening department has additional lab books and hard-copies of all results. These are stored in the Pepscan laboratory which is electronically secured.

STUDY DATES

Table 1. Study Dates and References

Order accepted:	30/09/2015
Synthesis of the array:	November – December 2015
Screening of the peptides:	Labbooks: Pep214: pp. 62, 64 Pep217: pp. 43, 48, 53 Pep218: pp. 44, 47, 50, 52, 54

PERSONNEL & FACILITIES

Table 2. Personnel

Study director:	Dr. JW Back
Study supervisor:	Dr. E. Shimanovskaya
Peptide synthesis:	Sonja Kerkhoff, Joshua Buijnink
Pepscan ELISA:	Drohpati Parohi, Joop Tibben, Paola Weert

MATERIALS

General materials used: See Methods section.

PROVIDED DESCRIPTION OF ANTIBODIES

Antibodies provided by University College Cork that recognize HCV-E1E2 glycoprotein are listed below (Table 3).

Table 3. Details of the antibodies

Name	Origin	Concentration	Location	Status
VF-Fab1b-5-1	human IgG	200 µg/ml	-20 C/95	finished
VF-Fab1b-10-1	human IgG	300 µg/ml	-20 C/95	finished

Pepscan Presto BV. CONFIDENTIAL

TARGET PROTEIN

PROVIDED PROTEIN SEQUENCE

Five sequences of HCV-E1E2 glycoprotein are listed below. Regions, which were used for the library design, are underlined. Highlighted in yellow is the major immunodominant region in HCV-E1E2 glycoprotein - hyper variable region, as reported in literature.

>HCVPP1B-5-1

MGCSFSIFPLALLSCLTIPASAIEVRNASGVYHVTNDCSNTSIVYEAADMIMHTPGCVPCVREGNPSRCWVALT
PTLAARNSSIPTTAIRRHIDLLVGTAAFCSAMYVGDLCGSVFLVSQLFTFSPRQHATVQDCNCSIYPGHVTGHR
MAWDMMMNWSPTTALVVSQLLRIPQAVVDVVAGAHWGVLAGLAYYS**MVGNWAKVLIVMLLFAGVDGRGTYTTGG**
AQAFTTHSFVRFFASGPSQNIQLVNTNGSWHINRTALNCNDSLNTGFLAALFYHNRFNSSGCPERMASCRPIDK
FVQGWGPITYARPANLDQKPYCWHYAPQPCGIVPASQVCGPVYCFTPSPVVAGTTDRLGVPTYSWGENETDVLL
LNNTRPPRGNWFGCTWMNSTGFTKTCGGPPCNIGGVGNDTLICPTDCFRKHPEATYAKCGSGPWLTPRCMVHYP
YRLWHYPCTINFTIFKVRMYVGGVEHRLEAACNWTRGERCDLEDRDRSELSPLLLSTTEWQVLPCSFTTLPALS
TGLIHLHRNIVDVQYLYGIGSAVVSYAIKWEYVLLLFLFLADARVCACLWMMLLIAQAEGSRQFCRYPAQWRPL
ESRGPAVRR

> HCVpp1b-8-1

MGCSFSIFLLALLSCLTIPASAIEVRNVSGVYHVTNDCSNASIVYEAADMIMHAPGCVPCVRENNSSRCWVALT
PTLAARNSSIPTTTIRRHVDLLVGTAAFCSAMYVGDLCGSVFLVSQLFTFSPRRHETVQDCNCSIYPGHVSGHR
MAWDMMMNWSPTTALVVSQLLRIPQAVVYMVAGAHWGVLAGLAYYS**MVGNWAKVLTVMLLFAGVDGVTHTLGGT**
QARAASGFASLFRLGPSQKIQLVNTNGSWHINRTALNCNDSLHTGFIAALFYARRFNASGCPERMASCRTIDKF
AQGWGPITYTKPPSLDQKPYCWHYAPQPCGIVPASQVCGPVYCFTPSPVVVGTTDRLGVPTYRWGENETDVLLL
NNTRPPRGNWFGCTWMNSTGFTKTCGGPPCNIGGLGNNTLICPTDCFRKHPEATYTKCGSGPWLTPRCMVHYPY
RLWHYPCTVNFTIFKVKMYVGGVEHRLEAACNWTRGERCDLEDRDRSELSPLLLSTTEWQVLPCSFTTLPALST
GLIHLHRNIVDVQYLYGIGSAVVSYAIKWEYVLLLFLFLADARVCACLWMMLLVAQAEGSRQFCRYPAQWRPLE
SRGPAVRR

> HCVpp1b-4-1

MGCSFSIFLLALLSCLTTPASAIEVRNVSGVYHVTNDCSNASIVYEAADMIMHTPGCVPCVLENNSSRCWVALT
PTLAARNASIPTTTIRRHVDLLVGTAAFCSAMYVGDLCGSVFLVSQLFTFSPRRHVTVQDCNCSIYPGHVSGHR
MAWDMMMNWSPTTALVVSQLLRIPQAVLDMVAGAHWGVLAGLAYYS**MVGNWAKVLIGKLLFAGVDGATHHTYRM**
GEAQGRTTRGLASIFTPGASQRIQLINTNGSWHINRTALNCNDSLHTGFLAALFYVNRFNASGCPERMASCRPI
DKFAQGWGPITYASPPISDQKPYCWHYAPQPCGIVPASQVCGPVYCFTPSPVVVGTTDRSGVPTYSWGANETDV
LLLSNTRPPRGNWFGCTWMNTTGFTKTCGGPPCNIGGAGNNTLICPTDCFRKHPEATYAKCGSGPWLTPRCMVD
YPYRLWHYPCTVNFSTFKVRMYVGGVEHRLDAACNWTRGERCDLEDRDRSELSPLLLSTTEWQVLPCSFTTLPA
LSTGLIHLHQNIVDVQYLYGIGSAVVSYAIKWEYVLLLFLFLADARVCACLWMMLLVAQTEA

> 1b-10-1

DAWDMMMNWSPTTALVVSQLLRIPQAVVDMVAGAHWGVLAGLAYYS**MAGNWAKVLIVMLLFAGVDGSTTTMGGS**
AAYNTSSLASFFSRGSAQKIQLVNTNGSWHTNRX

> 1b-7-1

DAWDMMMNWSPTTALVVSQLLRIPQAVVDIVAGAHWGVLAGLAYYS**MVGNWAKVLIVMLLFAGVDGTQTTGRVA**
ARNAHGFTSLFSPGASQNLQLINTNGSWHINRX

METHODS

2D HEATMAP ANALYSIS

A heatmap is a pseudocolored image, in which different samples are plotted horizontally, and peptide entries are plotted vertically. The magnitude of a response is color-coded and the key is included in the plot. Figure 1 below illustrates a response from a polyclonal serum screened on a library of overlapping peptides. The response is displayed in two complementary ways: as histogram and as 1D heatmap. While for a single serum the histogram is easily grasped, a comparison of responses from numerous samples is easier, when analyzed through a 2D heatmap.

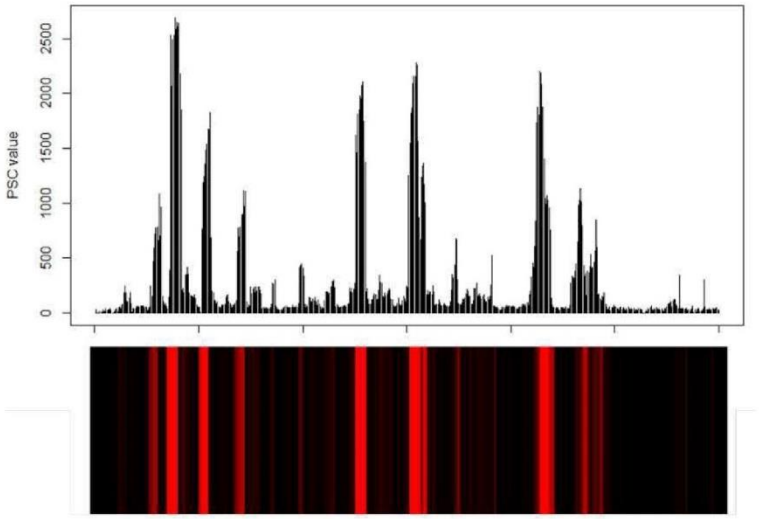

Figure 1. intensity profile and corresponding 2D heatmap representation of a response from a polyclonal serum screened on a library of overlapping linear peptides.

ELISA SCREENING

The binding of antibody to each of the synthesized peptides was tested in a PEPSCAN-based ELISA. The peptide arrays were incubated with primary antibody solution (overnight at 4°C). After washing, the peptide arrays were incubated with a 1/1000 dilution of an appropriate antibody peroxidase conjugate (SBA; Table 4) for one hour at 25°C. After washing, the peroxidase substrate 2,2'-azino-di-3-ethylbenzthiazoline sulfonate (ABTS) and 20 µl/ml of 3 percent H_2O_2 were added. After one hour, the color development was measured. The color development was quantified with a charge coupled device (CCD) - camera and an image processing system.

Table 4. Details of the antibodies

Name	Supplier	Cat. No
goat anti-human HRP conjugate	Southern Biotech	2010-05

DATA PROCESSING

The values obtained from the CCD camera range from 0 to 3000 mAU, similar to a standard 96-well plate ELISA-reader. The results are quantified and stored into the Peplab database. Occasionally a well contains an air-bubble resulting in a false-positive value, the cards are manually inspected and any values caused by an air-bubble are scored as 0.

SYNTHESIS QUALITY CONTROL

To verify the quality of the synthesized peptides, a separate set of positive and negative control peptides was synthesized in parallel. These were screened with antibody 57.9 (*ref.* Posthumus *et al.,* J. Virology, 1990, 64:3304-3309)

LITERATURE REFERENCES

Timmerman *et al.* (2007). Functional reconstruction and synthetic mimicry of a conformational epitope using CLIPS™ technology. *J. Mol. Recognit*. **20**:283-99

Langedijk *et al.* (2011). Helical peptide arrays for lead identification and interaction site mapping, *Analytical Biochemistry* **417**: 149–155

DESIGN OF PEPTIDES

Different sets of peptides were synthesized (see also Methods section) according to the following designs.

SET 1

Mimic Type: Linear peptides

Label: LIN

Description: Linear peptides of length 15 derived from the regions highlighted on page 7 with the one residue offset.

Sequences (first 10):

```
MVGNWAKVLIVMLLF
VGNWAKVLIVMLLFA
GNWAKVLIVMLLFAG
NWAKVLIVMLLFAGV
WAKVLIVMLLFAGVD
AKVLIVMLLFAGVDG
KVLIVMLLFAGVDGR
VLIVMLLFAGVDGRG
LIVMLLFAGVDGRGT
IVMLLFAGVDGRGTY
```

SET 2

Mimic Type: Linear peptides

Label: LIN.AA

Description: Peptides of set 1, but with residues on positions 10 and 11 replaced by Ala. When a native Ala would occur on either position, it is replaced by Gly. This set contains limited amounts of peptides.

Sequences (first 10):

```
MVGNWAKVLAAMLLF
VGNWAKVLIAALLFA
GNWAKVLIVAALFAG
NWAKVLIVMAAFAGV
WAKVLIVMLAAAGVD
AKVLIVMLLAGGVDG
KVLIVMLLFGAVDGR
VLIVMLLFAAADGRG
LIVMLLFAGAAGRGT
IVMLLFAGVAARGTY
```

SCREENING DETAILS

Antibody binding depends on a combination of factors, including concentration of the antibody and the amounts and nature of competing proteins in the ELISA buffer. Also, the pre-coat conditions (the specific treatment of the peptide arrays prior to incubation with the experimental sample) affect binding. These details are summed up in Table 5. For the Pepscan Buffer and Preconditioning (SQ), the numbers indicate the relative amount of competing protein (a combination of horse serum and ovalbumin).

Table 5. Screening conditions

Label	Dilution	Sample buffer	Pre-conditioning
VF-Fab1b-5-1	4 µg/ml	PBS-Tween	PBS-Tween
VF-Fab1b-10-1	5 µg/ml	10%SQ	10%SQ
Herceptin	5 µg/ml	PBS-Tween	0.1%SQ

SCREENING RESULTS

PRIMARY EXPERIMENTAL RESULTS AND SIGNAL TO NOISE RATIO DETERMINATION

The raw ELISA results of the screening are provided in the accompanying Excel data file. A graphical overview of the complete dataset is given in Figure 2. Here a box plot depicts each dataset and indicates the average ELISA signal, the distribution and the outliers within each dataset. Depending on experiment conditions (amount of antibody, blocking strength etc) different distributions of ELISA data are obtained.

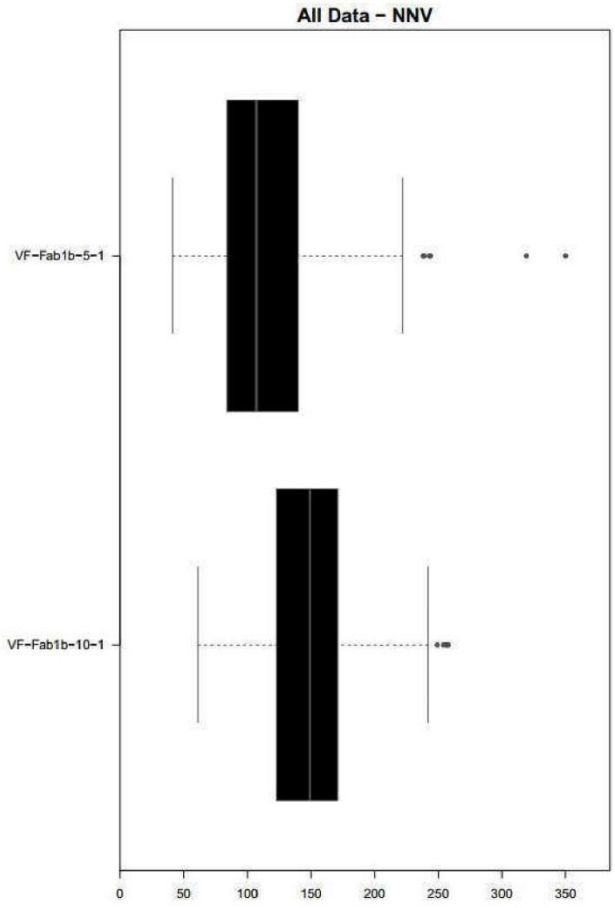

Figure 2. Box plot graphs of raw data of antibody screening. The bottom and top of the boxes are the 25th and 75th percentile of the data. The band near the middle of the box is the 50th percentile (the median). The whiskers are at 1.5 the inter-quantile range, an indication of statistical outliers within the dataset (ref Mcgill et al.,The American Statistician, 32: 12-16, 1978).

RESULTS IN DETAIL

ANTIBODY VF-FAB1B-5-1

When tested under high stringency conditions antibody VF-Fab1b-5-1 did not bind arrayed peptides. When tested under low stringency conditions the antibody bound few peptides present on the arrays. Cumulative data analysis indicates that antibody VF-Fab1b-5-1 dominantly binds peptides with sequences NIQLVNTNGSWHINR (HCVPP1B-5-1) and KIQLVNTNGSWHINR (HCVPP1B-8-1). Additional signal over background was recorded for peptides with sequences TGGAQAFTTHSFVR (HCVPP1B-5-1) and NLQLINTNGSWHINR (1b-7-1). The background subtracted intensity profile obtained for this sample is in Figure 3. Background values were obtained from the set of five Pepscan control peptides also present on the array.

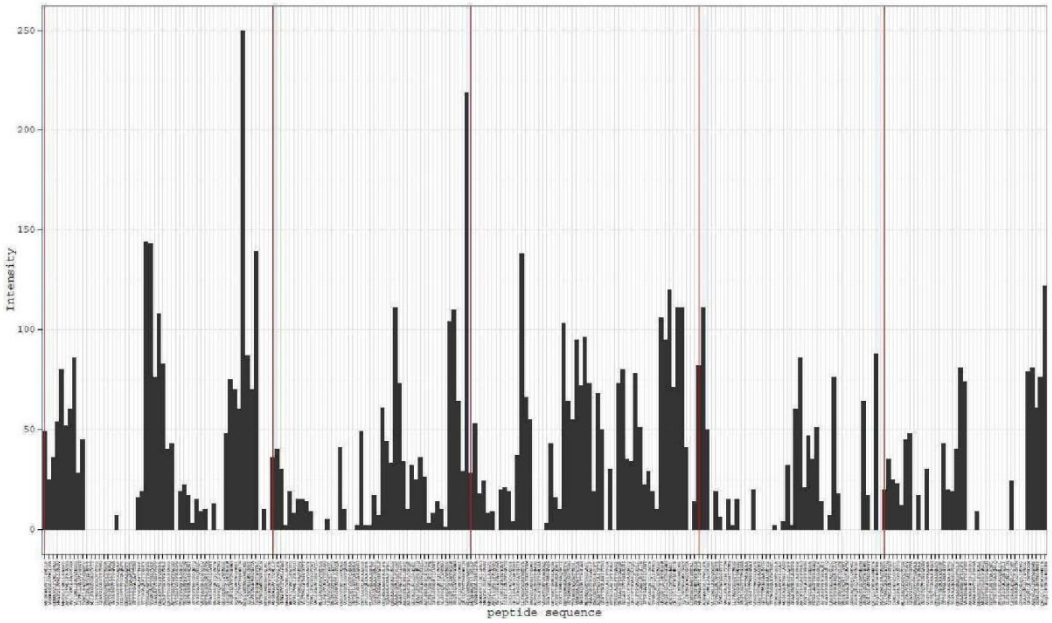

Figure 3. Background subtracted intensity profile recorded for antibody VF-Fab1b-5-1 on set 1.Red vertical lines indicates occurrences of the first unique peptide derived from the series of target sequences in the same order as listed on page 7.

ANTIBODY VF-FAB1B-10-1

When tested under high stringency conditions antibody VF-Fab1b-10-1 did not bind to the arrayed peptides. When tested under moderate stringency conditions the antibody repeatedly bound overlapping linear 15-mer peptides with core sequences HSFVRFFASGPSQN (HCVPP1B-8-1), GFASLFRLGPSQK (HCVPP1B-5-1) and MGEAQGRTTRGLA (HCVPP1B-4-1). The background subtracted intensity profile obtained for this sample is in Figure 4. Background values were obtained from the set of five Pepscan control peptides also present on the array.

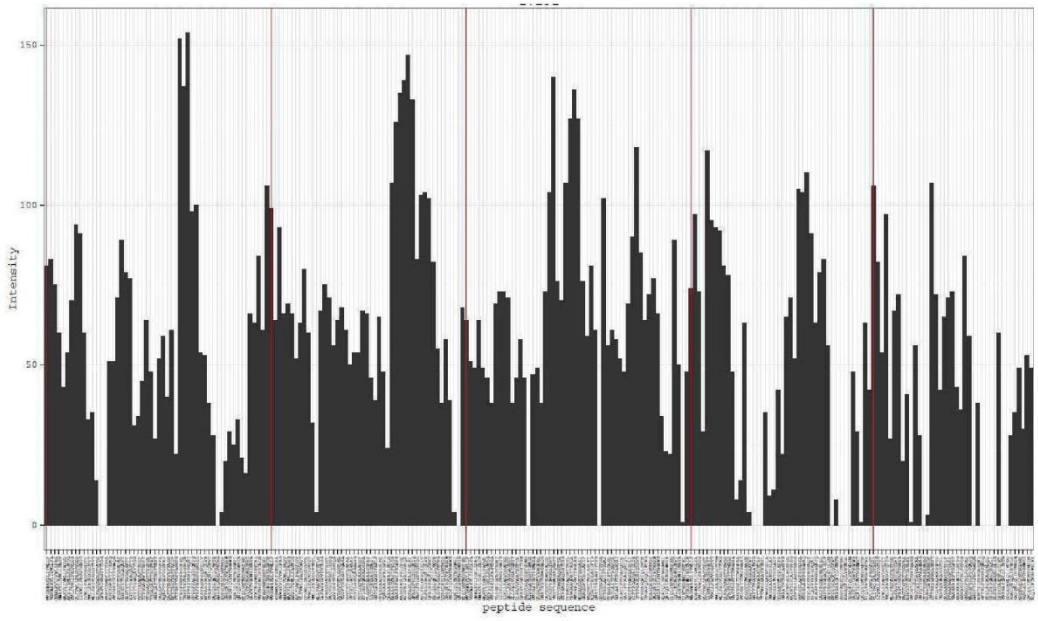

Figure 4. Background subtracted intensity profile recorded for antibody VF-Fab1b-10-1 on set 1. Red vertical lines indicates occurrences of the first unique peptide derived from the series of target sequences in the same order as listed on page 7.

HERCEPTIN

Herceptin was used as a negative control under conditions similar to those used for antibody VF-Fab1b-5-1. Herceptin weakly bound to a few peptides from the array. These peptides were accordingly excluded during the data analysis.

Pepscan Presto BV. CONFIDENTIAL

CONCLUSIONS

Two antibodies provided for this study were tested on HiSense linear array. While both antibodies did not bind arrays under high stringency conditions, they did result in detectable binding once stringency was reduced. The set of binding motifs was assigned to each sample is given in Table 6.

Table 6. Summary of the results acquired in this study

Antibody	Bound peptide	Target sequence name
VF-Fab1b-5-1	NIQLVNTNGSWHINR	HCVpp1b-5-1
	KIQLVNTNGSWHINR	HCVpp1b-8-1
VF-Fab1b-10-1	HSFVRFFASGPSQN	HCVpp1b-8-1
	GFASLFRLGPSQK	HCVpp1b-5-1
	MGEAQGRTTRGLA	HCVpp1b-4-1

The heatmap in Figure 5 gives an overview on the results obtained for each antibody.

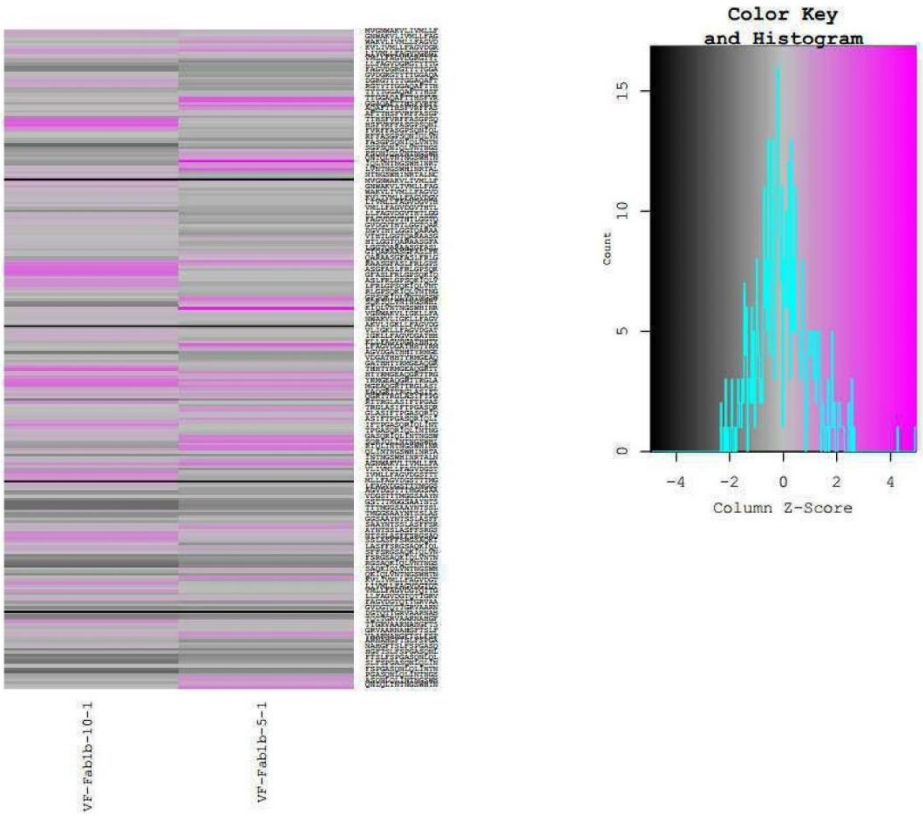

Figure 5. Heatmap representation of scaled and centered data recorded for two antibodies submitted for this study. Black horizontal lines show start positions of new target sequence in the same order as listed on page 7.

Since antibodies bound to linear peptides under reduced stringency conditions, it is possible that both antibodies recognize conformational or discontinuous epitopes, which might include parts of the protein not included in the current set of peptides.

Raw Data

__	Label	VF-Fab1b-10-1	VF-Fab1b-5-1
__	dilution	5µg/ml	4µg/ml
__	preconditioning	10%SQ	PT
__	Sample buffer	10%SQ	PT
__	conjugate	Humpo 1/1000	Humpo 1/1000
MVGNWAKVLIVMLLF	LIN	183	149
VGNWAKVLIVMLLFA	LIN	185	125
GNWAKVLIVMLLFAG	LIN	177	136
NWAKVLIVMLLFAGV	LIN	162	154
WAKVLIVMLLFAGVD	LIN	145	180
AKVLIVMLLFAGVDG	LIN	156	152
KVLIVMLLFAGVDGR	LIN	172	160
VLIVMLLFAGVDGRG	LIN	196	186
LIVMLLFAGVDGRGT	LIN	193	128
IVMLLFAGVDGRGTY	LIN	162	145
VMLLFAGVDGRGTYT	LIN	135	93
MLLFAGVDGRGTYTT	LIN	137	65
LLFAGVDGRGTYTTG	LIN	116	83
LFAGVDGRGTYTTGG	LIN	97	76
FAGVDGRGTYTTGGA	LIN	98	78
AGVDGRGTYTTGGAQ	LIN	153	95
GVDGRGTYTTGGAQA	LIN	153	84
VDGRGTYTTGGAQAF	LIN	173	107
DGRGTYTTGGAQAFT	LIN	191	96
GRGTYTTGGAQAFTT	LIN	181	85
RGTYTTGGAQAFTTH	LIN	179	95
GTYTTGGAQAFTTHS	LIN	133	86
TYTTGGAQAFTTHSF	LIN	136	116
YTTGGAQAFTTHSFV	LIN	147	119
TTGGAQAFTTHSFVR	LIN	166	244
TGGAQAFTTHSFVRF	LIN	150	243
GGAQAFTTHSFVRFF	LIN	129	176
GAQAFTTHSFVRFFA	LIN	154	208
AQAFTTHSFVRFFAS	LIN	161	183
QAFTTHSFVRFFASG	LIN	142	140
AFTTHSFVRFFASGP	LIN	163	143
FTTHSFVRFFASGPS	LIN	124	95
TTHSFVRFFASGPSQ	LIN	254	119
THSFVRFFASGPSQN	LIN	239	122
HSFVRFFASGPSQNI	LIN	256	117
SFVRFFASGPSQNIQ	LIN	200	103
FVRFFASGPSQNIQL	LIN	202	115
VRFFASGPSQNIQLV	LIN	156	109
RFFASGPSQNIQLVN	LIN	155	110
FFASGPSQNIQLVNT	LIN	140	82

FASGPSQNIQLVNTN	LIN	130	113
ASGPSQNIQLVNTNG	LIN	75	100
SGPSQNIQLVNTNGS	LIN	106	76
GPSQNIQLVNTNGSW	LIN	122	148
PSQNIQLVNTNGSWH	LIN	131	175
SQNIQLVNTNGSWHI	LIN	127	170
QNIQLVNTNGSWHIN	LIN	135	160
NIQLVNTNGSWHINR	LIN	123	350
IQLVNTNGSWHINRT	LIN	118	187
QLVNTNGSWHINRTA	LIN	168	170
LVNTNGSWHINRTAL	LIN	165	239
VNTNGSWHINRTALN	LIN	186	95
NTNGSWHINRTALNC	LIN	163	110
TNGSWHINRTALNCN	LIN	208	96
MVGNWAKVLTVMLLF	LIN	201	136
VGNWAKVLTVMLLFA	LIN	166	140
GNWAKVLTVMLLFAG	LIN	195	130
NWAKVLTVMLLFAGV	LIN	168	102
WAKVLTVMLLFAGVD	LIN	171	119
AKVLTVMLLFAGVDG	LIN	168	108
KVLTVMLLFAGVDGV	LIN	154	115
VLTVMLLFAGVDGVT	LIN	165	115
LTVMLLFAGVDGVTH	LIN	182	114
TVMLLFAGVDGVTHT	LIN	162	109
VMLLFAGVDGVTHTL	LIN	134	99
MLLFAGVDGVTHTLG	LIN	106	97
LLFAGVDGVTHTLGG	LIN	169	84
LFAGVDGVTHTLGGT	LIN	177	105
FAGVDGVTHTLGGTQ	LIN	173	99
AGVDGVTHTLGGTQA	LIN	158	83
GVDGVTHTLGGTQAR	LIN	166	141
VDGVTHTLGGTQARA	LIN	170	110
DGVTHTLGGTQARAA	LIN	163	99
GVTHTLGGTQARAAS	LIN	152	84
VTHTLGGTQARAASG	LIN	156	102
THTLGGTQARAASGF	LIN	156	149
HTLGGTQARAASGFA	LIN	169	102
TLGGTQARAASGFAS	LIN	168	102
LGGTQARAASGFASL	LIN	148	117
GGTQARAASGFASLF	LIN	141	107
GTQARAASGFASLFR	LIN	167	161
TQARAASGFASLFRL	LIN	150	144
QARAASGFASLFRLG	LIN	126	133
ARAASGFASLFRLGP	LIN	209	211
RAASGFASLFRLGPS	LIN	228	173
AASGFASLFRLGPSQ	LIN	237	134

ASGFASLFRLGPSQK	LIN	241	110
SGFASLFRLGPSQKI	LIN	249	132
GFASLFRLGPSQKIQ	LIN	235	125
FASLFRLGPSQKIQL	LIN	185	136
ASLFRLGPSQKIQLV	LIN	205	126
SLFRLGPSQKIQLVN	LIN	206	103
LFRLGPSQKIQLVNT	LIN	204	108
FRLGPSQKIQLVNTN	LIN	184	114
RLGPSQKIQLVNTNG	LIN	157	110
LGPSQKIQLVNTNGS	LIN	140	101
GPSQKIQLVNTNGSW	LIN	160	204
PSQKIQLVNTNGSWH	LIN	141	210
SQKIQLVNTNGSWHI	LIN	106	164
QKIQLVNTNGSWHIN	LIN	95	129
KIQLVNTNGSWHINR	LIN	170	319
MVGNWAKVLIGKLLF	LIN	166	128
VGNWAKVLIGKLLFA	LIN	153	153
GNWAKVLIGKLLFAG	LIN	151	118
NWAKVLIGKLLFAGV	LIN	166	124
WAKVLIGKLLFAGVD	LIN	151	108
AKVLIGKLLFAGVDG	LIN	148	109
KVLIGKLLFAGVDGA	LIN	140	95
VLIGKLLFAGVDGAT	LIN	171	120
LIGKLLFAGVDGATH	LIN	175	121
IGKLLFAGVDGATHH	LIN	175	119
GKLLFAGVDGATHHT	LIN	173	104
KLLFAGVDGATHHTY	LIN	140	137
LLFAGVDGATHHTYR	LIN	148	238
LFAGVDGATHHTYRM	LIN	160	166
FAGVDGATHHTYRMG	LIN	148	155
AGVDGATHHTYRMGE	LIN	91	83
GVDGATHHTYRMGEA	LIN	149	83
VDGATHHTYRMGEAQ	LIN	151	88
DGATHHTYRMGEAQG	LIN	140	103
GATHHTYRMGEAQGR	LIN	175	143
ATHHTYRMGEAQGRT	LIN	206	116
THHTYRMGEAQGRTT	LIN	242	110
HHTYRMGEAQGRTTR	LIN	178	203
HTYRMGEAQGRTTRG	LIN	172	164
TYRMGEAQGRTTRGL	LIN	209	155
YRMGEAQGRTTRGLA	LIN	229	195
RMGEAQGRTTRGLAS	LIN	238	172
MGEAQGRTTRGLASI	LIN	229	196
GEAQGRTTRGLASIF	LIN	178	173
EAQGRTTRGLASIFT	LIN	161	119
AQGRTTRGLASIFTP	LIN	183	168

QGRTTRGLASIFTPG	LIN	163	150
GRTTRGLASIFTPGA	LIN	95	74
RTTRGLASIFTPGAS	LIN	204	130
TTRGLASIFTPGASQ	LIN	158	100
TRGLASIFTPGASQR	LIN	163	173
RGLASIFTPGASQRI	LIN	160	180
GLASIFTPGASQRIQ	LIN	154	135
LASIFTPGASQRIQL	LIN	150	134
ASIFTPGASQRIQLI	LIN	171	178
SIFTPGASQRIQLIN	LIN	192	151
IFTPGASQRIQLINT	LIN	220	122
FTPGASQRIQLINTN	LIN	187	129
TPGASQRIQLINTNG	LIN	166	119
PGASQRIQLINTNGS	LIN	174	110
GASQRIQLINTNGSW	LIN	179	206
ASQRIQLINTNGSWH	LIN	168	195
SQRIQLINTNGSWHI	LIN	136	220
QRIQLINTNGSWHIN	LIN	125	171
RIQLINTNGSWHINR	LIN	124	211
IQLINTNGSWHINRT	LIN	191	211
QLINTNGSWHINRTA	LIN	152	141
LINTNGSWHINRTAL	LIN	103	72
INTNGSWHINRTALN	LIN	150	114
MAGNWAKVLIVMLLF	LIN	176	182
AGNWAKVLIVMLLFA	LIN	199	211
KVLIVMLLFAGVDGS	LIN	175	150
VLIVMLLFAGVDGST	LIN	131	71
LIVMLLFAGVDGSTT	LIN	219	119
IVMLLFAGVDGSTTT	LIN	197	106
VMLLFAGVDGSTTTM	LIN	195	97
MLLFAGVDGSTTTMG	LIN	194	115
LLFAGVDGSTTTMGG	LIN	183	102
LFAGVDGSTTTMGGS	LIN	180	115
FAGVDGSTTTMGGSA	LIN	150	90
AGVDGSTTTMGGSAA	LIN	110	93
GVDGSTTTMGGSAAY	LIN	116	84
VDGSTTTMGGSAAYN	LIN	165	120
DGSTTTMGGSAAYNT	LIN	106	75
GSTTTMGGSAAYNTS	LIN	77	62
STTTMGGSAAYNTSS	LIN	78	57
TTTMGGSAAYNTSSL	LIN	78	63
TTMGGSAAYNTSSLA	LIN	137	102
TMGGSAAYNTSSLAS	LIN	111	69
MGGSAAYNTSSLASF	LIN	113	104
GGSAAYNTSSLASFF	LIN	144	132
GSAAYNTSSLASFFS	LIN	124	102

SAAYNTSSLASFFSR	LIN	167	160
AAYNTSSLASFFSRG	LIN	173	186
AYNTSSLASFFSRGS	LIN	154	121
YNTSSLASFFSRGSA	LIN	207	147
NTSSLASFFSRGSAQ	LIN	206	135
TSSLASFFSRGSAQK	LIN	212	151
SSLASFFSRGSAQKI	LIN	193	114
SLASFFSRGSAQKIQ	LIN	165	75
LASFFSRGSAQKIQL	LIN	181	107
ASFFSRGSAQKIQLV	LIN	185	176
SFFSRGSAQKIQLVN	LIN	158	118
FFSRGSAQKIQLVNT	LIN	102	67
FSRGSAQKIQLVNTN	LIN	110	82
SRGSAQKIQLVNTNG	LIN	94	75
RGSAQKIQLVNTNGS	LIN	81	60
GSAQKIQLVNTNGSW	LIN	70	63
SAQKIQLVNTNGSWH	LIN	150	164
AQKIQLVNTNGSWHT	LIN	131	117
QKIQLVNTNGSWHTN	LIN	103	79
KIQLVNTNGSWHTNR	LIN	165	188
KVLIVMLLFAGVDGT	LIN	144	95
VLIVMLLFAGVDGTQ	LIN	208	120
LIVMLLFAGVDGTQT	LIN	184	135
IVMLLFAGVDGTQTT	LIN	156	125
VMLLFAGVDGTQTTG	LIN	199	123
MLLFAGVDGTQTTGR	LIN	129	112
LLFAGVDGTQTTGRV	LIN	169	145
LFAGVDGTQTTGRVA	LIN	174	148
FAGVDGTQTTGRVAA	LIN	122	78
AGVDGTQTTGRVAAR	LIN	143	117
GVDGTQTTGRVAARN	LIN	103	67
VDGTQTTGRVAARNA	LIN	158	130
DGTQTTGRVAARNAH	LIN	130	97
GTQTTGRVAARNAHG	LIN	95	63
TQTTGRVAARNAHGF	LIN	105	73
QTTGRVAARNAHGFT	LIN	209	143
TTGRVAARNAHGFTS	LIN	174	120
TGRVAARNAHGFTSL	LIN	144	119
GRVAARNAHGFTSLF	LIN	167	140
RVAARNAHGFTSLFS	LIN	173	181
VAARNAHGFTSLFSP	LIN	175	174
AARNAHGFTSLFSPG	LIN	145	99
ARNAHGFTSLFSPGA	LIN	138	73
RNAHGFTSLFSPGAS	LIN	186	109
NAHGFTSLFSPGASQ	LIN	161	98
AHGFTSLFSPGASQN	LIN	97	61

HGFTSLFSPGASQNL	LIN	140	94
GFTSLFSPGASQNLQ	LIN	85	64
FTSLFSPGASQNLQL	LIN	101	74
TSLFSPGASQNLQLI	LIN	86	81
SLFSPGASQNLQLIN	LIN	86	87
LFSPGASQNLQLINT	LIN	162	124
FSPGASQNLQLINTN	LIN	86	60
SPGASQNLQLINTNG	LIN	70	65
PGASQNLQLINTNGS	LIN	130	99
GASQNLQLINTNGSW	LIN	137	179
ASQNLQLINTNGSWH	LIN	151	181
SQNLQLINTNGSWHI	LIN	132	161
QNLQLINTNGSWHIN	LIN	155	176
NLQLINTNGSWHINR	LIN	151	222
MVGNWAKVLAAMLLF	LIN.AA	113	75
VGNWAKVLIAALLFA	LIN.AA	92	79
GNWAKVLIVAALFAG	LIN.AA	113	81
NWAKVLIVMAAFAGV	LIN.AA	92	59
WAKVLIVMLAAAGVD	LIN.AA	92	56
AKVLIVMLLAGGVDG	LIN.AA	111	111
KVLIVMLLFGAVDGR	LIN.AA	182	193
VLIVMLLFAAADGRG	LIN.AA	91	65
LIVMLLFAGAAGRGT	LIN.AA	105	74
IVMLLFAGVAARGTY	LIN.AA	113	83
VMLLFAGVDAAGTYT	LIN.AA	96	71
MLLFAGVDGAATYTT	LIN.AA	140	95
LLFAGVDGRAAYTTG	LIN.AA	160	85
LFAGVDGRGAATTGG	LIN.AA	154	89
FAGVDGRGTAATGGA	LIN.AA	121	86
AGVDGRGTYAAGGAQ	LIN.AA	187	99
GVDGRGTYTAAGAQA	LIN.AA	195	87
VDGRGTYTTAAAQAF	LIN.AA	93	72
DGRGTYTTGAGQAFT	LIN.AA	94	58
GRGTYTTGGGAAFTT	LIN.AA	191	135
RGTYTTGGAAGFTTH	LIN.AA	98	79
GTYTTGGAQGATTHS	LIN.AA	95	75
TYTTGGAQAAATHSF	LIN.AA	122	113
YTTGGAQAFAAHSFV	LIN.AA	110	98
TTGGAQAFTAASFVR	LIN.AA	149	161
TGGAQAFTTAAFVRF	LIN.AA	92	66
GGAQAFTTHAAVRFF	LIN.AA	87	64
GAQAFTTHSAARFFA	LIN.AA	105	84
AQAFTTHSFAAFFAS	LIN.AA	153	165
QAFTTHSFVAAFASG	LIN.AA	126	90
AFTTHSFVRAAASGP	LIN.AA	214	120
FTTHSFVRFAGSGPS	LIN.AA	191	97

TTHSFVRFFGAGPSQ	LIN.AA	257	152
THSFVRFFAAAPSQN	LIN.AA	228	122
HSFVRFFASAASQNI	LIN.AA	124	72
SFVRFFASGAAQNIQ	LIN.AA	163	135
FVRFFASGPAANIQL	LIN.AA	106	85
VRFFASGPSAAIQLV	LIN.AA	159	134
RFFASGPSQAAQLVN	LIN.AA	82	59
FFASGPSQNAALVNT	LIN.AA	79	67
FASGPSQNIAAVNTN	LIN.AA	85	63
ASGPSQNIQAANTNG	LIN.AA	61	65
SGPSQNIQLAATNGS	LIN.AA	69	62
GPSQNIQLVAANGSW	LIN.AA	77	79
PSQNIQLVNAAGSWH	LIN.AA	126	145
SQNIQLVNTAASWHI	LIN.AA	137	176
QNIQLVNTNAAWHIN	LIN.AA	96	99
NIQLVNTNGAAHINR	LIN.AA	148	166
IQLVNTNGSAAINRT	LIN.AA	130	102
QLVNTNGSWAANRTA	LIN.AA	183	114
LVNTNGSWHAARTAL	LIN.AA	141	93
VNTNGSWHIAATALN	LIN.AA	152	100
NTNGSWHINAAALNC	LIN.AA	119	100
TNGSWHINRAGLNCN	LIN.AA	76	64
VGNWAKVLTAALLFA	LIN.AA	133	146
GNWAKVLTVAALFAG	LIN.AA	147	121
NWAKVLTVMAAFAGV	LIN.AA	82	49
WAKVLTVMLAAAGVD	LIN.AA	80	50
AKVLTVMLLAGGVDG	LIN.AA	108	73
KVLTVMLLFGAVDGV	LIN.AA	161	146
VLTVMLLFAAADGVT	LIN.AA	88	46
LTVMLLFAGAAGVTH	LIN.AA	214	139
TVMLLFAGVAAVTHT	LIN.AA	198	120
VMLLFAGVDAATHTL	LIN.AA	145	101
MLLFAGVDGAAHTLG	LIN.AA	165	111
LLFAGVDGVAATLGG	LIN.AA	148	90
LFAGVDGVTAALGGT	LIN.AA	167	106
FAGVDGVTHAAGGTQ	LIN.AA	165	105
AGVDGVTHTAAGTQA	LIN.AA	119	87
GVDGVTHTLAATQAR	LIN.AA	154	121
VDGVTHTLGAAQARA	LIN.AA	123	98
DGVTHTLGGAAARAA	LIN.AA	165	101
GVTHTLGGTAGRAAS	LIN.AA	175	109
VTHTLGGTQGAAASG	LIN.AA	74	82
THTLGGTQAAGASGF	LIN.AA	68	57
HTLGGTQARGGSGFA	LIN.AA	70	58
TLGGTQARAGAGFAS	LIN.AA	71	41
LGGTQARAAAAFASL	LIN.AA	82	61

GGTQARAASAAASLF	LIN.AA	84	61
GTQARAASGAGSLFR	LIN.AA	165	101
TQARAASGFGALFRL	LIN.AA	153	85
QARAASGFAAAFRLG	LIN.AA	170	189
ARAASGFASAARLGP	LIN.AA	177	105
RAASGFASLAALGPS	LIN.AA	197	131
AASGFASLFAAGPSQ	LIN.AA	180	110
ASGFASLFRAAPSQK	LIN.AA	258	107
SGFASLFRLAASQKI	LIN.AA	107	62
GFASLFRLGAAQKIQ	LIN.AA	105	56
FASLFRLGPAAKIQL	LIN.AA	101	59
ASLFRLGPSAAIQLV	LIN.AA	159	95
SLFRLGPSQAAQLVN	LIN.AA	108	58
LFRLGPSQKAALVNT	LIN.AA	69	43
FRLGPSQKIAAVNTN	LIN.AA	80	59
RLGPSQKIQAANTNG	LIN.AA	61	48
LGPSQKIQLAATNGS	LIN.AA	107	83
GPSQKIQLVAANGSW	LIN.AA	144	170
PSQKIQLVNAAGSWH	LIN.AA	141	169
SQKIQLVNTAASWHI	LIN.AA	152	173
QKIQLVNTNAAWHIN	LIN.AA	146	149
KIQLVNTNGAAHINR	LIN.AA	150	129
MVGNWAKVLAAKLLF	LIN.AA	158	95
GNWAKVLIGAALFAG	LIN.AA	155	120
NWAKVLIGKAAFAGV	LIN.AA	193	128
WAKVLIGKLAAAGVD	LIN.AA	140	73
AKVLIGKLLAGGVDG	LIN.AA	131	83
KVLIGKLLFGAVDGA	LIN.AA	132	82
VLIGKLLFAAADGAT	LIN.AA	137	108
LIGKLLFAGAAGATH	LIN.AA	165	107
IGKLLFAGVAAATHH	LIN.AA	95	54
GKLLFAGVDAGTHHT	LIN.AA	82	63
KLLFAGVDGGAHHTY	LIN.AA	149	119
LLFAGVDGAAAHTYR	LIN.AA	129	144
LFAGVDGATAATYRM	LIN.AA	146	96
FAGVDGATHAAYRMG	LIN.AA	94	67
AGVDGATHHAARMGE	LIN.AA	146	86
GVDGATHHTAAMGEA	LIN.AA	107	74
VDGATHHTYAAGEAQ	LIN.AA	91	77
DGATHHTYRAAEAQG	LIN.AA	146	95
GATHHTYRMAAAQGR	LIN.AA	124	78
ATHHTYRMGAGQGRT	LIN.AA	135	66
THHTYRMGEGAGRTT	LIN.AA	119	58
HHTYRMGEAAARTTR	LIN.AA	141	140
HTYRMGEAQAATTRG	LIN.AA	152	145
TYRMGEAQGAATRGL	LIN.AA	97	64

YRMGEAQGRAARGLA	LIN.AA	89	65
RMGEAQGRTAAGLAS	LIN.AA	77	63
MGEAQGRTTAALASI	LIN.AA	127	94
GEAQGRTTRAAASIF	LIN.AA	158	172
EAQGRTTRGAGSIFT	LIN.AA	150	106
AQGRTTRGLGAIFTP	LIN.AA	113	94
QGRTTRGLAAAFTPG	LIN.AA	179	144
GRTTRGLASAATPGA	LIN.AA	139	57
RTTRGLASIAAPGAS	LIN.AA	187	95
TTRGLASIFAAGASQ	LIN.AA	108	73
TRGLASIFTAAASQR	LIN.AA	220	161
RGLASIFTPAGSQRI	LIN.AA	195	218
GLASIFTPGGAQRIQ	LIN.AA	168	115
LASIFTPGAAARIQL	LIN.AA	135	141
ASIFTPGASAAIQLI	LIN.AA	161	171
SIFTPGASQAAQLIN	LIN.AA	161	112
IFTPGASQRAALINT	LIN.AA	197	83
FTPGASQRIAAINTN	LIN.AA	154	87
TPGASQRIQAANTNG	LIN.AA	131	91
PGASQRIQLAATNGS	LIN.AA	157	95
GASQRIQLIAANGSW	LIN.AA	165	165
ASQRIQLINAAGSWH	LIN.AA	159	184
SQRIQLINTAASWHI	LIN.AA	141	183
QRIQLINTNAAWHIN	LIN.AA	139	141
RIQLINTNGAAHINR	LIN.AA	132	162
IQLINTNGSAAINRT	LIN.AA	129	94
QLINTNGSWAANRTA	LIN.AA	110	77
LINTNGSWHAARTAL	LIN.AA	166	145
INTNGSWHIAATALN	LIN.AA	113	92
MAGNWAKVLAAMLLF	LIN.AA	132	125
AGNWAKVLIAALLFA	LIN.AA	122	106
KVLIVMLLFGAVDGS	LIN.AA	186	134
VLIVMLLFAAADGST	LIN.AA	187	125
LIVMLLFAGAAGSTT	LIN.AA	186	107
IVMLLFAGVAASTTT	LIN.AA	204	120
VMLLFAGVDAATTTM	LIN.AA	154	83
MLLFAGVDGAATTMG	LIN.AA	160	102
LLFAGVDGSAATMGG	LIN.AA	149	85
LFAGVDGSTAAMGGS	LIN.AA	131	93
FAGVDGSTTAAGGSA	LIN.AA	135	98
AGVDGSTTTAAGSAA	LIN.AA	120	77
GVDGSTTTMAASAAY	LIN.AA	122	89
VDGSTTTMGAAAAYN	LIN.AA	136	74
DGSTTTMGGAGAYNT	LIN.AA	105	60
GSTTTMGGSGGYNTS	LIN.AA	135	76
STTTMGGSAGANTSS	LIN.AA	126	77

TTTMGGSAAAATSSL	LIN.AA	120	101
TTMGGSAAYAASSLA	LIN.AA	143	93
TMGGSAAYNAASLAS	LIN.AA	123	88
MGGSAAYNTAALASF	LIN.AA	130	116
GGSAAYNTSAAASFF	LIN.AA	139	106
GSAAYNTSSAGSFFS	LIN.AA	135	127
SAAYNTSSLGAFFSR	LIN.AA	140	146
AAYNTSSLAAAFSRG	LIN.AA	145	184
AYNTSSLASAASRGS	LIN.AA	128	112
YNTSSLASFAARGSA	LIN.AA	131	120
NTSSLASFFAAGSAQ	LIN.AA	139	89
TSSLASFFSAASAQK	LIN.AA	184	91
SSLASFFSRAAAQKI	LIN.AA	206	113
SLASFFSRGAGQKIQ	LIN.AA	184	64
LASFFSRGSGAKIQL	LIN.AA	127	76
ASFFSRGSAAAIQLV	LIN.AA	152	88
SFFSRGSAQAAQLVN	LIN.AA	157	88
FFSRGSAQKAALVNT	LIN.AA	184	85
FSRGSAQKIAAVNTN	LIN.AA	131	88
SRGSAQKIQAANTNG	LIN.AA	115	85
RGSAQKIQLAATNGS	LIN.AA	123	79
GSAQKIQLVAANGSW	LIN.AA	148	159
SAQKIQLVNAAGSWH	LIN.AA	137	169
AQKIQLVNTAASWHT	LIN.AA	124	90
QKIQLVNTNAAWHTN	LIN.AA	133	130
KIQLVNTNGAAHTNR	LIN.AA	123	106
KVLIVMLLFGAVDGT	LIN.AA	157	142
VLIVMLLFAAADGTQ	LIN.AA	185	174
LIVMLLFAGAAGTQT	LIN.AA	176	94
IVMLLFAGVAATQTT	LIN.AA	154	82
VMLLFAGVDAAQTTG	LIN.AA	127	92
MLLFAGVDGAATTGR	LIN.AA	96	80
LLFAGVDGTAATGRV	LIN.AA	127	73
LFAGVDGTQAAGRVA	LIN.AA	146	74
FAGVDGTQTAARVAA	LIN.AA	147	79
AGVDGTQTTAAVAAR	LIN.AA	133	113
GVDGTQTTGAAAARN	LIN.AA	105	96
VDGTQTTGRAGARNA	LIN.AA	137	106
DGTQTTGRVGGRNAH	LIN.AA	151	123
GTQTTGRVAGANAHG	LIN.AA	138	103
TQTTGRVAAAAAHGF	LIN.AA	128	94
QTTGRVAARAGHGFT	LIN.AA	128	105

Appendix III

PEPSCAN

FINAL REPORT FOR UNIVERSITY COLLEGE CORK

HCV-E1E2 GLYCOPROTEIN (HCVPP1B-1-3)

CONFORMATIONAL EPITOPE MAPPING

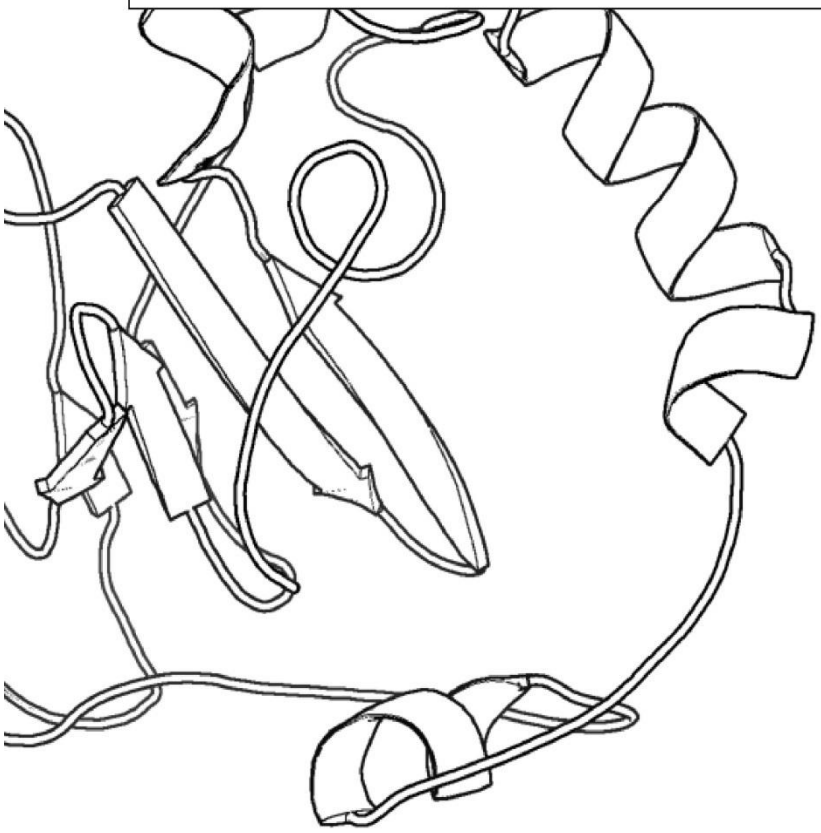

STUDY REPORT

STUDY NUMBER ES150122008A+B

TABLE OF CONTENTS

EXECUTIVE SUMMARY

GOAL

To map the epitopes of four Fabs targeting HCV-E1E2 glycoprotein (HCVpp1b-1-3) by means of conformational epitope mapping.

RESULTS

All four Fabs submitted for the study weakly bound sequence $_{10}$SRAAHRVTTFITR$_{22}$ under low stringency conditions. An additional binding motif $_{155}$LLNNTRPPRGNWF$_{167}$ was also identified for samples H, VF-Fab3a-1-1, and VF-FAB1B-3-1.

REFERENCES

The study was conducted at Pepscan Presto BV, (Zuidersluisweg 2, 8243RC Lelystad, The Netherlands). All Pepscan data is stored in the software package Peplab™, a proprietary database application developed in-house and built on a PostgreSQL storage back-end. The database has daily off-site back-ups on a private secure server. The screening department has additional lab books and hard-copies of all results. These are stored in the Pepscan laboratory which is electronically secured.

STUDY DATES

Table 1. Study Dates and References

Order accepted:	25th of January 2016
Synthesis of the array:	February – March 2016
Screening of the peptides:	Labbooks: Pep217: pp. 117, 119, 122, 124, 126 – 127, 131 Pep218: p. 128

PERSONNEL & FACILITIES

Table 2. Personnel

Study director:	Dr. JW Back
Study supervisor:	Dr. E. Shimanovskaya
Peptide synthesis:	Sonja Kerkhoff, Joshua Buijnink
Pepscan ELISA:	Drohpati Parohi, Joop Tibben, Paola Weert

MATERIALS

General materials used: See Methods section.

PROVIDED DESCRIPTION OF ANTIBODIES

Antibodies provided by University College Cork that recognize HCV-E1E2 glycoprotein (HCVpp1b-1-3) are listed below (Table 3).

Table 3. Details of the antibodies

Name	Origin	Concentration	Location	Status
VF-FAB1A-1-3	human	1,22 mg/ml	-20 C/95	ok
VF-FAB1B-1-3	human	1,20 mg/ml	-20 C/95	ok
VF-FAB1B-5-1	human	1,20 mg/ml	-20 C/95	ok
VF-FAB3A-1-1	human	1,10 mg/ml	-20 C/95	ok

TARGET PROTEIN

PROVIDED PROTEIN SEQUENCE

>fragment of HCV-E1E2 glycoprotein (HCVpp1b-1-3) (HCVpp1b-1-3)

```
  1 ETHTVGGSAS RAAHRVTTFI TRGPSQNIQL INTNGSWHIN RTALNCNDSL 50
 51 NTGFLAALFY THRFNASGCP ERMASCRPID KFAQGWGPIT HTEPPSSDQK 100
101 PYCWHYAPRP CGIVPAAQVC GPVYCFTPSP VVVGTTDRFG VPTYSWGENE 150
151 TDVLLLNNTR PPRGNWFGCT WMNSTGFTKT CGGPPCNIGG VGNDTLTCPT 200
201 DCFRKHPEAT YTRCGSGPWL TPRCMVHYPY 230
```

DATA VISUALIZATION

Results of epitope mapping are visualized using a homology model build based on pdb entry 4mwf that displays 82% of sequence identity with the target sequence.

Figure 1. Color ramped model of HCV-E1E2 glycoprotein (HCVpp1b-1-3).

METHODS

THE PRINCIPLES OF CLIPS TECHNOLOGY

CLIPS technology structurally fixes peptides into defined three-dimensional structures. This results in functional mimics of even the most complex binding sites. CLIPS technology is now routinely used to shape peptide libraries into single, double or triple looped structures as well as sheet- and helix-like folds (Figure 2).

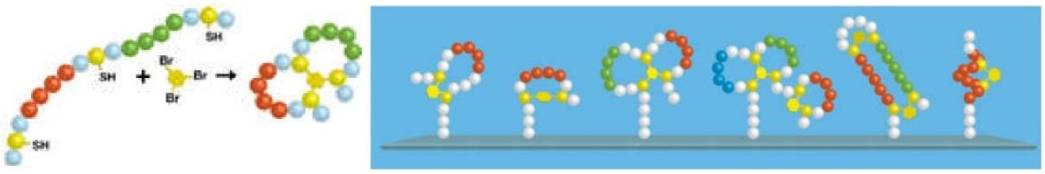

Figure 2. The CLIPS reaction takes place between bromo groups of the CLIPS scaffold and thiol sidechains of cysteines. The reaction is fast and specific under mild conditions. Using this elegant chemistry, native protein sequences are transformed into CLIPS constructs with a range of structures. From left to right: two different single T2 loops, T3 double loop, conjugated T2+T3 loops, stabilized beta sheet, and stabilized alpha helix (Timmerman et al., J. Mol. Recognit. 2007; 20: 283-29).

2D HEATMAP ANALYSIS

A heat map is a graphical representation of data where the values taken by a variable in a two-dimensional map are represented as colors.

In current example, different samples are plotted horizontally, and peptide entries are plotted vertically. The magnitude of a response is color-coded and the key is included in the plot. Figure 3 below illustrates a response from a polyclonal serum screened on a library of overlapping peptides. The response is displayed in two complementary ways: as histogram and as 1D heatmap. While for a single serum the histogram is easily grasped, a comparison of responses from numerous samples is easier, when analyzed through a 2D heatmap.

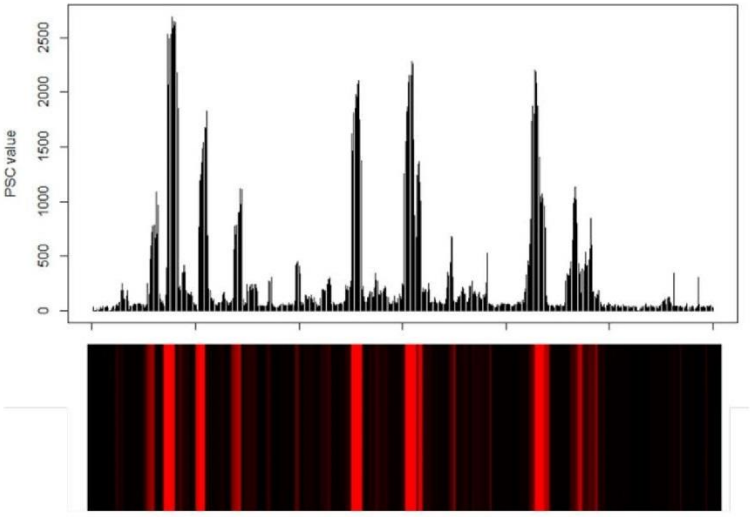

Figure 3. Intensity profile and corresponding 2D heatmap representation of a response from a polyclonal serum screened on a library of overlapping linear peptides.

SYNTHESIS OF PEPTIDES

To reconstruct epitopes of the target molecule a library of peptides was synthesized. An amino functionalized polypropylene support was obtained by grafting with a proprietary hydrophilic polymer formulation, followed by reaction with t-butyloxycarbonyl-hexamethylenediamine (BocHMDA) using dicyclohexylcarbodiimide (DCC) with Nhydroxybenzotriazole (HOBt) and subsequent cleavage of the Boc-groups using trifluoroacetic acid (TFA). Standard Fmoc-peptide synthesis was used to synthesize peptides on the amino-functionalized solid support by custom modified JANUS liquid handling stations (Perkin Elmer).

Synthesis of structural mimics was done using Pepscan's proprietary Chemically Linked Peptides on Scaffolds (CLIPS) technology. CLIPS technology allows to structure peptides into single loops, double-loops, triple loops, sheet-like folds, helix-like folds and combinations thereof. CLIPS templates are coupled to cysteine residues. The side-chains of multiple cysteines in the peptides are coupled to one or two CLIPS templates. For example, a 0.5 mM solution of the P2 CLIPS (2,6-bis(bromomethyl)pyridine) is dissolved in ammonium bicarbonate (20 mM, pH 7.8)/acetonitrile (1:3(v/v)). This solution is added onto the peptide arrays. The CLIPS template will bind to side-chains of two cysteines as present in the solid-phase bound peptides of the peptide-arrays (455 wells plate with 3 µl wells). The peptide arrays are gently shaken in the solution for 30 to 60 minutes while completely covered in solution. Finally, the peptide arrays are washed extensively with excess of H_2O and sonicated in disrupt-buffer containing 1 % SDS/0.1 % beta-mercaptoethanol in PBS (pH 7.2) at 70°C for 30 minutes, followed by sonication in H_2O for another 45 minutes. The T3 CLIPS carrying peptides were made in a similar way but now with three cysteines.

ELISA SCREENING

The binding of antibody to each of the synthesized peptides was tested in a PEPSCAN-based ELISA. The peptide arrays were incubated with primary antibody solution (overnight at 4°C). After washing, the peptide arrays were incubated with a 1/1000 dilution of an appropriate antibody peroxidase conjugate (SBA; Table 4) for one hour at 25°C. After washing, the peroxidase substrate 2,2'-azino-di-3-ethylbenzthiazoline sulfonate (ABTS) and 20 µl/ml of 3 percent H_2O_2 were added. After one hour, the color development was measured. The color development was quantified with a charge coupled device (CCD) - camera and an image processing system.

Table 4. Details of the antibodies

Name	Supplier	Cat. No
goat anti-human HRP conjugate	Southern Biotech	2010-05

DATA PROCESSING

The values obtained from the CCD camera range from 0 to 3000 mAU, similar to a standard 96-well plate ELISA-reader. The results are quantified and stored into the Peplab database. Occasionally a well contains an air-bubble resulting in a false-positive value, the cards are manually inspected and any values caused by an air-bubble are scored as 0.

SYNTHESIS QUALITY CONTROL

To verify the quality of the synthesized peptides, a separate set of positive and negative control peptides was synthesized in parallel. These were screened with antibody 57.9 (*ref.* Posthumus *et al.,* J. Virology, 1990, 64:3304-3309)

LITERATURE REFERENCES

Timmerman *et al.* (2007). Functional reconstruction and synthetic mimicry of a conformational epitope using CLIPS™ technology. *J. Mol. Recognit*. **20**:283-99

Langedijk *et al.* (2011). Helical peptide arrays for lead identification and interaction site mapping, *Analytical Biochemistry* **417**: 149–155

DESIGN OF PEPTIDES

Different sets of peptides were synthesized (see also Methods section) according to the following designs. Note that order of peptides in some sets was randomized and below only an actual order of peptides on mini-cards is shown.

SET 1

Mimic Type linear

Label LIN

Description Linear peptides of length 15 derived from the target sequence on page 7 with an offset of one residue. Cys are protected by acetamidomethyl (Acm; denoted "2").

Sequences (first 10)

2GPVY2FTPSPVVVG
TALN2NDSLNTGFLA
NRTALN2NDSLNTGF
SWGENETDVLLLNNT
DTLT2PTD2FRKHPE
STGFTKT2GGPP2NI
GVPTYSWGENETDVL
KHPEATYTR2GSGPW
KFAQGWGPITHTEPP
WFG2TWMNSTGFTKT

SET 2

Mimic Type Loop, mP2 CLIPS

Label LOOP

Description Constrained peptides of length 17. On positions 2 – 16 are 15-mer sequences derived from the target sequence of HCV-E1E2 glycoprotein (HCVpp1b-1-3). To introduce structural constraints Cys were inserted on positions 1 and 17, which then were constrained by mP2 CLIPS. Native Cys are protected by Acm (denoted "2").

Sequences (first 10)

CETHTVGGSASRAAHRC
CTHTVGGSASRAAHRVC
CHTVGGSASRAAHRVTC
CTVGGSASRAAHRVTTC
CVGGSASRAAHRVTTFC
CGGSASRAAHRVTTFIC
CGSASRAAHRVTTFITC
CSASRAAHRVTTFITRC
CASRAAHRVTTFITRGC
CSRAAHRVTTFITRGPC

SET 3

Mimic Type helical mimic, mP2 CLIPS

Label HEL

Description Structured peptides of length 23 derived from the target sequence on page 7 with an offset of one residue. On positions 1 and 5 are Cys residues which are joined by mP2 CLIPS. Native Cys are protected by Acm (denoted "2").

Sequences (first 10)

CETHCVGGSASRAAHRVTTFIT
CTHTCGGSASRAAHRVTTFITR
CHTVCGSASRAAHRVTTFITRG
CTVGCSASRAAHRVTTFITRGP
CVGGCASRAAHRVTTFITRGPS
CGGSCSRAAHRVTTFITRGPSQ
CGSACRAAHRVTTFITRGPSQN
CSASCAAHRVTTFITRGPSQNI
CASRCAHRVTTFITRGPSQNIQ
CSRACHRVTTFITRGPSQNIQL

SET 4

Mimic Type β-turn mimic, mP2 CLIPS

Label BET

Description Structured peptides of length 22. On positions 2- 21 are 20-mer sequences derived from the target sequence of HCV-E1E2 glycoprotein (HCVpp1b-1-3) with an offset of one residue. "PG" residues supplant the residues present on positions 10 and 11. On positions 1 and 22 are Cys residues which are joined by mP2 CLIPS. Native Cys are protected by Acm (denoted "2").

Sequences (first 10)

CHRVTTFITRPGSQNIQLINTC
CTYTR2GSGPPGTPR2MVHYPC
CQNIQLINTNPGWHINRTALNC
CNDTLT2PTDPGRKHPEATYTC
CNETDVLLLNPGRPPRGNWFGC
CETDVLLLNNPGPPRGNWFG2C
CP2GIVPAAQPGGPVY2FTPSC
C2RPIDKFAQPGGPITHTEPPC
CDSLNTGFLAPGFYTHRFNASC
CHYAPRP2GIPGAAQV2GPVYC

SCREENING DETAILS

Antibody binding depends on a combination of factors, including concentration of the antibody and the amounts and nature of competing proteins in the ELISA buffer. Also, the pre-coat conditions (the specific treatment of the peptide arrays prior to incubation with the experimental sample) affect binding. These details are summed up in Table 5. For the Pepscan Buffer and Preconditioning (SQ), the numbers indicate the relative amount of competing protein (a combination of horse serum and ovalbumin).

Table 5. Screening conditions

Label	Dilution	Sample buffer	Pre-conditioning
VF-FAB1A-1-3	5 µg/ml	PBS-Tween	0.1%SQ
VF-FAB1B-1-3	5 µg/ml	PBS-Tween	0.1%SQ
VF-FAB1B-5-1	5 µg/ml	PBS-Tween	0.1%SQ
Herceptin	5 µg/ml	PBS-Tween	0.1%SQ
VF-FAB3A-1-1	5 µg/ml	PBS-Tween	0.1%SQ

SCREENING RESULTS

PRIMARY EXPERIMENTAL RESULTS AND SIGNAL TO NOISE RATIO DETERMINATION

The raw ELISA results of the screening are provided in the accompanying Excel data file. A graphical overview of the complete dataset is given in Figure 4. Here a box plot depicts each dataset and indicates the average ELISA signal, the distribution and the outliers within each dataset. Depending on experiment conditions (amount of antibody, blocking strength etc) different distributions of ELISA data are obtained.

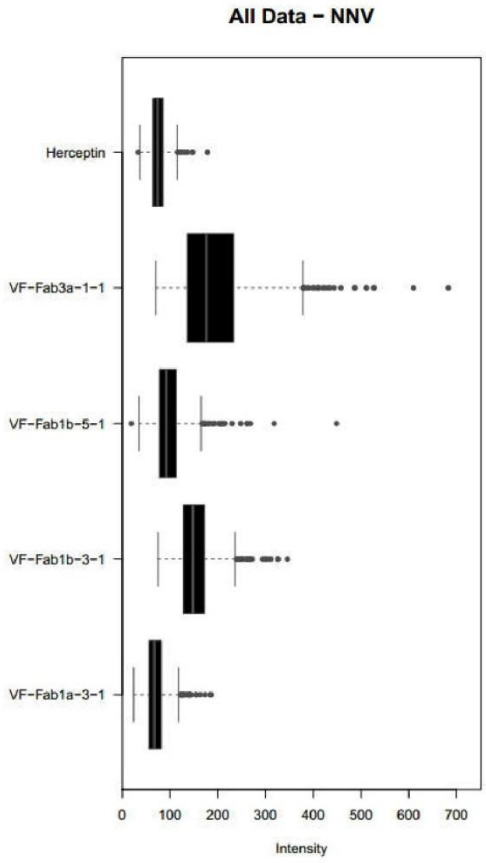

Figure 4. Box plot graphs of raw data of antibody screening. The bottom and top of the boxes are the 25th and 75th percentile of the data. The band near the middle of the box is the 50th percentile (the median). The whiskers are at 1.5 the inter-quantile range, an indication of statistical outliers within the dataset (ref Mcgill et al.,The American Statistician, 32: 12-16, 1978).

RESULTS IN DETAIL

HERCEPTIN

Herceptin was used as an internal negative control and was applied on the arrays under conditions used for profiling test samples. Herceptin did not result in any specific binding to the arrays.

FABS VF-FAB1A-1-3, VF-FAB1B-1-3, VF-FAB1B-5-1 & VF-FAB3A-1-1

When tested under high stringency conditions Fabs VF-FAB1A-3-1, B3, VF-Fab1b-5-1 and VF-Fab3a-1-1 did not bind any peptide present on the arrays. When tested under low stringency conditions Fabs VF-FAB1A-1-3, VF-FAB1B-1-3, VF-FAB1B-5-1 & VF-FAB3A-1-1 commonly bound peptides with core sequence $_{10}$SRAAHRVTTFITR$_{22}$ from all sets (Figure 5).

Additional binding was recorded for VF-FAB1A-1-3, VF-FAB1B-1-3 /VF-Fab1b-5-1 on linear peptides with core sequences $_{50}$LNTGFLAALFYTH$_{62}$ and $_{155}$LLNNTRPPRGNWF$_{167}$ respectively. Samples VF-Fab3a-1-1 and VF-Fab1b-5-1 similarly bound one β-turn mimic with core sequences $_{45}$NCNDSLNTGFLAALFYTHRF$_{64}$. Linear sequences $_{216}$SGPWLTPRCM$_{225}$, $_{155}$LLNNTRPPRGNWF$_{167}$ were additionally recognized by Fab VF-Fab3a-1-1.

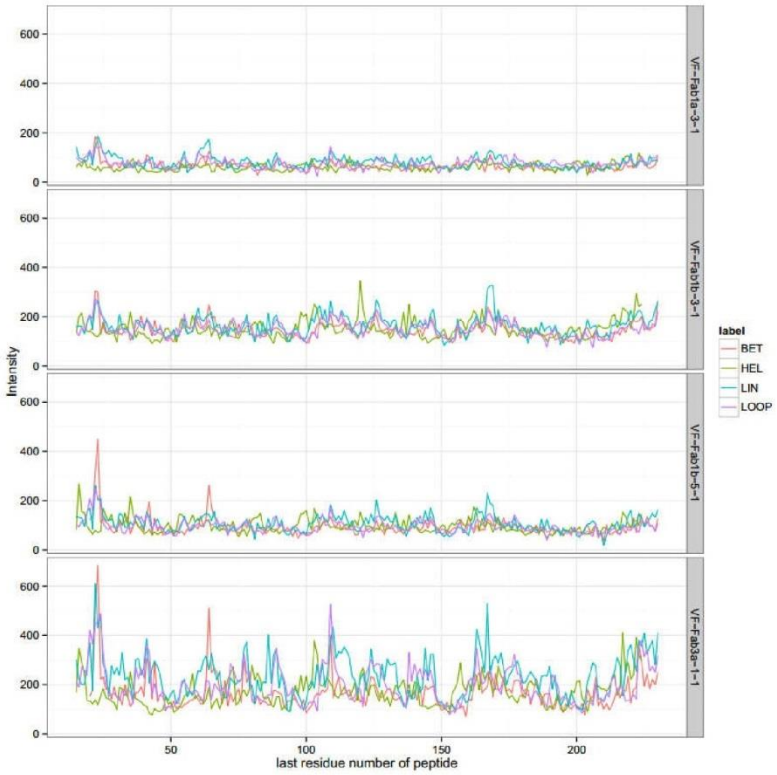

Figure 5. Overlay of intensity profiles recorded for all four Fabs on the arrays. Each sample intensity profile obtained with linear epitope mimics (blue) is overlaid with those obtained with structurally constrained peptides (green, red, purple). On the x-axis is the last residue number of each peptide with respect to the target sequence on page 7.

CONCLUSIONS

Four Fabs submitted for the study were tested using Pepscan peptide arrays. For each sample binding motifs were identified under low stringency conditions. A summary of the results is presented in Table 6.

Table 6. List of epitopes found in this study

Fabs	Bound sequences
VF-FAB1B-1-3	$_{10}$SRAAHRVTTFITR$_{22}$, $_{155}$LLNNTRPPRGNWF$_{167}$
VF-FAB1A-1-3	$_{10}$SRAAHRVTTFITR$_{22}$, $_{50}$LNTGFLAALFYTH$_{62}$
VF-FAB1B-5-1	$_{10}$SRAAHRVTTFITR$_{22}$*), $_{155}$LLNNTRPPRGNWF$_{167}$, $_{45}$NCNDSLNTGFLAALFYTHRF$_{64}$*)
VF-FAB3A-1-1	$_{10}$SRAAHRVTTFITR$_{22}$*), $_{216}$SGPWLTPRCM$_{225}$, $_{155}$LLNNTRPPRGNWF$_{167}$, $_{45}$NCNDSLNTGFLAALFYTHRF$_{64}$*)

*) for these sequences binding to β-turn mimics was higher when compared with that of linear mimics.

All Fabs similarly bound sequence $_{10}$SRAAHRVTTFITR$_{22}$. Fabs VF-FAB1B-1-3 VF-FAB1B-5-1 VF-Fab3a-1-1 also bound sequence $_{155}$LLNNTRPPRGNWF$_{167}$. The observed binding behavior of these samples opens two possibilities either these Fabs are of polyclonal nature or discontinuous epitopes are recognized.

The heatmap In Figure 6 shows the polyclonal nature of the antibody responses as recorded on Set 1 peptides.

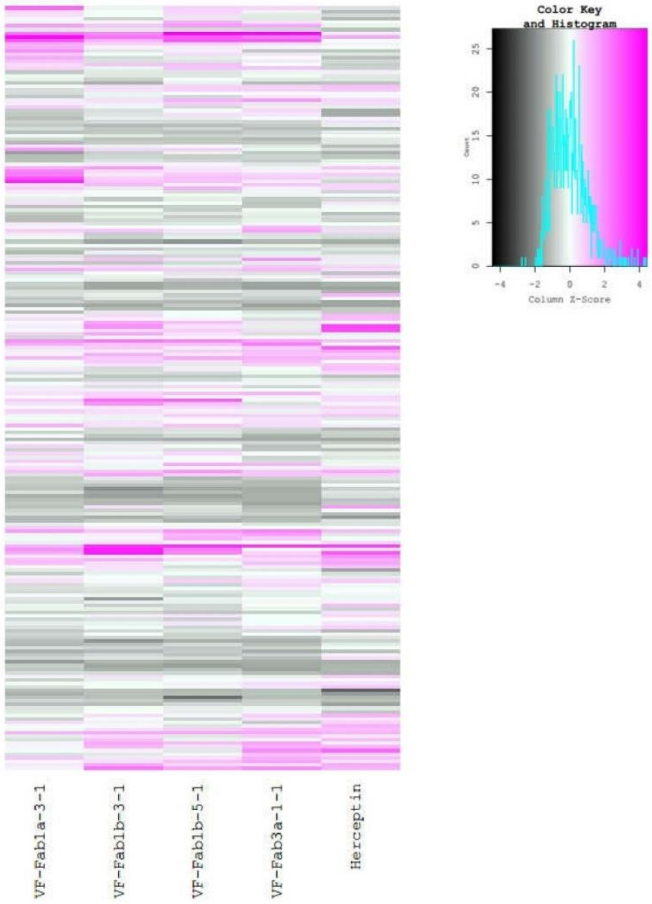

Figure 6. Heatmap representation of Fabs binding profiles recorded on set 1. Signals in each data set were scaled and then color coded (see the color key in the top right corner). In short, high signals are plotted in magenta, background signal is plotted in white.

To illustrate current findings 3D homology modeling was employed and identified binding motifs were highlighted (Figure 7). Dominantly bound sequence $_{10}$SRAAHRVTTFITR$_{22}$ is not modeled and thus cannot be shown.

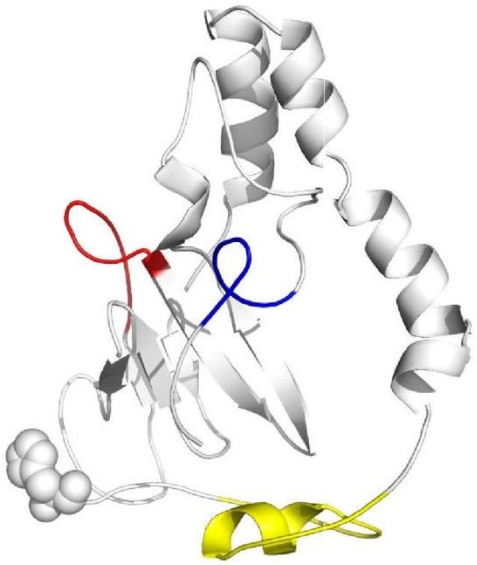

Figure 7. 3D representation of the current findings. The 3D model of HCV-E1E2 glycoprotein (HCVpp1b-1-3) *from Figure 1 is shown in white cartoon with flexible non-modeled VF-Fab3a-1-1-termini labeled with spheres. Sequence* $_{45}$*NCNDSLNTGFLAALFYTHRF*$_{64}$ *is highlighted in yellow,* $_{155}$*LLNNTRPPRGNWF*$_{167}$ *in red and* $_{216}$*SGPWLTPRCM*$_{225}$ *in blue.*

A. Linear Mimics

B.Loop Mimics

C. Helical Mimics

D. Beta turn Mimics

Heat map overview of peptides targeted by VF-Fab

Libraries of peptides beginning at the E2 N-terminus (residue 384-619 of the H77 reference strain AF011751) of the envelope protein were synthesized using chemically linked peptides on scaffolds (CLIPS) technology for conformational epitope mapping (Pepscan Presto; Lelystad, Netherlands).Individual peptides are listed on the right and VF-Fab are indicated at the base of the heatmap. Native Cys were protected by acetamidomethyl in all the libraries (denoted by "2"). The magnitude of colour (dark magenta) with higher z score represents the binding affinity of VF-Fab to the peptide. All the VF-Fabs commonly bound peptides with core sequence $_{393}$SRAAHRVTTFITR$_{405}$ from all the sets. Additional binding was recorded for VF-Fab1a-1-3, VF-Fab1b-1-3 and VF-Fab1b-5-1 on linear peptides with core sequences $_{433}$LNTGFLAALFYTH$_{445}$ and $_{539}$LLNNTRPPRGNWF$_{550}$ respectively. VF-Fab1b-5-1 and VF-Fab31-1-1 similarly bound one β- turn mimic with core sequences $_{428}$NCNDSLNTGFLAALFYTHRF$_{447}$. Linear sequences $_{599}$SGPWLTPRCM$_{608}$, $_{539}$LLNNTRPPRGNWF$_{550}$ were additionally recognized by VF-Fab3a-1-1 (Table 3). Herceptin was used as an internal negative control. In order to make Heatmap legible, only every second peptide in the study has been included in the figure.

A. Linear peptides of 15 residues **B**. loop mimics of constrained peptides of 17 residues. **C**. structured peptides of 23 residues mimic the helical structure **D**. structured peptides of 22 residues mimic the β-turn.

Appendix IV

JOURNAL OF GENERAL VIROLOGY

RESEARCH ARTICLE

Naik *et al.*, *Journal of General Virology* 2017;98:179–189

DOI 10.1099/jgv.0.000659

MICROBIOLOGY SOCIETY

Humoral immune system targets clonotypic antibody-associated hepatitis C virus

Amruta S. Naik,[1] Brendan A. Palmer,[1] Orla Crosbie,[2] Elizabeth Kenny-Walsh[2] and Liam J. Fanning[1,*]

Abstract

Hypervariable region 1 (HVR1) is one of the potential neutralization domains in the E2 glycoprotein of hepatitis C virus (HCV). Point mutations of the HVR1 can lead to humoral immune escape in HCV-infected patients. In this study, we segregated the chronically infected viraemic sera from HCV-infected patients into populations of antibody-free virus and antibody-associated virus (AAV) and mapped potential epitopes within the E1E2 gene junction of AAV sequences (residues 364–430). Furthermore, we generated HCV pseudoparticles (HCVpp) derived from AAV sequences to assess their infectivity. We studied the neutralization potential of virus-free Fab obtained from antibody–virus complexes, in the HCVpp system. We observed selective targeting of clonotypic HCV variants from the quasispecies pool. Moreover, we identified potential neutralizing epitopes within the HVR1 and an additional epitope that overlapped with a broadly neutralizing AP33 epitope (amino acid 412–423 in E2). We observed a marked difference in the infectivity of HCVpp generated using E1E2 sequences isolated from AAV. We document reduction in the infectivity of HCVpp-H77 and HCVpp derived from AAV sequences when challenged with virus-free Fab. Our results provide novel insights into the complexities of engagement between HCV and the humoral immune system.

INTRODUCTION

Globally, approximately 130–150 million people are chronically infected with hepatitis C virus (HCV) [1]. The quasispecies nature of HCV helps the virus to establish persistent infection [2–4]. The current focus in HCV management is to achieve an IFN-free regime. Direct-acting antivirals have emerged as an effective HCV treatment. However, prohibitive costs limit direct-acting antiviral access to discrete patient cohorts with cirrhosis and end-stage liver disease [5]. Vaccination is the most effective means of controlling an infectious disease, yet there is no prophylactic or therapeutic vaccine available to treat HCV [6].

A minority of infected individuals clear HCV infection spontaneously [7]. This requires a rapid, rigorous and multi-specific antiviral response by the host immune system [7]. Numerous studies have shown that broadly specific neutralizing antibodies (nAbs) are elicited early in infection [8–10]. Several experiments using HCV pseudoparticles (HCVpp) and cell-culture-derived HCV (HCVcc) have revealed that point mutations of immune dominant epitopes within viral E2 envelope protein aid humoral immune escape [11]. Hypervariable region 1 (HVR1) is one target of nAbs [2, 7, 12–14]. HVR1 is located in a stretch of 27 residues at the amino-terminus of E2 envelope glycoprotein (comprising amino acids 384–410), and is an immunodominant epitope with multiple linear epitopes [15]. Mutations within HVR1 are associated with humoral immune escape.

Potent and broadly nAbs are widely being considered as a potential therapy to treat viral infections [16–18]. However, over time, immune pressure drives replication of HCV variants to escape targeting by nAbs raised against dominant variants, even in cohorts infected with the same inoculum [13, 19]. Conversely, a note of caution needs to be applied here as cross-reactive nAbs may lead to antibody-dependant enhancement of infection [20]. It has been observed that selection pressure from nAb responses shapes the evolution of viral envelope protein [21–24].

To date, the neutralization potential of anti-HCV antibodies has been assessed in cell culture using HCVpp and HCVcc

Received 26 September 2016; Accepted 12 November 2016

Author affiliations: [1]Department of Medicine, Clinical Sciences Building, University College Cork, Cork, Ireland; [2]Department of Hepatology, Cork University Hospital, Cork, Ireland.

***Correspondence:** Liam J. Fanning, l.fanning@ucc.ie

Keywords: Hepatitis C virus; antibody-associated virus; HVR1.

Abbreviations: AAV, antibody-associated virus; AFV, antibody-free virus; HCV, hepatitis C virus; HCVcc, cell-culture-derived HCV; HCVpp, HCV pseudoparticle; HVR1, hypervariable region 1; nAb, neutralizing antibody; RLU, relative light unit; VF-Fab, virus-free Fab.

The GenBank/EMBL/DDBJ accession numbers for clones generated in this study are KT873141–KT873234 and KU888834–KU888837.

Three supplementary figures are available with the online Supplementary Material.

bearing glycoproteins of prototype laboratory strains. These clonotypic systems lack the diversity of the virus population within the serum [25–28]. In the current study, we fractionated viraemic HCV sera into antibody-associated virus (AAV) and antibody-free virus (AFV) subpopulations to investigate the viral variants targeted by the humoral immune system [29]. The presence of AAV is a key signature of active immune response to the antigenic epitopes. Virus-free Fab (VF-Fab) was obtained from the AAV complexes and used to challenge homologous sera where AAV was not detected. We mapped prospective epitopes within amino acid position 364–430, which includes HVR1 and AP33 epitopes using VF-Fab. Owsianka *et al.* [30] have shown that the mouse mAb AP33 recognizes a broadly neutralizing linear epitope in E2 (412–423) [30].

We generated HCVpp using sequence information from the AAV population. We further assessed the ability of VF-Fab to target viral variants from unrelated patients both in the HCVpp and serum-derived HCV system. Notably, we demonstrate that VF-Fab has distinct binding activity in the context of a homogeneous pseudoparticle system when compared to the complex heterogeneous serum environment. Our results provide an insight into the humoral immune response in chronic HCV infection.

RESULTS

Antibodies from AAV-positive sera capture viral variants from unrelated patients

Viraemic serum samples were obtained from 16 unrelated patients (Table 1). Out of 18 specimens, *n*=3/3 (1a), *n*=5/12 (1b) and *n*=2/3 (3a) genotypes were positive for AAV (Table 1). We further selected these AAV-positive sera for our antibody challenge experiment.

We postulated that antibodies that have targeted discrete viral variants in AAV-positive sera are isolate specific in the context of a complex mix of variants [23, 31–33]. In order to test this hypothesis, we challenged sera identified as negative for detectable AAV (Table 2, Fig. 1a) with total IgG purified from sera, which were classified as AAV positive (referred to as 1°AAV). We discovered the presence of a newly formed AAV (referred to as 2°AAV) in addition to the pre-existing parental 1°AAV (schematic representation in Fig. 1a). We observed that total IgG from 1b-5 targeted a viral variant from 1b-4 [KT873176–77, KT873180–81] and 1b-6 [KT873186, KT873194], total IgG from 1b-10 captured a variant from 1b-7 [KT873195, KT873197–204] and antibodies from 3a-2 were bound to viral variant in 3a-3 [KT873229]. However, we were not able to detect 2°AAV for 1b-8 when mixed with the total IgG from 1b-5. 1°AAV and 2°AAV sequences are unrelated and non-identical (Fig. 1b–d). Similarly, total IgG purified from 1b-4, 1b-6, 1b-7, 1b-8 and 1b-9, which were initially classified as AAV negative, were mixed from these experiments in a cross-panel challenge (e.g. total IgG from 1b-4 were mixed with sera 1b-6, 1b-7, 1b-8 and 1b-9). We observed that total IgG purified from AAV-negative sera did not capture any viral variant.

Separately, our sequence analysis observed that 1b-5 has a 28 amino acid HVR1 domain with an in-frame 3 bp insertion at nucleotide 1492-94 [ref: AF011751] at the 5′ end of E2 (Fig. 1b, Table 2). We observed an atypical 30 amino acid HVR1 sequence in both the 2°AAV and AFV fractions of serum 1b-4 (Fig. 1b, Table 2), as a result of 9 bp in-frame insertion at the 5′ end from nucleotide - 1492-1500 [ref: AF011751]. We also identified a 26 amino acid HVR1 profile from specimen 1b-7 (Fig. 1c) as a consequence of an in-frame deletion at the 5′ end from nucleotide - 1491-93 [ref: AF011751]. The rest of the targeted 2°AAV sequences harboured a classic 27 amino acid HVR1 (Fig. 1d).

Analysis of proteinase-K-treated sera

We obtained virus-free antibody fraction by treating AAV-positive sera with proteinase K. Absence of E1E2-junction-specific PCR product confirmed the virus-free status of the post-proteinase-K-treated samples. We further analysed the products of proteinase-K-treated sera eluted from Ab Spin Trap, LambdaFabSelect and Kappa Select on 4–12 % Bistris gradient gel. Analysis revealed that, in the process of dissociating the antibody–virus complex, the intact antibody was fractionated into several peptides. An intact Fab fragment was identified at ~50 kDa (Figs 2 and S1, available in the online Supplementary Material) from all three fractionation procedures, hence, VF-Fab (Ab Spin Trap), λ-VF-Fab (LambdaFabSelect) and κ-VF-Fab (KappaSelect). It has been previously shown that the CH1 domain of the Fab arm has a binding site for streptococcal protein G [34]. This is a likely explanation as to how we obtained VF-Fab from proteinase-K-treated AAV-positive serum samples.

Patient-derived VF-Fab selectively targets homologous genotypes

We used Fab fragments obtained from three different columns to challenge the AAV-negative sera. We observed that VF-Fabs were able to capture viral variants (2°AAV) in all instances in comparison to λ-VF-Fab and κ-VF-Fab (Table 2). Clonal analysis of 2°AAV variants revealed that 2°AAV variants were clonotypic in nature. Both intact mAb AP33 and proteinase-K-treated AP33 retained identical viral variants from 1b-9 and 3a-3 only (Table 2). The AAV fraction obtained from AP33-challenged 1b-9 and 3a-3 sera yielded a homogenous virus population of [KT873217] and [KT873229], respectively. Significantly, this mirrors the viral variants captured by VF-Fab1b-2 and VF-Fab3a-2.

Both VF-Fab and λ-VF-Fab derived from respective homologous genotypes captured identical viral variants from 1b-4, 1b-7 and 3a-3 forming a 2°AAV (Table 2). κ-VF-Fab did not capture viral variant from any of the challenge sera.

Source of VF-Fab does not affect the selective binding to viral variants

VF-Fab1b-2 was obtained from a serum that belongs to an anti-D cohort [35]. Patients in an anti-D cohort were iatrogenically infected with the same source of HCV genotype 1b [35]. Three of four HCV 1b sera which were challenged with

Table 1. Sample characteristics used in the current study

Genotype	No. of samples	1°AAV	Sample identifier*	Accession no. AFV†	Accession no. 1°AAV‡
1a	3	+	1a-1	KT873141	KT873142
		+	1a-2	KT873143	KT873144
		+	1a-3	KT873145	KT873146
1b	12	–	1b-1–1§, ‖	KT873147–57	–
		+	1b-1–2§, ‖	KT873158	KT873159
		+	1b-1–3§, ‖	KT873160	KT873161
		+	1b-2§	KT873162	KT873163
		–	1b-3	KT873164–71	–
		–	1b-4§	KT873173–81	–
		+	1b-5	KT873182	KT873183
		–	1b-6§	KT873184–94	–
		–	1b-7§	KT873195–04	–
		–	1b-8§	KT873205–11	–
		–	1b-9§	KT873212–17	–
		+	1b-10§	KT873218	KT873219
3a	3	+	3a-1	KT873220	KT873221
		+	3a-2	KT873234	KT873233
		–	3a-3	KT873222–32	–

+, Detectable AAV by reverse transcription PCR (RT-PCR); –, no detectable levels of AAV by RT-PCR.

*Genotype/subtype patient identifier.

†Samples positive for 1°AAV; both AFV and 1° AAV sequences were analysed by direct sequencing only.

‡Samples without accession numbers had no detectable levels of AAV.

§Source of infection: contaminated anti-D immunoglobulin [35].

‖Obtained from the same patient at three different time points (2002, 2013 and 2014, respectively). Genotype/subtype patient identifier-sample number.

VF-Fab1b-2 were from an anti-D cohort (1b-1-1, 1b-8 and 1b-9) (Table 2). However, viral variants from only two of viraemic sera (1b-1-1, 1b-9) were captured by the VF-Fab1b-2. Interestingly, the serum sample from which the VF-Fab1b-5 was obtained does not belong to an anti-D cohort yet successfully retained virus from anti-D sera 1b-4, 1b-6 and 1b-8. On the other hand, 1b-7 was targeted by VF-Fab1b-10 obtained from another anti-D serum. Of note, no shared reactivity with respect to capture viral variants (2°AAV) for VF-Fab1b-5 or VF-Fab1b-10 was observed.

Potential epitopes targeted by VF-Fab1b-5 and VF-Fab1b-10

Based on previous research by Guan *et al.* [4], we explored the 364–430 region for probable epitopes targeted by the humoral immune system [4]. Five different potential binding motifs were observed for included sequences. All the peptides in this study were designed as 15 mer with overlapping 14 mer peptides. The candidate epitopes are proposed by subtracting positive peptides and by aligning them to extract overlapping residues. VF-Fab1b-5 targeted a motif that shares amino acid residues 412, 413 and 415–423 with the AP33 epitope (QLINTNGSWHIN) in the 1°AAV fraction of 1b-5 and the 2°AAV fraction of 1b-8 (Table 3) [30]. VF-Fab1b-10 targeted a motif within the HVR1 domain of the 2°AAV fraction of 1b-4 [KU888835] and 1b-8 [KU888836] and the 1°AAV fraction of 1b-5 [KU888834]; it is the same antigenic domain targeted by mAb 3 C7 and 9/27 (396–407) (reviewed by Helle *et al.* [36]) (Table 3). Heatmap representation of scaled and centred data for each peptide recorded from both VF-Fabs is shown in Figs 3 and S3.

VF-Fab1b-5 efficiently neutralizes HCVpp-H77 and HCVpp1b-4

We generated five pseudotyped HCV particles. HCVpp-H77 was used as a reference clone. However, not all the expressed clones were infectious in Huh7 (Fig. 4a). Out of four AAV-E1E2 pseudotyped viruses, HCVpp1b-4 was infectious, yielding a 10-fold greater relative luminescence value [relative light unit (RLU)] than no envelope control.

We observed that VF-Fab1b-5 at a concentration of 0.167 mg ml^{-1} was highly neutralizing, reducing the HCVpp-H77 infection by 85 % (Fig. 4b). On the other hand, VF-Fab1b-10 reduced HCVpp-H77 infection by 75 % at 0.400 mg ml^{-1} (Fig. 4b). We used the highest neutralizing concentration of VF-Fab1b-5 and VF-Fab1b-10 in the neutralization assay for HCVpp1b-4. VF-Fab1b-5 reduced HCVpp1b-4 infection by 88 % at 0.167 mg ml^{-1} (Fig. 4c). VF-Fab1b-10 showed 72 % of inhibition of infection of HCVpp1b-4 at 0.400 mg ml^{-1} (Fig. 4c). In both neutralization assays, we found VF-Fab1b-5 to be highly neutralizing.

Table 2. Antibody challenge of serum samples without detectable AAV following initial fractionation

AAV-negative sera*	1°AAV-positive sera	Antibody challenge†						Unique HVR1‡	Accession nos. of 2°AAV
		Untreated		Proteinase-K-treated					
		Total IgG	AP33	VF-Fab	λ-VF-Fab	κ-VF-Fab	AP33		
1b-1–1§	1b-2§	–	ND	+	–	ND	ND	1	KT873154–57
1b-3§	1b-2§	ND	ND	+	ND	ND	ND	1	KT873166, KT873170–71
1b-4	1b-5	+	–	+	+	–	–	1	KT873176–77, KT873180–81
	1b-10	–	–	–	–	–	–	–	–
1b-6	1b-5	+	–	+	–	–	–	1	KT873186, KT873194
	1b-10	–	–	–	–	–	–	–	–
1b-7	1b-5	–	–	–	–	–	–	–	–
	1b-10	+	–	+	+	–	–	1	KT873195, KT873197–204
1b-8	1b-5	+	–	+	–	–	–	1	KT873205–11
	1b-10	–	–	–	–	–	–	–	–
1b-9§	1b-2§	+	+	+	–	ND	+	1	KT873216–17
3a-3	3a-2	+	+	+	+	–	+	1	KT873229

ND, Not done.

*Patient sera without detectable AAV following initial fractionation were subsequently challenged with genotype/subgenotype-matched 1°AAV-positive sera (as per Table 1).

†Individual antibody preparations originating from 1°AAV-positive serum or AP33 are described in Methods.

‡Cumulative number of unique HVR1 amino acid sequences identified in 2°AAV-positive samples.

§Insufficient amounts of AAV-negative sera and/or 1°AAV-positive sera limited the number of possible experimental combinations.

DISCUSSION

This is the first successful attempt to capture inter-patient viral variants from viraemic HCV sera using antibodies from homologous AAV-positive sera. It has been shown in HCVpp and HCVcc *in vitro* infection systems that antibodies obtained from patient sera are broadly reactive (reviewed in Ball *et al.* [37]). However, in our experiments, we observed that in the complex serum environment, antibodies target unique viral variants (from the quasispecies pool) from unrelated patient sera. We made similar observations for VF-Fab. From our results, we were unable to determine whether (i) the antibodies that targeted 1°AAV are the same antibodies that targeted 2°AAV and/or (ii) the antibodies were not saturated with antigen/virus. Additionally, we have shown that total IgG purified from AAV-negative sera were not capable of capturing viral variants from other AAV-negative sera. In this context, absence of AAV might represent a period when antibody-sensitive viral variants were removed (from a quasispecies pool), leaving behind the humoral immune escape mutants. Nonetheless, we acknowledge that these AAV-negative sera might have nAbs against previously culled viral variants. Analysis of the relative distribution of 2°AAV (Fig. S2) suggests that the viral variant targeted by VF-Fab need not dominate the heterogeneous virus population. Immunogenicity, accessibility and antibody–epitope binding kinetics might play a crucial role in selecting the clonotypic population out of the diverse mixture of variants in patient sera.

Extra-long HVR1 is a feature of the biology of HCV [23, 29, 38]. Guan *et al.* [4] in their experiments have shown that the first 13 amino acids do not affect infectivity in the HCVpp system. We are the first to report the capture of a non-classic 30 amino acid HVR1 (from sample 1b-4, Fig. 1b) using VF-Fab1b-5 from an unrelated sample. This latter variant harboured a non-classical 28 amino acid HVR1 (sample 1b-5, Fig. 1b). Our data indicate that this three amino acid insertion at the N-terminus of HVR1 did not interfere with the binding capacity of the aforementioned VF-Fab from sample 1b-5. This is likely because nAbs target the C-terminus of HVR1, and hence, deletion or insertion at the N-terminus doesn't affect this phenomenon [39].

In this study, we used human anti-HCV VF-Fabs for epitope mapping of viral sequences that were previously targeted by host humoral immune system. Our epitope mapping data showed that VF-Fab1b-5-targeted motifs in the 1°AAV fraction of 1b-5 [KU888834] and the 2°AAV fraction of 1b-8 [KU888836] overlap with the well-characterized AP33 epitope. It has been shown that the linear AP33 epitope is highly conserved across different HCV genotypes and is broadly neutralizing [30]. Importantly, mAb AP33 (either intact or proteinase-K-treated) was able to retain epitope-positive viral variant(s) from only 1b-9 and 3a-3 (Table 2). Deng *et al.* [40] in their research found no detectable antibody response to a peptide (PUHI 19) harbouring AP33 epitope (409–423), suggesting weak immunogenicity of the epitope, which might explain selective targeting of AP33-epitope-positive variants in our antibody-serum binding experiments [40].

Studies have shown that HCVpp and HCVcc lacking HVR1 are sensitive to neutralization by patient-derived

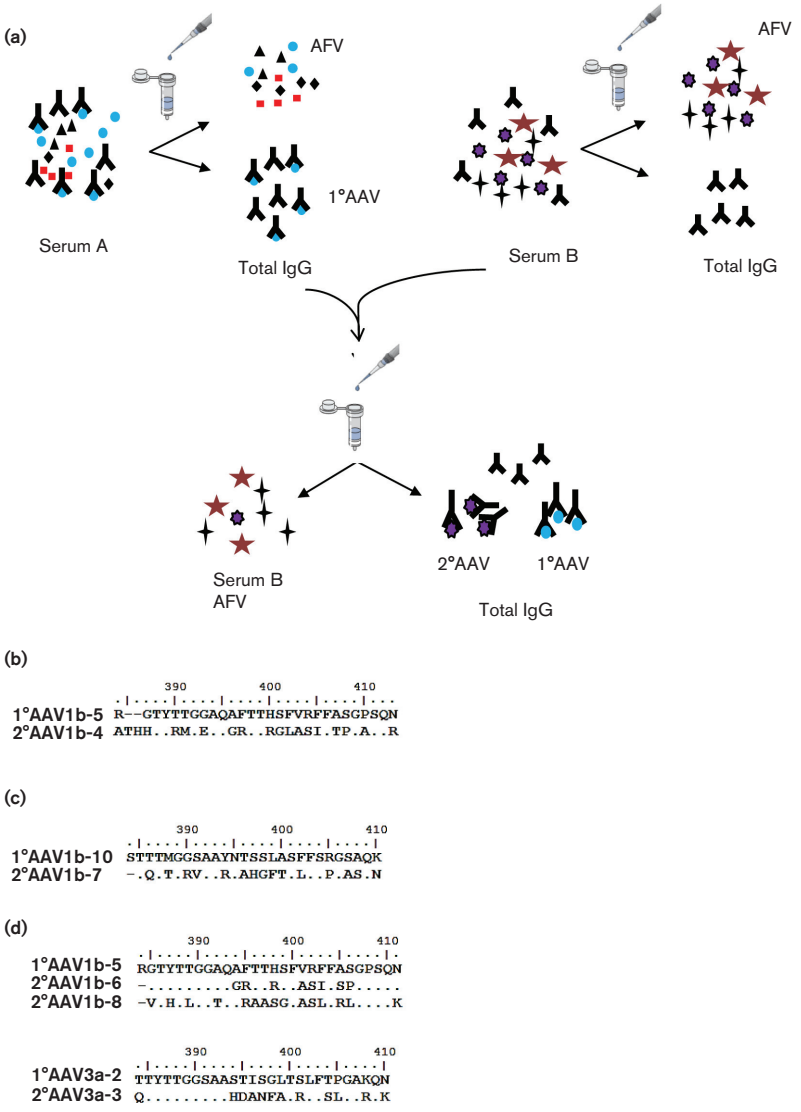

Fig. 1. 1°AAV (parental) is non-identical with 2°AAV (newly formed). (a) Schematic diagram of column-based separation of unbound AFV and 1°AAV fraction as described in Methods. Different coloured shapes represent the quasispecies nature of HCV. Total IgG from 1°AAV-positive sample (Serum A) were used to challenge an unrelated serum sample (Serum B) that had previously been classified as AAV negative. The output of this challenge was capture of a newly formed viral variant 2°AAV additional to the pre-existing parental 1°AAV. (b) 1°AAV sequence from 1b-5 has a 28 amino acid HVR1. Total IgG 1b-5 captured a 2°AAV [KT873177] from 1b-4, which harbours a non-classical 30 amino acid HVR1 [ref: AF011751]. HVR1 domain is marked by a black arrow on the top of the sequences. (c) 2°AAV [KT873195] from 1b-7 harbours a non-classical 26 amino acid HVR1 that was captured by total IgG from 1b-10. (d) Total IgG from 1b-5 captured two more viral variants (2°AAV) from unrelated sera that harboured a classical 27 amino acid HVR1 profile. Similar observations were made for total IgG from 3a-2, which captured a viral variant from serum 3a-3. Sequence analysis of 1°AAV with 2°AAV complex revealed to be non-identical.

antibodies, which again indicates an important role of HVR1 in overall viral fitness [41–43]. We observed fewer changes outside the HVR1 in all the isolates. VF-Fab1b-10 targeted a motif within HVR1 of the 2°AAV fraction of 1b-4 and 1b-8 and in the 1°AAV fraction of 1b-5 upon epitope mapping (Table 3, Fig. 3). Notably, these results suggest the existence of an immunodominant epitope on the C-terminal region of HVR1 recognized by patient-derived VF-Fabs. Our data are in strong agreement with that of previously published data, supporting that HVR1 is one of the potential antigenic epitopes under immune selection pressure [24, 32, 36, 44, 45].

In our study, we observed that both VF-Fab1b-5 and VF-Fab1b-10 neutralize HCVpp with different efficiencies, VF-Fab1b-5 being highly neutralizing (Fig. 4b, c). A likely explanation of the neutralizing activity of VF-Fab1b-5 is that it targeted a highly neutralizing epitope and captured

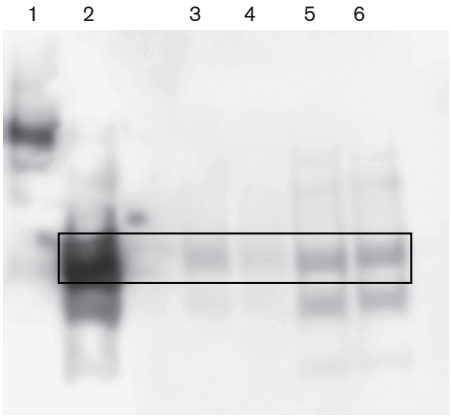

Fig. 2. Analysis of proteinase-K-treated serum samples. Products of post-proteinase-K-treated samples eluted on LambdaFabSelect (λ-Fab), KappaSelect (κ-Fab) and Ab Spin Trap (VF-Fab) were analysed on 4–12 % Bistris gradient gel under a non-reducing condition. Elutes were transferred onto nitrocellulose membrane. The blot was developed using HRP-labelled mouse anti-human IgG Fab antibody (Biorbyt). We identified intact Fab fragment post-proteinase K treatment (black box). 1, Control IgG [human plasma CTM (—)C, Roche Molecular Systems]; 2, natural human IgG Fab fragment protein (ab90352); 3, λ-VF-Fab; 4, κ-VF-Fab; 5, VF-Fab1b-5; 6, VF-Fab1b-10.

viral variants in all the antibody challenge experiments, when compared to VF-Fab1b-10 (Table 2). However, nAbs against HVR1 are mostly strain-specific and of limited cross-reactivity; hence, VF-Fab1b-10 is the lesser neutralizing between the two VF-Fabs (reviewed previously [36, 37]). A well-known caveat that needs to be appreciated when studying neutralization potential is that the pseudoparticle system provides a homogenous population of E1E2 glycoprotein, as compared to the complex heterogeneity and density of native glycoprotein in HCV virions.

It should be noted that both VF-Fab1b-5 and VF-Fab1b-10 were not able to recognize any epitope in the 2°AAV fraction of 1b-7 and the 1°AAV fraction of 1b-10. This may indicate a possible conformational or discontinuous epitope outside the HVR1, which is not included in our study. Our total IgG and VF-Fab binding studies strongly suggest that nAb responses are clonotypic in nature. However, this statement must be qualified by the fact that we have only examined AAV in the context of eight samples.

Table 3. Binding motifs targeted by VF-Fab

VF-Fab	Target sequence [accession nos.]	Putative epitope
VF-Fab1b-5	1b-5 [KU888834]	$_{410}$NIQLVNTNGSWHINR$_{424}$
	1b-8 [KU888836]	$_{410}$KIQLVNTNGSWHINR$_{424}$
VF-Fab1b-10	1b-4 [KU888835]	$_{388}$MGEAQGRTTRGLA$_{400}$
	1b-5 [KU888834]	$_{398}$GFASLFRLGPSQ$_{409}$
	1b-8 [KU888836]	$_{397}$HSFVRFFASGPSQ$_{410}$

In conclusion, we show differential binding behaviour of patient-derived anti-HCV antibodies, VF-Fab and mAb AP33 targeting clonotypic populations in unrelated viraemic sera. We have identified two epitopes that are subjected to humoral immune attack *in vivo*. Importantly, our data add new information on the *in vivo* humoral immune response to chronic HCV infection.

METHODS

Serum

This study was approved by the Clinical Research Ethics Committee of the Cork Teaching Hospitals, and written consent from patients was obtained. A panel of viraemic sera positive for HCV genotypes 1a (n=3), 1b (n=12) and 3a (n=3) was randomly selected (Table 1). Ten out of 12 1b serum samples belonged to a cohort of Irish women infected with a single source of HCV genotype 1b via contaminated anti-D immunoglobulin [35]. Patient 1b-1 was the only patient whose serum samples were obtained at three different time intervals (Table 1). The VERSANT HCV Genotype Assay was used to confirm the HCV genotype.

Nucleic acid extraction and E1E2 gene junction amplification

HCV RNA was extracted with QIAamp Viral RNA mini kit where applicable (Qiagen). The E1E2 gene junction (318 bp) of HCV was amplified as previously described [29]. All PCRs were carried out using Pfu DNA polymerase (Thermo Scientific) to guard against unequal template selection due to the quasispecies nature of the virus [46].

Fractionation of serum samples into AFV and AAV

The Ab Spin Trap columns were used to separate the samples into (i) AFV and (ii) AAV populations following the manufacturer's protocol with a few modifications (GE Healthcare Life Sciences). The protein G columns were used to purify total IgG from serum or plasma. Briefly, 200 µl of patient sera was applied to the column followed by incubation for 15 min at room temperature with end-over-end mixing. The first flow-through (W0) was retained as the AFV fraction. Eight washes (W1–W8) of 300 µl binding buffer were applied to the column, while the last wash (W8) was tested by PCR amplicon analysis to confirm the absence of HCV virions. The column was then incubated for 5 min with 200 µl elution buffer with end-over-end mixing. The elute is now identified as total IgG. Total IgG contains AAV (HCV targeted by antibodies), along with free antibodies bound by the column.

Dissociation of antibody–virion complexes and collection of VF-Fab, λ-VF-Fab and κ-VF-Fab

Proteinase K was used to dissociate the antibodies from the antibody–virion complex. This was achieved by adding 1 : 1 (v/v) of proteinase K (5 mg ml^{-1}) to AAV-positive sera. The Ab Spin Trap protocol was followed post-proteinase K treatment. We analysed the functional component in post-proteinase-K-treated samples using HiTrap LambdaFabSelect

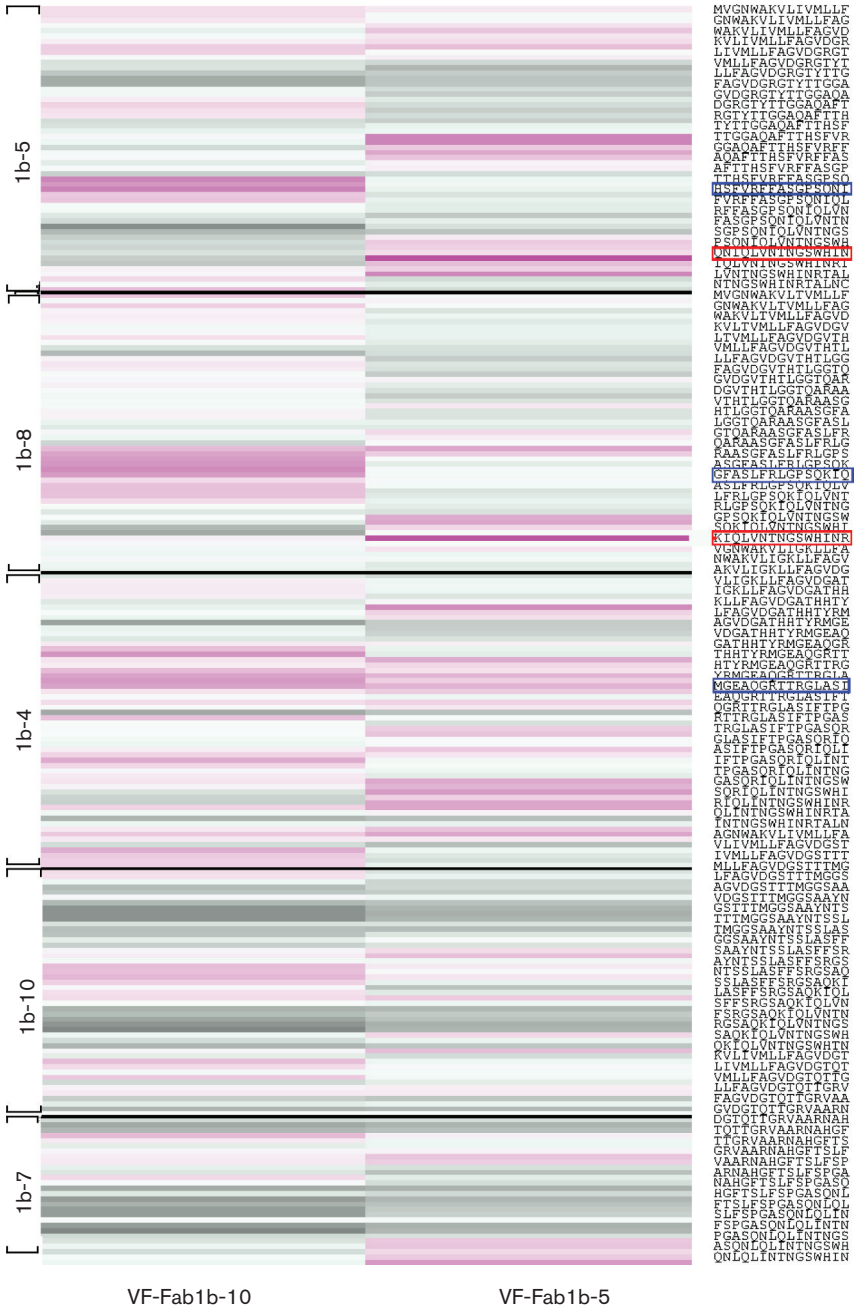

Fig. 3. Heatmap overview of binding motifs targeted by VF-Fab1b-5 and VF-Fab1b-10. 1°AAV fractions of 1b-5 and 1b-10 and 2°AAV fractions of 1b-4, 1b-7 and 1b-8 were assessed for epitope mapping with VF-Fab1b-5 and VF-Fab1b-10 from amino acid 364–430 including the HVR1 in E2. Individual peptides are listed on the right-hand side, and VF-Fab is indicated at the base of the heatmap. Black horizontal lines show the start position of a new target sequence in that particular set of peptides. Target sequences are flanked by black brackets on the left. The magnitude of colour (dark magenta) with higher *z* score represents the binding affinity of Fab to the peptide. The sequence in a red box (on the right) represents a motif targeted by VF-Fab1b-5. The sequence in a blue box (on the right) represents a motif targeted by VF-Fab1b-10. In order to make the heatmap legible, only every second peptide in the study has been included in the figure.

and KappaSelect pre-packed columns (GE Healthcare Life Sciences). These columns have a ligand that binds to the constant region of lambda or the kappa light chain of human IgG, respectively. Briefly, 1 ml proteinase-K-treated serum samples were passed through both the columns as per the manufacturer's protocol. Columns were washed to remove unbound material with 5 vols binding buffer (PBS, pH 7.4). Fab fragments were eluted with 0.5 ml elution

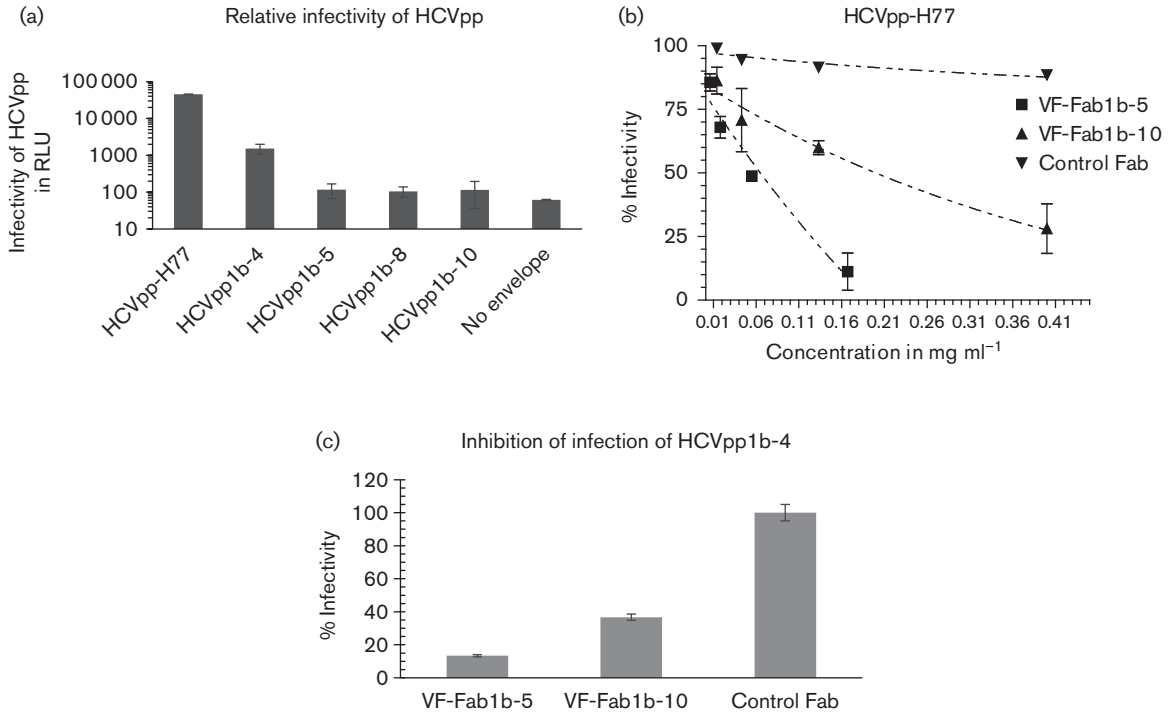

Fig. 4. Infectivity and neutralization of AAV HCVpp. (a) From a panel of 1°AAV and 2°AAV E1E2, only 2°AAV 1b-4 was found to be infectious. phCMV-ΔC/E1/E2 H77 was used as a reference clone. No envelope control HCVpp reproducibly gave RLU values less than 100; therefore, a cut-off of 1000 RLUs was used to determine the infectivity of a clone. The x-axis depicts HCVpp clones in this study. The y-axis denotes percentage of infectivity. (b) Neutralization curve for HCVpp-H77 shows 0.167 and 0.400 mg ml^{-1} as the most effective concentrations to inhibit the HCVpp infection for VF-Fab1b-5 and VF-Fab1b-10 by 85 and 75 %, respectively. (c) VF-Fab1b-5 at 0.167 mg ml^{-1} inhibits 88 % of HCVpp1b-4 infection, whereas VF-Fab1b-10 at 0.400 mg ml^{-1} inhibits only 72 % of infection. Each experiment was repeated three times with two technical replicates.

buffer (0.1 M glycine buffer, pH 2.5, for KappaSelect, 0.1 M acetate buffer, pH 3.5, for LambdaFabSelect). The eluted fractions were concentrated by an Amicon Ultra-0.5 centrifugal unit with Ultracel 50 (Millipore). Confirmation of the virus-free status of this proteinase-K-treated preparation was determined by the absence of an E1E2-specific amplification following reverse transcription PCR (RT-PCR). Furthermore, elutes obtained post-proteinase K treatment from Ab Spin Trap (VF-Fab), LambdaFabSelect (λ-VF-Fab) and KappaSelect (κ-VF-Fab) were analysed by Western blotting. Elutes, natural human IgG Fab fragment protein (ab90352, Abcam) and control IgG obtained from human plasma CTM (−)C (Roche Molecular Systems), were blotted on a nitrocellulose membrane. The samples were then incubated with HRP-labelled mouse anti-human IgG Fab antibody (Biorbyt) at 1 : 10 000 concentration in 0.05 % (v/v) PBS Tween-20.

Antibody-sera (non-detectable AAV) challenge

Total IgG that contains AAV (hereafter referred to as 1°AAV) along with free antibodies, VF-Fab, λ-VF-Fab and κ-VF-Fab, were used to challenge the AAV-negative sera in 1 : 5 ratios (Table 2). This mixture was then incubated at 37 °C for 2 h. AP33 is a mouse mAb that targets the partially confirmation-dependent epitope within amino acid residues 412–423 (a kind gift from Dr Arvind Patel, University of Glasgow, UK). Simultaneously, we challenged the sera (Table 2) with both intact AP33 and Ab-Spin-Trap-eluted post-proteinase-K-treated AP33 (25 μg ml^{-1}). The Ab Spin Trap protocol was followed, and the challenged samples were tested for the presence of a newly formed 2°AAV by PCR.

Molecular cloning and sequencing analysis

The AFV and 1°AAV fractions obtained on initial analysis of sera were analysed by direct sequencing only. cDNA obtained from 1°AAV and 2°AAV was diluted 1 : 100 to ensure that there was no template resampling. AFV and 2°AAV amplicon obtained from total IgG, VF-Fab and AP33 antibody (Table 2) were cloned into pJET1.2/blunt cloning vector (Thermo Scientific). Ten colonies each for AFV and three colonies each for 2°AAV fractions were analysed for sequencing (MWG Operon).

Epitope mapping

Linear peptides were synthesized for 1°AAV 1b-5 [KU888834] and 1b-10 [KT873219] and 2°AAV 1b-4 [KU888835], 1b-7 [KT873204] and 1b-8 [KU888836] covering amino acid region 364–430 in the E1E2 glycoprotein [ref:

AF011751] to study the epitopes targeted by the host immune system. (For 1b-7 [KT873204] and 1b-10 [KT873219], since we did not have full-length sequences at the time, peptides were designed for region 364–423.)

Two sets (hence, set 1 and set 2) of overlapping peptides of 15 amino acid lengths with an overlap of 14 were synthesized for these sequences. Set 2 comprised linear peptides of 15 amino acid length; however, amino acids at positions 10 and 11 were replaced by Ala. When a native Ala would occur on either position, it was replaced by Gly. Control peptides unrelated to our test sequences that are propriety of Pepscan were designed based on epitopes of monoclonal antibodies 57.9 and 3C9 [47]. The binding of VF-Fab1b-5 and VF-Fab1b-10 to peptides was assessed in a Pepscan-based ELISA as described below (Pepscan Presto) [48]. Each well in the card contained covalently linked peptides that were incubated overnight at 4 °C with VF-Fab1b-5 and VF-Fab1b-10, between 0.1 and 10 % Pepscan buffer and preconditioning blocking buffer (SQ) (a mixture of horse serum, Tween 80 and ovalbumin in PBS). After washing, the plates were incubated with goat anti-human HRP conjugate (1 : 1000, Southern Biotech 2010–05) for 1 h at 25 °C. After further washing, peroxidase activity was assessed using substrate 2,2′-azino-di-3-ethyl-benzthiazolinesulfonate and 20 µl ml^{-1} of 3 % H_2O_2. The colour development was quantified after 60 min using a charge-coupled device camera and an image-processing system.

Production of infectious HCVpp

Full-length E1E2 glycoprotein sequences 1b-5 [KU888834] and 1b-10 [KU888837] positive for 1°AAV on initial serum analysis and 1b-4 [KU888835] and 1b-8 [KU888836] targeted by VF-Fab1b-5 and VF-Fab1b-10 forming 2°AAV (Table 2), respectively, were cloned in pcDNA3.1V5his D-TOPO expression vector (Life Technologies) as previously described [28]. HCVpp were generated according to the protocol of Bartosch *et al.* [25]. Briefly, HEK-293T cells were co-transfected with plasmids expressing the HCV E1E2 glycoproteins, the murine leukaemia virus Gag-Pol packaging vector (Inserm Transfert) and a transfer construct with luciferase reporter gene (a gift from Dr Arvind Patel, University of Glasgow, UK). Pseudoparticles generated without E1E2 glycoprotein (no envelope) were used as a negative control. phCMV-ΔC/E1/E2 H77 clone was used as a positive control (Inserm Transfert). Infectivity of the HCVpp was tested as previously described [25, 28]. To characterize the capacity of our VF-Fab to recognize different isolates, E1E2 glycoproteins from the clarified lysates of transfected HEK 293T cells were captured onto GNA (*Galanthus nivalis*) lectin (Sigma Aldrich)-coated microtitre plates and then detected by the anti-E2 mouse mAb AP33 and VF-Fab1b-5, VF-Fab1b-10 and control Fab [human plasma CTM (−)C, Roche Molecular Systems].

Neutralization of HCVpp infection in Huh7 cells

Neutralization was tested only for those HCVpp with infectivity at least 10 times greater than mock pseudoparticle (no envelope) values. Huh7 cells were cultured in 24 well plates at 2.5×10^4 cells density for 2°AAV HCVpp1b-4 and 4×10^3 cells in 96 well plates for HCVpp-H77. HCVpp-H77 were mixed with VF-Fab1b-5, VF-Fab1b-10 and control Fab [human plasma CTM (−)C, Roche Molecular Systems], at concentrations from 0.015 to 0.400 mg ml^{-1} to estimate the highest neutralization working concentration. HCVpp1b-4 were mixed with VF-Fab1b-5 (0.167 mg ml^{-1}), VF-Fab1b-10 (0.400 mg ml^{-1}) and control Fab (0.400 mg ml^{-1}) and incubated for 1 h at 37 °C. The mixture was added to the Huh7 cells and was incubated for 4 h at 37 °C. Inoculum was removed and replaced with fresh media and incubated at 37 °C for 72 h. After 72 h, media was removed from the cells, and 50 µl Cell Culture Lysis Reagent (Promega) for 96 well plate and 100 µl for 24 well plate were added and left to incubate for >15 min. The lysate was then transferred to a white low-luminescence 96 well plate, and luciferase activity was measured in RLUs in a GloMax. The percentage of neutralization was calculated as 100 %×[1−(HCVppRLUtest/HCVppRLUcontrol)]. Each sample was tested in duplicate following three independent experiments.

Funding information
A. N.'s work was funded by Molecular Medicine Ireland as part of the Clinical and Translational Research Programme.

Acknowledgements
We would like to thank Dr Arvind Patel and Dr Ania Owsianka of CVR, University of Glasgow, UK for training to generate HCV pseudoparticles and critical reviewing of the manuscript. We would also like to thank John Levis and Dr Kevin Hegarty of Molecular Virology Diagnostic and Research Laboratory, Cork University Hospital, University College Cork, Cork, Ireland for initial characterization of patient sera.

Conflicts of interest
The authors declare that there are no conflicts of interest.

References

1. Wong JA, Bhat R, Hockman D, Logan M, Chen C *et al.* Recombinant hepatitis C virus envelope glycoprotein vaccine elicits antibodies targeting multiple epitopes on the envelope glycoproteins associated with broad cross-neutralization. *J Virol* 2014;88:14278–14288.
2. Allain JP, Dong Y, Vandamme AM, Moulton V, Salemi M. Evolutionary rate and genetic drift of hepatitis C virus are not correlated with the host immune response: studies of infected donor-recipient clusters. *J Virol* 2000;74:2541–2549.
3. Farci P, Shimoda A, Coiana A, Diaz G, Peddis G *et al.* The outcome of acute hepatitis C predicted by the evolution of the viral quasispecies. *Science* 2000;288:339–344.
4. Guan M, Wang W, Liu X, Tong Y, Liu Y *et al.* Three different functional microdomains in the hepatitis C virus hypervariable region 1 (HVR1) mediate entry and immune evasion. *J Biol Chem* 2012;287:35631–35645.
5. Chhatwal J, Kanwal F, Roberts MS, Dunn MA. Cost-effectiveness and budget impact of hepatitis C virus treatment with sofosbuvir and ledipasvir in the United States. *Ann Intern Med* 2015;162:397–406.
6. Drummer HE. Challenges to the development of vaccines to hepatitis C virus that elicit neutralizing antibodies. *Front Microbiol* 2014;5:329.
7. Zeisel MB, Baumert TF. HCV entry and neutralizing antibodies: lessons from viral variants. *Future Microbiol* 2009;4:511–517.
8. Bailey JR, Wasilewski LN, Snider AE, El-Diwany R, Osburn WO *et al.* Naturally selected hepatitis C virus polymorphisms confer

broad neutralizing antibody resistance. *J Clin Invest* 2015;125: 437–447.

9. **Pestka JM, Zeisel MB, Bläser E, Schürmann P, Bartosch B *et al.*** Rapid induction of virus-neutralizing antibodies and viral clearance in a single-source outbreak of hepatitis C. *Proc Natl Acad Sci USA* 2007;104:6025–6030.
10. **Thimme R, Oldach D, Chang KM, Steiger C, Ray SC *et al.*** Determinants of viral clearance and persistence during acute hepatitis C virus infection. *J Exp Med* 2001;194:1395–1406.
11. **Thimme R, Lohmann V, Weber F.** A target on the move: innate and adaptive immune escape strategies of hepatitis C virus. *Antiviral Res* 2006;69:129–141.
12. **Lavie M, Goffard A, Dubuisson J.** HCV glycoproteins: assembly of a functional E1–E2 heterodimer. In: Tan SL (editor). *Hepatitis C Viruses: Genomes and Molecular Biology*. Norfolk, UK: Horizon Bioscience; 2006.
13. **Ray R, Meyer K, Banerjee A, Basu A, Coates S *et al.*** Characterization of antibodies induced by vaccination with hepatitis C virus envelope glycoproteins. *J Infect Dis* 2010;202:862–866.
14. **Vieyres G, Dubuisson J, Patel AH.** Characterization of antibody-mediated neutralization directed against the hypervariable region 1 of hepatitis C virus E2 glycoprotein. *J Gen Virol* 2011;92:494–506.
15. **Law M, Maruyama T, Lewis J, Giang E, Tarr AW *et al.*** Broadly neutralizing antibodies protect against hepatitis C virus quasispecies challenge. *Nat Med* 2008;14:25–27.
16. **Doria-Rose NA, Schramm CA, Gorman J, Moore PL, Bhiman JN *et al.*** Developmental pathway for potent V1V2-directed HIV-neutralizing antibodies. *Nature* 2014;509:55–62.
17. **Qiu X, Wong G, Audet J, Bello A, Fernando L *et al.*** Reversion of advanced Ebola virus disease in nonhuman primates with ZMapp. *Nature* 2014;514:47–53.
18. **Stiegler G, Katinger H.** Therapeutic potential of neutralizing antibodies in the treatment of HIV-1 infection. *J Antimicrob Chemother* 2003;51:757–759.
19. **Ray SC, Fanning L, Wang XH, Netski DM, Kenny-Walsh E *et al.*** Divergent and convergent evolution after a common-source outbreak of hepatitis C virus. *J Exp Med* 2005;201:1753–1759.
20. **Dejnirattisai W, Supasa P, Wongwiwat W, Rouvinski A, Barba-Spaeth G *et al.*** Dengue virus sero-cross-reactivity drives antibody-dependent enhancement of infection with zika virus. *Nat Immunol* 2016;17:1102–1108.
21. **Basavapathruni A, Yeh WW, Coffey RT, Whitney JB, Hraber PT *et al.*** Envelope vaccination shapes viral envelope evolution following simian immunodeficiency virus infection in rhesus monkeys. *J Virol* 2010;84:953–963.
22. **Dowd KA, Netski DM, Wang XH, Cox AL, Ray SC.** Selection pressure from neutralizing antibodies drives sequence evolution during acute infection with hepatitis C virus. *Gastroenterology* 2009; 136:2377–2386.
23. **Palmer BA, Moreau I, Levis J, Harty C, Crosbie O *et al.*** Insertion and recombination events at hypervariable region 1 over 9.6 years of hepatitis C virus chronic infection. *J Gen Virol* 2012;93: 2614–2624.
24. **Palmer BA, Schmidt-Martin D, Dimitrova Z, Skums P, Crosbie O *et al.*** Network analysis of the chronic Hepatitis C virome defines HVR1 evolutionary phenotypes in the context of humoral immune responses. *J Virol* 2015;90:3318–3329.
25. **Bartosch B, Dubuisson J, Cosset FL.** Infectious hepatitis C virus pseudo-particles containing functional E1–E2 envelope protein complexes. *J Exp Med* 2003;197:633–642.
26. **Giang E, Dorner M, Prentoe JC, Dreux M, Evans MJ *et al.*** Human broadly neutralizing antibodies to the envelope glycoprotein complex of hepatitis C virus. *Proc Natl Acad Sci USA* 2012;109:6205–6210.
27. **Meunier JC, Russell RS, Goossens V, Priem S, Walter H *et al.*** Isolation and characterization of broadly neutralizing human monoclonal antibodies to the e1 glycoprotein of hepatitis C virus. *J Virol* 2008;82:966–973.
28. **Tarr AW, Owsianka AM, Szwejk A, Ball JK, Patel AH.** Cloning, expression, and functional analysis of patient-derived hepatitis C virus glycoproteins. *Methods Mol Biol* 2007;379:177–197.
29. **Moreau I, O'Sullivan H, Murray C, Levis J, Crosbie O *et al.*** Separation of hepatitis C genotype 4a into IgG-depleted and IgG-enriched fractions reveals a unique quasispecies profile. *Virol J* 2008;5:103.
30. **Owsianka A, Tarr AW, Juttla VS, Lavillette D, Bartosch B *et al.*** Monoclonal antibody AP33 defines a broadly neutralizing epitope on the hepatitis C virus E2 envelope glycoprotein. *J Virol* 2005;79: 11095–11104.
31. **Palmer BA, Schmidt-Martin D, Dimitrova Z, Skums P, Crosbie O *et al.*** Network analysis of the chronic hepatitis C virome defines hypervariable region 1 evolutionary phenotypes in the context of humoral immune responses. *J Virol* 2015;90:3318–3329.
32. **Naik AS, Palmer BA, Crosbie O, Kenny-Walsh E, Fanning LJ.** A single amino acid change in the hypervariable region 1 of hepatitis C virus genotype 4a aids humoral immune escape. *J Gen Virol* 2016;97:1345–1349.
33. **Palmer BA, Dimitrova Z, Skums P, Crosbie O, Kenny-Walsh E *et al.*** Analysis of the evolution and structure of a complex intrahost viral population in chronic hepatitis C virus mapped by ultradeep pyrosequencing. *J Virol* 2014;88:13709–13721.
34. **Derrick JP, Wigley DB.** The third IgG-binding domain from streptococcal protein G. An analysis by X-ray crystallography of the structure alone and in a complex with Fab. *J Mol Biol* 1994;243: 906–918.
35. **Kenny-Walsh E.** Clinical outcomes after hepatitis C infection from contaminated anti-D immune globulin. Irish Hepatology Research Group. *N Engl J Med* 1999;340:1228–1233.
36. **Helle F, Duverlie G, Dubuisson J.** The hepatitis C virus glycan shield and evasion of the humoral immune response. *Viruses* 2011;3:1909–1932.
37. **Ball JK, Tarr AW, McKeating JA.** The past, present and future of neutralizing antibodies for hepatitis C virus. *Antiviral Res* 2014; 105:100–111.
38. **Gerotto M, Dal Pero F, Loffreda S, Bianchi FB, Alberti A *et al.*** A 385 insertion in the hypervariable region 1 of hepatitis C virus E2 envelope protein is found in some patients with mixed cryoglobulinemia type 2. *Blood* 2001;98:2657–2663.
39. **Cashman SB, Marsden BD, Dustin LB.** The humoral immune response to HCV: understanding is key to vaccine development. *Front Immunol* 2014;5:550.
40. **Deng K, Liu R, Rao H, Jiang D, Wang J *et al.*** Antibodies targeting novel neutralizing epitopes of hepatitis C virus glycoprotein preclude genotype 2 virus infection. *PLoS One* 2015;10: e0138756.
41. **Bankwitz D, Steinmann E, Bitzegeio J, Ciesek S, Friesland M *et al.*** Hepatitis C virus hypervariable region 1 modulates receptor interactions, conceals the CD81 binding site, and protects conserved neutralizing epitopes. *J Virol* 2010;84:5751–5763.
42. **Bartosch B, Vitelli A, Granier C, Goujon C, Dubuisson J *et al.*** Cell entry of hepatitis C virus requires a set of co-receptors that include the CD81 tetraspanin and the SR-B1 scavenger receptor. *J Biol Chem* 2003;278:41624–41630.
43. **Prentoe J, Jensen TB, Meuleman P, Serre SB, Scheel TK *et al.*** Hypervariable region 1 differentially impacts viability of hepatitis C virus strains of genotypes 1 to 6 and impairs virus neutralization. *J Virol* 2011;85:2224–2234.
44. **Sautto G, Tarr AW, Mancini N, Clementi M.** Structural and antigenic definition of hepatitis C virus E2 glycoprotein epitopes targeted by monoclonal antibodies. *Clin Dev Immunol* 2013;2013: 450963.
45. **Tarr AW, Khera T, Hueging K, Sheldon J, Steinmann E *et al.*** Genetic diversity underlying the envelope glycoproteins of

hepatitis C virus: structural and functional consequences and the implications for vaccine design. *Viruses* 2015;7:3995–4046.

46. **Mullan B, Sheehy P, Shanahan F, Fanning L.** Do *Taq*-generated RT-PCR products from RNA viruses accurately reflect viral genetic heterogeneity? *J Viral Hepat* 2004;11:108–114.
47. **Posthumus WP, Lenstra JA, Van Nieuwstadt AP, Schaaper WM, Van der Zeijst BA *et al.*** Immunogenicity of peptides simulating a neutralization epitope of transmissible gastroenteritis virus. *Virology* 1991;182:371–375.
48. **Langedijk JP, Brandenburg AH, Middel WG, Osterhaus A, Meloen RH *et al.*** A subtype-specific peptide-based enzyme immunoassay for detection of antibodies to the G protein of human respiratory syncytial virus is more sensitive than routine serological tests. *J Clin Microbiol* 1997;35:1656–1660.

Journal of General Virology (2016), **97**, 1345–1349 DOI 10.1099/jgv.0.000447

Short Communication

A single amino acid change in the hypervariable region 1 of hepatitis C virus genotype 4a aids humoral immune escape

Amruta S. Naik,[1] Brendan A. Palmer,[1] Orla Crosbie,[2] Elizabeth Kenny-Walsh[2] and Liam J. Fanning[1]

Correspondence
Liam J. Fanning
l.fanning@ucc.ie

[1]Department of Medicine, Clinical Sciences Building, University College Cork, Cork, Ireland
[2]Department of Hepatology, Cork University Hospital, Cork, Ireland

Received 25 January 2016
Accepted 3 March 2016

Longitudinal analysis of chronic hepatitis C virus (HCV) infection has shown that the virus has several adaptive strategies that maintain persistence and infectivity over time. We examined four serum samples from the same chronically infected HCV genotype 4a patient for the presence of IgG antibody-associated virus. RNA was isolated from antibody-associated and antibody-free virions. Subsequent to sequence analysis, 27 aa hypervariable region 1 (HVR1) peptides were used to test the humoral immune escape. We demonstrated that differential peptide binding of Fab was associated with a single amino acid change. We provide direct evidence of natural humoral immune escape by HCV within HVR1.

Hepatitis C virus (HCV) infects 2–3 % of the world population and is a leading cause of liver disease (Freeman *et al.*, 2001; Zhou *et al.*, 2014). Early in infection the host immune system responds by producing neutralizing antibodies (Terilli & Cox, 2013). Although HCV infection stimulates a strong immune response, it is generally insufficient to eradicate infection, as 50–80 % of the infected individuals develop chronic liver disease (Deng *et al.*, 2013; Freeman *et al.*, 2001; Inchauspé *et al.*, 2008; Kenny-Walsh, 1999). The high rate of viral persistence is thought to be a result of a complex interplay between viral diversity and suboptimal immunity. Viruses with hypervariable genomic regions evade host humoral immune response by several mechanisms (Brown *et al.*, 2005; Quaranta *et al.*, 2012; Thimme *et al.*, 2006). The best understood mechanism for viral immune escape is single-point mutation which results in non-synonymous changes within the immunodominant viral envelope glycoprotein and NS3 (Cox *et al.*, 2005; Ray *et al.*, 2005; Thimme *et al.*, 2006, 2012). Multiple linear epitopes within the 27 aa hypervariable region 1 (HVR1), in the N terminus of the E2 envelope protein, have been identified as the principle target of neutralizing antibodies (Ball *et al.*, 2014; Fafi-Kremer *et al.*, 2012; Tarr *et al.*, 2015). Antibodies specific for epitopes within HVR1 have been reported to inhibit the binding of the E2 glycoprotein to cells and to block HCV infectivity *in vitro* and *in vivo* (Farci *et al.*, 1996; Habersetzer *et al.*, 1998; Owsianka *et al.*, 2001). However, HCV pseudoparticle and cell-culture-derived HCV experiments have shown poor cross-neutralization potential of isolate-specific neutralizing antibody response to HVR1 (Brown *et al.*, 2005; Cashman *et al.*, 2014; Larrubia *et al.*, 2014). Cytotoxic T-lymphocytes drive evolution of the HVR1, which can lead to the emergence of escape variants (Cox *et al.*, 2005; Ray *et al.*, 2005). However, there is an absence of direct *in vivo* evidence of humoral immune escape by host-derived antibodies and viral glycoproteins (Chung *et al.*, 2013).

Previous research from our group has observed, over a near 10 year period, the emergence, dominance and disappearance of distinct but related lineages (L1 and L2) in a treatment-naive patient chronically infected with HCV genotype 4a (Palmer *et al.*, 2014). L1 dominated the virome for the first 8 years of the sampling period prior to population collapse and this led to the concomitant rise to prominence of L2. During the initial dominance of L1, IgG targeting of L1 was detected in five of the first seven samples which, in part, contributed directly to the extinction of this group of variants (Palmer *et al.*, 2012, 2014). In spite of the near total dominance of L2 sequences in later samples (96.9 and 99.9 % at T9 and T10, respectively; see Fig. 1 for details of sampling times), no IgG targeting of L2 virions was detected in this previous study (Palmer *et al.*, 2014). Furthermore, the HVR1 of L2 variants remained predominantly under purifying selection across the 10 year period with a single principle HVR1 amino acid variant persisting during this time. Follow-up clonal analysis 1 year later (T11) revealed that a HVR1 variant with a single-point mutation had superseded the principle variant. There was no antibody-associated virus (AAV) found at T11 (Palmer *et al.*, 2014) (Fig. 1). Fig. 1 summarizes the AAV profile of all samples analysed.

The GenBank/EMBL/DDBJ accession numbers for the hepatitis C virus isolate sequences are KT595215–KT595226.

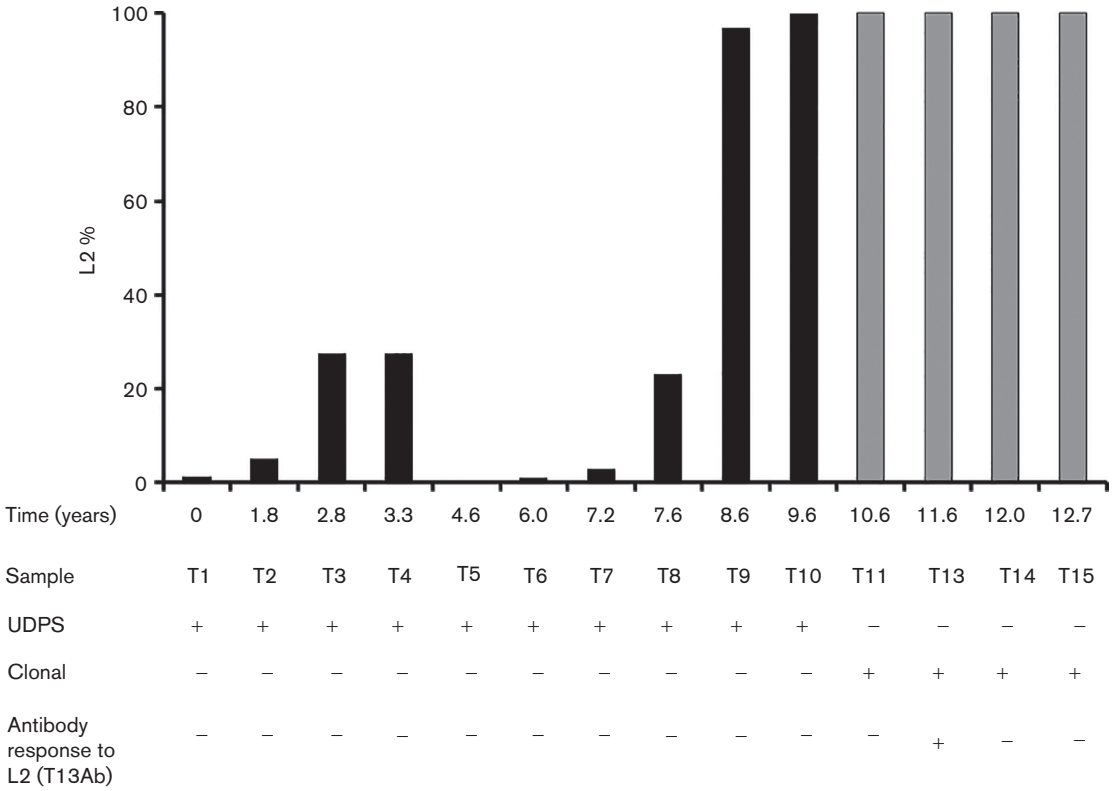

Fig. 1. Ultra-deep pyrosequencing (UDPS) and clonal analysis of serum samples over 13 years. All the samples were screened for the presence or absence of AAV. The *y*-axis depicts the percentage of lineage L2 in all the samples in the study. The *x*-axis demonstrates antibody response to L2 over the period of 13 years. The black columns indicate dominance of L1, grey columns indicate dominance of L2. The plus sign in the bottom row at 11.6 years indicates detectable levels of T13Ab to L2. Neither clonal nor UDPS data is available for T12.

In the current follow-up study to Palmer *et al.* (2014) we mapped a further four serum samples T12–T15 that extended the sampling period to 13 years (Fig. 2). Serum samples were obtained from a treatment-naive patient. This study was approved by the Clinical Research Ethics Committee of the Cork Teaching Hospital and written consent from the patient was obtained. The clonal sequence analysis of these samples identify the continued dominance of L2 sequences. The constituent virions were partitioned into antibody-free virus (AFV) and AAV fractions, as described previously (Moreau *et al.*, 2008; Palmer *et al.*, 2014). Of these samples, only T13 contained detectable levels of AAV (GenBank accession numbers KT595222 and KT595223) (Fig. 1). The antibody–virus complex of this fraction was dissociated and disruption of the virion was achieved by treatment with proteinase K (5 mg ml^{-1}) for 2 h at 37 °C with end-over-end mixing followed by overnight incubation at room temperature. Confirmation of the virus-free status of this proteinase K-treated T13 antibody (T13Ab) preparation was determined by the absence of an E1E2-specific amplicon following reverse transcription PCR; the virus-free T13Fab fragment was designated VF-T13Fab.

T11 had three different HVR1 amino acid variants, i.e. H_{395}-X-X-X-F_{399}, N_{395}-X-X-X-F_{399} and N_{395}-X-X-X-L_{399} (subscript numbering identifies specific amino acid positions within the 27 aa HVR1 with reference to GenBank accession number NC_004102). The presence of HVR1 variant H_{395}-X-X-X-F_{399} in the AFV fraction of T12 was confirmed by amplicon sequencing only. The subsequent AFV fraction of T13 also had the H_{395}-X-X-X-F_{399} amino acid profile (frequency 0.40). However, the N_{395}-X-X-X-L_{399} variant was now dominant in T13 (frequency 0.60). Interestingly, the predicted HVR1 sequence from AAV RNA detected at T13 indicated N_{395}-X-X-X-L_{399} motif targeting (Fig. 2). This Leu-containing motif was isolated in the succeeding samples, i.e. T14 and T15 (Fig. 2). AAV was not detected in samples T11, T12, T14 and T15. However, in order to exclude the possibility that the P2 variant motif containing N_{395}-X-X-X-L_{399} was not accessible to antibodies, we similarly tested VF-T11Fab, VF-T12Fab and VF-T15Fab for binding affinity to the HVR1 peptide variants.

A recent study by Guan *et al.* (2012) showed that neutralization epitopes can be between amino acid positions 16 and 24 (i.e. 399–407) in HVR1. It is interesting to note that

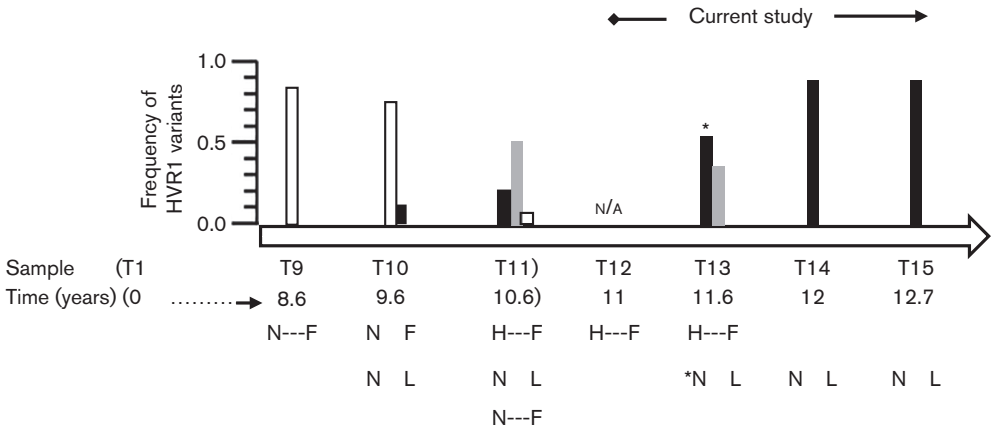

Fig. 2. Clonal DNA sequence analysis of the antibody-free fraction of T11 (Palmer *et al.*, 2014), T13–T15 yielded the following predicted amino acid variants: (i) three unique AFV HVR1 variants for T11 (GenBank accession numbers KC689336–KC689341), (ii) two unique AFV HVR1 variants for T13 (GenBank accession numbers KT595216–KT595221), (iii) a clonotype amino acid quasispecies from the AAV in T13 (GenBank accession numbers KT595222 and KT595223), and (iv) an identical amino acid clonotype profile to T13 AAV in T14 (GenBank accession number KT595224) and T15 (GenBank accession numbers KT595225 and KT595226). T12 (GenBank accession number KT595215) was analysed by amplicon sequencing only. Columns are representative of the relative abundance of that sequence at that time point: black, N_{395}-X-X-L_{399} (N- - -L); grey, H_{395}-X-X-F_{399} (H- - -F); white, N_{395}-X-X-F_{399} (N- - -F). In this study the antibody response was detected at T13. The detectable antibody response identified at T13 and the variant associated with it is denoted by an asterisk. NA, Data not available.

in our study, amino acid variation was observed only at amino acid positions 395 and 399 within the entire HVR1. Based on the Guan *et al.* (2012) data, we hypothesized that the HVR1 variants with N_{395}-X-X-X-F_{399} (T11-AFV) and H_{395}-X-X-X-F_{399} (T13-AFV) motifs were potential humoral immune escape mutants which have Phe at position 399. To confirm the escape phenotype hypothesis, three N-terminally His_6-tagged, 27 aa HVR1 peptides were synthesized, i.e. P1 (H-HHHHHHETHITGAVASSNAQK**F**TSLFTFGPQQN-OH), P2 (H-HHHHHHETHITGAVASSNAQK**L**TSLFTFGPQQN-OH) and P3 (HHHHHHETHITGAVASS**H**AQK**F**TSLFTFGPQQN-OH) (Pepscan Presto), where underlining indicates the His_6-tag and bold indicates the variant amino acid at position 395 or 399. The HVR1 sequence of P1 and P3 corresponded to the dominant L2 HVR1 variant for the initial 10 years of *in vivo* infection for which no AAV was detected (Palmer *et al.*, 2014). The P2 sequence corresponded to the predicted HVR1 of AAV RNA isolated at T13. Peptides were reconstituted in 100 % DMSO at a concentration of 1 mg ml^{-1} and stored at − 20 °C. Peptide (100 ng μl^{-1}) was used in an ELISA-based method. These peptides were incubated with VF-T11Fab, VF-T12Fab, VF-T13Fab and VF-T15Fab at 1 : 10 dilution for 1 h followed by incubation with anti-human IgG (H&L)–HRP conjugate secondary antibody (Promega) at 1 : 5000 dilution for 1 h (Fig. 3). The ELISA results confirmed that the peptide containing the N_{395}-X-X-X-L_{399} mutation was recognized by VF-T13Fab. The binding phenotype of VF-T13Fab had the strongest affinity to P2 (P2>>P1>>P3) with Leu at position 399, compared with the predicted escape variant Phe *in vitro* ($P = 0.06$, Kruskal–Wallis test using Prism 4; GraphPad) (Fig. 3). Our results prove that, in this case, a naturally occurring single amino acid change to Phe in the HVR1 alone at position 399 can drive humoral immune escape after >10 years of immune silence. Our results demonstrated that none of VF-T11Fab, VF-T12Fab and VF-T15Fab bound to the HVR1 peptide variants P1–P3.

In our current study, analysis of serum samples over a 13 year period showed two distinct periods when AAVs were present. A window period of 5 years existed between the two points during which AAVs were detectable. The antibody specificity of the latter time point, i.e. T13, targeted a different HVR1 lineage from that found previously (Palmer *et al.*, 2012, 2014). The HVR1 variant captured by the T13Ab was first observed in pyrosequencing data at T10 (1.1 %) (Palmer *et al.*, 2014). A further 2 years elapsed before T13Ab to this latter variant was detected (Fig. 2).

Interestingly, the HVR1 genomic sequence associated with virus captured by T13Ab was found to be present in the subsequent samples, i.e. T14 and T15. Analysis of samples T14 and T15 revealed that the T13Ab response was not sustained to detectable levels. The loss of neutralization antibodies is a recognized feature of the natural history of HCV infection (Shimizu *et al.*, 1994). Additionally, it is also recognized that a sustained antibody response is likely a prerequisite for complete removal of viral variant(s). The

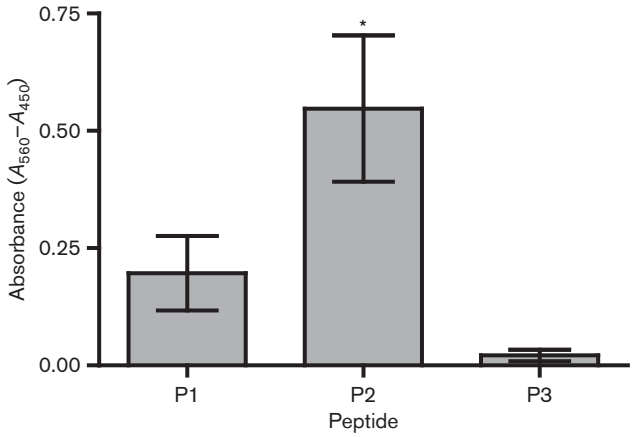

Fig. 3. ELISA-based detection of the binding of the VF-T13Ab to the predicted HVR1 derived His_6-tag peptide epitopes (P1–P3, see text). The P1 and P3 variants were observed in the AFV fraction of T11, and the P2 variant was observed in the AAV fraction of T13. The control reference points included only peptides, peptides with only primary antibodies and peptides with only secondary antibodies. VF-T13Fab showed the strongest affinity towards P2 and baseline activity towards P3. The data were obtained from three independent experiments. The *x*-axis indicates the peptide used in the ELISA, i.e. P1, P2 and P3. The *y*-axis indicates the absorbance obtained by subtracting the A_{450} reading from the A_{560}. *$P = 0.06$.

notable absence of a sustained and neutralizing antibody response (in T14 and T15), and likely fitness superiority, explains why the motif (N_{395}-X-X-X-L_{399}) persisted in subsequent samples.

In conclusion, our proof-of-concept study has confirmed that antibodies were naturally generated against a discrete viral variant (Fig. 3). We additionally confirmed that naturally occurring amino acid variations in this epitope represent one mechanism by which HCV escapes humoral immunity.

Acknowledgements

This work was funded by Molecular Medicine Ireland as a part of the Clinical & Translational Research programme. We would also like to thank John Levis and Dr Kevin Hegarty for initial characterization of patient sera.

References

Ball, J. K., Tarr, A. W. & McKeating, J. A. (2014). The past, present and future of neutralizing antibodies for hepatitis C virus. *Antiviral Res* **105**, 100–111.

Brown, R. J., Juttla, V. S., Tarr, A. W., Finnis, R., Irving, W. L., Hemsley, S., Flower, D. R., Borrow, P. & Ball, J. K. (2005). Evolutionary dynamics of hepatitis C virus envelope genes during chronic infection. *J Gen Virol* **86**, 1931–1942.

Cashman, S. B., Marsden, B. D. & Dustin, L. B. (2014). The humoral immune response to HCV: understanding is key to vaccine development. *Front Immunol* **5**, 550.

Chung, R. T., Gordon, F. D., Curry, M. P., Schiano, T. D., Emre, S., Corey, K., Markmann, J. F., Hertl, M., Pomposelli, J. J. & other authors (2013). Human monoclonal antibody MBL-HCV1 delays HCV viral rebound following liver transplantation: a randomized controlled study. *Am J Transplant* **13**, 1047–1054.

Cox, A. L., Mosbruger, T., Mao, Q., Liu, Z., Wang, X. H., Yang, H. C., Sidney, J., Sette, A., Pardoll, D. & other authors (2005). Cellular immune selection with hepatitis C virus persistence in humans. *J Exp Med* **201**, 1741–1752.

Deng, Y., Guan, J., Wen, B., Zhu, N., Chen, H., Song, J., Yang, Y., Wang, Y. & Tan, W. (2013). Induction of broadly neutralising HCV antibodies in mice by integration-deficient lentiviral vector-based pseudotyped particles. *PLoS One* **8**, e62684.

Fafi-Kremer, S., Fauvelle, C., Felmlee, D. J., Zeisel, M. B., Lepiller, Q., Fofana, I., Heydmann, L., Stoll-Keller, F. & Baumert, T. F. (2012). Neutralizing antibodies and pathogenesis of hepatitis C virus infection. *Viruses* **4**, 2016–2030.

Farci, P., Shimoda, A., Wong, D., Cabezon, T., De Gioannis, D., Strazzera, A., Shimizu, Y., Shapiro, M., Alter, H. J. & Purcell, R. H. (1996). Prevention of hepatitis C virus infection in chimpanzees by hyperimmune serum against the hypervariable region 1 of the envelope 2 protein. *Proc Natl Acad Sci U S A* **93**, 15394–15399.

Freeman, A. J., Marinos, G., Ffrench, R. A. & Lloyd, A. R. (2001). Immunopathogenesis of hepatitis C virus infection. *Immunol Cell Biol* **79**, 515–536.

Guan, M., Wang, W., Liu, X., Tong, Y., Liu, Y., Ren, H., Zhu, S., Dubuisson, J., Baumert, T. F. & other authors (2012). Three different functional microdomains in the hepatitis C virus hypervariable region 1 (HVR1) mediate entry and immune evasion. *J Biol Chem* **287**, 35631–35645.

Habersetzer, F., Fournillier, A., Dubuisson, J., Rosa, D., Abrignani, S., Wychowski, C., Nakano, I., Trépo, C., Desgranges, C. & Inchauspé, G. (1998). Characterization of human monoclonal antibodies specific to the hepatitis C virus glycoprotein E2 with in vitro binding neutralization properties. *Virology* **249**, 32–41.

Inchauspé, G., Honnet, G., Bonnefoy, J. Y., Nicosia, A. & Strickland, G. T. (2008). Hepatitis C vaccine: supply and demand. *Lancet Infect Dis* **8**, 739–740.

Kenny-Walsh, E. & Irish Hepatology Research Group (1999). Clinical outcomes after hepatitis C infection from contaminated anti-D immune globulin. *N Engl J Med* **340**, 1228–1233.

Larrubia, J. R., Moreno-Cubero, E., Lokhande, M. U., García-Garzón, S., Lázaro, A., Miquel, J., Perna, C. & Sanz-de-Villalobos, E. (2014). Adaptive immune response during hepatitis C virus infection. *World J Gastroenterol* **20**, 3418–3430.

Moreau, I., O'Sullivan, H., Murray, C., Levis, J., Crosbie, O., Kenny-Walsh, E. & Fanning, L. J. (2008). Separation of hepatitis C genotype 4a into IgG-depleted and IgG-enriched fractions reveals a unique quasispecies profile. *Virol J* **5**, 103.

Owsianka, A., Clayton, R. F., Loomis-Price, L. D., McKeating, J. A. & Patel, A. H. (2001). Functional analysis of hepatitis C virus E2 glycoproteins and virus-like particles reveals structural dissimilarities between different forms of E2. *J Gen Virol* **82**, 1877–1883.

Palmer, B. A., Moreau, I., Levis, J., Harty, C., Crosbie, O., Kenny-Walsh, E. & Fanning, L. J. (2012). Insertion and recombination events at hypervariable region 1 over 9.6 years of hepatitis C virus chronic infection. *J Gen Virol* **93**, 2614–2624.

Palmer, B. A., Dimitrova, Z., Skums, P., Crosbie, O., Kenny-Walsh, E. & Fanning, L. J. (2014). Analysis of the evolution and structure of a

complex intrahost viral population in chronic hepatitis C virus mapped by ultradeep pyrosequencing. *J Virol* **88**, 13709–13721.

Quaranta, M. G., Mattioli, B. & Vella, S. (2012). Glances in immunology of HIV and HCV Infection. *Adv Virol* **2012**, 434036.

Ray, S. C., Fanning, L., Wang, X. H., Netski, D. M., Kenny-Walsh, E. & Thomas, D. L. (2005). Divergent and convergent evolution after a common-source outbreak of hepatitis C virus. *J Exp Med* **201**, 1753–1759.

Shimizu, Y. K., Hijikata, M., Iwamoto, A., Alter, H. J., Purcell, R. H. & Yoshikura, H. (1994). Neutralizing antibodies against hepatitis C virus and the emergence of neutralization escape mutant viruses. *J Virol* **68**, 1494–1500.

Tarr, A. W., Khera, T., Hueging, K., Sheldon, J., Steinmann, E., Pietschmann, T. & Brown, R. J. (2015). Genetic diversity underlying the envelope glycoproteins of hepatitis C virus: structural and functional consequences and the implications for vaccine design. *Viruses* **7**, 3995–4046.

Terilli, R. R. & Cox, A. L. (2013). Immunity and hepatitis C: a review. *Curr HIV/AIDS Rep* **10**, 51–58.

Thimme, R., Lohmann, V. & Weber, F. (2006). A target on the move: innate and adaptive immune escape strategies of hepatitis C virus. *Antiviral Res* **69**, 129–141.

Thimme, R., Binder, M. & Bartenschlager, R. (2012). Failure of innate and adaptive immune responses in controlling hepatitis C virus infection. *FEMS Microbiol Rev* **36**, 663–683.

Zhou, X., Sun, P., Lucendo-Villarin, B., Angus, A. G., Szkolnicka, D., Cameron, K., Farnworth, S. L., Patel, A. H. & Hay, D. C. (2014). Modulating innate immunity improves hepatitis C virus infection and replication in stem cell-derived hepatocytes. *Stem Cell Rep* **3**, 204–214.